Design of multifunctional polymeric nanoparticles for biomedical applications

Stefanie Leitner

DESIGN OF MULTIFUNCTIONAL POLYMERIC NANOPARTICLES FOR BIOMEDICAL APPLICATIONS

STEFANIE LEITNER

Universitat de Barcelona

Consejo Superior de Investigaciones Científicas
Insistuto de Química Avanzada de Cataluña
Departamento de Nanotecnología Química y Biomolecular

Programa de doctorat “Ciència i Tecnologia de Materials”

DESIGN OF MULTIFUNCTIONAL POLYMERIC NANOPARTICLES FOR BIOMEDICAL APPLICATIONS

_____
Stefanie Leitner

_____
Dr. Gabriela Calderó Linnhoff
Consejo Superior de Investigaciones Científicas (CSIC)

_____
Dr. Conxita Solans Marsà
Consejo Superior de Investigaciones Científicas (CSIC)

_____
Dr. María José García-Celma
Universitat de Barcelona

TABLE OF CONTENTS

1. INTRODUCTION

1.1. NANO-EMULSIONS

1.1.1. DEFINITION AND CHARACTERISTICS

Nano-emulsions are a class of emulsions with droplet sizes in the nanometer range, consisting of at least two immiscible liquids, one of them being dispersed as very small droplets in the other and stabilized by surfactant molecules [Tadros, 2009]. Generally, one of the liquids is polar (usually referred to as water or aqueous solution/component) while the other is nonpolar (also referred to as oil). Depending on the nature of the continuous phase, nano-emulsions can be classified into oil-in-water (O/W) nano-emulsions, where oil droplets are dispersed in water, and water-in-oil (W/O) nano-emulsions, where water droplets are dispersed in the nonpolar liquid [Solans, 2005; Tadros, 2005; McClements, 2011 and 2012].

Nano-emulsions droplet diameters are typically between 20 and 500 nm. Due to the small size, they have a transparent or translucent appearance to the naked eye (Figure 1.1) and show kinetic stability against gravitational separation (sedimentation or creaming).

Figure 1.1. Visual aspect of a nano-emulsion.

Nano-emulsions, being thermodynamically unstable systems (non-equilibrium systems), cannot form spontaneously. Hence, energy input is needed for creating an interface between both immiscible liquids. The total free Energy of (nano-)emulsion formation (ΔG_T) is defined as [Tadros, 2004]:

$$\Delta G_T = \gamma \Delta A - T\Delta S \qquad \text{[Equation 1]}$$

where ΔA is the interfacial area increase, γ the interfacial tension, T the temperature and ΔS the configuration entropy of the dispersion.

By forming many droplets with the Area A_2 from the bulk liquid with an Area A_1, the interfacial area increases (as $A_2 >> A_1$), making ΔA positive. The interfacial tension γ is also positive which makes the term very large and overweighs the entropy of droplet formation $T\Delta S$ with the configuration entropy ΔS being small and positive [Tadros 2004; Solans, 2005; Anton, 2008; McClements, 2011 and 2012].

In the literature, nano-emulsions are also referred to as submicron emulsions [Benita, 1993; Yang, 2000] or miniemulsions [Ugelstad, 1973; Asua, 2002; El-Aasser, 2004].

Nano-emulsion formation involves the generation of new water-oil interfaces which require the presence of stabilizing components. Surfactants, due to their amphiphilic character (i.e. having a hydrophilic and a lipophilic moiety), can be arranged at the interfacial liquid-liquid film. In this way, they diminish the surface tension γ and thus the total free Energy ΔG_T of the system [Equation 1] which hence enables the formation of small droplets.

Aside from lowering the surface tension, strongly adsorbed surfactants also create a monolayer at the droplet interface which functions as a steric, mechanical and/or electrical barrier, preventing the direct contact between neighbour droplets and thus avoiding destabilization phenomena like flocculation or coalescence [Tadros, 2004].

1.1.2. STABILITY

(Nano-)Emulsions are thermodynamically unstable systems and tend to break down with time. The mechanisms involved in the destabilization are schematically represented in Figure 1.2.

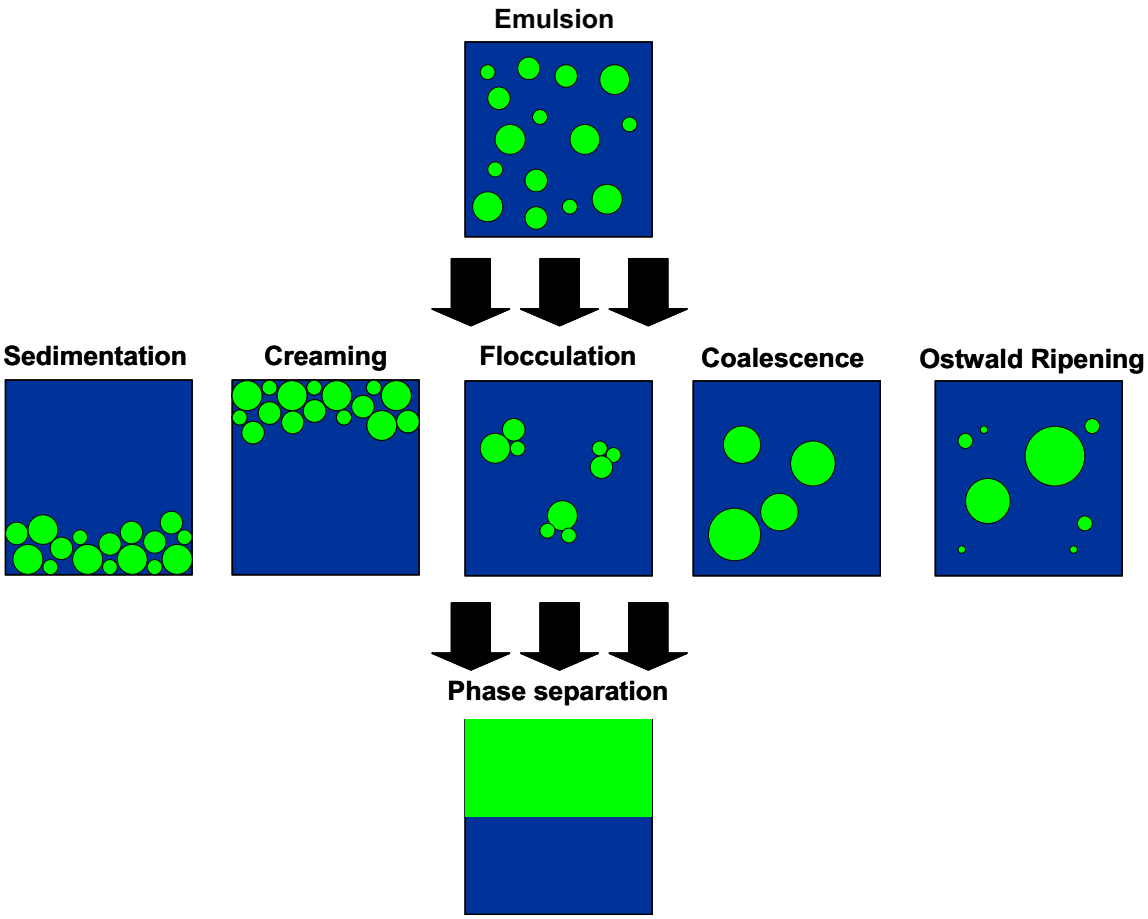

Figure 1.2. Schematic representation of emulsion breakdown processes.

Creaming / sedimentation is a reversible process which takes place due to the relative densities of the dispersed and continuous phases, exceeding the Brownian motion. While droplets having a lower density than the bulk phase move upwards (creaming), those which have a higher density than the continuous phase move downwards (sedimentation). As mentioned earlier, high kinetic stability against these phenomena are usually given through small droplet sizes. However, when droplets are polydisperse in size, large ones cream or sediment while small ones remain dispersed. The creaming / sedimentation rate v_{Stokes} can be calculated applying the *Stokes' law* [Tadros, 2005]

$$v_{Stokes} = \frac{2\ g\ r^2(\rho_2 - \rho_1)}{9\eta} \qquad \text{[Equation 2]}$$

where g is the acceleration due to gravity, r the droplet radius, ρ_1 and ρ_2 the density of the continuous and dispersed phase, respectively, and η the viscosity of the continuous phase. The phenomena of creaming and sedimentation can be prevented by decreasing the nano-emulsion droplet size, thickening of the continuous phase or density-matching of the two immiscible liquids [Tadros, 2004 and 2005; McClements, 2011].

Flocculation is the formation of aggregates/clusters by two or more drops of the dispersed phase, a process which is mainly reversible. The driving force of this phenomenon is the van der Waals forces between the droplets, which becomes significant at short separation distances. Flocculation leads to an increase in droplet size (aggregates of droplets) and may also cause coalescence of the drops. Flocculation can be prevented by sufficient large droplet surface charge (electrostatic barrier) or by selected surfactants (steric barrier) [Borwankar, 1992; Tadros, 2009].

Coalescence may take place when droplets come in close contact in a flocculated or creamed layer or due to Brownian motion. Possible consequences are a thinning or disruption of the interfacial film, leading to a breakup of the droplets and merging into a single droplet with the same total volume but a reduced surface energy which is energetically favored. Therefore, this process is irreversible. The change of droplet size with time can be described with following equation [Deminière, 1998]:

$$\frac{1}{r^2} = \frac{1}{r_0^2} - \left(\frac{8\pi}{3}\right)\omega t \qquad \text{[Equation 3]}$$

where r is the average droplet radius at time t, r_0 the value at t = 0 and ω the coalescence rate [Deminière, 1998].

Ostwald ripening describes the irreversible growth of larger droplets at the expense of smaller ones in polydisperse systems, a process driven by the diffusion of molecules of the dispersed phase. The small droplets will dissolve and redeposit their material onto the larger droplets which will increase the

average droplet radius. This effect is a result of polydispersity and thus different chemical potentials in the droplets due to different radii of curvature of the droplets, resulting in a greater solubility of smaller droplets compared to larger ones. The Lifshitz-Slezov and Wagner (LSW) theory [Lifshitz, 1961; Wagner 1961] gives an expression for the rate of ripening by following equation:

$$\omega = \frac{dr_c^3}{dt} = \frac{8C_\infty \gamma V_m D}{9RT\rho} \qquad \text{[Equation 4]}$$

It is based on the assumptions that droplets are spherical, separated from each other by distances larger than the droplet diameter and the mass transport is merely by molecular diffusion in the continuous phase [Kabalnov, 1992; Taylor, 1998; Tadros, 2009]

Summarizing the instability mechanisms in nano-emulsions, the following conclusions/assumptions can be made:

- Creaming / sedimentation and flocculation are prevented by the small droplet sizes (high Brownian motion and great curvature of small droplets)
- Coalescence is considered as possible destabilization mechanism
- Ostwald ripening is considered as the main destabilization process

1.1.3. PREPARATION METHODS

As mentioned earlier, energy input is required for nano-emulsion formation. The energy may come from mechanical devices (high-energy approach) or from the chemical potential of the components (low-energy approach) [Walstra, 1983]. High-energy emulsification approaches (dispersion emulsification methods) such as high pressure homogenizers, ultrasound generators, high-shear stirrers or fluidizers own intensive disruptive forces, capable to produce small and uniform droplets [Tadros, 2004; Solans, 2005; Jafari, 2007; Anton, 2008]. However, the energy level required to obtain nanosized droplets is rather high. Therefore, low-energy emulsification methods (condensation emulsification methods), based on the use of the chemical energy stored in the components to

achieve emulsification have received increasing attention. Only simple stirring is required and allows the formation of smaller droplets than with high-energy methods [Forgiarini, 2001; Bouchemal, 2004; Usón, 2004; Solè, 2006; Kelmann, 2007; Anton, 2009]. Among different low-energy emulsification methods, the phase inversion methods are well-known in which phase inversion of the surfactant spontaneous curvature is produced during emulsification either by changing temperature at constant composition (phase inversion temperature (PIT) method) or by changing composition at constant temperature (phase inversion composition (PIC) method).

The Phase Inversion Temperature (PIT) method

The Phase Inversion Temperature (PIT) method, which was introduced by Shinoda and Saito in 1968 [Shinoda, 1968], is based on changes in the surfactant spontaneous curvature (molecular geometry) or solubility of non-ionic surfactants induced upon temperature changes [Izquierdo, 2002; Solans, 2005; Morales, 2006; Anton, 2008 and 2009]. This method can only be applied when temperature-sensitive surfactants are involved such as polyethoxylated nonionic surfactants.

At low temperatures (T < PIT), the surfactant molecules are hydrated and thus water-soluble. Therefore, O/W nano-emulsions can be formed. When increasing the temperature, the head groups of the surfactant molecules are dehydrated which makes them more lipophilic. At the PIT, the surfactant is equally soluble in the water and in the oil phase and the formation of a bicontinuous system is favored. By further increasing the temperature (T > PIT), the surfactant becomes completely lipophilic and W/O nano-emulsions are formed. The phase transitions can be followed by measuring the turbidity and/or conductivity of the nano-emulsion as a function of temperature.

The importance of phase transitions through a microemulsion phase or a lamellar liquid crystalline phase (multiphase) has been shown by numerous studies. Izquierdo *et al.* described nano-emulsion formation in the water/$C_{12}E_4$/isohexadecane system by the PIT method. Smallest droplet sizes were obtained with both, an initial single or multiphase region [Izquierdo, 2004].

Similar results were reported by Morales *et al.* in the water/$C_{16}E_6$/mineral oil system [**Morales, 2003**].

The Phase Inversion Composition (PIC) method

The Phase Inversion Composition (PIC) method is based on changes of the composition at constant temperature. One of the components (water or oil) is added progressively to a mixture of the other two components (oil-surfactant or water-surfactant, respectively). This method is not restricted to polyethoxylated surfactants which are, nevertheless, frequently involved. **Figure 1.3** gives a schematic representation. When water is stepwise added to the oil phase containing the surfactant, initially, water-in-oil (W/O) microemulsions are formed with water droplets being dispersed in the continuous oil phase. By adding more water, the surfactant spontaneous curvature will change from negative to zero, forming consequently bicontinuous structures as the surfactant affinity to water and to oil is balanced. By further addition of water, oil-in-water (O/W) nano-emulsions will be formed with very small droplet sizes suggesting a very high positive curvature of surfactant layer [**Forgiarini, 2001; Pey, 2006; Wang, 2008 and 2009; Solè, 2006 and 2010; Calderó, 2011; Solans, 2012**].

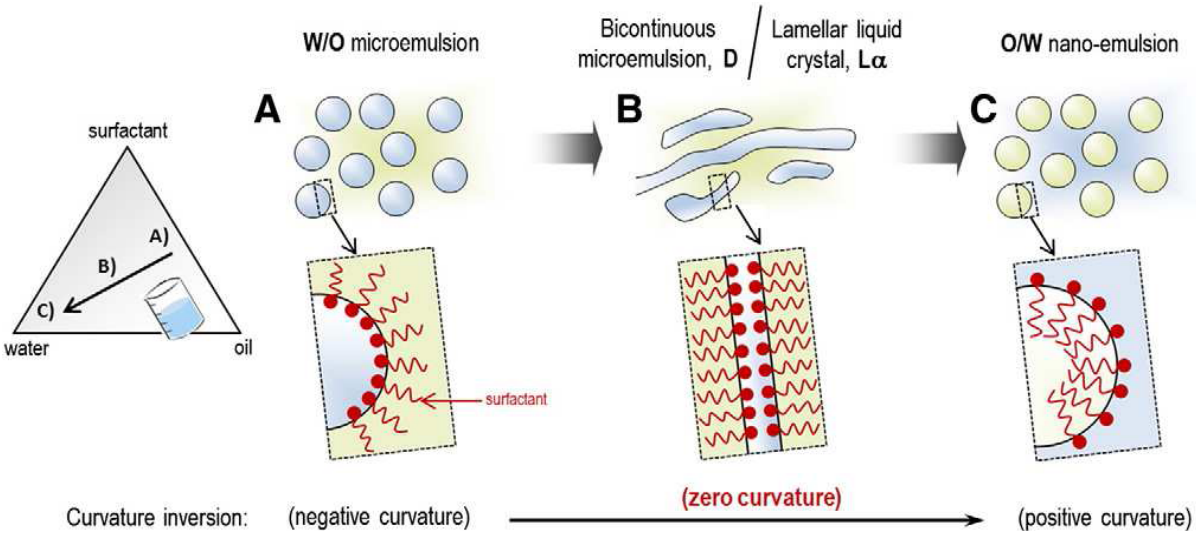

Figure 1.3. Schematic representation of nano-emulsion formation by the phase inversion composition (PIC) method [**Solans, 2012**].

Oil-in-water (O/W) nano-emulsions by the PIC method have been studied extensively. Sonneville-Aubrun *et al.* reported O/W nano-emulsions with homogenous size distribution and mean diameter of 100 nm formed in the water/polyethylene glycol 400 monoisostearate/hydrogenated polyisobutene system by the PIC method. A lamellar liquid crystalline phase with zero mean curvature was detected by SANS [Sonneville-Aubrun, 2009]. Roger *et al.* demonstrated that emulsification took place by the PIC method in the water/$C_{16}E_8$/hexadecane system. A swelling of a reverse micellar phase was followed by the formation of a bicontinuous sponge phase. Further addition of water lead to the nucleation of oil droplets in the sponge phase and then resulted in nano-emulsions with bimodal size distributions [Roger, 2011]. O/W nano-emulsions, formed by the PIC method, with bimodal size distributions have also been reported by Heunemann *et al.* [Heunemann, 2011]. Lamellar liquid crystal structures have been described as one of the key factors for the formation of the O/W nano-emulsions with small droplet sizes (Ø ≤ 50 nm) in the water/Cremophor EL/Miglyol 812 system by Sadurni *et al.* [Sadurní, 2005] and in the water/Brij 30/decane system by Forgiarini *et al.* [Forgiarini, 2001].

1.1.4. APPLICATIONS

The characteristic properties of nano-emulsions such as their small droplet sizes, their high kinetic stability and/or their optical transparency make them attractive for applications in many fields like food, personal care products and medical and pharmaceutical industries. In food industry, they have been used for modification of food characteristics like food texture, taste or stability during shelf life [McClements, 2007; Huang, 2010; Silva, 2012]. Troncoso *et al.* carried out studies focused on the influence of disperse phase composition (oil-to-solvent ratio) on the physicochemical properties and in vitro digestion of Tween 20-stabilized O/W nano-emulsions, prepared by a high-energy method. This information is crucial for determining the design and production of edible delivery systems based on nano-emulsions and the control of lipid digestion [Troncoso, 2012]. In cosmetics they found applications due to their low viscosity and transparency [Sonneville-Aubrut, 2004; Alves, 2007; Gutierrez, 2008]. In the pharmaceutical and medical field, nano-emulsions were applied as

carriers/delivery systems for e.g. vaccines, DNA encoded drugs or antibiotics through various administration routes (oral, pulmonary, ocular, transdermal) [Calvo, 1996; Santos-Magalhães, 2000; Wu, 2001; Pan, 2003; Nicolaos, 2003; Tamilvanan, 2004; Tiwari, 2006]. In regard to nano-emulsions as carriers for ocular drugs, Ammar *et al.* formulated a nano-emulsion containing the antiglaucoma drug dorzolamide hydrochloride. It was reported that this nano-emulsion had higher therapeutic efficiency, faster onset of action and prolonged effect relative to either drug solution or market products [Ammar, 2009]. Especially nano-emulsions containing a positive charge have gained increasing attention due to their ability to develop electrostatic interactions with negatively charged drugs [Bivas-Benita, 2004; Hagigit, 2008; Liu, 2010; Ott, 2002; Torchilin, 2006]. Teixeira *et al.* prepared cationic nano-emulsions from medium-chain triglycerides, poloxamer 188 and stearylamine for the delivery of oligonucleotides. It has been shown that oligonucleotides in a wide range of size could be associated and have been protected in culture medium containing serum [Teixeira, 1999].

Another significant application of nano--emulsions is their use as templates for nanoparticle preparation [Solans, 2005; Anton, 2008] which was also the purpose in this work. Calderó *et al.* described that polymeric nanoparticles could be obtained from O/W nano-emulsions formed in a water/polyoxyethylene 4 sorbitan monolaurate/[10 wt% ethylcellulose in ethyl acetate] system. The nano-emulsions were obtained by the PIC method and were used as templates for nanoparticle preparation by solvent evaporation [Calderó, 2011].

1.2. NANOPARTICLES

1.2.1. DEFINITION AND CHARACTERISTICS

Nanoparticles are solid materials with sizes usually below 500 nm. They can be categorized into nanospheres and nanocapsules. *Nanospheres* consist of homogenous matrix systems and are in general spherical. However, also non-spherical shapes have been reported [Moinard-Chécot, 2008]. *Nanocapsules*

are particles with a solid shell surrounding a liquid or semisolid core (Figure 1.4) [Soppimath, 2001; Pinto Reis, 2006; Anton, 2008; Kumari, 2010; Rao, 2011]. Depending on the particular application, the properties of the nanoparticles can be optimized by choosing the right materials and preparation method. The materials used for nanoparticle preparation are either of inorganic or organic nature like e.g. metal oxides [Matijević, 1993; Willert, 2001; Stoimenov, 2002] or polymers [Fernández-Urrusuno, 1999; Xu, 2004].

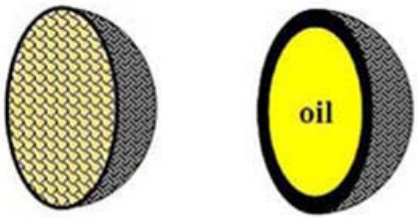

Figure 1.4. Structure of different types of nanoparticles, nanospheres and nanocapsules [**Vauthier, 2009**].

1.2.2. PREPARATION METHODS

Nanoparticles can be prepared from a variety of inorganic and organic materials. Among organic materials, polymers (natural, synthetic, semisynthetic) have been frequently used for the preparation of polymeric nanoparticles. Two general approaches exist, namely the preparation by polymerization of monomers [Landfester, 2001; Asua, 2002; Rao, 2011] or from preformed polymers [Soppimath, 2001; Pinto Reis, 2006; Calderó, 2011; Rao, 2011]. The latter approach bears several advantages over the direct polymerization of monomers. It avoids purification processes necessary to remove undesired side products or excess of reactants (monomers, surfactants, etc.) and the application of additional reactive components (e.g. initiators) [Pinto Reis, 2006; Calderó, 2011]. Several methods exist to obtain polymeric nanoparticles by using a preformed polymer such as e.g. the solvent displacement method (nanoprecipitation method), the solvent evaporation method or by applying the supercritical fluid technology (SCF) [Soppimath, 2001; Vauthier, 2009; Rao, 2011]. The solvent evaporation method was the first method developed to

prepare polymeric nanoparticles from a preformed polymer [Vanderhoff, 1979]. Figure 1.5 gives a schematic representation of this method.

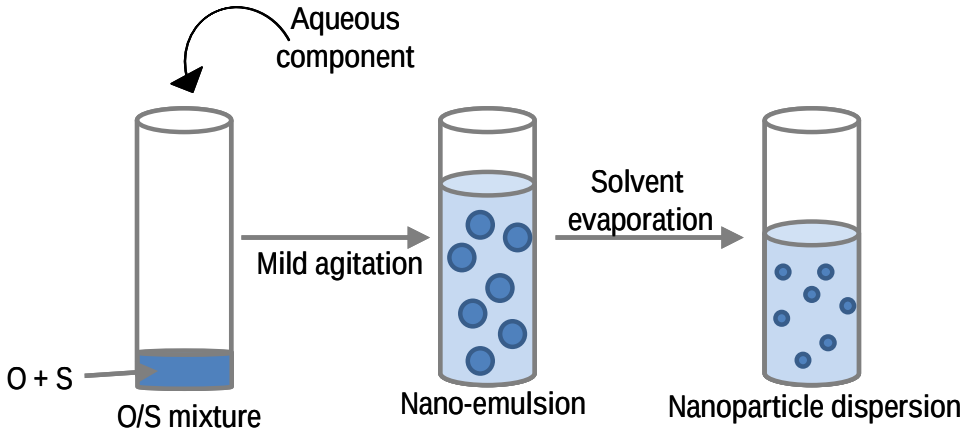

Figure 1.5. Scheme of the nanoparticle preparation process with oil phase abbreviated as O and surfactant(mixture) as S.

In a first step, a nano-emulsion is formed with a volatile, organic solvent as oil phase, containing the polymer, dispersed into droplets in an aqueous solution, stabilized by surfactant molecules. In a second step, the nano-emulsion is converted into a nanoparticle dispersion by evaporating the solvent which is able to diffuse through the continuous phase of the nano-emulsion. Solvent evaporation is achieved e.g. by continuous magnetic stirring at room temperature or under reduced pressure [Pinto Reis, 2006; Rao, 2011]. In the work of Calderó *et al.*, in order to obtain ethylcellulose nanoparticles the organic solvent, ethyl acetate, was evaporated overnight under continuous stirring at room temperature [Calderó, 2011]. Ethyl acetate was also the organic solvent in the work of Desgouilles *et al.* where ethylcellulose and poly(lactic acid) nanoparticles were formed by solvent evaporation under vacuum and at elevated temperature (30°C) during 30 minutes [Desgouilles, 2003]. Song *et al.* prepared poly(lactic-co-glycolic acid) (PLGA) nanoparticles with a particle size between 60 and 200 nm by employing a mixture of dichloromethane and acetone (8:2, v:v) as solvent system, using Poly(vinyl alcohol) (PVA) as stabilizing agent [Song, 1997].

1.2.3. Applications

Depending on their nature, nanoparticles find application in various fields like in textile industry as coatings for antimicrobial fabrics [Lee, 2003; Dubas, 2006], in

optics as anti-reflection coatings [Chen, 2001; Hiller, 2002; Krogman, 2005], as Magnetic Resonance Imaging (MRI) contrast agents in magnetic devices [Shultz, 2007; Hadjipanays, 2008; Na, 2009], as well as in pharmaceutical and medical industries where they are widely used as carriers for drugs and bioactive compounds [Cortesi, 2002; Hans, 2002].

The use of nanoparticles to enhance the *in vivo* efficiency of drugs has been well established over the last years in pharmaceutical and clinical research. Surface modification of nanoparticles is used to control their biological properties and makes them to simultaneously preform various therapeutically or diagnostically important functions. The most important results of such modification include an increased stability and half-life of nanoparticles in the blood circulation, ability to accumulate in the required pathological zone, responsiveness to local physiological stimuli, effective intracellular drug delivery and ability to serve as imaging/contrast agents allowing the real-time observation of their accumulation inside the target [Torchilin, 2006].

Numerous studies have been carried out encapsulating drugs into polymeric nanoparticles. Sheng *et al.*, for example, reports the encapsulation of hemoglobin by polylactic acid (PLA) nanoparticles, obtained by the double emulsion method [Sheng, 2009]. Targeting of nanoparticles with the aid of ligands specific to cell surface characteristic structures allows the selective drug delivery to those cells. A variety of methods have been developed to attach corresponding vectors (antibodies, peptides, folate and others) to the nanoparticle surface. Targeting tumors with folate-modified nanocarriers represents a useful approach, since folate receptors are frequently overexpressed in many tumor cells [Gabizon, 2004]. Other studies have reported that drugs were linked to the nanoparticle surface by means of a cleavable linker which could be cut by enzymes. Kohler *et al.* reported an in vitro study on the release of the chemotherapeutic drug methotrexate (MTX) by using iron oxide nanoparticles as cargo system. The bond between the MTX and the particle surface was triggered at low pH by lysozymes [Kohler, 2005]. In the work of Arias *et al.* 5-fluorouracil (5-FU), a drug used for the treatment of solid tumors was adsorbed onto different pol(alkylcyanoacrylate) (PACA) nanoparticles. The adsorption has been found to be low, probably due to the

lack of interaction between 5-FU and the hydrophobic PACA which demonstrated the importance of the nature of the nanoparticle surface. However, for these nanoparticles the sorption method has been found to be more efficient than the entrapment method [Arias, 2008]. Many biologically active compounds need to be delivered intracellularly to exert their therapeutic action inside the cell onto nucleus or other specific organelles. However, the lipophilic nature of the biological membranes restricts the direct intracellular delivery of proapoptotic drugs, lysosomal compounds, gene and antisense agents and some others. Moreover, large molecules such as DNA, which are internalized via endocytosis and transferred within endosomes, end in lysosomes resulting in the degradation of these molecules by lysosomal enzymes [Varga, 2000]. This is especially important in gene therapy. From this point of view, the development of nanoparticles to deliver DNA or oligonucleotides into the cytoplasm of the target cells would be highly desirable. The use of cationic lipids and cationic polymers as transfection vectors for intracellular delivery of DNA was suggested in the last decades [Xu, 1996]. The delivery of drugs/ nucleic acid by nanoparticles has been described through different approaches that involve covalent binding, adsorption, encapsulation or electrostatic interactions. In terms of electrostatic interactions, the positive surface charge of a nanoparticle can arise from incorporation of a cationic polymer or cationic (surfactant) molecules. An example is given by Li *et al.*, who studied the gene transfection efficiency of cationic liposomes containing amino-acid based lipids. Transfection generally refers to the introduction of nucleic acid into cells. In the work of Li *et al.*, transfection activity was reported for lipoplexes containing lysine or arginine as head groups. It was assumed that based on the structure of the cationic lipids, DNA was packed compactly which increased the permeability of the complex through cell membranes [Li, 2011].

Oligonucleotides are important biomolecules as they can be effective drugs themself. An antisense oligonucleotide (ASO) is a single-stranded, chemically modified DNA-like molecule, 17-22 nucleotides long and designed to be complementary to a selected gene's mRNA. ASOs have been widely accepted to inhibit expression of different genes and delay tumor progression in many preclinical models (gene silencing) [Gleave, 2005]. The activity of ASO *in vivo* is

compromised due to several factors such as low stability to endonucleases present in serum. For that reason, there is the interest of improving cellular uptake of the ASO molecules by taking advantage of their negative charge and, given through that, their ability to develop electrostatic interactions with opposed charged nano-carriers. For example polyalkylcyanoacrylate (PACA) nanoparticles, prepared by the emulsion polymerization process, were combined with DEAE-dextran, a cationic polymer, or with hexadecyltrimethylammonium bromide (CTAB), a cationic hydrophobic surfactant. *In vitro* cellular uptake of the DEAE-PHCA was followed and confirmed by fluorescence microscopy [Zimmer, 1999].

In conclusion, multifunctional nanoparticles can provide opportunities in producing highly efficient and specialized systems for drugs, genes and diagnostic agents. Although the approach is just emerging, it shows a promising future.

2. OBJECTIVES

Nano-emulsions are emulsions of very small droplet sizes, usually below 200 nm. They can be prepared by high-energy methods based on mechanical energy input or by low-energy methods which take advantage of the physicochemical properties of the components of a system. Commonly used low energy-methods are the phase inversion temperature (PIT) and the phase inversion composition (PIC) method. In these methods, nano-emulsions are obtained through phase inversion, either by changing temperature at constant composition (PIT) or by changing the composition at constant temperature (PIC). It is reported that **low-energy emulsification methods** produce smaller and more uniform droplets than high-energy methods. Two major applications of nano-emulsions are their use as drug delivery systems and as templates for the preparation of nanoparticles. **Cationic nano-emulsions** are of particular interest as they have found application as non-viral nanocarriers in the pharmaceutical and medical field through various routes due to their ability to develop electrostatic interactions with negatively charged bioactives. The cationic charge derives either from cationic polymers or other cationic molecules [**Solans, 2005 and 2012**].

Polymeric nanoparticles have gained significant interest due to their small size and their suitability for controlled and sustained drug release. The use of preformed polymers is advantageous over monomer polymerization as it avoids purification steps and the use of additional reactants. In this context, numerous synthetic polymers have been used such as polylactic acid (PLA) [**Cheng, 2008; Mainardes, 2009**], poly-ε-caprolactone (PCL) [**Damgé, 2007; Zheng, 2009**] or poly(lactic-co-glycolic acid) (PLGA) [**Labhasetwar, 1998; Danhier, 2009**]. Also natural polymers have been applied such as gelatin [**Lu, 2004; Kaur, 2008**] or chitosan [**Janes, 2001; Wu, 2005**]. In recent years, ethylcellulose has received increasing attention. This semisynthetic cellulose derivative has been approved for oral and topical applications and applied in food, cosmetics and pharmaceutical products [**Rekhi, 1995; Calderó, 2011**]. Ethylcellulose

nanoparticles have been prepared usually from nano-emulsions by high-energy methods such as high pressure homogenizers [**Ubrich, 2004**] or high shear stirrers [**Perugini, 2002**]. Only few reports have been published on their preparation by low-energy methods [**Spernath, 2007**; **Generalova, 2009; Calderó, 2011**].

The preparation of nanoparticles from preformed polymers is generally performed by the **solvent evaporation** method. However, low-polarity organic solvents like benzene [**Arias, 2010**] or toluene [**Generalova, 2009**], which bear a high toxicity and are thus not recommended for the production of agents for biomedical applications have been widely used. As an effort to design environmental friendly nanoparticulate systems, the use of high-polarity oils such as ethyl acetate, which belong to ICH class 3 (solvent regarded as less toxic and of lower risk to human health) [**ICH Guideline, 2011**], is of great interest [**Desgouilles 2003; Calderó 2011**].

The general objective of this research was the **design of polymeric cationic nanoparticles from nano-emulsions obtained by low-energy methods for biomedical applications**.

This general objective includes the following specific *objectives*:

1) Preparation of oil-in-water (O/W) cationic nano-emulsions by low-energy methods and their characterization
2) Preparation and characterization of cationic polymeric nanoparticles using the O/W cationic nano-emulsions as templates
3) Functionalization of the polymeric nanoparticles
4) *In vitro* studies of functionalized nanoparticles

In order to achieve these objectives, the following *working plan* was established:

- Selection of nano-emulsion components
- Formation of cationic nano-emulsions in Aqueous solution / surfactant(s) / polymer solution systems by low-energy methods and

determination of the extent of nano-emulsion regions in the corresponding systems

- Characterization of nano-emulsion droplet size and surface charge using techniques such as dynamic light scattering (DLS) and electrophoretic mobility, respectively, and assessment of stability by light backscattering
- Formation of nanoparticles from cationic nano-emulsions by the solvent evaporation method
- Characterization of particle size and shape, surface charge and stability assessment of the obtained nanoparticles using transmission electron microscopy (TEM) in addition to the techniques used for nano-emulsion characterization
- Functionalization of nanoparticles with a targeting agent and characterization of the functionalized nanoparticles
- Functionalization of nanoparticles with oligonucleotides as therapeutic agents and characterization of the nanoparticle:oligonucleotide complexes
- *In vitro* studies on nanoparticle dispersions and nanoparticle:oligonucleotide complexes by means of *in vitro* cell viability tests and determination of transfection efficiency

3. MATERIALS AND METHODS

3.1. MATERIALS

3.1.1. SURFACTANTS

Nonionic surfactants

Sorbitan esters

Sorbitan esters are fatty acid esters of sorbitan (generally referred to as Span®) and their ethoxylated derivatives (generally referred to as polysorbates or Tween®). They are widely used in cosmetics, food products and pharmaceutical formulations as emulsifying agents [Tadros, 2005; Rowe, 2009].

Sorbitan monooleate (Span® 80)

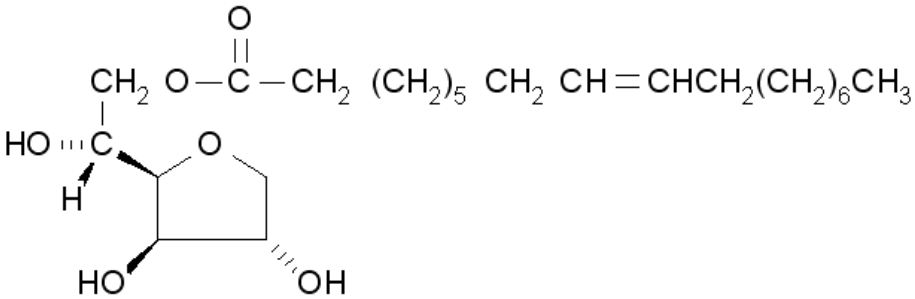

Figure 3.1. Structural formula of Sorbitan monooleate (Span® 80).

Span® 80 (Fluka; $C_{24}H_{44}O_6$) is a yellow viscous liquid at room temperature. Its molecular weight is 428.6 g/mol. Its hydrophilic-lipophilic balance (HLB) number is 4.3. The hydroxyl value is 193 – 215. It is soluble in ethanol, isopropyl alcohol and mineral oil and insoluble in water and propylene glycol [Osol, 1980; Rowe, 2009].

Sorbitan monolaurate (Span® 20)

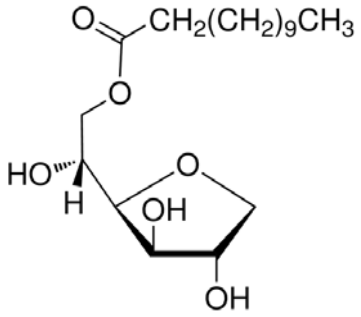

Figure 3.2. Structural formula of Sorbitan monolaurate (Span® 20).

Span® 20 (Fagron; $C_{18}H_{34}O_6$) is a viscous and yellow fluid. Its molecular weight is 346.5 g/mol. Its HLB number is 8.6. The hydroxyl value is 330 – 360. It is soluble in mineral oil, methanol, ethanol and ethylene glycol and insoluble in water and propylene glycol [Osol, 1980; Rowe, 2009].

Polyoxyethylene (4) sorbitan monolaurate (Tween® 21)

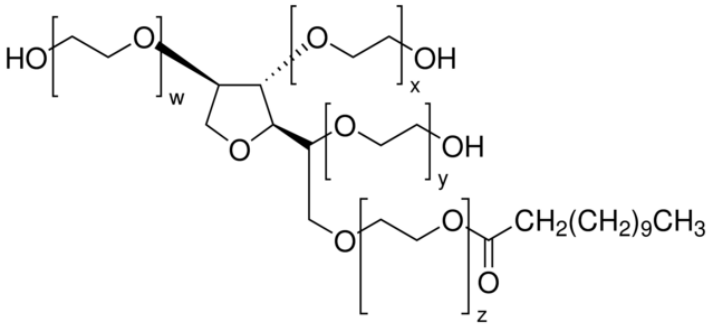

with w + x + y + z = 4

Figure 3.3. Structural formula of Polyoxyethylene (4) sorbitan monolaurate (Tween® 21) with w + x + y + z = 4.

Tween® 21 (Croda; $C_{26}H_{50}O_{10}$), also known as Polysorbate 21, is a yellow liquid at 25°C. This sorbitan ester has a molecular weight of 522.7 g/mol. The HLB number is 13.3. Its hydroxyl value is between 225 and 255. The number of oxyethylene –(CH_2CH_2O)– units in the molecule is four. It is soluble in ethanol, dispersible in water and insoluble in mineral oil and vegetable oil [Rowe, 2009].

Polyoxyethylene alkyl ethers

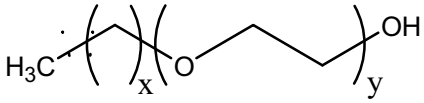

Figure 3.4. General structural formula of a polyoxyethlene alky ether with (x + 1) carbon atoms in the alkyl chain and y ethylene oxide groups.

Polyoxyethylene alkyl ethers are nonionic surfactants produced by the polyethoxylation of fatty alcohols. Products are homologues with different degree of ethoxylation. They are used in pharmaceutical formulations and cosmetics as emulsifiers and stabilizers [Rowe, 2009].

Polyoxyethylene 2 stearyl ether (Brij® 72)

Brij® 72 (Aldrich) is a white waxy solid at 25°C. Its HLB number is 4.9. The hydroxyl value is 150 – 170. The melting point is 43°C. It is insoluble in water, propylene glycol and mineral oil and soluble in ethanol and in nonvolatile, natural, so-called fixed oils [Rowe, 2009].

Polyoxyethylene 2 oleyl ether (Brij® 92v)

Brij® 92v (Fluka) is a liquid with a pale yellow color. Its HLB number is 4.9. The hydroxyl value is 160 – 180. The melting point is 10°C and the boiling point is above 100°C. It is water-insoluble but soluble in ethanol, mineral oils, propylene glycol and in fixed oils [Rowe, 2009].

Polyoxyethylene 10 oleyl ether (Brij® 96v)

Brij® 96v (Fluka) is a white viscous liquid to semi-solid substance at 25°C with a HLB number of 12.4. The hydroxyl value is 80 – 95. The melting point is 16°C and the boiling point is above 100°C. It is soluble in water, propylene glycol, mineral oils and ethanol [Rowe, 2009].

Ethoxylated castor oil surfactants

Polyethoxylated castor oil derivatives are complex mixtures of various hydrophobic and hydrophilic components. They are obtained by reaction of

varying amounts of ethylene oxide with either castor oil or hydrogenated castor oil. Hydrogenated polyethoxylated castor oils have the same chemical structure as castor oils with the difference that the double bond in the fatty chain is saturated [Rowe, 2009].

PEG-7 Hydrogenated Castor Oil (Cremophor® WO7)

Cremophor® WO7 (BASF) is a cloudy, slightly yellow, viscous liquid. Its HLB number is 5 ± 1. Its hydroxyl value is 100 – 130. The manufacturing is made by reaction of hydrogenated castor oil with 7 moles of ethylene oxide. It is insoluble in water and is used as emulsifying agent in pharmaceutical and cosmetic formulations [BASF a].

PEG-35 Castor Oil (Kolliphor® EL, Cremophor® EL)

Kolliphor® EL (BASF), also known as Cremophor® EL, appears as a yellow liquid. The HLB number ranges between 12 and 14. The hydroxyl value is 65 – 78. It is obtained from the reaction between one mole of castor oil and 35 moles of ethylene oxide. It is soluble in water and various organic solvents such as ethanol, toluene, ethyl acetate and chloroform. It is used as emulsifier and solubilizer [BASF b].

Cationic surfactants

Esterquats

Esterquats are quaternary ammonium compounds where the hydrophobic part is linked to the positively charged head group, the ammonium ion, via an ester bond. They can be classified as mono-, di- and triesterquats. Most often, the esterquats are prepared by reaction of a tertiary alkanolamine with fatty acids, followed by reaction with an alkylation agent to the corresponding quarternary. The ester function in the molecule can be hydrolysed which makes this compound biodegradable. Formation of toxic compounds through biodegration is circumvented and the products formed are nontoxic. Esterquats are used in cosmetics and personal care products e.g. as conditioners in hair care or in

sunscreen formulations. They are also used in textile and plastic industries as they possess antistatic properties [Mishra, 2007].

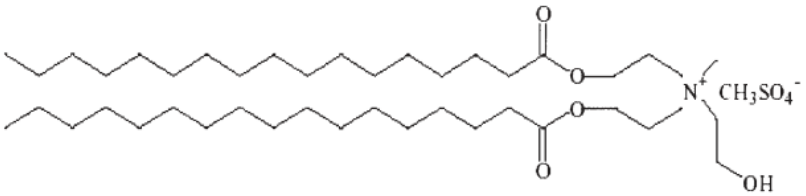

Figure 3.5. General structure of a double chained esterquat.

Dicocoylethyl Hydroxyethylmonium Methosulfate (Dehyquart® L80)

Dehyquart® L80 (Cognis) is a double chain esterquat. It is a yellowish, clear to slightly turbid liquid. It is commercially used in hair aftertreatment agents. It contains propylene glycol. It is soluble in water (20°C). Its LD_{50} oral is above 2000 mg/kg body weight. When combined with emulsifying ingredients, it is suitable for the preparation of hair conditioning creams and emulsions at concentrations of 1.5 – 5%. The pH value at 5% in water at 20°C is between 2.0 and 3.5.

Bis (acyloxyethyl)hydroxyethyl methylammonium Methosulfate (Dehyquart® AU-04)

Dehyquart® AU-04 (Cognis) is a double chain esterquat and at room temperature a yellow liquid. Its LD_{50} oral is above 2000 mg/kg body weight. It is used for the production of transparent softeners. Being an esterquat, it is stated to be highly biodegradable, with a high softening capacity and a good antistatic power. Its pH at 5% in water is 2.5 – 3.5.

Quaternized amido amine

Ricinoleamidopropyltrimonium Methosulfate (Varisoft® RTM 50)

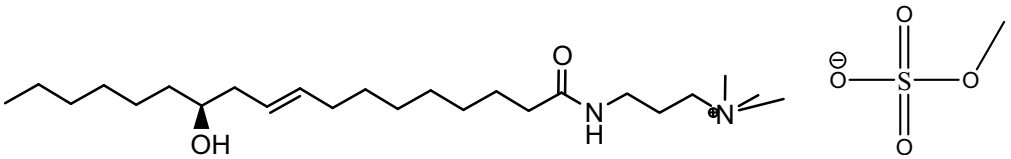

Figure 3.6. Structural formula of Ricinoleamidopropyltrimonium Methosulfale (Varisoft® RTM 50).

Varisoft® RMT 50 (Evonik) is a single chain cationic surfactant. It appears clear yellow with tendency to cloudiness at 20°C. It is fluid at room temperature, contains 60% of water and hypophosphoric acid (catalyst) at a concentration of 0.05%. Its boiling point is about 100°C. It has a density of 1.03 g/cm^3 at 20°C and is easily soluble in water at room temperature. It is used in hair (e.g. conditioning shampoos) and skin treatment (e.g. provides soft skin feeling in skin cleansers).

3.1.2. POLYMERS

Hydrophobically modified cellulose

Ethylcellulose is a semisynthetic cellulose derivative. It consists of a long-chain of beta-anhydroglucose units joined together by acetal linkages. It is characterized by its molecular weight and its degree of substitution with ethyl groups. This polymer is widely used in oral and topical pharmaceutical formulations and also in food applications, e.g. for flavor encapsulation. In general it is considered as nontoxic, nonallergic and nonirritating material [Rowe, 2009].

For this research, two different ethylcellulose types were used showing different molecular weights but the same degree of substitution.

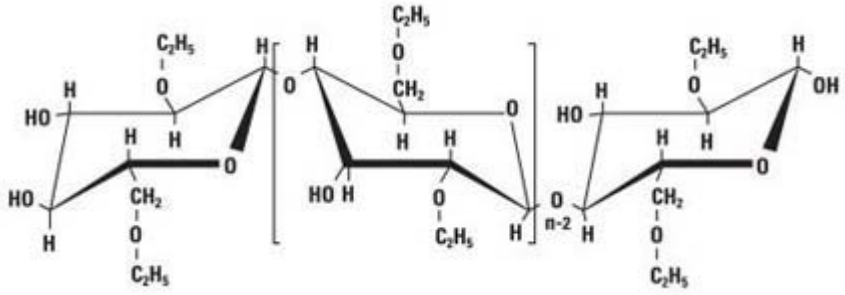

Figure 3.7. Structural formula of Ethylcellulose.

Ethocel Std 4 Premium and Ethocel Std 10 Premium (DOW Chemicals; Colorcon), abbreviated as EC4 and EC10, respectively, are both white and free-flowing powders with the melting point in the range 165 – 173°C and the density 1.15 g/cm^3. They are insoluble in water and freely soluble in organic solvents

like chloroform, ethyl acetate, acetone and ethanol. Relevant properties of both polymers are summarized in Table 3.1 [Rowe, 2009; Dow Cellulosics].

Table 3.1. Properties of EC4 and EC10 [**Rowe, 2009; Dow Cellulosics**].

Property	EC10	EC4
Molecular weight (g/mol)	65000 (1)	~25000 (2)
Viscosity range (cP) (3)	9 – 11	3 – 5.5
Viscosity in ethyl acetate, 99% (cP) (4)	360	not available
Ethoxyl content (%)	48.0 – 49.5	
Solubility in ethyl acetate, 85-88%(5)	2 g ETHOCEL is soluble in 18 mL of solvent	

(1) determined by gel permeation chromatography; (2) estimated value considering the molecular weight; (3) viscosities for a 5% solution measured at 25°C in an Ubbelohde viscometer in a mixture of 80% toluene and 20% ethanol; (4) 15 g polymer in 100 mL solvent at 25°C; (5) Solubility rated on a mixture of 2 g ETHOCEL in 18 mL of solvent.

3.1.3. AQUEOUS COMPONENTS

Water

The water used was “purified water” [Rowe, 2009], obtained by a Millipore Milli-Q lab water system and preserved in tightly sealed containers. Purified water can be used as vehicle and solvent for the manufacture of drug products and pharmaceutical preparation. For parenteral preparations “sterile water for injections” has to be used which was applied for cytotoxicity and transfection studies in this work.

4-(2-Hydroxyethyl)piperazine-1-ethanesulfonic acid (HEPES)

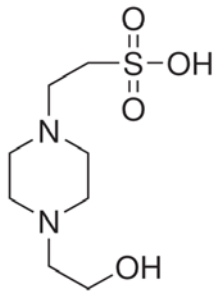

Figure 3.8. Structural formula of 4-(2-Hydroxyethyl)piperazine-1-ethanesulfonic acid (HEPES).

4-(2-Hydroxyethyl)piperazine-1-ethanesulfonic acid (Sigma; $C_8H_{18}N_2O_4S$) abbreviated as HEPES, is a colorless and crystalline solid with a molecular weight of 238.3 g/mol. Its melting point is 234°C. This organic water-soluble molecule has an effective pH buffering range of 6.8 – 8.2 and a pK_a of 7.48 (at 25ºC) [Stoll, 2009]. The measured refractive index (RI) at a concentration of 20 mM was 1.334 and is very similar to pure water (RI 1.333). It was found to be suitable as buffer for biological research [Good, 1966; Ferguson, 1980; Stoll, 2009]. In this work, it was used as a buffer solution with a concentration of 20 mM in water, appropriate for biochemical processes [Stoll, 2009].

D-(+)-Glucose

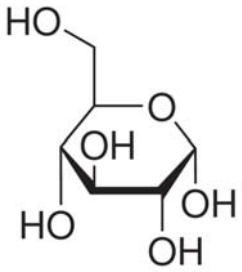

Figure 3.9. Structural formula of D-(+)-Glucose.

D-(+)-glucose (Sigma, $C_6H_{12}O_6$) is a white, crystalline and hygroscopic powder. The molecular weight is 180.2 g/mol. This monosaccharide is soluble in water (1 g dissolves in about 1.1 mL water at 25°C) and has a melting point of 150 – 152°C [Sweetman, 2005]. It was used to adjust the osmolarity of the HEPES buffer solution to applicable conditions for endovenous use. An abbreviation used in literature for the HEPES buffer solution containing glucose is HBG (HEPES-buffered glucose) [Ogris, 2000; Merkel, 2011].

Phosphate buffer solutions

Phosphate buffers are applied in physiological systems. In the present work, buffers based on phosphoric acid salts, dissolved in water, with different compositions have been used in order to adapt nano-emulsions and nanoparticle dispersions to physiological conditions (e.g. pH, isotonicity) of human blood. Phosphate buffered saline (PBS) is nontoxic to cells and is

commonly used in biological research e.g. as a wash buffer for cell cultures [The United States Pharmacopeia, 1985; Aparicio, 2005].

All used components were purchased from Merck. Table 3.2 summarizes relevant data of the buffer components used.

Table 3.2. Formula, molecular weight (MW) and mass concentration of used phosphate buffer components.

Name	Formula	MW (g/mol)	Mass concentration (g/L)		
			PB (0.02 M)	PBS (0.16 M)	PBS (0.33 M)
Sodium dihydrogen phosphate monohydrate	$NaH_2PO_4 \cdot H_2O$	138.0	0.55	0.22	3.45
di-Sodium hydrogen phosphate dihydrate	$Na_2HPO_4 \cdot 2 H_2O$	178.0	2.85	2.98	1.07
Sodium chloride	NaCl	58.4	-	8.00	8.47

3.1.4. ORGANIC SOLVENTS

Ethyl acetate

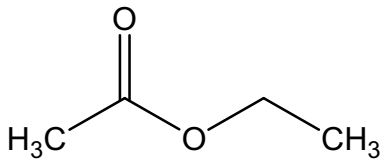

Figure 3.10. Structural formula of ethyl acetate.

Ethyl acetate (Merck; $C_4H_8O_2$) is a clear, colorless, aprotic and volatile liquid with a density of 0.902 g/cm^3. Its molecular weight is 88.1 g/mol. It is flammable and has a boiling point of 77°C. The refractive index is 1.372 [Osol, 1980; Rowe, 2009;]. It is partially soluble in water (solubility at 20 – 25ºC: 8.70 wt%) and, reversely, water is soluble in ethyl acetate at 3.3 wt.% at the same temperature [Sah, 1997]. This liquid is regarded as less toxic and of lower risk to human

health than other organic solvents and accepted in pharmaceuticals. For this reason it can be found among the class 3 solvents of the ICH Guidelines [Pinto Reis, 2006; ICH Guideline, 2011]. It is considered that amounts of up to 50 mg per day (5000 ppm) would be acceptable without justification in pharmaceutical products for human use. In food industry it is used as flavoring agent. The estimated acceptable daily intake was set by the World Health Organization (WHO) at up to 25 mg/kg body weight. Due to its high volatility it has been used in solvent evaporation methods for nanoparticle preparation [Osol, 1980; Rowe, 2009].

3.1.5. BIOMOLECULES

(2S)-2-[(4-{[(2-amino-4-hydroxypteridin-6-yl)methyl]amino}phenyl)formamido]pentanedioic acid) (Folic acid)

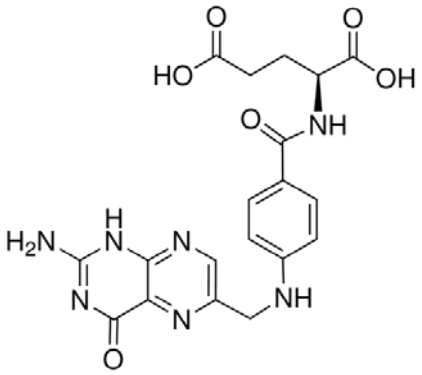

Figure 3.11. Structural formula of (2*S*)-2-[(4-{[(2-amino-4-hydroxypteridin-6-yl)methyl]amino}phenyl)formamido]pentanedioic acid) (folic acid).

Folic acid (Sigma Aldrich, 98%; $C_{19}H_{19}N_7O_6$), also known as folate, folacin, vitamin M, vitamin B_9, pteroylglutamic acid etc., is a crystalline yellow solid with a molecular weight of 441.4 g/mol. Its melting point is about 285°C and is very slightly soluble in water (0.0016 mg/ml at 25ºC) [Maynard, 1996]. It is insoluble in alcohols, acetone, chloroform and ethers and dissolves in dilute acid solutions and in solutions of alkali hydroxides and carbonates [Sweetman, 2005]. Its pk_a values (pK_1=2.38, pK_2=3.38, pK_3=4.83, pK_4=7.85) have been determined with pressure-assisted capillary electrophoresis (PACE) [Szakács, 2006]. Folate, the folic acid salt, cannot be synthesized by the human body. It is found in natural products like e.g. vegetables and wheat. It serves as

coenzymes for various metabolic processes like the carbon transfer reaction in the synthesis of DNA nucleotides and in cell growth and division [Hilgenbrink, 2005]. Among health benefits, reported are the prevention of neural tube defects (NTDs) and occlusive vascular disease (OVD). It has also been described that it influences various disorders like cancer, Alzheimer's disease, Down's syndrome, etc. Deficiency of folate, caused e.g. by malabsorption through coeliac disease or alcohol consumption, will cause anemia and inadequate nucleic acid synthesis which will thus impair cellular division and DNA synthesis [Lucock, 2000]. Folate receptors bind folic acid with a high affinity (dissociation constant K_d ~10^{-10} M) [Pan, 2009]. The presence of the folate receptors on a cell surface is regulated by the cell function. Nearly all cells express folate receptors, however, tumoral cells of e.g. ovary, kidney, breast or lung express a much greater amount of folate receptors (above 500 times more than healthy cells) [Weitman, 1992; Sudimack, 2000; Hilgenbrink, 2005; Dixit, 2006]. Due to these facts, the high affinity of folic acid/folate for folate receptors and the overexpression of these on cancer tissues, there is the opportunity provided to use folic acid/folate as targeting ligand for selective delivery of anticancer agents to tumor cells [Dixit 2006; Pan 2009].

3.1.6. MATERIALS FOR *IN VITRO* ASSAYS

Oligonucleotide

Phosphorothioate oligonucleotide (5'-CGTTTCCTTTGTTCTGGA) was synthesized in an automated DNA synthesizer (Applied Biosystems 3400) by coupling sequentially and growing the oligonucleotide chain in the order required by the sequence of the product. The cycle starts with a detritylation reaction from the dimethoxytrityl (DMT) group with a 2% trichloroacetic acid (TCA) solution. Then, a 0.02–0.2 M solution of nucleoside in acetonitrile is activated by 1*H*-tetrazole. The mixing is usually very quick and occurs in fluid lines of oligonucleotide synthesizers while the components are being delivered to the reactors containing solid support. The activated phosphoramidite in 1.5 – 20-fold excess over the support-bound material is then brought in contact with the starting solid support (first coupling) or a support-bound oligonucleotide

precursor (following couplings). The capping step is performed by treating the solid support-bound material with a mixture of acetic anhydride and 1-methylimidazole since a small percentage of the solid support-bound 5'-OH groups (0.1 to 1%) remains unreacted and needs to be permanently blocked from further chain elongation to prevent the formation of oligonucleotides with an internal base deletion. Finally, the step of oxidation is substituted with a sulfurization step to obtain the resultant oligonucleotide phosphorothioate on solid-support. Upon the completion of the chain assembly, the product is released from the solid phase (with a solution of 32% ammonia at 55ºC, overnight), protecting groups were deprotected, and the solution was collected. The resultant phosphorothioathe oligonucleotide was used in the following steps without further purification [Zhang, 2003].

3.1.7. OTHERS

Oleylamine

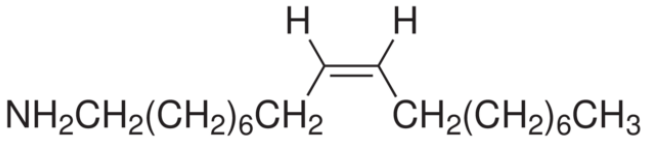

Figure 3.12. Structural formula of oleylamine.

Oleylamine (Fluka; $C_{18}H_{37}N$), abbreviated as OA, is a slightly yellow and clear liquid with a molecular weight of 267.5 g/mol and a density of 0.813 g/mL (25°C). Its melting point is 18 – 26°C and the boiling point 348 – 350°C. It is soluble in polar and nonpolar solvents, but insoluble in water. It has a pK_a value of about 10.7 [Sahraneshin, 2012] and is therefore positively charged at lower pH values. It was added to nano-emulsion systems in order to enhance the cationic properties.

3.2. EQUIPMENTS

3.2.1. PHOTON CORRELATION SPECTROMETER

Dynamic Light Scattering (DLS) is a common technique for measuring size and size distribution of submicron-sized objects dispersed in a liquid. Measurements are based on the Brownian motion of colloidal particles, that is, their irregular motion due to interactions with solvent molecules. When treated with a laser beam at a known scattering angle, the particles scatter the light at different intensities. These fluctuations depend on several parameters like e.g. particle size and shape but also the diffusion coefficient D of the particle given by *Einstein's equation:*

$$D = \frac{k_B T}{f} \qquad \text{[Equation 5]}$$

where k_B is the Boltzmann's constant, T the temperature and f the friction coefficient of the solute.

For spherical particles the equation, known as *Stokes-Einstein equation*, is given as

$$D = \frac{k_B T}{6\ \pi\ \eta\ R_H} \qquad \text{[Equation 6]}$$

where η is the viscosity of the continuous phase and R_H the hydrodynamic radius of the solute. As molecules in solution are usually solvated, the radius calculated is indicative for the apparent size of the hydrated/solvated particle. This explains the term "hydrodynamic radius". Thus, particle sizes by DLS might be larger than those obtained by other techniques like transmission electron microscopy.

A 3D photon correlation spectrometer (PCS) (LS Instruments, Switzerland) was used to determine the particle hydrodynamic radius at an angle of 90º. Multiple scattering is suppressed by using 3D cross-correlation technology. The instrument is equipped with a He–Ne laser (λ = 633 nm). During the measurement, samples were kept at 25ºC in a decaline bath.

A Malvern 4700 instrument (Malvern Instruments, Malvern, UK) equipped with an argon laser (λ = 488 nm) was also used for determining both, particle size and polydispersity index at an angle of 90º. Measurements were carried out at 25°C. The reported polydispersity index is ranging from 0.0 for completely monodisperse samples up to 1.0 for very polydisperse dispersions.

3.2.2. LIGHT BACKSCATTERING (LBS) APPARATUS

Stability of nano-emulsions was assessed by light backscattering measurements at 25ºC with a TurbiscanLab®Expert. This characterization method is based on the analysis of transmittance and photon backscattering. The light source is a pulsed near infrared light emitting diode LED (λ = 880nm). The detector consists of two synchronous optical sensors: the transmission detector and the backscattering detector. While the former receives the light which is transmitted through the sample at 180º, the backscattering sensor detects the light backscattered by the sample at 45º. Both measure along the height of the sample which is placed in a cylindrical borosilicate tube. Information about stability processes in the sample like migration of particles (e.g. sedimentation) and particle size changes (e.g. coalescence) are monitored.

3.2.3. ZETASIZER

The Zetasizer Nano Z from Malvern Instruments Ldt., Malvern, U.K. was used for measuring the surface charge or so called zeta potential. The zeta potential is a physical property which is exhibited by any particle in suspension. It can be considered as an index of magnitude of the electrostatic repulsive interaction between particles. As visualized in **Figure 3.13**, any particle in solution is surrounded by ions. Depending on the net charge of the particle, it will be surrounded by the corresponding counter ions, ions carrying the opposite charge to that of the particle. In **Figure 3.13**, the net charge of the particle is negative which explains why it is surrounded by positively charged ions. There are two layers formed, one layer where the counter ions are strongly bound to the particle, the so-called Stern layer, and another layer, the outer layer, where ions are less firmly attached. Both together are called the electrical double layer.

Within this outer diffuse region, there is a boundary which marks a stable formation of particles with ions. Gravity makes particles move and the ions within this boundary move with them. Ions beyond it do not travel. This boundary is called slipping plane and the potential which exists at this boundary is known as zeta potential.

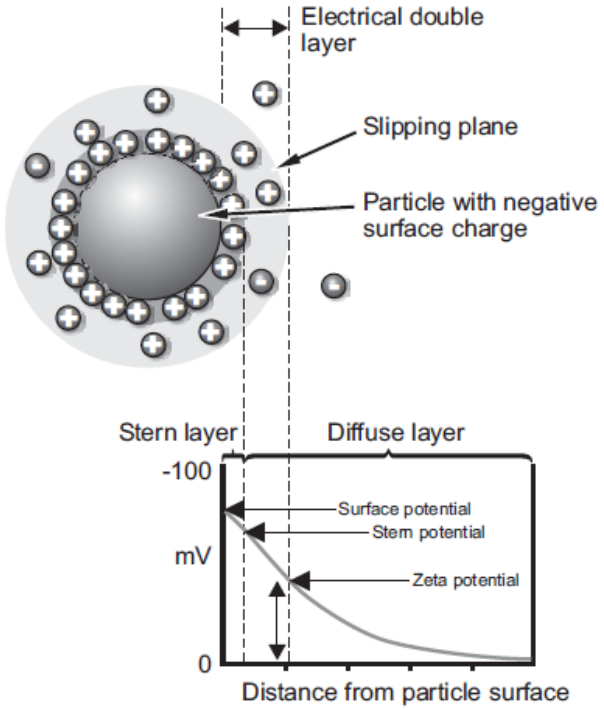

Figure 3.13. Illustration of zeta potential and the electrical double layer which surrounds each particle in suspension.

When an electric field is applied, charged particles suspended in the electrolyte are attracted towards the electrode of opposite charge. Viscous forces acting on the particles tend to oppose this movement. When equilibrium between these two opposing forces is reached, the particles move with constant velocity. The velocity is dependent on the strength of electric field, the dielectric constant of the medium, the viscosity of the medium and the zeta potential. The velocity of a particle in a unit electric field is referred to as its electrophoretic mobility. The zeta potential is related to the electrophoretic mobility by the *Henry equation*

$$\mu = \frac{2\ \varepsilon\ \varepsilon_0\ \zeta\ f(\kappa r)}{3\ \eta} \qquad \text{[Equation 7]}$$

where μ is the electrophoretic mobility, ε the dielectric constant in medium, ε_0 the dielectric constant in vacuum, ζ the zeta potential, η the viscosity and $f(\kappa r)$ the Henry's function.

Electrophoretic determinations of zeta potential are most commonly made in aqueous media and moderate electrolyte concentrations. For particles larger than 200 nm and the aqueous solution containing more than 10^{-3}M of electrolytes, $f(\kappa r)$ has a value of 1.5 and this is referred to as the *Smoluchowski approximation*. For small particles in low dielectric constant media (e.g. non-aqueous media) $f(\kappa r)$ becomes 1.0 and allows an equal calculation which is called the *Hückel approximation*.

Particles with large positive or negative zeta potentials will repel each other. By contrast, if the zeta potential is low, particles will not be prevented to come together and flocculation might occur. Zeta potential values considered to ensure electrostatic stabilization are those more negative than -30mV or more positive than +30mV.

The laser, a He–Ne gas laser (λ = 633 nm), is used to provide a light source to illuminate the particles within the sample. For zeta potential measurements, this light source is split to provide an incident and reference beam. The incident laser beam passes through the center of the sample cell and the scattered light at an angle of about 13° is detected. When an electric field is applied to the cell, any particles moving through the measurement volume will cause the intensity of light detected to fluctuate with the frequency proportional to the particle speed and this information is passed to a digital signal processor and then to a computer. The Zetasizer Nano software produces a frequency spectrum from which the electrophoretic mobility and hence the zeta potential is calculated. The intensity of the detected scattered light must be within a specific range for the detector to successfully measure it. This is achieved using an attenuator which adjusts the intensity of the light reaching the sample and hence the intensity of the scattering. Compensation optics are installed to maintain optimum alignment (**Figure 3.14**).

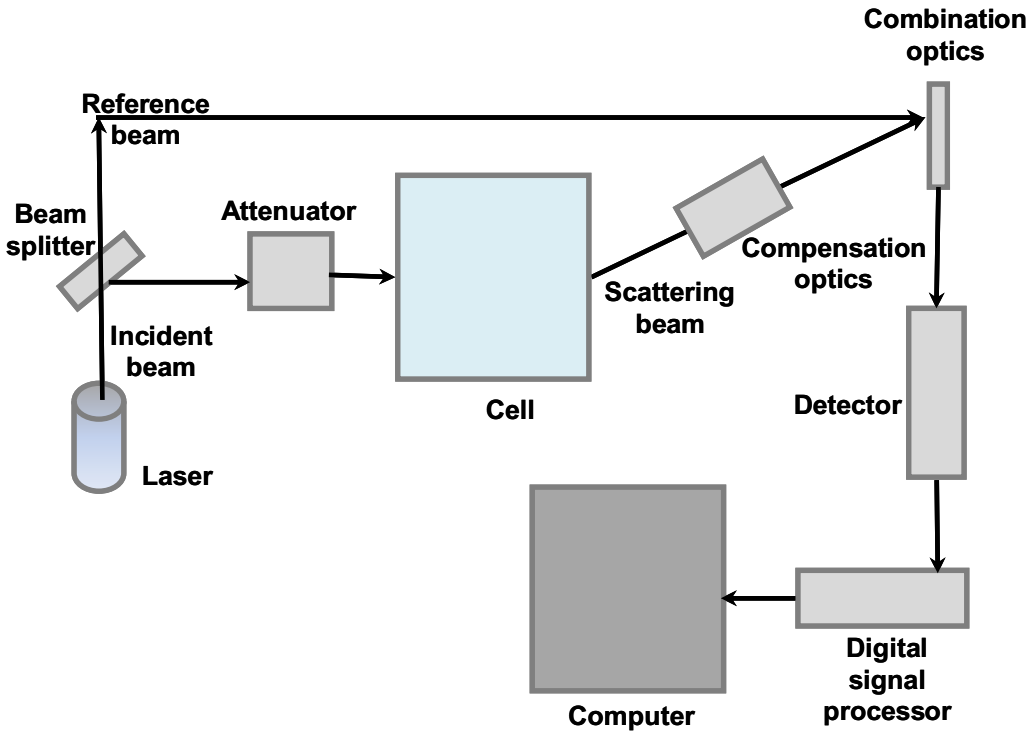

Figure 3.14. Visualization of the functional principle of Zetasizer Nano Z.

3.2.4. TRANSMISSION ELECTRON MICROSCOPE (TEM)

Nanoparticle size was determined by using the transmission electron microscope JEOL 1010 (Jeol Korea Ltd.). This instrument operates with an accelerating voltage of 80kV. Images were captured with the Charge Coupled Device Megaview III (SIS) camera (Munster, Germany). In order to characterize the nanoparticles, negative staining was applied to enhance the electron-density as organic compounds such as polymers do not conduct electrons. The negative staining method consists of adding a heavy metal salt onto a sample that has been deposited on a carbon film. They are used as they will interact with the electron beam. The particles which compose the sample are not stained themselves but they are surrounded by the dense stain layer of the heavy metal solution. An image is formed in negative contrast from the interaction of the electrons transmitted through the specimen. However, electron beams are easily scattered by air molecules. For this reason, the TEM columns must be kept under high vacuum. As a result, the specimen appears in negative contrast [Harris, 1999].

Nano-emulsion droplet size and shape was also determined using the cryogenic transmission electron microscope JEOL JEM 2011, operating at 200kV. The vitrification was done with a CPC Leica. Samples were placed on QUANTIFOIL®R 1.2/1.3 grids.

3.2.5. OSMOMETER

Osmolality is a measurement of the total number of solutes in a liquid solution. For the determination of the osmolality of samples, the Micro-Osmometer Type 15 of the brand Löser Messtechnic was used. This osmometer is a freezing point osmometer, that is, it determines the osmotic strength of a solution by using freezing point depression. The freezing point of a sample is the temperature (at atmospheric pressure) at which the solid and liquid phases co-exist in equilibrium (see **Figure 3.15**). When a solute is dissolved in a solvent (e.g. water), the freezing point of the solution is lowered compared to that of the solvent alone. When more solute is added, the freezing point decreases further. The method makes use of the thermoelectric cooling, the so-called Peltier effect, through which small amounts of liquid can be cooled and frozen. Measurements can be carried out from 0 to 2500 mOsm/kg water with a reproducibility of ±0.5%. Samples of 100 or 50 μL are transferred into eppendorf tubes with an automatic pipette. The measuring time for a sample of 100 μL is about 1.5 min. Values are expressed in milliosmoles of solute (e.g. particles) per kilogram of solvent (mOsm/kg). In this work, the osmolarity of solutions was adjusted to isotonic values (275–300 mOsm/kg) of pig blood in order to study the potential of materials to damage the red blood cells (hemolysis).

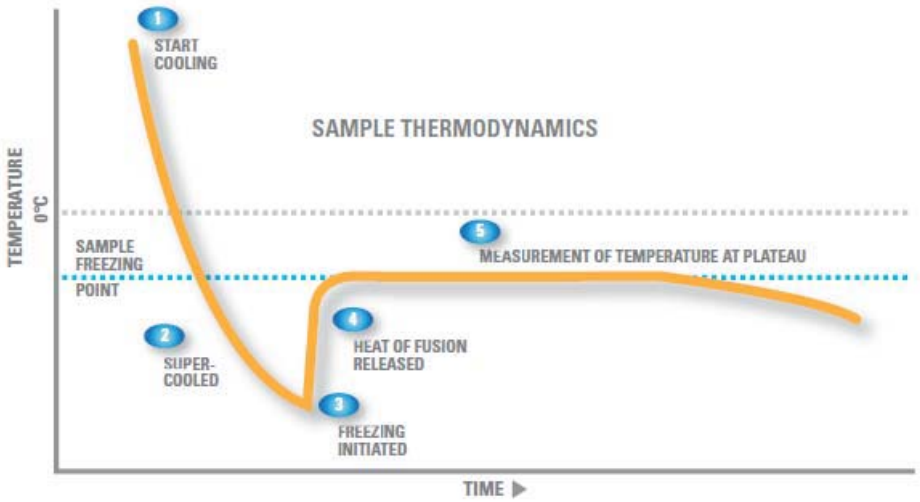

Figure 3.15. Measurement principle of the Micro Osmometer Type 15, Löser Messtechnik [**Advanced Instruments, Inc.**].

3.2.6. CONDUCTIMETER

For measuring the electrical conductivity, the conductimeter model GLP-31 of the trademark Crison was used. This instrument is equipped with a conductivity cell made of a platinum electrode (cell constant = 1 cm^{-1}), model 52-92, and a temperature sensor, model 55-31. For proper measuring, at first, calibration is required. Hence, calibration standards of 1413 μS/cm and 12.88 mS/cm were used.

3.2.7. DIFFERENTIAL REFRACTOMETER

The Abbe Refractometer Type 3T from ATRAGO® was used for refractive index measurements. The refractive index range is 1.3000 ~ 1.7100 with an accuracy of ± 0.0001. Applicable temperatures are from 0 to about 50°C.

3.2.8. OTHERS

Rotary Evaporator

For solvent evaporation, the Rotavapor®R-210/215 from BUCHI Labortechnik AG was used. The rotary evaporator principle is a common method to separate liquids. Solvents can be evaporated in a controlled and safe manner. The operating voltage is 100 – 240V, the frequency is 50/60Hz. The rotation speed

can be varied from 20 to 280 rpm. The heating bath can be adjusted from +20 to +180°C.

Mixer

Vortex-Genie **2** (Scientific Industries, Model-Nr G-560E, Serial Number: 2-126816, 50Hz, Voltage 230/240) with variable speed control allows slow speed shaking action up to high speed vortexing of 2700 rpm. Samples were permanently vortexed during the time needed for nano-emulsion preparation.

Water bath

The thermostat DC10 from Thermo Scientific HAAKE and the cryostat EK20 were used for temperature regulation in a water bath. The working temperature range is from 25 to 100°C with a temperature accuracy of 0.02 and a pump pressure of 300 mbar.

Balance

For determining the weight of chemical materials the Balance AB204S/FACT from Mettler Toledo was used. The balance has a maximum capacity of 220g and is equipped with a fully automatic time- and temperature-controlled internal adjustment (FACT).

3.3. METHODS

3.3.1. PHASE INVERSION DETERMINATION

The phase inversion was determined by conductivity measurements using a Pt/platinised electrode. Samples (4 g) were prepared by addition of water to the oil/surfactant mixtures at intervals of 10 wt% of water up to 90 or 95 wt%. Samples were kept at constant temperature with the help of a thermostat at 25ºC and homogenized during the electrical conductivity measurement by means of magnetic stirring. The water present in the cationic surfactant was considered in the conductivity plots.

3.3.2. NANO-EMULSION PREPARATION BY THE LOW-ENERGY PHASE INVERSION COMPOSITION (PIC) METHOD

About 4 g or 8 g of the nano-emulsions were prepared at a constant temperature of 25°C by adding drop wise the aqueous solution (water or buffer solution) from a syringe to the mixture of oil and surfactant, which was previously homogenized. The addition was performed under permanent vortex stirring at about 2700 rpm.

3.3.3. NANO-EMULSION REGION DETERMINATION

The region of nano-emulsion formation was determined in the Aqueous solution / Mixed surfactants / Oil systems at room temperature. Samples with various O/S ratios and water contents were prepared by drop wise addition of water to previously homogenized mixtures of the surfactants and the oil. Compositions with a transparent or translucent to opaque appearance and a reddish or bluish shine when observed in lamp light were identified as nano-emulsions.

3.3.4. NANOPARTICLE PREPARATION

Nanoparticles were prepared from the nano-emulsions by the solvent evaporation method, schematically represented in Figure 1.5. This method is based on the evaporation of the organic solvent from O/W nano-emulsions in which the oil component consists of a preformed polymer dissolved in ethyl acetate, leading to precipitation of the polymer as nano-sized nanoparticles [Vanderhoff, 1979; Desgouilles, 2003]. In this work, solvent evaporation was carried out during 45 or 60 minutes, depending on the prepared amount of nano-emulsion (4 g and 8 g, respectively) under reduced pressure of 43 mbar and at 25°C. These evaporation conditions ensure a residual solvent content below 5000 ppm [ICH Guideline, 2011] as determined by Head-Space Gas Chromatography [Calderó, submitted]. After evaporation, the evaporated amount was replaced by adding water to the system.

Nanoparticle functionalization with folic acid

4 g of nanoparticle dispersion were prepared with MilliQ® water, HEPES solution (20 mM) or HEPES-buffered glucose (HBG) solution as described above. Folic acid was dissolved in the aqueous solutions. In order to coat the nanoparticles with folic acid, different dilutions of a mother solution of the acid were mixed with the nanoparticles. On that basis, complexes with different nanoparticle:folic acid charge ratios c^+/a^- were generated, whereas c^+ stands for the cationic charge coming from the cationic surfactant CatA and a^- for the anionic charge coming from the anionic group of folic acid. The mixtures were vortexed for a few seconds and after approximately 10 min used for characterization.

Formation of nanoparticle:oligonucleotide complexes

Nanoparticle dispersion was mixed with dried antisense oligonucleotide (ASO) in eppendorf vials at different nanoparticle:antisense oligonucleotide ratios, which are expressed in terms of the ratio between the equivalents of cationic charge (provided by the cationic surfactant) and those of anionic charge (provided by the antisense oligonucleotide). This ratio is often called N/P ratio and is equivalent to the c^+/a^- ratios described above. The mixtures were shortly vortexed (10 seconds) and centrifuged (10 seconds) and then incubated during 40 minutes at 37°C for allowing the complexes to form. Complex formation was confirmed with gel electrophoresis and zeta potential measurements (25°C).

3.3.5. PARTICLE SIZE DETERMINATION BY DLS

Two different equipment were used to determine the particle size, a Photon Correlation Spectrometer (PCS) and a PCS 3D, as described in Section 3.2. Depending on the scattering intensity, samples were diluted 1/100 with water and water saturated with ethyl acetate, respectively, at 25ºC or measured without dilution. The water bath temperature was set to be 25°C and the angle to 90°. Measurements were carried out as triplicates. The determined refractive indexes of water saturated with ethyl acetate and of water were respectively 1.349 and 1.333. When using HEPES solution (20 mM, pH 7.4) as aqueous phase, the refractive index of 1.334 was taken. The polydispersity index was

given by the equipment when working with the conventional PCS. When working with the PCS 3D, polydispersity was calculated by dividing the width output of the instrument by the average hydrodynamic radius.

3.3.6. PARTICLE SIZE DETERMINATION BY TEM

TEM samples were prepared just after solvent evaporation. A drop of the nanoparticle dispersion was placed on a parafilm strip. The carbon coated cupper grid was placed with the carbon coated side on top of the drop for one minute. The grid was then dabbed with filter paper and twice placed onto a water droplet for a short time (about 15-30 seconds). After repetitive dabbing it was placed for one minute onto one drop of the stain solution. A negative stain, a 2 wt% phosphotungstic acid (PTA) or a 2 wt% uranyl acetate water solution, was used. The excess solution was then removed by using filter paper and the grid was air-dried at room temperature. Pictures of the nanoparticles were taken at different magnifications. About 1000 particles were sized manually on the pictures using the program Image J and evaluated with the program Origin which made a histogram of particle size distribution in intervals of 5 nm or 10 nm.

3.3.7. NANO-EMULSION AND NANOPARTICLE DISPERSION STABILITY

Macroscopic observation: Nano-emulsions and nanoparticle dispersions were kept in a glass vial in a thermostated bath at 25°C. They were visually checked as a function of time. Some nano-emulsion instabilities are clearly visible with the naked eye. A layer in the meniscus area indicates creaming whereas when it is on the bottom of the vial, it is called sedimentation.

The creaming and sedimentation rate was calculated form *Stokes 'law* [Equation 2, see Section 1.1.2]. It is assumed that droplet size keeps constant in time and that the system is sufficiently diluted to disregard interactions among droplets. The densities of ethyl acetate and ethylcellulose were taken as 0.902 g/mL and 1.15 g/mL respectively.

Dynamic Light Scattering: Nano-emulsion and nanoparticle dispersion stability was determined by measuring the size as a function of time. Measurements were performed as triplicates at a dispersion angle of 90° and at 25°C. Samples were kept between measurements in a thermostated bath at constant temperature of 25°C.

Light Backscattering: Stability of nano-emulsions was also assessed by light backscattering measurements at 25ºC with Turbiscan®Lab Expert. For this experiment, 15 g of freshly prepared sample was transferred into a glass cell which was tightly stoppered in order to prevent solvent evaporation. Backscattering data of the sample were collected each hour during 24 hours at 25°C. Backscattering intensity was expressed as a function of time.

3.3.8. SURFACE CHARGE DETERMINATION

The zeta potential, which was calculated from the electrophoretic mobility measure by the Zetasizer Nano Z equipment (Smoluchovsky equation, see Section 3.2.3), is a measure of the net surface charge. A standard folded capillary cell was used. About 1 mL of nano-emulsion, nanoparticle dispersion or complex was placed with either a syringe or an automatic pipette into the cell avoiding bubble formation. Three measurements per 20 scans were carried out per sample at room temperature. The refractive index of the continuous phase was taken as that of water (1.33). If necessary, samples were diluted (concentration of 20 mg/g with water and/or PB/PBS) before measuring. For the measurement of nanoparticle:oligonucleotide complexes, 1 mL HEPES buffer (20 mM, pH 7.4) was added to enable measurements.

3.3.9. REMOVAL OF SURFACTANT EXCESS FROM NANOPARTICLE DISPERSIONS

About 4 or 8 g of nanoparticle dispersion were filled in a SpectraPor dialysis bag (MWCO of 12000 – 14000) and immersed in 0.8 or 2 L, respectively, of MilliQ filtered water or phosphate buffered saline (PBS) solution during minimum 3 hours up to 11 days // until a plateau was reached during constant stirring at 25°C. If not stated in the corresponding section, dialysis was carried out without changing the dialysate. Conductivity measurements were carried out either in

the dialysate solution or in the nanoparticle dispersion inside of the flexible tube at intervals of 5 or 60 min. It was monitored by means of a Crison-GLP 31 conductimeter with a Pt/platinised electrode. Conductivity data were automatically collected on a computer. Zeta potential measurements from the nanoparticle dispersion diluted to 20 mg/g with MilliQ® water were carried out using the Zetasizer Nano-z. The sample volume was 1 mL and three measurements per 20 scans were carried out per sample at 25°C.

3.3.10. ELECTROPHORETIC MOBILITY SHIFT ASSAY (EMSA)

In this work, the Electrophoretic Mobility Shift Assay (EMSA), usually used as a technique to characterize protein:DNA/RNA interactions, was used to confirm the complex formation between nanoparticles and oligonucleotide. Several gel shift assays were carried out. A polyacrylamide gel and the antisense oligonucleotide (ASO) phosphorothioate (PS, MW 5712 g/mol) were used. The nanoparticle dispersion was prepared as described in Section 3.3.4 using HEPES solution (20 mM, pH 7.4) as aqueous phase. The concentration of the oligonucleotides was fixed at 5 μg. The dried oligonucleotide was mixed with the nanoparticle dispersion in different ratios, then briefly (~30 seconds) vortexed and centrifuged (~30 seconds). Mixtures were subsequently incubated during 40 minutes at 37°C. As running buffer TBE 1x was used. Shifts were visualized with a Gel Logic 200 imaging system after staining the gel with the fluorescent dye SYBR® Green (TBE 1x 200 mL; 20 μl) for 20 minutes under smooth shaking.

3.3.11. CYTOTOXICITY ASSAY BY MTT

The MTT assay is one of the most common cell proliferation and cytotoxicity assays used in *in vitro* toxicology studies. It is a colorimetric assay developed by Mosmann [Mosmann, 1983] and is mainly attributed to mitochondrial enzymes and electron carriers (i.e. NADH, NADPH or succinate). 3-(4,5-dimethylthiazol-2-yl)-2,5 diphenyl tetrazolium bromide (MTT), a water-soluble yellow dye, is reduced by the dehydrogenase system of active cells to water-insoluble purple formazan crystals through a ring-opening redox reaction. The

assay is not well understood in terms of the enzyme systems that reduce MTT, however, a general principle is illustrated in Figure 3.16 [Slater, 1963; Mosmann, 1983].

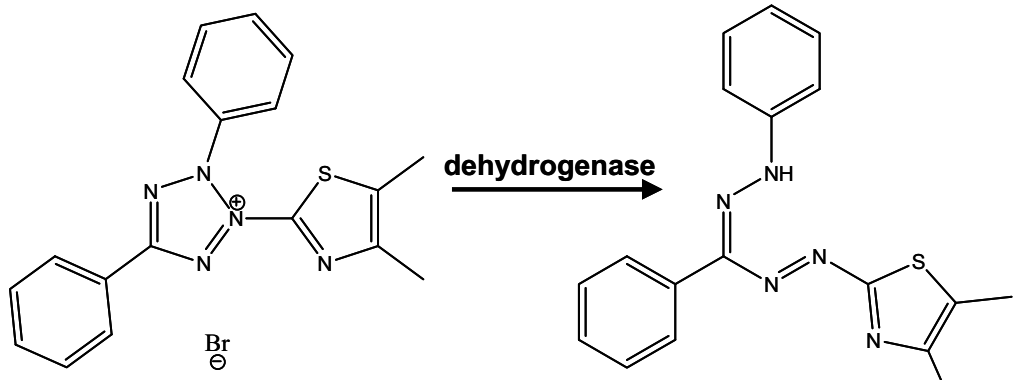

3-(4,5-dimethylthiazol-2-yl)-2,5 diphenyl tetrazolium bromide (MTT, yellow)

Formazan (purple)

Figure 3.16 MTT reduction in live cells by mainly mitochondrial reductase, resulting in the formation of insoluble formazan.

The formazan crystals can be quantified spectrophotometrically by dissolution in an organic solvent. One of the most suitable solvents used for the dissolution of the formazan crystals is dimethyl sulfoxide (DMSO) as it has a high solubilizing efficiency and a low volatility [Twentyman, 1987; Wang, 2010]. For that reason, it was selected for this experiment. The absorbance is measured at a certain wavelength, usually between 500 and 600 nm. The concentration is directly proportional to the number of metabolically active cells in the culture [Hart, 2002; Wang, 2010]. The MTT reduction has been reported to be carried out also by non-mitochondrial enzymes e.g. in the endoplasmic reticulum or in endosome/lysosome membranes [Bernas, 2002; Berridge, 2005; Liu, 2007]. Cell lines used for MTT assays are e.g. HepG2 (human hepatoma cell line), HTC (rat hepatoma cell line), rat lung epithelia cells or HeLa cells (human cervical cancer cell line) [Ishiyama, 1996; Hart, 1999; Fotakis, 2006; Fisichella, 2009] which have found application also in this work. The HeLa cell line is an immortal cell line often used in medical research. It was derived from cervical cancer cells taken from and named after Henrietta Lacks who died from her cancer in 1951.

HeLa viability and proliferation in the presence of nanoparticles at different concentrations was tested using a 3-(4,5- dimethylthiazol-2-yl)-2,5-diphenyltetrazolium bromide (MTT) assay. For each assay, between 5 x 10^3 and 10 x 10^3 cells/cm^2 were seeded on a 96-well plate (Nange Nunc) (100 µL/hole) and cultured for 24 hours. After complete adhesion to the plate, the culture medium was discarded. Nanoparticle dispersion was added at growing concentrations between 1.5 and 8.0 mM. The cells were incubated for 4 hours at 37ºC under 5% CO_2 atmosphere. Then, the nanoparticle dispersion was discarded and DMEM (200 µL) was added. Cells were incubated for 15 hours at 37°C. MTT was added at a final concentration of 0.5 mg/mL per (25 µL) and was incubated for 2 hours at 37°C. The medium was absorbed, DMSO (200 µL) was added to dissolve formazan, a dark blue colored crystal observed in the wells. Absorbance was measured (Spectra Max M5 by Molecular Devices) at λ = 570 nm, 30 min after the addition of DMSO. The cell viability was expressed as a percent ratio of cells treated with nanoparticle dispersion against cells untreated used as control.

3.3.12. RED BLOOD CELL (RBC) HEMOLYSIS

Hemolysis is the destruction of red blood cells (RBC) whereby hemoglobin is released which, *in vivo*, can lead to adverse health effects like anemia, hypertension, jaundice and other adverse health effects [**Rother, 2005; Fitzgerald, 2011**]. Therefore, the hemolytic potential of all intravenously administered pharmaceuticals must be evaluated. In general, the hemolytic test is used as a screening method for the toxicity of surfactants and formulations by estimating the erythrocyte damage that they will induce *in vivo* [**Schreier, 1997**]. Many studies have reported on nanoparticle-induced hemolysis using variations in the protocols which makes their comparison difficult [**Dobrovolskaia, 2008; Fitzgerald, 2011**]. After incubating the nanoparticles with blood and the separation of undamaged cells by centrifugation, the percentage of particle-induced hemolysis is evaluated by spectrophotometric detection of hemoglobin derivatives.

Hemolysis assay was performed using fresh pig blood as previously reported [Chen, 2008; Morral-Ruíz, 2012]. The pig blood was purchased from AbD Serotec (Raleigh, NC, USA). All materials employed in biocompatibility studies, Dulbecco's Modified Eagle Medium (DMEM), Ham's F-12 Nutrient Mix (F-12), fetal bovine serum (FBS), penicillin/streptomycin antibiotic and endothelial cell growth supplement were supplied from Life Technologies Ltd. (Paisley, UK).
The erythrocytes were collected by centrifugation (Heraeus Megafuge 16R centrifuge, Thermo Scientific) at 3000 rpm for 10 minutes and then washed three times with phosphate buffered saline (PBS) at pH 7.4. A stock dispersion was prepared by mixing 3 mL of centrifuged erythrocytes into 11 mL of PBS. Nanoparticles were prepared as described in Section 3.3.4 while the osmolarity of the aqueous phase (HEPES solution) was adjusted to isotonic values (range 275 – 300 mOsm/L) by adding glucose. One hundred microliter of stock erythrocyte dispersion (pig blood) was added to 1 mL of the nanoparticle dispersion. The tubes were then incubated for 10 minutes at 37°C in an Incubator Shaker (80 rpm). After incubations, the tubes were centrifuged at room temperature (15 minutes at 13000 rpm, ICE MicroCL 21R centrifuge, Thermo Scientific) and the percentage of hemolysis was determined by comparing the absorbance (λ = 540 nm) of the supernatant with that of control samples totally hemolyzed with 1 mL distilled water as previously reported [Aparicio, 2005]. The supernatant absorbance of a blood sample not treated with nanoparticles and incubated with 1 mL of PBS was used as negative control to obtain only the percentage particle-induced hemolysis. All experiments were reproduced 3x with each type of formulation and data have been presented as the percentage of the complete hemolysis.

3.3.13. TRANSFECTION EFFICIENCY ASSAY

Transfection is the process of transferring genetic material (DNA, oligonucleotides) into cells. The transfected genetic material may be able to mediate gene silencing. Gene silencing is the interruption or suppression of a gene and can occur during either transcription or translation. This method has been used to study gene functions and also for therapeutical applications like

cancer, autoimmune diseases or viral infections. In this context, the therapeutic use of oligonucleotide like **antisense oligonucleotides**, has gained a lot of attention. Their high specificity, covering a wide range of biomedical applications, allows the inhibition of target proteins that are not easily accessed and modulated by conventional drugs [**Gleave, 2005**].

HeLa cells were cultured at 37ºC, 5% CO_2 in Dulbecco's Modified Eagle's Medium (DMEM; GIBCO) partially supplemented with 10% fetal bovine serum (FBS), 100 μg/mL penicillin and 100 μg/mL streptomycin. Cells were regularly passaged to maintain exponential growth. 24 hours before transfection at 50 – 80% confluency, cells were trypsinized and diluted 1:5 with fresh medium without antibiotics (1-3 x 10^5 cells/mL) and transferred to 24-well plates (500 μL per well). Two luciferase plasmids, *Renilla* luciferase (pRL-TK) and Firefly luciferase (pGL3) from Promega, were used as reporter and as control, respectively. *Renilla* and Firefly luciferase vectors (0.1 μg and 1.0 μg per well, respectively) were transfected into the cells using Lipofectamine 2000. Cells were incubated with the plasmids for 6 hours. Medium was discarded and the cells were washed with PBS. Then, 500 μL of fresh medium without antibiotics were added to each well. The oligonucleotide was prepared at concentrations of 60, 150 and 270 nM. Nanoparticle:antisense oligonucleotide complexes which were incubated previously for 40 minutes at 37°C using HEPES solution (20 mM, pH 7.4) as buffer, were prepared at different concentrations. 100 μL nanoparticle:antisense oligonucleotide complex were added to each well. 24 hours after transfection, cell lysates were prepared and analyzed using the Dual-Luciferase Reporter Assay System. Also for these studies the Gel Logic 200 imaging system was used [**Grijalvo, 2010 and 2012**].

4. RESULTS AND DISCUSSION

4.1. NANO-EMULSIONS: FORMATION AND CHARACTERIZATION

4.1.1. SELECTION OF NANO-EMULSION COMPONENTS AND PRELIMINARY SCREENING OF SYSTEMS FOR NANO-EMULSION FORMATION

The first specific objective of the thesis was the preparation of oil-in-water (O/W) nano-emulsions in Water / Surfactant / Oil systems by low-energy methods for pharmaceutical and cosmetical applications. One of the focal points was to obtain cationic nano-emulsions wherefore positively charged surfactants were incorporated. Another intention was to use these cationic nano-emulsions as templates for the preparation of polymeric nanoparticles. For this reason, a preformed polymer was dissolved in a volatile solvent, constituting the oil phase. The components used and hence nano-emulsions and nanoparticles have to accomplish the requirements for the intended pharmaceutical route of administration and have to be biocompatible and nontoxic or, at least, effective in a nontoxic concentration range. Nano-emulsions were formulated at room temperature. At high temperatures, the volatile solvent would evaporate easily and pharmaceutical components could get degraded.

Selection of nano-emulsion components

Considering the requirements, that is, the presence of a cationic component, a preformed polymer and a volatile solvent and all with low toxicity, the following components were selected for the preparation of the nano-emulsions:

Aqueous components

Water was mainly used as aqueous component. For potential applications of the nanoparticle dispersion for pharmaceutical purposes, several requirements have to be accomplished. Water must be purified by e.g. distillation and should be free from antimicrobial agents or other added substances [The United States Pharmacopeia Twenty-first Revision 1985]. In this work, MilliQ® water was mainly used. For some studies, a certain pH value and isotonicity are important. Therefore, a phosphate buffer or a HEPES solution (Section 3.1.3) was used in order to achieve pH 7.4, the physiological pH of the blood. Other studies require the existence a certain osmolarity. In this work, the osmolarity of the nanoparticle dispersions prepared with HEPES solution was adjusted to that of the blood (275 – 300 mOsm/kg) by adding a glucose solution. When prepared with phosphate buffer, orthophosphoric acid was added in order to achieve isotonicity.

Oil components

The polymeric nanoparticles were aimed to be obtained from nano-emulsions by solvent evaporation. Therefore, a preformed polymer and a volatile solvent should be the main components of the oil phase. Using a preformed polymer for nano-emulsion formation instead of performing polymerization reactions entails several advantages as explained in Section 1.2.2: Purification steps which are needed to remove undesired side products or excess of reactants are avoided. Furthermore biocompatibility of the nano-emulsion system is improved as no reactive substances are used which might increase the toxicity of the system.

Ethyl acetate was selected as organic solvent. This colorless liquid is regarded as a relatively nontoxic (ICH, class 3) and nonirritant material (concentration limit in pharmaceutical products intended for human use is 5000 ppm [ICH Guideline, 2011]. It is used in food as well as in oral and topical pharmaceutical formulations (Section 3.1.4). Since ethyl acetate is a volatile solvent it is suitable for the preparation of nanoparticles by solvent evaporation. In any case, is it required to ensure residue below the limits set by competent authorities

Ethylcellulose was chosen as it is suitable for applications in pharmaceutical formulations [**Rowe, 2006**]. The main part of this work was carried out with EC10 (MW 65000 g/mol). It is widely used in oral and topical formulations. However, EC4 was also used as it might also be suitable for parenteral administration due to its lower molecular weight (MW 25000 g/mol).

Surfactants

The cationic surfactants were chosen among commercially available quaternized biocompatible and biodegradable amphiphiles. **Table 4.1** shows the selected cationic surfactants: Two double chain esterquats and a single chain amide of a quaternized amine derivative.

Table 4.1. Commercial name and purity of selected cationic surfactants.

Cationic surfactant	Commercial name	Purity
Esterquat	Dehyquart® L 80	74 – 79%
	Dehyquart® AU-04	87 – 91%
Amido amine, quaternized	Varisoft® RTM 50	40%

A preliminary screening of *Water / Cationic surfactant / [EC10 in ethyl acetate] systems* was carried out by changing the concentration of polymer in the oil phase from 2 up to 10 wt% in order to assess their suitability for the preparation of nano-emulsions at room temperature. At each polymer concentration, samples with O/S ratios ranging from 10/90 to 90/10 were prepared by addition of water up to a concentration of 90 wt%. Formation of nano-emulsions was assessed visually as explained in **Section 3.3.3**. No nano-emulsions were formed in any of the systems containing *only* cationic surfactant as emulsifier.

In order to achieve nano-emulsion formation in the presence of cationic surfactants, they were mixed with different nonionic amphiphiles of different chemical nature and HLB number.

Ethoxylated as well as nonethoxylated nonionic surfactants belonging to different chemical families were selected. **Table 4.2** summarizes the nonionic surfactants used.

Table 4.2. Commercial name and HLB values of selected nonionic surfactants.

Nonionic surfactants	Commercial name	HLB value
Sorbitan esters	Span® 80	4.3
	Span® 20	8.6
	Tween® 21	13.3
Ethoxylated fatty alcohols	Brij® 72	4.9
	Brij® 92 v	4.9
	Brij® 96 v	12.4
Ethoxylated castor oil surfactants	Cremophor® WO7	5.0
	Cremophor® EL	12.0 - 14.0

Preliminary Screening of Water / Cationic:nonionic surfactant / [EC10 in ethyl acetate] systems for nano-emulsion formation

Dehyquart® AU-04:nonionic surfactant mixtures

The cationic surfactant Dehyquart® AU-04, which belongs to the family of esterquats, was tested with two nonionic surfactants, Span® 80 and Brij® 92 v, in different mixed surfactant ratios and two polymer concentrations (6 and 10 wt% EC10) and with 90 wt% water content. Table 4.3 shows the results for 6 wt% EC10. The nonionic surfactants are differing in their chemical structure but have similar HLB values (see Table 4.2).

Table 4.3. Nano-emulsion (NE) formation in Water / Dehyquart® AU-04 : nonionic surfactant / [6 wt% EC10 in ethyl acetate] systems with a water content of 90 wt%, at 25ºC.

Surfactants			NE formation: Range of O/S ratios
Cationic surfactant	Nonionic surfactant	Cationic : nonionic surfactant ratio	
Dehyquart® AU-04	Span® 80	3:1	10/90 - 30/70
		1:1	none
	Brij® 92 v	3:1	none
		1:1	none

Nano-emulsions could only be obtained from systems containing the sorbitan ester Span® 80 with the cationic:nonionic ratio 3:1 and only at low O/S ratios. With 10 wt% EC10, similar results were obtained: Nano-emulsion formation took only place with the cationic:nonionic surfactant ratio 3:1 while the formation range was even smaller (O/S ratio 10/90 – 20/80). As only few nano-emulsions were obtained and only with high surfactant concentrations, which is not favorable for the intended applications, studies on this system were discontinued.

Dehyquart® L 80:nonionic surfactant mixtures

Table 4.4 shows the tested cationic:nonionic surfactant mixtures. For all systems, the polymer concentrations studied were 6 and 10 wt% EC10 and the water content was 90 wt%. The nonionic surfactants tested belong to different families and show different HLB numbers. All listed systems did not yield any nano-emulsion. For this reason, further studies on systems containing this amphiphile mixture were discontinued.

Table 4.4. Cationic:nonionic surfactant ratios studied in the Water / Dehyquart® L 80 : nonionic surfactant / [EC10 in ethyl acetate] systems.

Cationic surfactant	Nonionic surfactant	Cationic : nonionic surfactant ratio
Dehyquart® L 80	Span® 80	3:1
		1:1
	Tween® 21	1:1
		1:3
		1:4
		1:9
	Brij® 92 v	3:1
		1:1
	Brij® 96 v	1:9

Varisoft® RTM 50:nonionic surfactant mixtures

A cationic surfactant with a different structure from the previous ones, Varisoft® RTM 50, in the following abbreviated as CatA, was mixed with several nonionic surfactants. The results of nano-emulsion formation are shown in **Table 4.5**.

Table 4.5. Nano-emulsion (NE) formation in Water / CatA : nonionic surfactant / [EC10 in ethyl acetate] systems with a water content of 90 wt%, at 25ºC.

Surfactants			NE formation: Range of O/S ratios	
Cationic surfactant	Nonionic surfactant	Cationic : nonionic surfactant ratio	6% EC10 (1)	10% EC10 (1)
Varisoft® RTM 50 (CatA)	Span® 80	3:1	none	none
		1:1	30/70 – 80/20	30/70 - 80/20
		1:3	50/50 - 70/30	50/50 - 70/30
		1:5	none	none
	Span® 20	3:1	20/80 - 30/70, 50/50 - 70/30	60/40 - 80/20
		1:1	10/90 - 30/70	10/90 - 30/70, 70/30
	Brij® 92 v	3:1	none	60/40 - 70/30
		1:1	30/70 - 70/30	30/70 - 40/60, 60/40 - 70/30
	Brij® 72	1:1	none	not studied
	Cremophor® WO7	3:1	60/40 - 70/30	not studied
		1:1	60/40 - 70/30	none
		1:3	60/40 - 70/30	70/30
	Cremophor® EL	1:1	50/50 – 80/20	not studied
		1:3	60/40 - 80/20	70/30 – 80/20

(1) Polymer concentration in the oil component.

Concerning the nonionic surfactants, among the sorbitan esters, Span® 80 was chosen for further studies instead of Span® 20 because nano-emulsions with Span® 80 were less opaque. Furthermore, nano-emulsions with Span® 20

were obtained with slightly lower O/S ratios, which is not suitable for certain applications, as mentioned previously.

Among the ethoxylated fatty alcohols, no nano-emulsions were formed with Brij® 72. Nano-emulsions were obtained with Brij® 92 v in a broad range of O/S ratios but with a very opaque shine. For this reason, further studies on systems with CatA mixed with this type of nonionic surfactants were discontinued.

Although, among the tested ethoxylated castor oil surfactants, nano-emulsions were obtained in a small range of O/S ratios, they showed a transparent or translucent appearance with bluish shine and were for this reason considered for more detailed studies.

Comparing all three types of nonionic surfactants, nano-emulsions were formed in a similar range of O/S ratios in the system containing sorbitan ester (Span) derivatives mixed with CatA and the systems containing mixtures of CatA with ethoxylated fatty alcohol derivatives (Brij). From their visual aspect, systems containing any of the Cremophor derivatives, regardless of their HLB number, were much more transparent, thus indicating smaller droplet sizes than systems formed with a sorbitan ester or an ethoxylated fatty alcohol. The HLB number was not found to play a decisive role in nano-emulsion formation within the same group of nonionic surfactant. Nano-emulsions were obtained with high and low HLB values, e.g. Span® 80 and Span® 20. However, when comparing systems with nonionic surfactants of different types with similar HLB values, a difference is remarkable. While no nano-emulsions were obtained with Brij® 72 (HLB 4.9) and only at low O/S ratios with Brij® 92 v (HLB 4.9), they were formed at higher O/S ratios with Cremophor® WO 7 (HLB 5.0). This might also be related to the role of the surfactant structure.

Regarding the cationic:nonionic surfactant ratios, nano-emulsion formation was mostly favored at the ratio 1:1. Also the ratio 1:3 yielded nano-emulsions in almost all studied systems.

Nano-emulsions were formed with both polymer concentrations, 6 and 10 wt% with slight differences in the range of O/S ratios.

SUMMARY on Selection of nano-emulsion components (4.1.1)

For nano-emulsion formation, the following components have been selected: Apart from water, HEPES solution and phosphate buffers were chosen as *aqueous phase*. The *oil phase* consisted mainly of the polymer ethylcellulose EC10 which was dissolved in ethyl acetate, an organic, volatile solvent, appropriate for nanoparticle preparation by the solvent evaporation method. Minor studies were carried out using a polymer with a lower molecular weight, EC4. As one of the objectives was to obtain nanoparticles with a positive surface charge, it was decided to use a nonionic *surfactant* in combination with a cationic surfactant as no nano-emulsions could be formed by using only the cationic surfactant.

Based on the preliminary screening of Water / cationic:nonionic surfactant / [EC10 in ethyl acetate] systems, the following conclusions were made:

- The quaternized amido amine *Varisoft® RTM 50 (CatA)* yielded nano-emulsions in combination with various nonionic surfactants, unlike the tested esterquats, and was therefore selected for systematic studies.
- Among the nonionic surfactants, it was focused on *Span® 80, Cremophor® WO7 and Cremophor® EL.*
- It was decided to mainly study the cationic:nonionic surfactant ratios of 1:1 and 1:3 with the polymer concentrations of 6 and 10 wt%.

4.1.2. NANO-EMULSIONS IN THE WATER / CATA:SPAN® 80 / POLYMER SOLUTION SYSTEM

Based on the screening performed in the previous section, the system CatA:Span® 80 with the ratio 1:1 and 6 wt% EC10 in ethyl acetate was selected for systematic studies.

Nano-emulsion formation region and Phase Inversion determination

Nano-emulsions were obtained at O/S ratios between 25/75 and 85/15 and water contents above 75 wt%, as shown in **Figure 4.1**. Their visual appearance was opaque. Nano-emulsions were only formed when the surfactant was first mixed with the oil and then the water was added drop wise as described in **Section 3.3.2**.

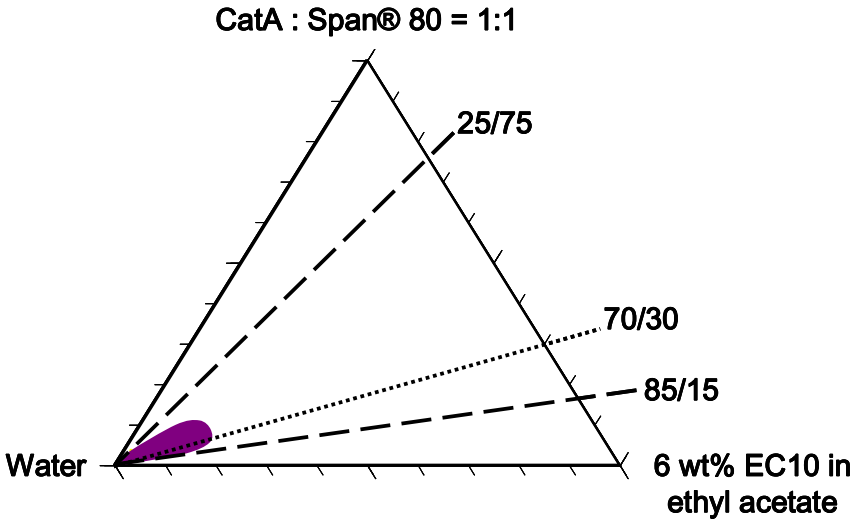

Figure 4.1. Oil-in-water (O/W) nano-emulsion region in the Water / [CatA:Span® 80 = 1:1] / [6 wt% EC10 in ethyl acetate] system at 25ºC. The dotted line for the O/S ratio 70/30 indicates the dilution path which was followed for conductivity measurements.

To assess if the nano-emulsions were formed through a phase inversion mechanism, conductivity measurements were carried out along experimental paths with constant O/S ratio at 25°C, as described in **Section 3.3.1**. **Figure 4.2** shows the conductivity as a function of total water content along the dilution path with O/S ratio 70/30 (dotted line in **Figure 4.1**).

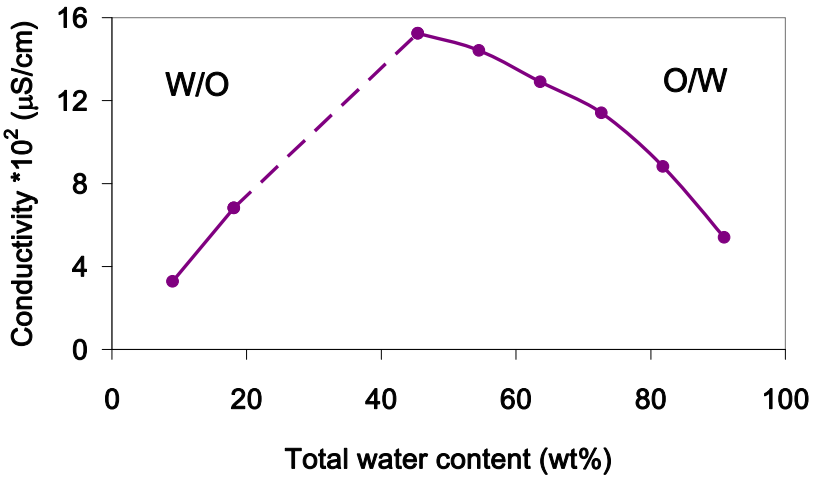

Figure 4.2. Conductivity (*10^2) as a function of total water content in the Water / [CatA:Span® 80 = 1:1] / [6 wt% EC10 in ethyl acetate] system along the dilution path at the O/S ratio 70/30, at 25ºC. The dashed line indicates that the conductivity could not be measured with accuracy. Water-in-oil (W/O) and oil-in water (O/W) regions are indicated.

The amount of water present in the surfactant CatA (40 wt% of active matter) was considered in the total water content in the plot. For this reason the lowest water concentration that could be studied was about 9 wt% of water. At low water contents, conductivity values increase with the increase of water content. Between about 20 and 40 wt% of water, conductivity could not be measured with accuracy due to fast phase separation of the samples. Values reach a maximum at about 45 wt% and then gradually decrease. The increase in conductivity at low water content is indicative of water-in-oil (W/O) structures which experience a transition at higher water concentration. The decrease in conductivity after the conductivity maximum can be attributed to the effect of dilution of the conducting species present in the system [Clausse, 1983; Meziani, 1997]. Therefore, bell-shaped curves as obtained here had previously been described in literature [Clausse, 1983; Meziani, 1997; Calderó, 2011]. It has been assessed that inversion from a W/O to an O/W system takes place when fluctuations in conductivity occurred.

There is a remarkable difference with regard to the conductivity values of nano-emulsions of the present study and those of similar systems formulated only with nonionic surfactants [Calderó, 2011]. While conductivity in these systems was close to zero at water contents of 0 – 20 wt% and reached a maximum of

about 320 μS/cm at 42 wt%, conductivity values in the present system are quite high due to the presence of the cationic surfactant.

Nano-emulsion characterization

Nano-emulsions with O/S ratios of 50/50, 60/40 and 70/30 and a water content of 90 wt% were selected for further studies. **Table 4.6** summarizes droplet sizes and polydispersity indices obtained by DLS at 25ºC. The pH values of the chosen nano-emulsions are also indicated. The nano-emulsions show droplet sizes up to approximately 300 nm and polydispersity indices below 0.15 at room temperature.

Table 4.6. pH values of as-prepared nano-emulsions and droplet diameters and polydispersity indices (PI) of nano-emulsions of the Water / [CatA:Span® 80 = 1:1] / [6 wt% EC10 in ethyl acetate] system with 90 wt% of water content as obtained with DLS upon dilution 1/100 with water saturated with ethyl acetate, at 25ºC.

O/S ratio	pH	Droplet size	
		Diameter (nm)	PI
50/50	5.1	297.6	0.12
60/40	5.2	305.1	0.15
70/30	5.5	261.7	0.11

Although there is not a clear tendency in the droplet size as a function of the O/S ratio, the smallest droplet size is achieved at the highest O/S ratio, that is 70/30, which may be attributed to solvent diffusion.

The surface charge of the nano-emulsions was determined by zeta potential measurements. To allow suitable measurements, the nano-emulsions were diluted. As dilution has an influence on the zeta potential values, the effect of the degree of dilution and the nature of the diluting medium were determined. Two different dilution media were studied, water and a phosphate buffer solution (PB, 0.02 M) with a pH similar to that of the blood (7.4). The results are shown in **Figure 4.3**. When diluting in water, zeta potential increased with increasing nano-emulsion concentration from slightly negative values (about -1 mV) until a plateau was nearly reached in the positive range (about +54 mV). Zeta potential values measured with PB as diluting media showed a similar tendency, starting with negative values at low concentration and raising to

higher positive values with increasing concentration. However, values in water (pH = 5.6) are generally about 20 mV higher than in PB (pH = 7.4) in the studied dilution range. The reason may be that in the buffer solution the phosphate anionic species may shield the cationic charges provided by the surfactant CatA, thus producing a decrease of the zeta potential values.

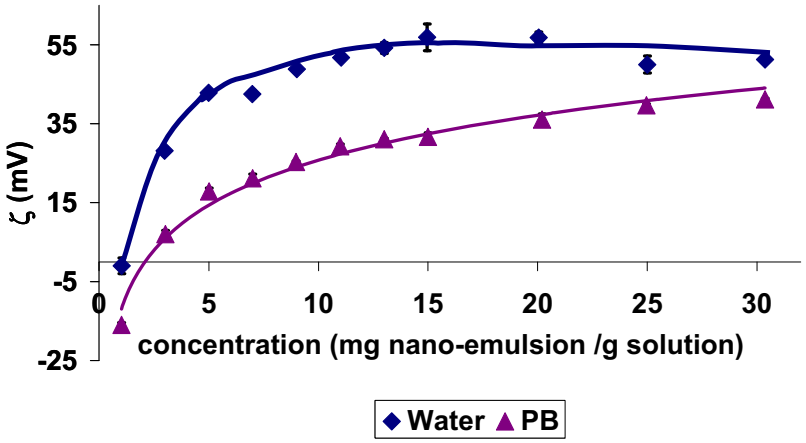

Figure 4.3. Zeta potential (ζ) values of nano-emulsions of the Water / [CatA:Span® 80 = 1:1] / [6 wt% EC10 in ethyl acetate] system as a function of the concentration of nano-emulsion in the diluting medium (water (pH = 5.6) or PB (pH=7.4)), at 25°C. The nano-emulsion composition was: O/S ratio 60/40 and 90 wt% water. The symbols are the experimental data and the lines a guide to the eye.

Based on these results and for comprehensive studies, further measurements were performed by diluting to a concentration of 20 mg/g, which is within (water as diluting medium) or close (PB as diluting medium) to the plateau range. **Figure 4.4** shows the zeta potential as a function of the O/S ratio of the nano-emulsions, using the two mentioned diluting media. As previously observed, one main factor influencing the zeta potential seems to be the diluting medium: The presence of anionic shielding species, as noted before, strongly decreases the zeta potential also with varying the O/S ratio. While in water the zeta potential is around 60 mV, in PB this value drops down to about the half. It is also observed that, as expected, zeta potential decreases slightly at increasing O/S ratio, due to the decrease in CatA content. Values are summarized in **Table 4.7**.

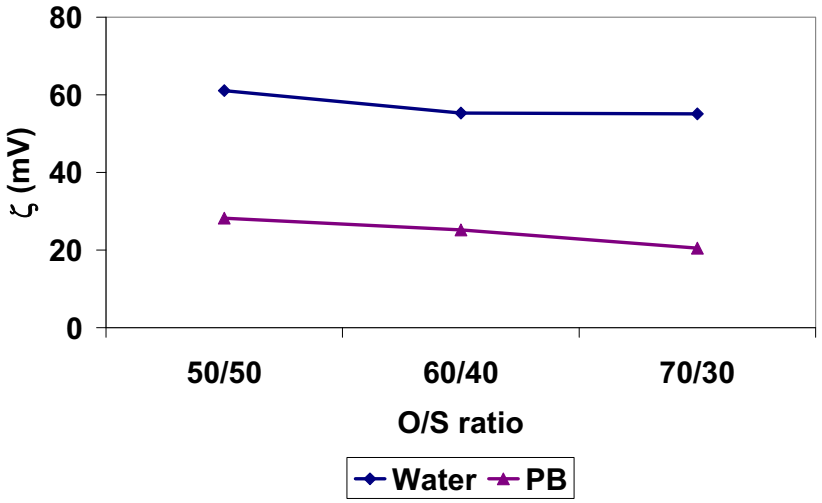

Figure 4.4. Zeta potential (ζ) values of nano-emulsions of the Water / [CatA:Span® 80 = 1:1] / [6 wt% EC10 in ethyl acetate] system as a function of the O/S ratio, at 25°C. The nano-emulsions, initially with 90 wt% water, were diluted to a concentration of 20 mg/g either in water or PB.

Table 4.7. Electrophoretic mobility (μ) and zeta potential (ζ) values of nano-emulsions of the Water / [CatA:Span® 80 = 1:1] / [6 wt% EC10 in ethyl acetate] system, initially with 90 wt% water, in water (pH 5.6) and PB (pH 7.4) as diluting media, at a concentration of 20 mg/g.

O/S ratio	Water		PB	
	μ (μmcm/Vs)	ζ (mV)	μ (μmcm/Vs)	ζ (mV)
50/50	4.8	61.1	2.3	28.2
60/40	4.3	55.3	2.0	25.2
70/30	4.3	55.1	1.6	20.5

Comparing the values obtained in this system with those reported for cationic nano-emulsions of other systems, they are of the same order of magnitude. E.g. Ott *et al*. reported positively charged nano-emulsions by incorporation of the cationic component 1,2-dioleoyl-3-tri-methylammonium-propane lipid (DOTAP) in the formulation. While the nano-emulsion without the cationic component showed negative zeta potential (about -39 mV, dilution in deionized water), the nano-emulsion containing DOTAP showed positive zeta potential (about +54 mV, dilution in deionized water) [Ott, 2002].

Due to high zeta potential values of the nano-emulsions obtained in this study, a good stability was expected as a result of electrostatic repulsion among droplets.

However, the visual stability assessment of the samples stored at room temperature revealed that seven hours after nano-emulsion preparation, a layer in the upper part of the sample was observed, indicating creaming. For a closer analysis, tests by light backscattering were undertaken. The results are shown in **Figure 4.5**. The backscattering intensity (expressed in percentage compared to internal standards) is plotted as a function of sample height (horizontal axis) at different times. The grey shaded regions in the graphics indicate the bottom and meniscus of the sample in the glass cell. At the bottom of the cell, a slight increase in backscattering is observed which is due to multiple light diffractions of the glass cell. No physical meaning is assigned to this phenomenon. Backscattering intensity did not change throughout the complete sample height during 24 hours indicating that clarification of the continuous phase, caused by a decrease in droplet size or in quantity of dispersed droplets, does not occur. However, at the meniscus, a peak appeared after 5 (O/S ratio 60/40) and 3 hours (O/S ratio 70/30) which is an indication of creaming. It should be noted that the peak is sharper at higher O/S ratio.

(a) O/S ratio 60/40

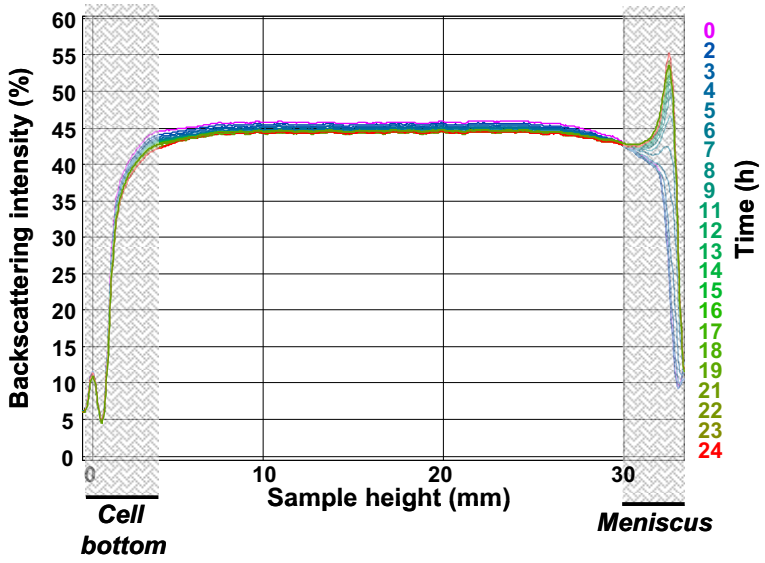

(b) O/S ratio 70/30

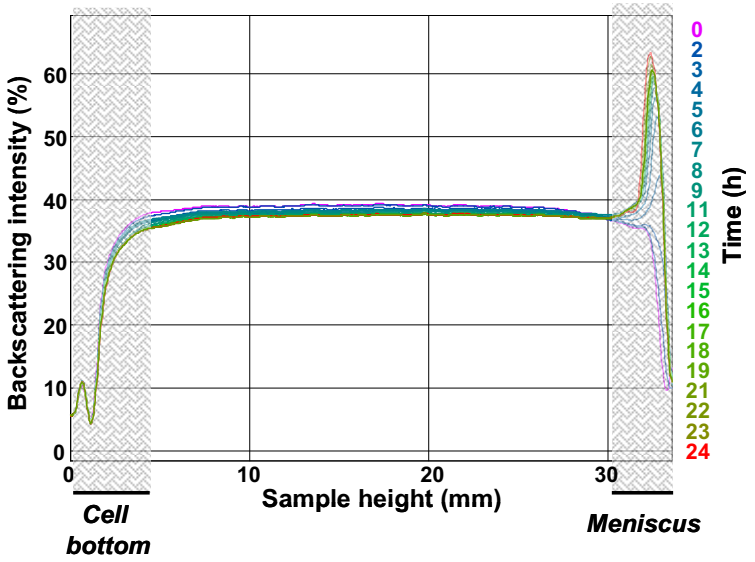

Figure 4.5. Backscattering data during 24 hours of nano-emulsions of the Water / [CatA:Span® 80 = 1:1] / [6 wt% EC10 in ethyl acetate] system with 90 wt% water and O/S ratio of a) 60/40 and b) 70/30, at 25ºC. Grey shaded regions indicate the bottom and meniscus of the sample in the glass cell.

Table 4.8 summarizes the stability assessment performed by visual observation and light backscattering at 25°C, and calculated from Stokes' law (Section 1.1.2 using values obtained by DLS). According to the rate of creaming, the observed layer is supposed to appear faster with O/S ratio 60/40 than with 50/50 or 70/30 which could not be confirmed by light backscattering or visual evaluation. This discrepancy can be attributed to the lack of accuracy in the droplet size volumes due to polydispersity and solvent evaporation.

Table 4.8. Stability assessment of the three selected O/S ratios of nano-emulsions of the Water / [CatA:Span® 80 = 1:1] / [6 wt% EC10 in ethyl acetate] system by visual observation and light backscattering at 25ºC, and calculated from Stokes' law.

O/S ratio	Visual assessment (h)	Backscattering – appearance of a peak in meniscus (h)	Theoretical creaming rate (nm/s)
50/50	≤ 7	-	4
60/40	≤ 7	5	5
70/30	≤ 7	3	3

It was tested if the nano-emulsions with the O/S ratios 50/50, 60/40 and 70/30 could be formed also with PBS (0.16 M) or HEPES buffer (20 mM, pH 7.4). No

nano-emulsions were formed with the phosphate buffer, however, with HEPES solution, nano-emulsion could successfully be obtained.

It was furthermore studied if nano-emulsions could be obtained using EC4, a polymer with a lower molecular weight, at a concentration of 6 wt%. As continuous phases MilliQ® water, HEPES solution (20 mM, pH 7.4) and phosphate buffer (0.16 M) were chosen. Nano-emulsions could be formed with MilliQ® water and HEPES buffer solution, however, with PBS (0.16 M), no nano-emulsions were obtained.

Effect of oleylamine

In order to enhance the cationic properties of the system, oleylamine (OA) was incorporated in the selected nano-emulsions. This fatty amine has a pK_a of about 10.7 [Sahraneshin, 2012] and is therefore positively charged at lower pH values (e.g. the physiological pH of the blood, 7.4). Oleylamine was mixed with the oil component in an ratio [ethylcellulose in ethyl acetate]:oleylamine of 3:1. Droplet size and polydispersity indices (PI) of the nano-emulsions prepared with this component are summarized in Table 4.9.

Table 4.9. pH values, droplet diameters and polydispersity indices (PI) of nano-emulsions of the Water / [CatA:Span® 80 = 1:1] / [6 wt% EC10 in ethyl acetate and oleylamine] system with 90 wt% water. Droplet size values were obtained by DLS upon dilution 1/100 with water saturated with ethyl acetate, at 25ºC.

O/S ratio	pH	droplet size	
		diameter (nm)	PI
50/50	8.6	250.7	0.14
60/40	9.2	238.9	0.10
70/30	9.3	230.8	0.13

In the presence of oleylamine, the pH values of the nano-emulsions increase up to around 9 while the pH values of the system without OA were slightly acidic (see Table 4.6). It was found that in both cases, the pH value increases slightly with the O/S ratio, which is consistent with the higher amount of oleylamine when the O/S ratio increases. The nano-emulsion droplet sizes, as characterized by DLS (Section 3.3.5), were around 240 nm with polydispersitiy

indices similar to those of the system without OA. A decrease of droplet sizes with the increase of O/S ratio is noted which may be explained due to the presence of fatty amine, placing itself at the interfacial film and acting as a cosurfactant, as this molecule consists of a polar head group and a hydrocarbon chain and may therefore display amphiphilic properties. It is noteworthy that also in the presence of the fatty amine, the smallest droplet sizes were achieved at the highest O/S ratio (70/30) which is attributed to solvent diffusion.

Based on the previous zeta potential measurements, the dilution used was 20 mg nano-emulsion / g water or PB. **Figure 4.6** shows the trend of surface charge with increasing amount of oil component with incorporated fatty amine, compared to the values of the system without this component. The values in water were significantly higher than those obtained when diluted with PB which can be explained by the shielding effect of the anions present in the buffer. Furthermore, in all diluted systems containing OA, the values are higher than without this component. This can be explained by the fact that these nano-emulsions contain more cationic charge caused by the presence of the OA which carries a positive charge at the studied pH values. However, while a slight decrease in zeta potential with increasing oil content can be observed with the systems without OA in both diluting solvents, the surface charge of nano-emulsions with OA keeps almost constant (**Figure 4.6**, **Table 4.10**).

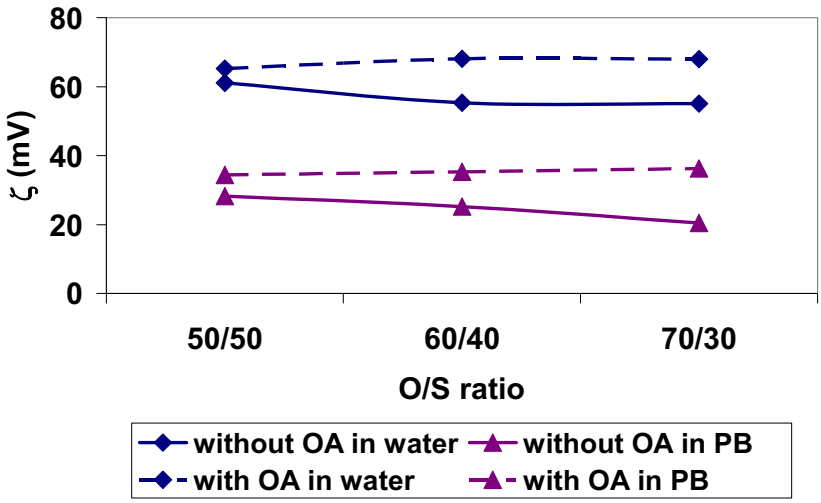

Figure 4.6. Zeta potential (ζ) values of nano-emulsions of the Water / [CatA:Span® 80 = 1:1] / [6 wt% EC10 in ethyl acetate (and oleylamine)] system as a function of the O/S ratio. The nano-emulsions, initially with 90 wt% water, were diluted to a concentration of 20 mg/g, either in water or PB.

Table 4.10. Electrophoretic mobility (μ) and zeta potential (ζ) values of nano-emulsions of the Water / [CatA:Span® 80 = 1:1] / [6 wt% EC10 in ethyl acetate and oleylamine] system in water (pH 5.6) and PB (pH 7.4) as diluting media, at a concentration of 20 mg/g, at 25°C.

O/S ratio	Water		PB	
	μ (μmcm/Vs)	ζ (mV)	μ (μmcm/Vs)	ζ (mV)
50/50	5.1	65.1	2.7	34.8
60/40	5.3	67.9	2.8	35.8
70/30	5.4	68.0	2.8	36.3

In spite of the high zeta potential values, a creaming layer was observed only few hours (< 7) after sample preparation. **Figure 4.7** shows the stability assessed by light backscattering. The backscattering intensity increase at the meniscus of the samples is significantly reduced as compared to the nano-emulsions in the absence of OA which is in good agreement with the lower creaming rate predicted by Stokes' law (**Tables 4.8 and 4.11**). However, a striking decrease in the backscattering intensity is observed along the sample height.

(a) O/S ratio 50/50

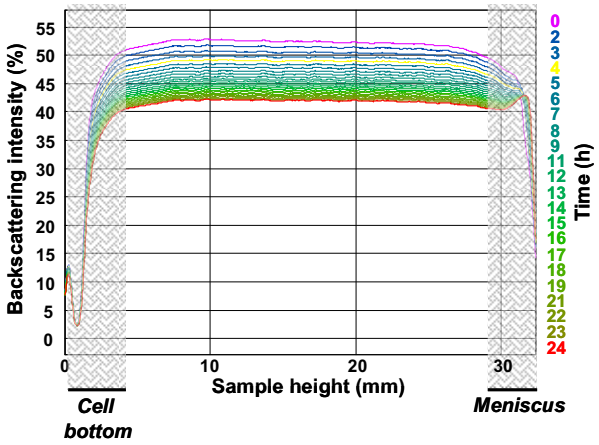

(b) O/S ratio 60/40

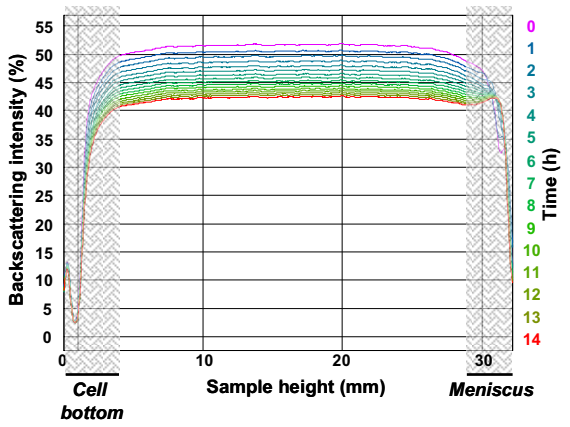

(c) O/S ratio 70/30

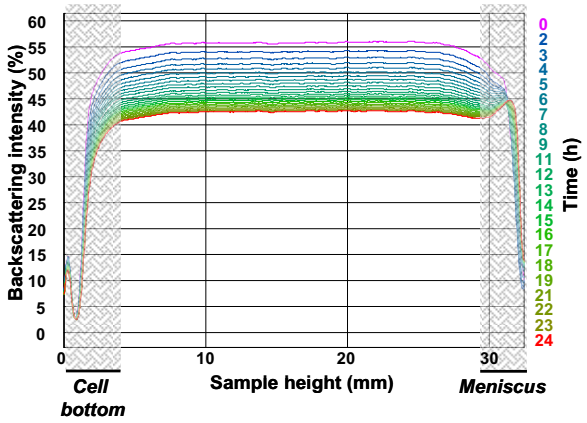

Figure 4.7. Backscattering data of nano-emulsions of the Water / [CatA:Span® 80 = 1:1] / [6 wt% EC10 in ethyl acetate with oleylamine] system with 90 wt% water and O/S ratio of a) 50/50 during 24 hours b) 60/40 during 14 hours and c) 70/30 during 24 hours, at 25ºC.

This phenomenon has been related to a clarification of the continuous phase, which can be caused either by a decrease in the size or in the number of the dispersed droplets. On the one hand, a decrease in size can be caused by the diffusion of the partially water-soluble ethyl acetate from the dispersed droplets to the aqueous continuous phase. On the other hand, a decrease of the number of dispersed entities can occur as a consequence of coalescence, flocculation or Ostwald ripening. Since nano-emulsions showed high surface charge values, flocculation and coalescence of the droplets should not be favorable here. Ostwald ripening however, which implies a growth of the larger droplets at an expense of the smallest ones is prone to happen in polydisperse nano-emulsion systems and would lead to a reduction of the number of drops. The clarification observed and identified as Ostwald ripening, which started right in the first hour after sample preparation, can be regarded as consistent with the visual

observation of samples where creaming was observed within 7 hours after sample preparation.

For a better illustration of the significant change in backscattering intensity throughout the sample height of nano-emulsions, a middle part (10 – 20 mm sample height) of the nano-emulsions with O/S ratio 70/30 and 90 wt% water with and without OA is plotted in **Figure 4.8**. The decrease in backscattering intensity, which was attributed to clarification due to Ostwald Ripening, is about 13% while in the sample without the fatty amine backscattering intensity keeps constant.

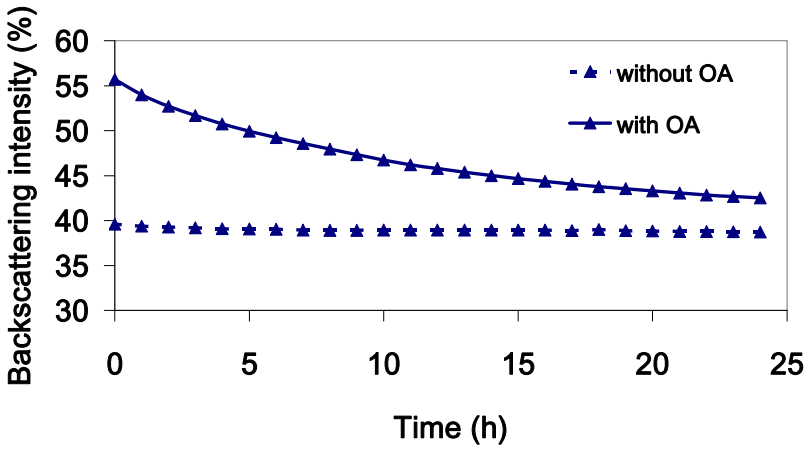

Figure 4.8. Backscattering intensity at a sample height between 10 and 20 mm (total sample height: about 32 mm) as a function of time of nano-emulsions with O/S ratio 70/30 and 90 wt% water of the Water / [CatA:Span® 80 = 1:1] / [6 wt% EC10 in ethyl acetate] system at 25°C.

Table 4.11 summarizes the stability assessment performed by visual observation and light backscattering at 25°C as well as calculated from Stokes' law.

Table 4.11. Stability assessment of the three selected O/S ratios of nano-emulsions of the Water / [CatA Span® 80 = 1:1] / [6 wt% EC10 in ethyl acetate and oleylamine] system by visual observation and light backscattering at 25ºC, and calculated from Stokes' law.

O/S ratio	Visual assessment (h)	Backscattering – appearance of a peak in meniscus (h)	Theoretical creaming rate (nm/s)
50/50	< 7	1	3
60/40	< 7	1	3
70/30	< 7	1	3

The rate of creaming indicates that no difference in stability is found in nano-emulsions with all three O/S ratios. Comparing samples with and without oleylamine it can be noticed that in both systems, the visual assessment is consistent with data obtained by light backscattering measurements but less consistent with calculations of the creaming rate.

As pH values of nano-emulsions formed with water were slightly basic (**Table 4.9**), it was studied if the pH could be adjusted to the physiological pH of the blood, pH 7.4, by using HEPES solution and hydrochloric acid (HCl, 0.1 M and 0.01 M) solutions as aqueous phases. Values are summarized in **Table 4.12**.

Table 4.12. pH values obtained with HEPES solution (20 mM, pH 7.4), HCl (0.1 M, pH 1.2) and HCl (0.01 M, pH 2.1) for nano-emulsions of the Water / [CatA:Span® 80 = 1:1] / [6 wt% EC10 in ethyl acetate and oleylamine] system.

O/S ratio	Aqueous phases with pH values		
	HEPES (20 mM, pH 7.4)	HCl (0.1 M, pH 1.2)	HCl (0.01 M, pH 2.1)
50/50	8.5	1.6	8.4
60/40	8.6	1.7	8.5
70/30	8.7	1.8	8.6

It can be noted that with HEPES solution (20 mM, pH 7.4) and HCl (0.01 M, pH 1.2) , pH values were in about the same range as in the formulations with water. However, when using HCL (0.1 M), pH values strongly decreased to the very acid range.

Summary

Nano-emulsions have been obtained in the Water / [CatA:Span® 80 = 1:1] / [6 wt% EC10 in ethyl acetate] system between O/S ratios 25/75 and 85/15. Phase Inversion from a W/O to an O/W system was confirmed by conductivity measurements and takes place between 20 and 45 wt% of water content. Nano-emulsions showed droplet sizes of about 300 nm and a polydispersity values below 0.15. Zeta potential values in diluted systems (fixed concentration of 20 mg/g in water and PB) were about +60 mV (in water) and +30 mV (in PB). The incorporation of oleylamine increases the zeta potential of nano-emulsions (+67 mV in water and +35 mV in PB) due to the extra positive charge coming

from the fatty amine and it is the higher, the higher the oil content in the nano-emulsion is. Nano-emulsion droplet size with oleylamine was slightly smaller (250 nm) than in nano-emulsions without the fatty amine. However, nano-emulsions were less stable than with OA as creaming appears faster.

The following conclusions can be made:

- Nano-emulsion formation using Span® 80 as nonionic surfactant yielded droplet sizes larger than 250 nm with high zeta potential values (about 60 mV in water) with little stability visually assessed.
- The use of oleylamine did not improve the system properties and therefore this strategy was discontinued.

4.1.3. NANO-EMULSIONS IN THE WATER / CATA : CREMOPHOR® WO7 / POLYMER SOLUTION SYSTEM

Nano-emulsions of the system containing the surfactant mixture CatA:Span® 80, described in the previous chapter, showed relative large droplet sizes (above 200 nm) and low stability. The preliminary studies, described in Section 4.1.1, showed that nano-emulsions with mixtures of CatA and Cremophor® WO7 were less opaque than those obtained with CatA and Span® 80. It should be noted that apart from a different chemical structure, Cremophor® WO7 has a slightly higher HLB number (HLB 5.0) than Span® 80 (HLB 4.3). In order to find out if using a surfactant with a different chemical structure and a slightly higher HLB number would improve the formation of kinetically stable nano-emulsions with lower droplet sizes, studies were carried out with the surfactant mixture CatA:Cremophor® WO7. In the following, Cremophor® WO7 is abbreviated as CWO7.

Effect of cationic:nonionic surfactant ratio

Nano-emulsion formation region and Phase Inversion determination

Based on the results of the preliminary screening, CatA:CWO7 ratios of 1:3 and 1:1 were studied. As mentioned above, the visual appearance of nano-emulsions with 90 wt% water, obtained with both cationic:nonionic surfactant ratios, was more transparent than that of those with the mixed CatA:Span® 80 surfactant system, which was interpreted as a sign of smaller droplet size. Transparency of nano-emulsions also increased with increasing water content. For this reason, nano-emulsions with higher water content, 95 wt%, were also studied.

The region of nano-emulsion formation was identical for both cationic:nonionic surfactant ratios (**Figure 4.9**). Nano-emulsions were formed between O/S ratios of 55/45 and 75/25 and above 88 wt% water. Nano-emulsions of the CatA:CWO7 1:3 ratio appeared more transparent than those with 1:1 ratio. Compared to the nano-emulsion region obtained in the CatA:Span® 80 system, nano-emulsions are formed in a narrower range of O/S ratios and at higher water content.

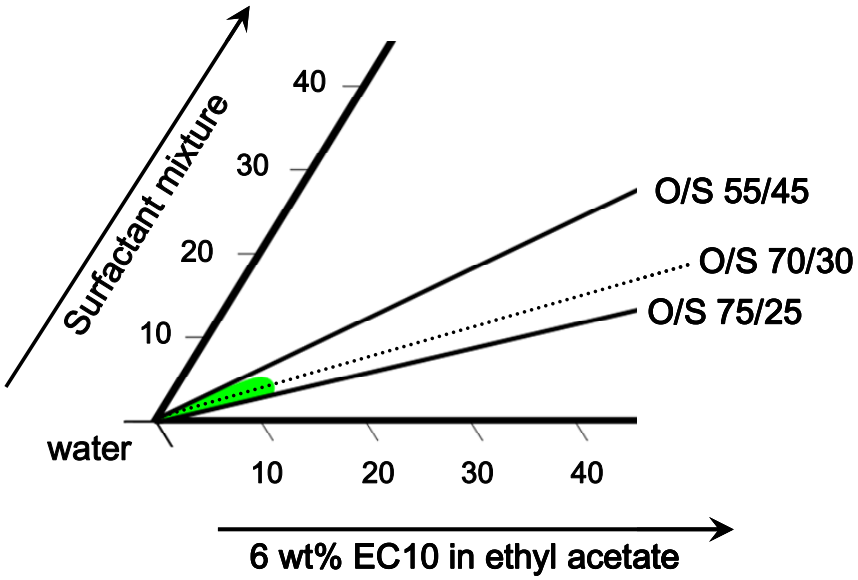

Figure 4.9. Oil-in-water (O/W) nano-emulsion region in the Water / [CatA:CWO7] / [6 wt% EC10 in ethyl acetate] system for CatA:CWO7 ratios of 1:1 and 1:3, at 25ºC. The dotted line indicates the dilution path for the O/S ratio 70/30, followed for conductivity measurements.

Conductivity measurements were carried out in order to assess if a transition from W/O to O/W structures took place during emulsification. **Figure 4.10** shows the results obtained in the CatA:CWO7 ratio 1:3 system with an O/S ratio of 70/30, at 25ºC. No conductivity values could be obtained below 5 wt% water due to the water already present in CatA, as mentioned in **Section 3.3.1**. Conductivity values of samples with a water content around 25 wt% fluctuated due to their instability which could be indicative of phase transition. As described in the previous chapter for the CatA:Span® 80 system, conductivity values increase with the increase of water content, reaching a maximum and then gradually decrease due to the effect of dilution of the conducting species. Conductivity values (about 1000 μS/cm) are slightly lower than those obtained with the CatA:Span® 80 system (about 1400 μS/cm). This can be explained taking into account the different cationic:nonionic surfactant ratios (ratio 1:1 with the Span® 80 system and ratio 1:3 with the Cremophor® WO7 system) and thus the lower amount of cationic species. It has been assessed that phase inversion takes place when fluctuation in conductivity occurred, that is, at around 25 wt% water which is about the same phase inversion region assessed for the CatA:Span® 80 system.

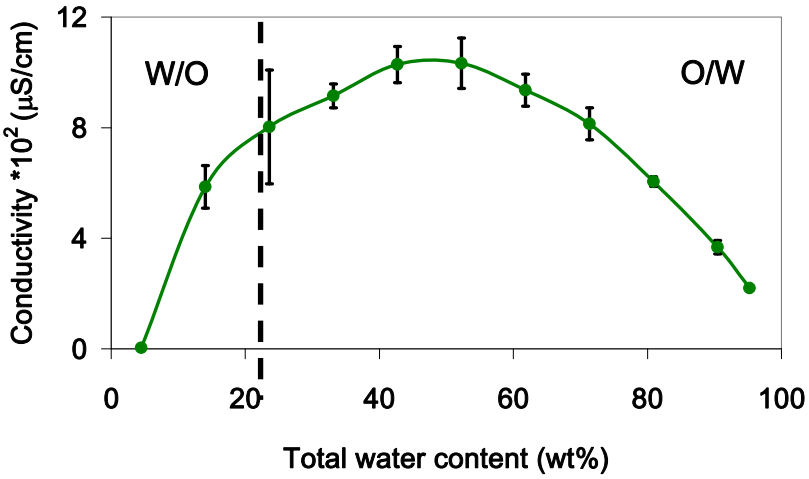

Figure 4.10. Conductivity (*10^2) as a function of total water content in the Water / [CatA:CWO7 = 1 : 3] / [6 wt% EC10 in ethyl acetate] system along the dilution path with an O/S ratio of 70/30, at 25ºC. Water-in-oil (W/O) and oil-in water (O/W) regions are indicated.

Nano-emulsion characterization

Droplet size and surface charge of nano-emulsions with 90 and 95 wt% water and with O/S ratios between 60/40 and 75/25 were characterized at 25ºC. **Table 4.13** shows nano-emulsion droplet diameters and polydispersity indices obtained by DLS measurements. Some nano-emulsions could not be measured without dilution (shown in shadowed cells in **Table 4.13**) due to their high turbidity. Dilution, when needed, was performed at a ratio of 1/100 with water saturated with ethyl acetate in order to prevent diffusion of ethyl acetate from the droplets to the continuous phase. However, dilution may cause destabilization of the oil droplets by displacement of surfactant molecules from the droplet interface into the continuous phase.

Table 4.13. Droplet diameters and polydispersity indices (PI) of nano-emulsions of the Water / [CatA:CWO7] / [6 wt% EC10 in ethyl acetate] systems with 90 and 95 wt% of water content obtained by DLS, at 25ºC. Shadowed areas correspond to samples diluted (1/100) with water saturated with ethyl acetate.

CatA:CWO7 ratio	O/S ratio	90 wt% water		95 wt% water	
		droplet diameter (nm)	PI	droplet diameter (nm)	PI
1:1	60/40	260.3	0.25	173.1	0.20
	70/30	218.6	0.29	163.2	0.36
1:3	60/40	133.2	0.33	133.9	0.41
	65/35	127.3	0.38	130.9	0.20
	70/30	119.9	0.41	127.6	0.33
	75/25	167.5	0.43	150.4	0.46

As the polydispersity of all samples is rather high (polydispersity indices between 0.20 and 0.46) the droplet size values shown in the **Table 4.13** have to be taken with caution. Therefore, only the tendency of the values is discussed. In the CatA:CWO7 ratio 1:1 system nano-emulsion droplets decrease with the increase of O/S ratio. This could be attributed to the diffusion of ethyl acetate from the droplets to the aqueous phase.

Nano-emulsion droplet sizes in the CatA:WO7 ratio 1:3 system do not differ significantly when increasing the water content from 90 to 95 wt%. However,

when increasing the oil content (increase of O/S ratio), droplet size is decreasing up to a minimum at the O/S ratio 70/30 and then it increases again. This trend, which has been described in similar systems [Calderó, 2011], may be due to two antagonizing effects: The effect of solvent diffusion from the droplets towards the continuous phase, which was mentioned above, leading to a decrease in droplet size and, on the other hand, the increase of the dispersed fraction leading to an increase of droplet size. At the higher O/S ratios, the dispersed phase fraction effect would dominate over the diffusion effect producing a droplet size increase. The observed behavior is different from that described in systems with less polar oils where no diffusion of the dispersed phase is produced and where the droplet diameter increases with increasing O/S ratio [Sadurní, 2005].

A nano-emulsion of the CatA:CWO7 ratio 1:3 system with an O/S ratio of 70/30 and 95 wt% of water was chosen for imaging by cryogenic transmission electron microscopy (cryoTEM) as it showed the smallest droplet size by DLS. The results shown in Figure 4.11 confirmed the high polydispersity of the nano-emulsion as already evidenced by DLS.

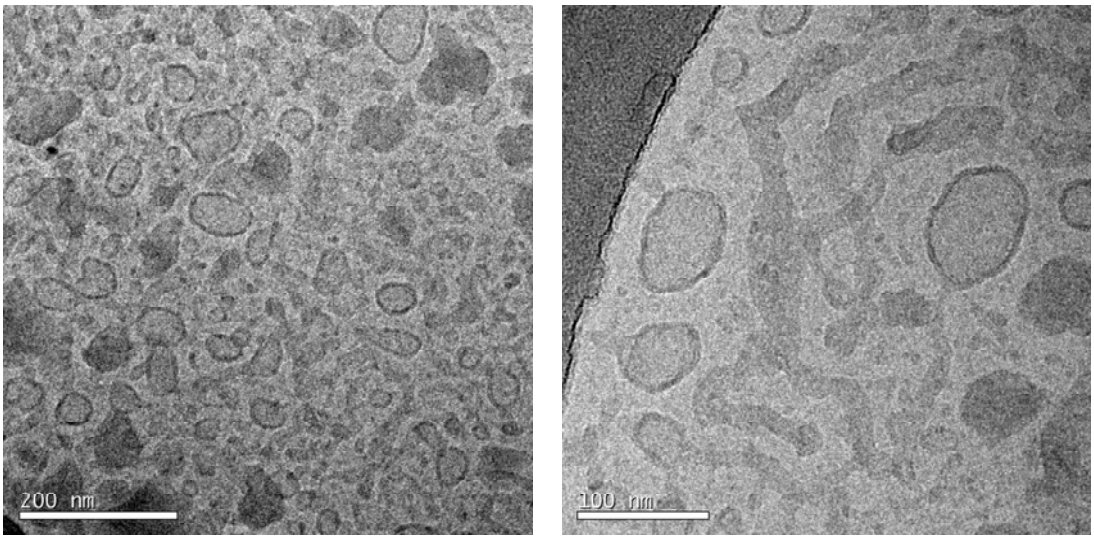

Figure 4.11. CryoTEM images of the nano-emulsion of the Water / [CatA:CWO7 = 1:3] / [6 wt% EC10 in ethyl acetate] system with an O/S ratio of 70/30 and 95 wt% of water content, at 25ºC.

The nano-emulsion displays a broad range of structures such as droplets of irregular shapes and sizes with a lighter inside surrounded by a darker layer, darker spots also of irregular shapes or darker tunnel structures. The

interpretation of these images should be carried out cautiously, as during sample preparation, which requires for example freezing at low temperature, modification of the original sample may occur, such as the formation of crystals. However, the droplets with darker surrounding and lighter inside observed in this nano-emulsion could eventually be interpreted as vesicles, compared to cryoTEM images from liposomes found in literature [**Maurer, 2001; Kuntsche, 2011**]. The sizes of the droplets shown on the images have an estimated diameter lower than 50 nm. This was confirmed by an image analysis of cryoTEM images. About 500 droplets, in particular those with a rounded shape were manually measured. The size distribution is shown in **Figure 4.12**.

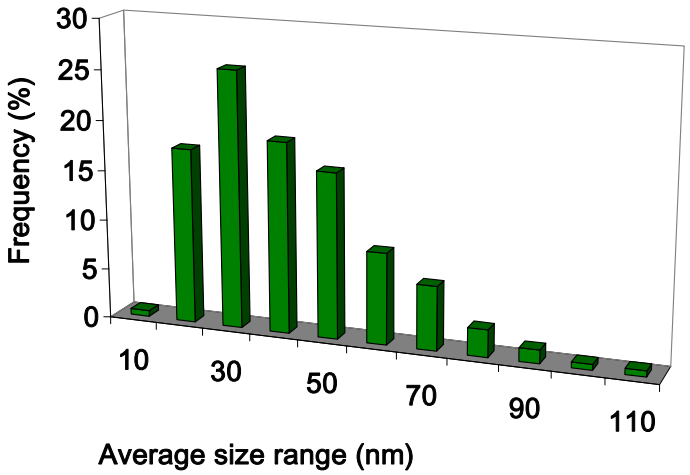

Figure 4.12. Droplet size distribution of the nano-emulsion of the Water / [CatA:CWO7 = 1:3] / [6 wt% EC10 in ethyl acetate] system with O/S ratio 70/30 and 95 wt% of water content, assessed from cryoTEM image analysis.

The graph shows a roughly monomodal but broad Schulz-like size distribution at 25°C. The calculated mean droplet size is 37 ± 18 nm. The droplets are significantly smaller than those obtained with DLS (**Table 4.13**). It has to be considered that the DLS measures the hydrodynamic radius/diameter while the diameter given by cryoTEM is the hard sphere diameter. Furthermore, this difference in size could be explained by droplet aggregation.

Electrophoretic mobility and zeta potential values of nano-emulsions are summarized in **Table 4.14**. Nano-emulsions of the CatA:CWO7 ratio 1:1 system show values around +50 mV for both, 90 and 95 wt% of water and O/S ratios of 60/40 and 70/30. However, with the CatA:CWO7 ratio 1:3 system, a change in zeta potential with O/S ratio is noticeable. While at O/S 60/40 zeta potential

values are about +45 mV, surface charge is decreased for 10 – 15 mV in samples with an O/S ratio of 70/30. This can be explained by the decrease of cationic surfactant in the sample with increasing O/S ratio. The higher zeta potential values in samples with CatA:CWO7 ratio 1:1 can also be attributed to the greater amount of cationic species present in the mixture, compared to the ratio 1:3. The zeta potential values of the mixed CatA:CWO7 surfactant system (**Table 4.14**) are lower than those obtained for the mixed CatA:Span® 80 surfactant system. This could be due to structural differences of both nonionic surfactants and to more cationic surfactant available at the droplet interface in the CatA:Span® 80 system.

Table 4.14. Electrophoretic mobility (μ), zeta potential (ζ) of nano-emulsions of the Water / [CatA:CWO7] / [6 wt% EC10 in ethyl acetate] system, initially prepared with 90 and 95 wt% water content, respectively, after dilution with MilliQ® water to 20 mg/g, at 25ºC.

CatA:CWO7 surfactant ratio	O/S ratio	90 wt% water		95 wt% water	
		μ (μmcm/Vs)	ζ (mV)	μ (μmcm/Vs)	ζ (mV)
1:1	60/40	3.9	49.7	3.9	49.2
	70/30	3.9	49.4	3.7	47.2
1:3	60/40	3.5	44.7	3.6	45.7
	65/35	3.1	39.8	2.6	32.6
	70/30	2.7	34.4	2.4	30.5
	75/25	2.6	34.0	2.1	35.1

The high zeta potential values of all the samples might indicate a good electrostatic stability. **Table 4.15** shows the stability assessed visually (time to observe sedimentation) of samples prepared with 90 and 95 wt% of water, at a constant temperature of 25ºC.

Table 4.15. Stability by visual observation of nano-emulsions of the Water / [CatA:CWO7] / [6 wt% EC10 in ethyl acetate] system with 90 and 95 wt% water content, at 25ºC.

CatA:C WO7 surfactant ratio	O/S ratio	Stability (days)	
		90 wt% water	95 wt% water
1:1	60/40	1	1
	70/30	1	2
1:3	60/40	4	7
	65/35	50	53
	70/30	66	71
	75/25	6	6

The stability data obtained by visual assessment suggest that there is no direct correlation between the electrostatic stability predicted through high zeta potential values and the stability assessed visually. Nevertheless, it is worth noting that all samples with the CatA:CWO7 ratio 1:1 system show stability of maximum 2 days while nano-emulsions of the CatA:CWO7 ratio 1:3 system show a considerably higher stability. The most stable nano-emulsions were formed with the O/S ratios 65/35 and 70/30 with a visually assessed stability of about 2 months. The compositions of these nano-emulsions seemed to enhance nano-emulsion stability, presumably due to beneficial electrostatic and sterical conditions.

The main instability detected in most nano-emulsions was sedimentation. A possible reason for the low stability can be the precipitation of polymer in excess, observed shortly after nano-emulsion preparation. It must be kept in mind that, apart from the high density of EC10 (1.15 g/cm^3),the high polydispersity of the nano-emulsion (>0.2), and electrostatic effects, there might be sterical effects playing a role in the stability of these nano-emulsions.

Further accelerated stability tests were carried out with nano-emulsions with O/S ratio of 70/30 and 95 wt% water by measuring the backscattering intensity along the sample height with time (**Figure 4.13**). This method allows detecting stability changes of nano-emulsions which cannot be seen with the naked eye. Backscattering intensity of the CatA:CWO7 ratio 1:1 system is constant on the

whole sample height at a value of about 14%. This indicates that the sample was homogenous and stable during the first 24 hours after its preparation.

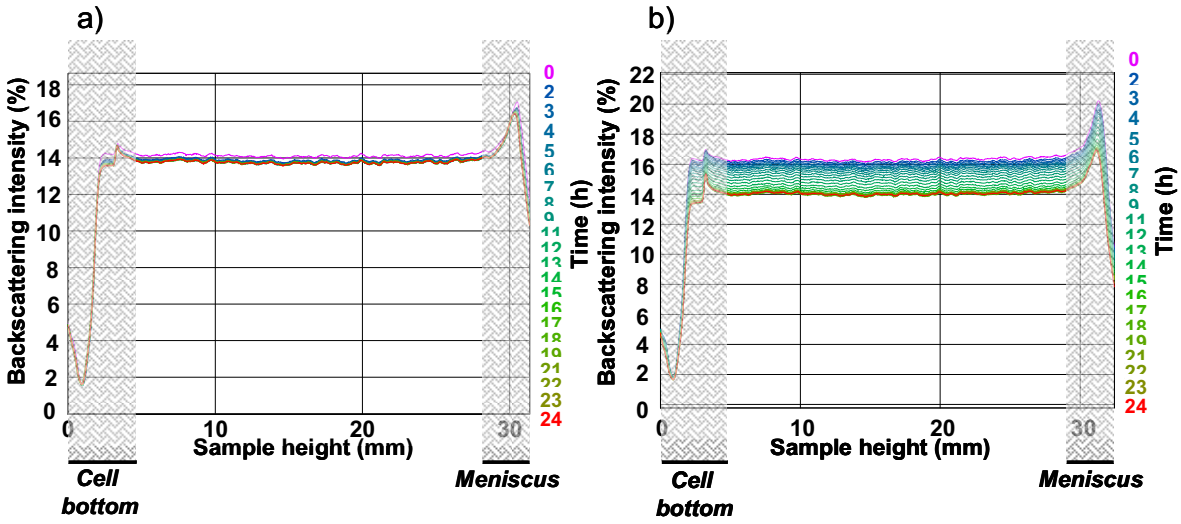

Figure 4.13. Backscattering data of the nano-emulsions with the O/S ratio 70/30, 95 wt% of water content and 6 wt% EC10 with the mixed CatA:CWO7 ratio of **a)** 1:1 and **b)** 1:3, during 24 hours. Grey shaded regions indicate the bottom and meniscus of the sample in the glass cell.

By contrast, at first glance, backscattering intensity in the sample of the CatA:CWO7 = 1:3 system (**Figure 4.13b**) decreases as a function of time which could not be detected by visual observation. As described in **Section 4.1.2**, this could be attributed to the clarification of the continuous phase caused by a decrease in number of droplets as a consequence of coalescence or Ostwald ripening or by a decrease in size due to diffusion of ethyl acetate from the droplets to the outer phase. As less CWO7 is available in the mixture CatA:CWO7 1:1 (**Figure 4.13a**), this diffusion effect would be less distinctive and thus less evident in the spectrum. However, it can also be noticed that the change is minor (backscattering intensity drop below 2%) compared to results obtained with the CatA:Span® 80 ratio 1:1 system with incorporated oleylamine, where the same phenomenon was observed (backscattering intensity drop of about 11%). Also with this sample, no sedimentation or creaming was observed during the first 24 hours. Thus, nano-emulsions with this composition can be considered as relatively stable during measurement time.

The hydrodynamic droplet diameter of the nano-emulsion of the CatA:CWO7 ratio 1:3 system with an O/S ratio of 70/30 and 95 wt% of water was measured

as a function of time for 14 days (**Figure 4.14**). Droplet size does not change significantly during this period of time indicating stability of the nano-emulsion which is in agreement with results obtained from backscattering analysis and visual assessment.

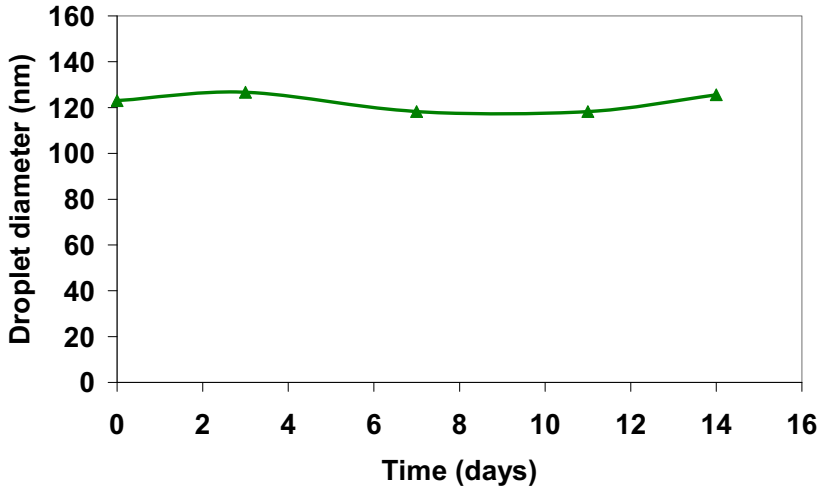

Figure 4.14. Droplet diameter of the nano-emulsion of the Water / [CatA:CWO7 = 1:3] / [6 wt% EC10 in ethyl acetate] system with an O/S ratio of 70/30 and 95 wt% of water content as a function of time, at 25ºC.

The results shown above suggest that by increasing the nonionic surfactant content the formation and stability of nano-emulsions is enhanced. Therefore, decreasing the cationic:nonionic surfactant ratio on the formation and stability of nano-emulsions was studied. For these studies, CatA:CWO7 ratios of 1:4, 1:6 and 1:8 were chosen. The O/S ratio of 70/30, which formed the most stable systems by visual observation and which also possessed the smallest droplet size was selected. The water contents were 90 and 95 wt%, respectively, and the polymer concentration was 6 wt%. Droplet diameters and polydispersity indices of these nano-emulsions are plotted in **Figure 4.15** and summarized in **Table A 9.1** in the Appendix. Nano-emulsions are polydisperse. Polydispersity indices do not show a clear trend and are similar for both water contents. Nevertheless they are rather high wherefore only droplet diameter tendencies can be discussed.

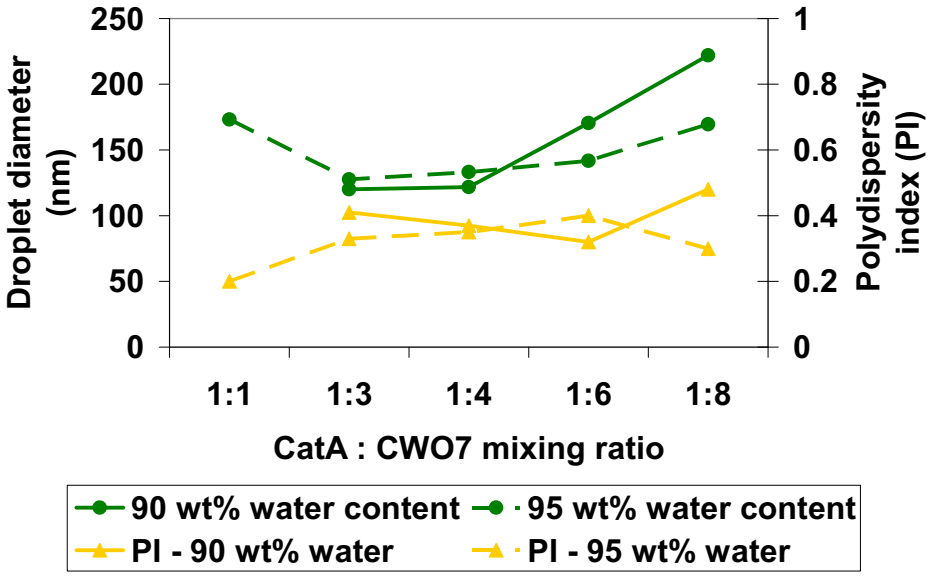

Figure 4.15. Droplet diameters and polydispersity indices (PI) of nano-emulsions of the Water / [CatA:CWO7] / [6 wt% EC10 in ethyl acetate] systems with the O/S ratio 70/30 and 90 and 95 wt% water content as a function of CatA:CWO7 mixing ratio, at 25ºC.

With 90 wt% water content, the droplet size increases with decreasing cationic:nonionic surfactant ratio while with 95 wt% water, droplet sizes at high CatA:CWO7 ratios (ratio 1:1) are large, then notably decrease (ratios 1:3 till 1:6) before they increase again (ratio 1:8). For both tendencies, droplet sizes are minimal (about 120 nm) at CatA:CWO7 ratios 1:3 and 1:4.

The sedimentation rate values of nano-emulsions, calculated applying Stokes' law, are summarized in Table 4.16.

Table 4.16. Theoretical stability assessment of nano-emulsions of the Water / [CatA:CWO7] / [6 wt% EC10 in ethyl acetate] system with an O/S ratio of 70/30 and 90 and 95 wt% water, calculated from Stokes' law.

CatA:CWO7 ratio	90 wt% water	95 wt% water
	Rate of sedimentation (nm/s)	
1:1	2.3	1.3
1:3	0.7	0.8
1:4	0.7	0.9
1:6	1.4	1.0
1:8	2.4	1.4

The sedimentation rates for nano-emulsions with the CatA:CWO7 surfactant mixing ratios 1:3 and 1:4 are below 1.0, an indication of a higher stability of

these nano-emulsions compared to those with higher or lower CatA:CWO7 mixing ratios. Compared to sedimentation rates obtained for the CatA:Span® 80 system which were equal to or greater than 3 nm/s (see **Tables 4.8 and 4.11**), sedimentation rates are much lower (between 0.7 and 2.5 nm/s) which confirms the higher stability of this system.

Figure 4.16 show the visually assessed stability of nano-emulsions prepared with 90 and 95 wt% of water. Values are also summarized in **Table A 9.2** in the Appendix. It was found that nano-emulsions formed with the CatA:CWO7 ratio of 1:3 possess an optimum in stability. Also nano-emulsions with the CatA:CWO7 ratio 1:4 showed a higher stability assessed visually. However, no clear tendency is found comparing the stability of nano-emulsions with both water contents.

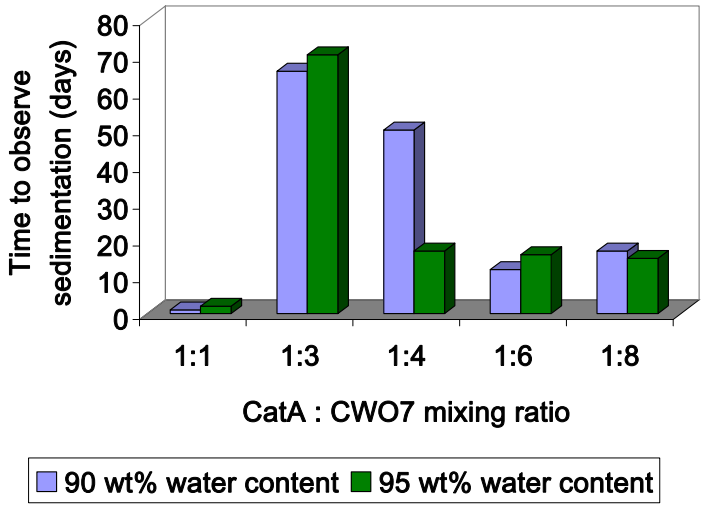

Figure 4.16. Stability by visual observation of nano-emulsions of the Water / [CatA:CWO7] / [6 wt% EC10 in ethyl acetate] system with the O/S ratio 70/30 and 90 and 95 wt% water content as a function of the CatA:CWO7 mixing ratio, at 25°C.

The visually assessed stability values are in good agreement with the sedimentation rates obtained from Stokes' law (**Table 4.16**). With the CatA:CWO7 mixing ratios 1:1, 1:6 and 1:8 the sedimentation values are equal to or slightly higher than 1.0, indicating less stability of these nano-emulsions. No clear trend is observed comparing the stability of nano-emulsions with 90 and 95 wt% of water.

The results obtained by visual assessment also suggest that electrostatic stabilization might play a role for certain CatA:CWO7 mixing ratios, aside from facts such as the high polymer density and polydispersity (>0.20). Most stable nano-emulsions with the CatA:CWO7 ratio 1:3 have a surface charge of around +30 mV. With decreasing surface charge the visually assessed stability is decreasing. However, nano-emulsions of the CatA:CWO7 ratio of 1:1 have the highest surface charge (+50 mV). In this case, the sterical effects might be dominant over electrostatic stabilization. The surface charge values are shown in **Table 4.17** and in **Figure 4.17**.

Table 4.17. Electrophoretic mobility (μ) and zeta potential (ζ) values of nano-emulsions of the Water / [CatA:CWO7] / [6 wt% EC10 in ethyl acetate] system with the O/S ratio 70/30, initially prepared with 90 and 95 wt% water content, respectively, after dilution with MilliQ water to 20 mg/g, at 25°C.

CatA:CWO7 ratio	90 wt% water		95 wt% water	
	μ (μmcm/Vs)	ζ (mV)	μ (μmcm/Vs)	ζ (mV)
1:1	3.9	49.4	3.7	47.2
1:3	2.7	34.4	2.4	30.5
1:4	2.6	32.5	2.0	25.4
1:6	2.0	25.5	1.3	16.5
1:8	1.9	24.7	0.8	10.3

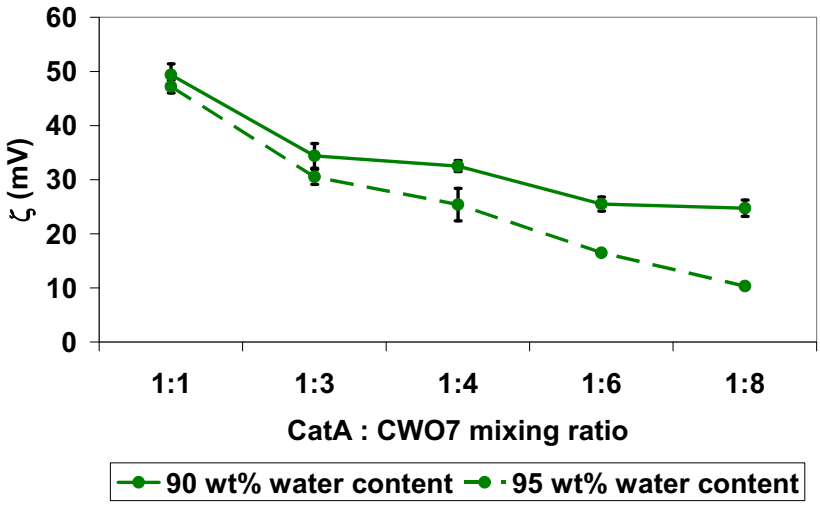

Figure 4.17. Zeta potential (ζ) values of nano-emulsions of the Water / [CatA:CWO7] / [6 wt% EC10 in ethyl acetate] system as a function of CatA:CWO7 mixing ratio with an O/S ratio of 70/30 and 90 and 95 wt% of water content, respectively, after dilution with MilliQ water to 20 mg/g, at 25ºC.

With increasing content of nonionic surfactant the zeta potential decreases. It is an expected behavior, as the amount of cationic surfactant decreases with increasing nonionic surfactant concentration. This trend can be observed for both water contents. Zeta potential values with 95 wt% water are lower than those with 90 wt% which might be explained by the effect of dilution.

Effect of polymer concentration

Nano-emulsion formation region

The formation of nano-emulsions with a higher polymer concentration, 10 wt% EC10, was studied in order to determine if there was an improvement in the formation and stability of nano-emulsions.

Nano-emulsions were not obtained in the CatA:CWO7 ratio 1:1 system with 10 wt% EC10. Although nano-emulsions were formed with a CatA:CWO7 ratio of 1:3, the nano-emulsion region was very narrow (Figure 4.18). As displayed in the figure, nano-emulsions were formed between O/S ratios 65/35 and 75/25 and above 88 wt% of water. These two facts, that is, no formation of nano-emulsions with the cationic:nonionic surfactant ratio 1:1 and only in a very narrow region for the ratio 1:3 indicates that higher polymer concentrations do not favor the formation of nano-emulsions with these cationic:nonionic surfactant mixtures. It might also suggest that nano-emulsion formation at higher polymer concentrations requires low cationic:nonionic surfactant ratios.

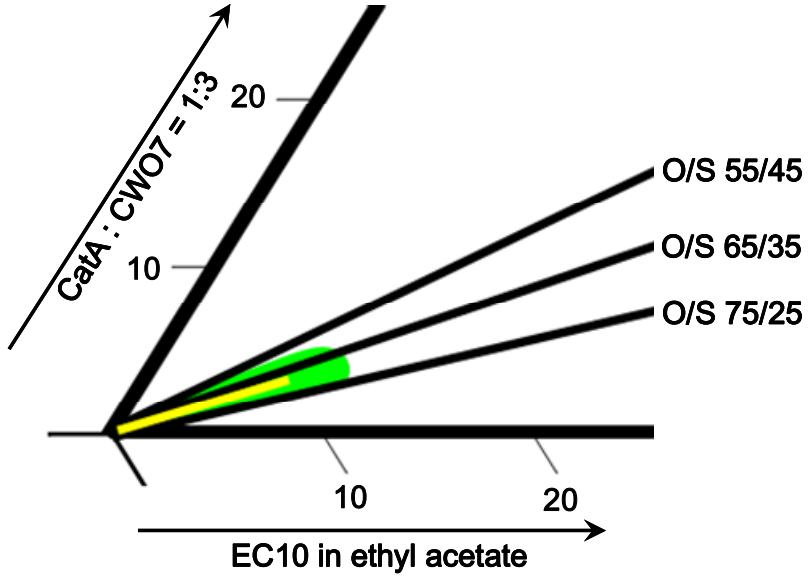

Figure 4.18. Oil-in-water (O/W) nano-emulsion region in the Water / [CatA:CWO7] / [EC10 in ethyl acetate] system at 25ºC. The nano-emulsion region with 6 wt% of polymer concentration is shown in light green color while the region with 10 wt% is shown as the yellow line along the O/S ratio 70/30.

It was tested if nano-emulsions could be formed with 8 wt% of polymer concentration. Samples with the O/S ratios 60/40 and 70/30 and 95 wt% of water content were studied. For the CatA:CWO7 ratio 1:1 nano-emulsions were only obtained with the O/S ratio 70/30 and for the CatA:CWO7 ratio 1:3 with both O/S ratios. This confirms that higher cationic:nonionic surfactant ratio in combination with a higher EC10 concentration is less suitable for nano-emulsion formation.

Nano-emulsion characterization

Droplet size, surface charge and stability by visual observation of the nano-emulsions of the O/S ratio 70/30 and with 90 and 95 wt% water were determined. **Table 4.18** shows droplet sizes obtained for samples with 10 wt% and 6 wt% EC10.

Table 4.18. Droplet diameters and polydispersity indices of nano-emulsions of the Water / [CatA:CWO7 = 1:3] / [EC10 in ethyl acetate] system with the O/S ratio 70/30 and 90 and 95 wt% of water content at 25ºC.

O/S ratio	wt% polymer	90 wt% water		95 wt% water	
		droplet diameter (nm)	PI	droplet diameter (nm)	PI
70/30	6	119.9	0.42	127.6	0.33
	10	136.1	0.35	150.6	0.41

Taking into account the high polydisperity indices (above 0.30) which do not allow a straight-forward analysis, the tendency observed is that nano-emulsions with 10 wt% polymer show larger droplet sizes with both water contents than the corresponding nano-emulsion prepared with 6 wt% polymer. This could be attributed to the formation of larger droplets with the increase in polymer concentration.

Table 4.19 shows electrophoretic mobility and surface charge values obtained for samples with 6 and 10 wt% EC10. With 10 wt% polymer concentration, zeta potential values of nano-emulsions are about 10 mV lower than those with 6 wt%. This may be due to a higher shielding effect of the polymer on the cationic surfactant placed at the drop surface.

Table 4.19. Electrophoretic mobility (μ) and zeta potential (ζ) values of nano-emulsions of the Water / [CatA:CWO7 = 1:3] / [EC10 in ethyl acetate] system with the O/S ratio 70/30 at a concentration of 20 mg/g, at 25°C.

O/S ratio	wt% polymer	90 wt% water		95 wt% water	
		μ (μmcm/Vs)	ζ (mV)	μ (μmcm/Vs)	ζ (mV)
70/30	6	2.7	34.4	2.4	30.5
	10	2.0	25.9	1.8	23.1

The estimated number of droplets in the nano-emulsion was calculated using the following equation [Némati, 1994]:

$$n = \frac{[mass\ of\ polymer\ in\ the\ medium\ (M)]}{[mass\ of\ one\ particle]} = \frac{M\ x\ 10^{12}}{\frac{4}{3}\pi\ r^3\ x\ 1.1}$$ [Equation 8]

where M should be expressed in ng and the radius r of the droplets in nm.

Table 4.20 summarizes estimative numbers of droplets calculated, using droplet diameter values of Table 4.18.

For nano-emulsions with 90 wt% water, the number of droplets is slightly increased with 10 wt% EC10 towards 6 wt% EC10. The same trend can be observed for nano-emulsions with 95 wt% water. However, the difference in droplet numbers between nano-emulsions formed with 90 and 95 wt% water is significant. With 90 wt%, the amount is about the double of droplets formed with 95 wt%.

Table 4.20. Estimated droplet number in 1 mL of nano-emulsion of the Water / [CatA:CWO7 = 1:3] / [EC10 in ethyl acetate] system with the O/S ratio 70/30.

O/S ratio	wt% polymer	number of droplets (x 10^{12})	
		90 wt% water	95 wt% water
70/30	6	1.01	0.42
	10	1.15	0.42

For nano-emulsions with 90 wt% water, the number of droplets is slightly increased with 10 wt% EC10 towards 6 wt% EC10 and are of the same magnitude for nano-emulsions with 95 wt% water. There is a significant difference in droplet numbers between nano-emulsions formed with 90 and 95 wt% of water. With 90 wt%, the amount is about the double of droplets formed with 95 wt%.

Table 4.21 shows the stability assessed visually of samples prepared with 90 and 95 wt% of water and 6 wt% and 10 wt% EC10. Nano-emulsions formed with 10 wt% polymer were significantly less stable than those obtained with 6 wt%. The observed destabilization was sedimentation.

Table 4.21. Stability by visual observation of nano-emulsions of the Water / [CatA:CWO7 = 1:3] / [EC10 in ethyl acetate] system with the O/S ratio 70/30 and with 90 and 95 wt% water content, at 25ºC.

O/S ratio	wt% polymer	Stability (days)	
		90 wt% water	95 wt% water
70/30	6	66	70.5
	10	3	3

The reduced stability of nano-emulsions formed with 10% EC10 could be explained by the high polydispersity indices (> 0.30), the high polymer density and early precipitation of polymer in excess and by the larger droplet sizes and eventually denser droplet structure leading to a faster sedimentation.

The sedimentation rate for nano-emulsions with 10 wt% polymer concentration was calculated to be 0.8 and 1.0 for 90 and 95 wt% of water content, respectively. These values are comparable to those obtained with 6 wt% EC10 (0.7 and 0.8, respectively, **Table 4.16**) which would allow assuming similar stabilities, which was not confirmed by visual observation of nano-emulsions.

The use of a higher concentration of polymer resulted in a narrower region of nano-emulsion formation. The droplet size is larger than with 6 wt% EC10 and surface charges are lower. The visually assessed stability is strongly decreased while the sedimentation rate is comparable to that obtained with 6 wt% polymer concentration. These let conclude that the use of a higher polymer concentration with the surfactant mixture CatA:CWO7 does not improve the formation of kinetically stable nano-emulsions.

Summary

Nano-emulsions have been obtained in the Water / [CatA:CWO7] / [6 wt% EC10 in ethyl acetate] system between O/S ratio 55/45 and 75/25 and above 88 wt% water content with both, CatA:CWO7 ratios 1:1 and 1:3. The nano-emulsion region is thus slightly narrower than with the CatA:Span® 80 system and appears at higher water contents. Nano-emulsions of the CatA:CWO7 ratio 1:3 were more transparent than those of the CatA:CWO7 ratio 1:1 and also than those of the CatA:Span® 80 system. Phase Inversion from W/O to O/W

structures at the O/S ratio 70/30 of the CatA:CWO7 = 1:3 system was confirmed by conductivity measurements and takes place at about the same range of water content as with the CatA:Span® 80 system (about 30 wt%). Conductivity values were comparably high to those obtained with the surfactant mixture CatA:Span® 80 of 1:1. Nano-emulsions of both cationic:nonionic surfactant ratios showed droplet sizes below 260 nm and a polydispersity ranging between 0.20 and 0.46. Compared to the CatA:Span® 80 system, droplet sizes are significantly smaller and the polydispersity is larger. Zeta potential values are between +30 and +50 mV (dilution to 20 mg/g with MilliQ® water). Surface charge values with CatA:CWO7 ratio 1:1 are higher than those of 1:3 due to the presence of more cationic species in the nano-emulsions. Visual stability assessment shows that nano-emulsions with CatA:CWO7 ratio 1:3 are more stable than those of the ratio 1:1 or those of the CatA : Span® 80 system. Nano-emulsions with lower CatA:CWO7 ratios than 1:3 could successfully be obtained. With decreasing cationic:nonionic surfactant ratio droplet size increases whereby the surface charge decreases. Decreasing the CatA:CWO7 mixing ratio did not improve droplet size, surface charge and visually assessed stability of nano-emulsions compared to the CatA:CWO7 ratio 1:3 system. Nano-emulsions with 10 wt% polymer concentration could only be obtained for the surfactant mixture CatA:CWO7 of 1:3 and the O/S ratio 70/30. They showed larger droplet sizes and lower surface charge values than corresponding nano-emulsions with 6 wt% polymer and were visually less stable. It is noteworthy that using Cremophor® WO7 slightly improved the nano-emulsion formation with respect to the CatA:Span® 80 system.

The following conclusions can be made:

- Nano-emulsion formation using a hydrogenated castor oil derivative surfactant, CWO7, mixed with CatA, was improved compared to that using a sorbitan ester which suggests that the surfactant structure plays a significant role.
- With regard to the cationic:nonionic surfactant ratio there is an optimum CatA : CWO7 ratio (1:3) for stability and small droplet size.

- Higher zeta potential values are obtained with high cationic:nonionic surfactant ratios, i.e. 1:1.
- High O/S ratios (e.g. O/S ratio 70/30) are favorable for the formation of nano-emulsions.
- Nano-emulsions were obtained with both, 90 and 95 wt% of water with a comparable visually assessed stability and comparable droplet sizes.
- The use of a higher polymer concentration does not improve the formation of kinetically stable nano-emulsions.

These conclusions suggest that surfactants derived from castor oil may favor nano-emulsion formation. It also suggests that high O/S ratios, a polymer concentration of 6 wt% and high water content may be the most favorable factors for nano-emulsion formation in this system.

In order to study if the formation of kinetically stable nano-emulsions could be further improved, in a next step, CWO7 was mixed with another nonionic surfactant with a similar chemical structure but with a higher HLB number.

4.1.4. NANO-EMULSIONS IN THE WATER / CATA:(CREMOPHOR® WO7:CREMOPHOR® EL) / POLYMER SOLUTION SYSTEM

As reported in the previous chapter, the cationic surfactant CatA mixed with the low HLB value nonionic hydrogenated castor oil derivative surfactant, Cremophor® WO7 (CWO7), improved the formation of nano-emulsions with smaller droplet size and higher stability compared to the CatA:Span® 80 mixture. In a next step, it was investigated if mixing Cremophor® WO7 with another nonionic surfactant with similar structure, Cremophor® EL, with a high HLB number (12 – 14), would contribute to further improvement of nano-emulsion formation. Cremophor® WO7 will be abbreviated as CWO7 and Cremophor® EL will be shortened to CEL.
The studies were focused on the characterization of nano-emulsions with an O/S ratio of 70/30 and a water content of 95 wt%. The cationic surfactant was

mixed with different mixing ratios of both nonionic surfactants with CatA:(CWO7:CEL) ratios of 1:1 and 1:3.

Effect of cationic:mixed nonionic surfactant ratios

Nano-emulsion formation

Table 4.22 summarizes studied nano-emulsions of the Water / [CatA:(CWO7:CEL)] / [EC10 in ethyl acetate] system. In some cases, nano-emulsions were very turbid and unstable and were for that reason not characterized.

Table 4.22. Formation of nano-emulsions of the Water / [CatA:(CWO7:CEL)] / [EC10 in ethyl acetate] system with the O/S ratio 70/30, 95 wt% water and 6 and 10 wt% polymer, at 25ºC.

CWO7:CEL ratio	CatA:(CWO7:CEL) = 1:1		CatA:(CWO7:CEL) = 1:3	
	6 wt% EC10	10 wt% EC10	6 wt% EC10	10 wt% EC10
1:3	yes	N.D.	yes	N.D.
1:2	yes	N.D.	yes	N.D.
1:1	yes	yes	yes	yes
2:1	yes	N.D.	yes	yes
3:1	yes	yes	yes	yes

(1) N.D.: not determined

Nano-emulsion characterization

Nano-emulsions were characterized regarding droplet size, surface charge and stability assessed visually. **Figure 4.19** shows droplet sizes and **Table A 9.3** in the Appendix also indicates polydispersity indices of nano-emulsions for several cationic:mixed nonionic surfactant ratios.

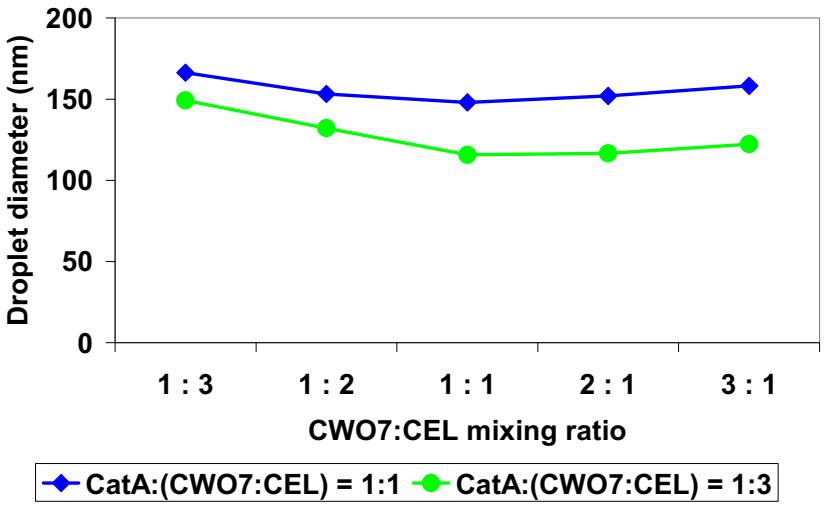

Figure 4.19. Droplet sizes of nano-emulsions of the Water / [CatA:(CWO :CEL)] / [6 wt% EC10 in ethyl acetate] system as a function of CWO7:CEL mixing ratio with the O/S ratio 70/30 and 95 wt% of water content, at 25ºC.

With both ratios, CatA:(CWO7:CEL) ratio 1:1 and 1:3, droplet sizes decrease with increasing CWO7 content until a plateau is reached starting from the CWO7:CEL mixing ratio 1:1. The droplet sizes are smaller with the CatA:(CWO7:CEL) ratio 1:3 system than those with the 1:1 system. The results suggest that the CWO7:CEL mixing ratio of 1:1 favors the formation of small droplets.

Droplet sizes for the CWO7:CEL mixing ratio 0:1 (not shown in the graph) were significantly smaller (98.4 nm) than those obtained when CWO7 was mixed with CEL, with a similar polydispersity (0.32). Droplet size values obtained for the CWO7:CEL mixing ratio 1:0 (not shown in the graph, see **Table 4.13**) were both in the range of the values in **Figure 4.19**, following the trend displayed in the graphs.

Based on droplet sizes obtained by DLS (and summarized in **Table A 9.3** in the Appendix), the sedimentation rate could be calculated applying Stokes' Law. The values obtained (listed in **Table A 9.4** in the Appendix) in the range between 0.6 and 1.3 nm/s are comparable to those obtained with the CatA:CWO7 system (see **Table 4.16**). While with CatA:(CWO7:CEL) ratio 1:1, nano-emulsions with a very low CWO7 content (CWO7:CEL mixing ratio of 1:3) or a very high CWO7 content (CWO7:CEL mixing ratio of 3:1) seem to show a

faster sedimentation, no clear trend is visible for samples prepared with CatA:(CWO7:CEL) = 1:3.

Zeta potential values are summarized in **Table 4.23** and displayed in **Figure 4.20**. The surface charge increases with increasing content of CWO7 for both CatA:(CWO7:CEL) ratios. This increase is slightly more noticeable with the CatA:(CWO7:CEL) ratio 1:3 (about 12 mV) than with ratio 1:1 (about 8 mV). With the latter mentioned ratio, a plateau seems to be reached at around +32 mV which might be due to structural effects of the surfactants and the polymer on the droplet surface. Surface charge values are about 10 mV higher with CatA:(CWO7:CEL) ratio 1:1 than with ratio 1:3 due to the higher content of cationic surfactant present at the 1:1 ratio.

Table 4.23. Electrophoretic mobility (μ) and zeta potential (ζ) values of nano-emulsions of the Water / [CatA:(CWO7:CEL)] / [6 wt% EC10 in ethyl acetate] system with the O/S ratio 70/30 and 95 wt% of water content, after dilution to a concentration of 20 mg/g, at 25°C.

CWO7:CEL mixing ratio	CatA:(CWO7:CEL) = 1:1		CatA:(CWO7:CEL) = 1:3	
	μ (μmcm/Vs)	ζ (mV)	μ (μmcm/Vs)	ζ (mV)
1:3	1.9	24.2	0.9	11.0
1:2	2.4	30.0	1.2	15.4
1:1	2.5	31.7	1.4	18.2
2:1	2.6	32.9	1.7	22.1
3:1	2.5	32.5	1.8	23.3

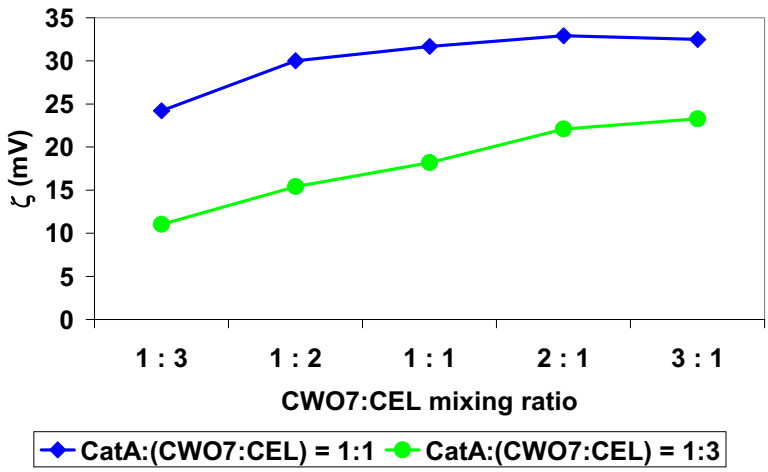

Figure 4.20. Zeta potential (ζ) values of nano-emulsions of the Water / [CatA:(CWO7:CEL)] / [6 wt% EC10 in ethyl acetate] system as a function of CWO7:CEL mixing ratio with the O/S ratio 70/30 and 95 wt% of water content after dilution to a concentration of 20 mg/g, at 25°C.

Surface charge values for the CWO7:CEL mixing ratio 0:1 (CatA:CEL ratio 1:1) are 32.2 mV (μ = 2.5) and hence comparable to the values of the plateau, obtained for CatA:(CWO7:CEL) of 1:1. Zeta potential values for the CWO7:CEL mixing ratio 1:0, that is, for the CatA:CWO7 ratio 1:1 (30.5 mV, μ = 2.4) and for the CatA:CWO7 ratio 1:3 (47.2 mV, μ = 3.7, see **Table 4.14**), are higher than those shown in the graphs in **Figure 4.20**.

Nano-emulsions showed sedimentation within less than 24 hours after preparation. They are significantly less stable than those of the CatA:CWO7 system with the same ratios. Possible reasons for this phenomenon like sterical effects, high polymer density and high polydispersity have been mentioned earlier.

Effect of polymer concentration

The same compositions as described previously were tested with 10 wt% polymer concentration. Droplet sizes and polydispersity indices are represented in **Table 4.24**.

Table 4.24. Droplet diameters and polydispersity indices (PI) of nano-emulsions of the Water / [CatA:(CWO7:CEL)] / [10 wt% EC10 in ethyl acetate] system with the O/S ratio 70/30 and 95 wt% of water content at 25ºC, as obtained with DLS.

CWO7:CEL mixing ratio	CatA:(CWO7:CEL) = 1:1		CatA:(CWO7:CEL) = 1:3	
	droplet diameter (nm)	PI	droplet diameter (nm)	PI
1:1	172.3	0.20	174.0	0.27
2:1	N.D.		157.3	0.27
3:1	165.2	0.47	144.5	0.36

N.D.: not determined

Droplet sizes are above 140 nm and show polydispersity indices between 0.20 and 0.50. Compared to the corresponding nano-emulsions formed with 6 wt% EC10 (**Table A 9.3** in the Appendix), droplets are significantly larger. The same phenomenon has been observed with nano-emulsions of the CatA:CWO7

system containing 6 and 10 wt% EC10, described in **Section 4.1.3.** The increase of polymer concentration might lead to the formation of larger droplets as mentioned earlier.

With the CatA:CWO7 system, where nano-emulsions with 10 wt% EC10 were only obtained for the ratio 1:3, droplet sizes were in the same size range (150 nm) with similar polydispersity (PI 0.41).

Surface charge values, shown in **Table 4.25**, with CatA:(CWO7:CEL) ratio 1:1 system are between +30 and +35 mV. For nano-emulsions of the CatA:(CWO7:CEL) ratio 1:3 system, zeta potential values are reduced to about half due to less amount of cationic surfactant present in the mixture. With the latter mentioned ratio, surface charge values are slightly increasing with increasing content of CWO7. It is likely that the surfactant structures and their arrangement along the interface of the droplets might play a role.

Table 4.25. Electrophoretic mobility (μ) and zeta potential (ζ) values of nano-emulsions of the Water / [CatA:(CWO7:CEL)] / [10 wt% EC10 in ethyl acetate] system with the O/S ratio 70/30 and 95 wt% of water content, at a concentration of 20 mg/g, at 25°C.

CWO7:CEL mixing ratio	CatA:(CWO7:CEL) = 1:1		CatA:(CWO7:CEL) = 1:3	
	μ (μmcm/Vs)	ζ (mV)	μ (μmcm/Vs)	ζ (mV)
1:1	2.4	31.2	1.4	17.6
2:1	N.D.		1.6	20.7
3:1	2.6	33.1	1.7	21.5

N.D.: not determined

Compared to these results, zeta potential values of the nano-emulsions of the CatA:CWO7 ratio 1:3 system are in the same order (+23 mV; μ = 1.8).

Nano-emulsions obtained with 10 wt% EC10 showed visual low stability with sedimentation the same day of preparation. The sedimentation rates calculated from Stokes' law (**Table A 9.5** in the Appendix) are between 0.9 and 1.3 nm/s and thus are equal to or slightly higher than those calculated for corresponding nano-emulsions with 6 wt% EC10 (see **Table A 9.4** in the Appendix) which would mean that nano-emulsions with both polymer concentrations would show a comparable stability. This is in agreement with the stability assessed visually.

Nano-emulsions are visually less stable than those obtained with 10 wt% EC10 of the CatA:CWO7 = 1:3 system (3 days).

Summary

Nano-emulsions with O/S ratio 70/30 and 95 wt% water content have been obtained in the Water / [CatA:(CWO7:CEL)] / [6 wt% EC10 in ethyl acetate] systems with CatA:(CWO7:CEL) ratios 1:1 and 1:3. They showed droplet sizes between 115 and 160 nm and polydispersity indices between 0.25 and 0.36. Smallest nano-emulsions were obtained with CWO7:CEL mixing ratio 1:1. Surface charge values for nano-emulsions were between +11 and +33 mV and showed an increase with increasing CWO7 content. Zeta potential values for the CatA:(CWO7:CEL) ratio 1:3 were significantly lower than those of the CatA:(CWO7:CEL) ratio 1:1 which was attributed to a lower content of cationic surfactant. Stability assessed visually of all nano-emulsions was below 1 day. Droplet sizes, using a higher polymer concentration, were larger than those obtained with 6 wt% EC10, surface charges were in the same range and stability assessed visually revealed that nano-emulsions were less stable.

The following conclusions can be made:

- Mixing the two castor oil derived surfactants with significantly different HLB numbers did not contribute to a further improvement of the formation of kinetically stable nano-emulsions.
- Droplet sizes are similar to those of the CatA:CWO7 system.
- Nano-emulsions stability, assessed visually, was not improved.
- It was confirmed that the use of a higher polymer concentration (10 wt%) does not improve the formation of kinetically stable nano-emulsions.

4.1.5. NANO-EMULSIONS IN THE AQUEOUS SOLUTION / CATA:CREMOPHOR® EL / POLYMER SOLUTION SYSTEM

As reported in the previous chapter, mixing CatA with a mixture of the two castor oil derived surfactants with significantly different HLB numbers did not improve the formation of kinetically stable nano-emulsions. It was considered of

interest to study if nano-emulsion formation could be improved by mixing CatA with only the high HLB surfactant, CEL. As it was assumed that for the CatA:CEL ratio 1:1 system zeta potential values would be higher than those of the ratio 1:3, which was already evidenced with the CatA:CWO7 system (**Section 4.1.3**, **Table 4.14**), the CatA:CEL mixing ratio of 1:1 was chosen in order to have a surface charge suitable for future applications (e.g. complexation with biomolecules). Different types of aqueous solutions, such as phosphate buffered saline or HEPES solution which provide physiological pH values (see **Section 4.1.1**), were used. The aqueous solution content was fixed at 95 wt%. As evidenced in the studies with the CatA:CWO7 and the CatA:(CWO7:CEL) systems, formation of kinetically stable nano-emulsions was not improved using a high polymer concentration (10 wt%). Therefore, the polymer solution content was kept at 6 wt%.

Effect of buffer solution

Nano-emulsion formation region and Phase Inversion determination

Nano-emulsion formation was studied using MilliQ® water and two buffer solutions set at the physiological pH (7.4), a phosphate saline buffer (PBS, 0.16 M) and a HEPES solution (20 mM). **Table 4.26** lists all relevant properties of these aqueous solutions. **Figure 4.21** shows the nano-emulsion region obtained with water as aqueous phase.

Table 4.26. pH, osmolarity, conductivity and solutes of each aqueous solution.

	PBS (0.16 M)	Water	HEPES solution
Solutes	$NaH_2PO_4 \cdot H_2O$ (Sodium dihydrogen phosphate monohydrate) $Na_2HPO_4 \cdot 2\ H_2O$ (di-Sodium hydrogen phosphate dihydrate) NaCl (Sodium chloride)	H_3O^+ (hydronium cation) OH^- (hydroxide anion)	$C_8H_{18}N_2O_4S$ (4-(2-Hydroxyethyl)piperazine-1-ethanesulfonic acid)
pH	7.4	5.6	7.4
Osmolarity (mOsm/kg)	~280	~0	~33
Conductivity (µS/cm)	~15970	~1.66	~640

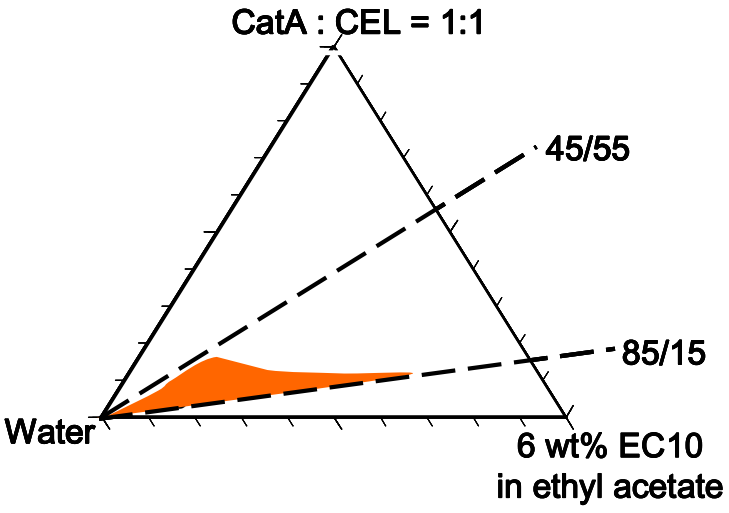

Figure 4.21. Oil-in-water (O/W) nano-emulsion region in the Water / [CatA:CEL = 1:1] / [6 wt% EC10 in ethyl acetate] system, at 25°C.

Nano-emulsions were obtained between the O/S ratios 45/55 and 85/15 and above 30 wt% of water content. As observed in the previously studied systems, the nano-emulsions also appeared more transparent at higher water contents. **Figure 4.22** shows nano-emulsion regions obtained using buffer solutions instead of water.

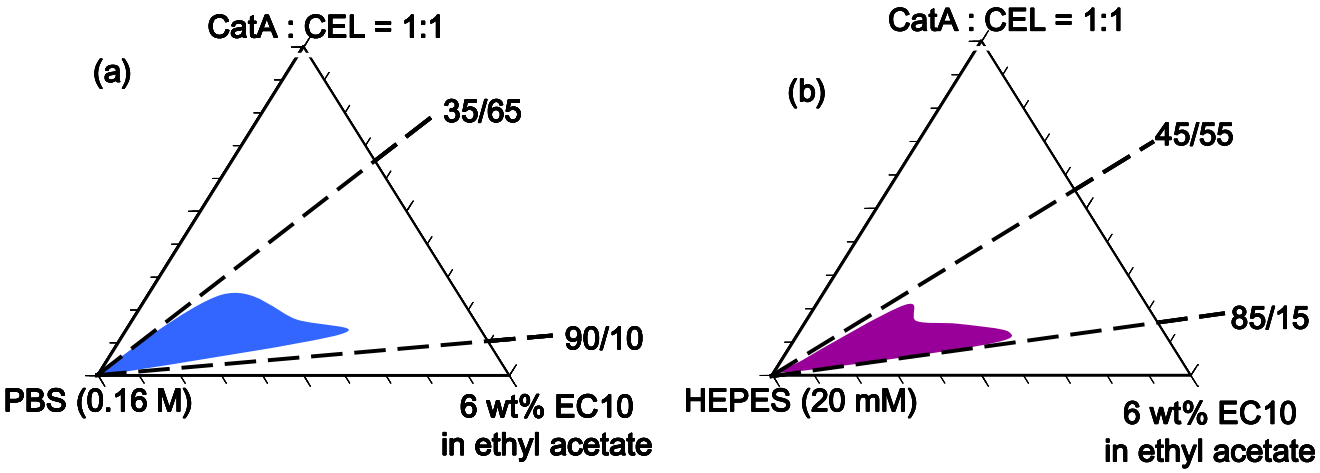

Figure 4.22. Oil-in-water (O/W) nano-emulsion region in the Aqueous solution / [CatA:CEL = 1:1] / [6 wt% EC10 in ethyl acetate] system at pH 7.4 with **a)** PBS solution (0.16 M), and **b)** HEPES solution (20 mM), at 25°C.

Independently of the aqueous solution, nano-emulsion regions of the CatA:CEL system were larger than those obtained with CatA:Span® 80 or CatA:CWO7 system.

In the system with PBS, nano-emulsions were formed in a wider range of O/S ratios, between 35/65 and 90/10, and above 33 wt% PBS content (**Figure 4.22a**). Nano-emulsions in the system with HEPES solution formed between the same O/S ratios as with water and above 35 wt% HEPES solution content. The nano-emulsion regions obtained with the different aqueous solutions show a similar shape, stretching to lower aqueous solution contents at higher O/S ratios, suggesting that O/S ratios between 70/30 and 85/15 favor the formation of nano-emulsions. The largest region is formed with PBS. As the pH of both, HEPES and PBS solution, is 7.4, the differences could be attributed to the nature of the solutes might play a role.

To confirm that nano-emulsions were formed through phase inversion, conductivity measurements were performed along an experimental path with a

constant O/S ratio. **Figure 4.23** provides the conductivity values of samples with constant O/S ratio of 70/30 as a function of aqueous solution content at 25°C.

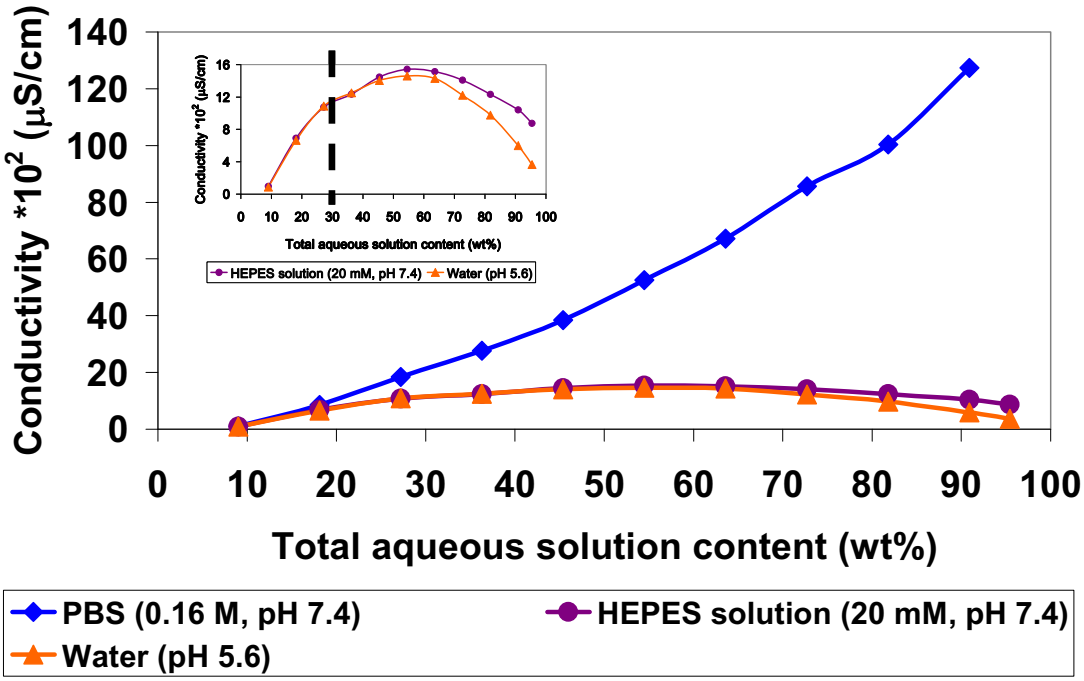

Figure 4.23. Conductivity (*10^2) as a function of total aqueous solution content in the Aqueous solution / [CatA:CEL = 1:1] / [6 wt% EC10 in ethyl acetate] system along the dilution path with the O/S ratio of 70/30, with water (pH 5.6), phosphate buffered saline (PBS, 0.16 M, pH 7.4) and HEPES solution (20 mM, pH 7.4), at 25°C. The inset corresponds to a magnification of the graphs obtained with water and HEPES solution.

Conductivity values with PBS show a different trend than those with water and HEPES. With increasing amount of phosphate buffer, the conductivity increases due to the increasing amount of electrolyte species. Therefore, inversion could not be assessed by conductivity for this system. Conductivity values of samples containing water or HEPES solution do not differ significantly. HEPES solution contains zwitterionic molecules. At neutral pH the quantity of cationic and anionic charges are equal which makes the buffer solution to behave like water. As observed in the conductivity studies of the previous systems, conductivity values increase with increasing aqueous solution content and reach a maximum, which in this system is produced at about 1500 µS/cm. Then, conductivity values gradually decrease due to the effect of dilution of the conducting species. Conductivity values with both continuous phases are comparable to the values obtained with the CatA:Span® 80 system. This could be explained due to the same cationic:nonionic surfactant mixing ratio of 1:1 and thus the same conductive species in both systems as well as by the same concentration of

polymer. The phase inversion was assessed to take place at about 30 wt% aqueous solution where conductivity values fluctuated.

Nano-emulsion characterization

Nano-emulsions formed with 95 wt% of PBS (0.16 M, pH 7.4) were very unstable. A possible reason for the instability could be the high concentration of ions in the buffer. However, some trials were undertaken by diluting the PBS buffer so that the content of NaCl (initially 8 g) decreased up to 0.08 g. Nano-emulsions were prepared with 95 wt% of different PBS dilution and with the O/S ratio 70/30. With each dilution, transparent nano-emulsions were obtained which, however, were very unstable and showed sedimentation directly after preparation. Furthermore, it was noted that with decreasing NaCl content, sedimentation seemed to appear less strongly. For that reason, another trial was undertaken using a buffer solution without NaCl, PB (0.01M). The nano-emulsion with the O/S ratio 70/30 and 95 wt% PB could be formed with a transparent appearance and an improved visual stability (up to 2 days). These results let conclude that the presence and quantity of ions has an influence on the formation of nano-emulsions. No further characterization studies on the PBS or PB systems were carried out.

Figure 4.24 provides the droplet sizes and **Table A 9.6** in the Appendix also polydispersity indices (PI) of nano-emulsions with 95 wt% of water and HEPES solution.

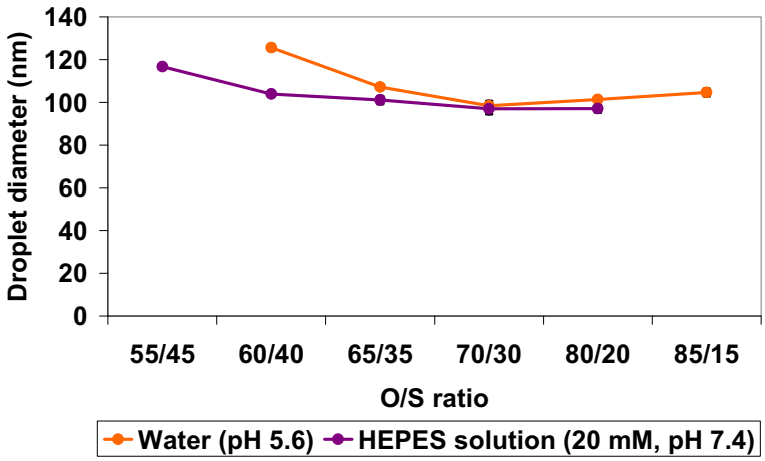

Figure 4.24. Droplet diameters of nano-emulsions of the Aqueous solution / [CatA:CEL = 1:1] / [6 wt% EC10 in ethyl acetate] system as a function of O/S ratio with 95 wt% of aqueous solution content, with water (pH 5.6) and HEPES solution (20 mM, pH 7.4), at 25ºC, as obtained with DLS.

As the polydispersity is high, only trends can be discussed. Nano-emulsion droplet size with both continuous phases decreases with increasing O/S ratio, reaching a minimum / plateau at the O/S ratio 70/30. This effect is more striking at lower O/S ratios and is shifted to higher O/S ratios for water. The reason for the decrease in droplet size might be explained by the solvent diffusion effect as discussed earlier. This trend is similar to that observed for nano-emulsions of the CatA:CWO7 system with a ratio of 1:3 whereas droplet sizes are smaller than those. Polydispersity indices (PIs) are high (up to 0.51) and fairly constant with both aqueous solutions with increasing O/S ratio (see **Table A 9.6** in the Appendix).

From droplet size values, the sedimentation rates of nano-emulsions were calculated applying the Stokes' law in order to have an estimation on nano-emulsion stability. Sedimentation rates range between 0.4 and 0.8 nm/s (**Table A 9.7** in the Appendix) which suggests a significantly higher stability than nano-emulsions of the CatA:Span® 80 system (values equal to or greater than 3 nm/s, see **Section 4.1.2, Table 4.8**). They are also lower in comparison to the CatA:CWO7 (between 0.7 and 2.4 nm/s, **Section 4.1.3, Table 4.16**) and the CatA:(CWO7:CEL) system (between 0.6 and 1.3 nm/s, Section 4.1.4, **Table A 9.4** in the Appendix).

The surface charge values of as-prepared nano-emulsions of the systems with water and HEPES solution are shown in **Table 4.27** and plotted in **Figure 4.25**.

With both studied aqueous phases, electrophoretic mobility and therefore zeta potential decreases slightly with increasing O/S ratio. As mentioned earlier, this can be explained by the decrease of cationic species with increasing O/S ratio. Values in water are around +32 mV while values in HEPES solution are about +20 mV. This decrease in surface charge may be attributed to the fact that HEPES molecules, which are zwitterionic, might have a shielding effect by placing themselves on the droplet interface and thus lowering the zeta potential. Zeta potential values in water are about 20 mV lower than those of the CatA:CWO7 = 1:1 (about +50 mV, **Table 4.14**).

Table 4.27. Electrophoretic mobility (μ) and zeta potential (ζ) values of nano-emulsions of the Aqueous solution / [CatA:CEL = 1:1] / [6 wt% EC10 in ethyl acetate] system with 95 wt% of aqueous solution content , in water (pH 5.6) and HEPES solution (20 mM, pH 7.4), at 25°C.

O/S ratio	Water		HEPES solution	
	μ (μmcm/Vs)	ζ (mV)	μ (μmcm/Vs)	ζ (mV)
55/45	x[(1)]	x[(1)]	1.7	21.5
60/40	2.8	35.6	1.7	21.9
65/35	2.6	33.4	1.6	20.2
70/30	2.5	32.2	1.5	19.1
80/20	2.4	30.2	1.4	18.4
85/15	2.4	30.2	x[(1)]	x[(1)]

. [(1)] As nano-emulsions were very instable, values are not included

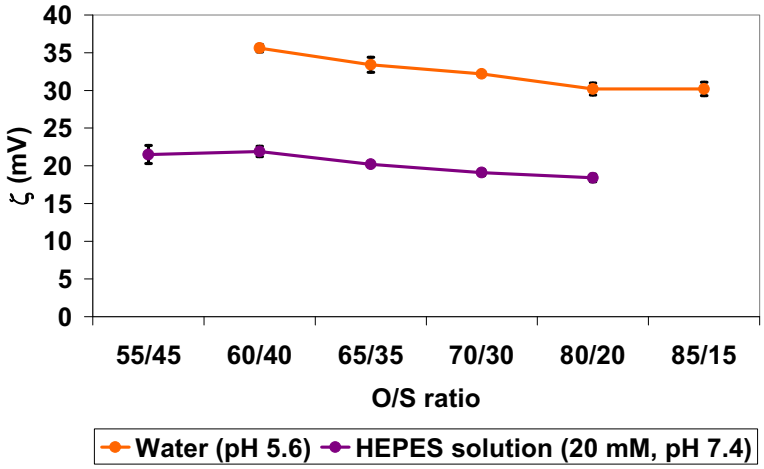

Figure 4.25. Zeta potential (ζ) values of nano-emulsions of the Aqueous solution / [CatA:CEL = 1:1] / [6 wt% EC10 in ethyl acetate] system as a function of O/S ratio with 95 wt% of aqueous solution content, with water and HEPES solution (20 mM, pH 7.4), at 25°C.

The stability of the nano-emulsions was first followed by visual observation. Results are shown in **Figure 4.26**. The occurring instability observed was sedimentation which could, among others, be explained by the high polymer density and polydispersity which have been mentioned several times. Nano-emulsions with very low (O/S ratio 55/45) and very high O/S ratios (O/S ratios 80/20 and 85/15) show the lowest stability. A possible explanation could be that with low O/S ratios, larger droplets are formed resulting in less stable nano-emulsions. Furthermore, it can be assumed that with high oil phase content in the nano-emulsion, the low surfactant concentration might not be sufficient for stabilizing the droplets, resulting in the formation of large droplets and in a reduced nano-emulsion stability. However, droplet size is lower at high O/S ratios than at low O/S ratios (**Figure 4.24**). It should be noted that diffusion of solvent from the oil to the aqueous phase may account for the lower droplet size at high O/S ratios.

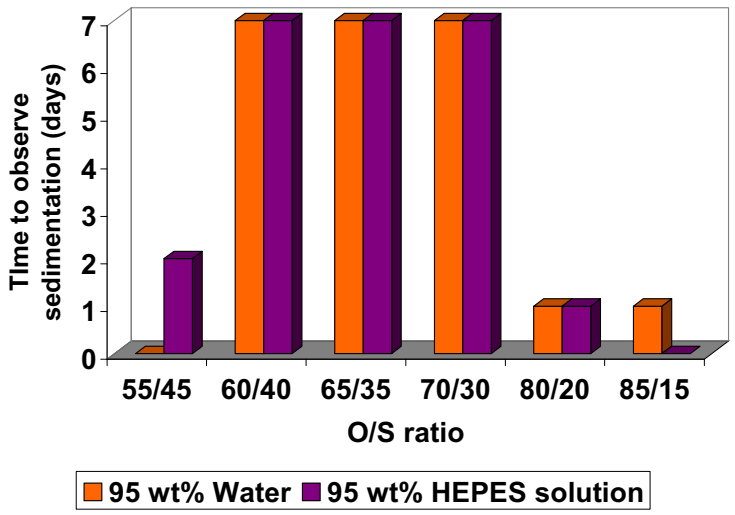

Figure 4.26. Stability by visual observation of nano-emulsions of the Aqueous solution / [CatA:CEL = 1:1] / [6 wt% EC10 in ethyl acetate] system with 95 wt% aqueous solution content as a function of the O/S ratio, at 25°C.

The nano-emulsions with O/S ratios from 60/40 to 70/30 show a visual stability of about a week with both aqueous solutions. Surface charges are in water around +30 mV and which might let assume a good electrostatic stability while values in HEPES solution are about +20 mV where less electrostatic stabilization is expected.

Therefore, further studies were focussed on nano-emulsions with O/S ratio 70/30, the most stable visually and with the smallest droplet size.

Apart from assessing stability visually, further stability analysis was carried out by measuring the backscattering intensity with time along the sample height. **Figure 4.27** shows the backscattering intensity of nano-emulsions (O/S ratio 70/30, 95 wt% aqueous solution content) with both aqueous phases. It is visible that in both graphics the intensity is flat on the whole sample height and remains constant (at 12% with water, at about 14% with HEPES solution) with time. This indicates that samples are homogenous and stable during the first 24 hours after their preparation.

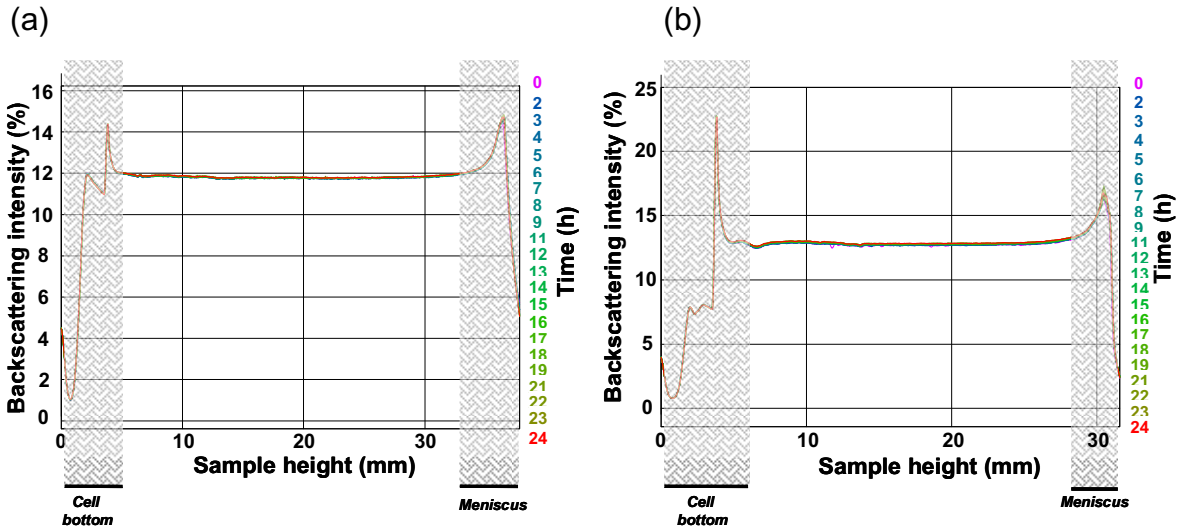

Figure 4.27. Backscattering data of the nano-emulsions of the Aqueous solution / [CatA:CEL = 1:1] / [6 wt% EC10 in ethyl acetate] system with the O/S ratio 70/30 and 95 wt% aqueous solution content a) in water and b) in HEPES solution, at 25°C.

Nano-emulsion stability was also assessed by measuring the changes of nano-emulsion droplet size as a function of time (**Figure 4.28**). These measurements were carried out in the supernatant. No sedimentation was observed in the DLS tubes during the indicated timeframe which may let assume that nano-emulsions were stable during 7 days. It has to be taken into account that, as mentioned above, due to the high polydispersity values (PI > 0.3), the real value can not be shown.

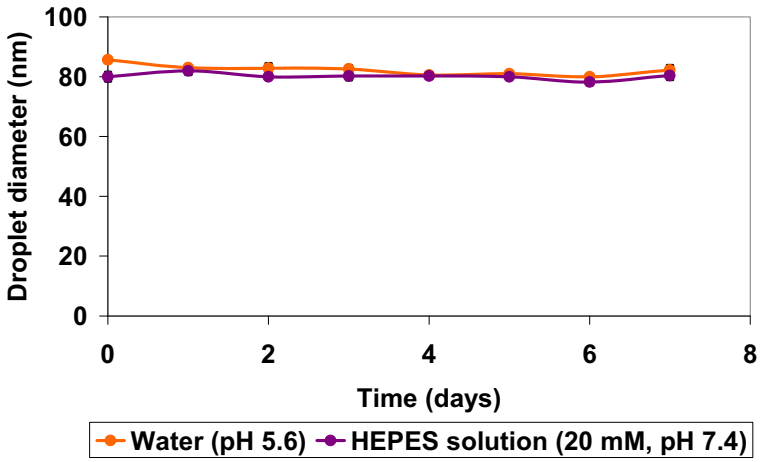

Figure 4.28. Droplet diameter of the nano-emulsion of the Aqueous solution / [CatA:CEL = 1:1] / [6 wt% EC10 in ethyl acetate] system with an O/S ratio of 70/30 and 95 wt% of aqueous solution content as a function of time, at 25ºC.

The main purpose of this thesis was to use nano-emulsions as templates for nanoparticles for biomedical applications. In preclinical tests, e.g. in *in vitro* hemolysis, adjustment of the osmolarity is required. Therefore, preliminary studies were carried out adjusting the osmolarity of the aqueous phase. Thus, it was intended to adjust the osmolarity of the HEPES solution (~ 33 mOsm/kg, see **Table 4.25**) to the value of the PBS solution (~280 mOsm/kg) which is known to be appropriate for the above mentioned tests on cells as its osmolarity value is in the range of the that of the used blood (275 – 300 mOsm/kg). HEPES buffered glucose (HBG) solutions with different glucose concentrations were prepared in order to find out the right conditions for subsequent studies. **Figure 4.29** shows osmolarity values obtained for different HBG solutions.

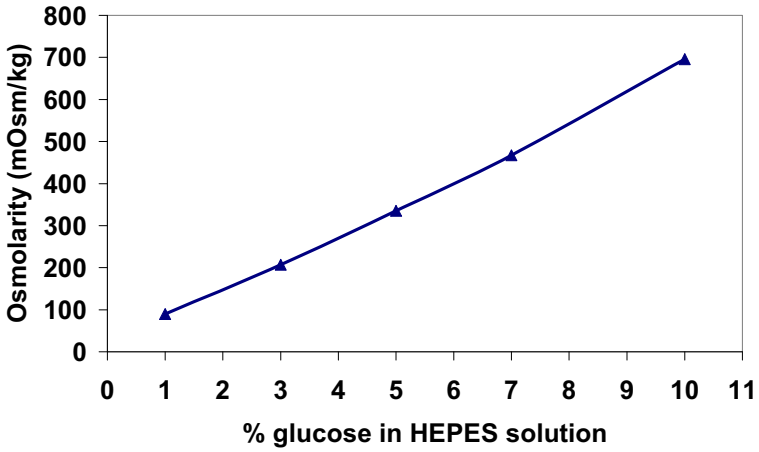

Figure 4.29. Osmolarity of the HEPES buffered glucose (HBG solution) as a function of glucose content (%) in the buffer solution.

From the graph it can be seen that osmolarity increases with increasing glucose concentration and that the required blood osmolarity is reached at a glucose concentration between 3 and 5%. Therefore, further precise studies were carried out, shown in **Figure 4.30**.

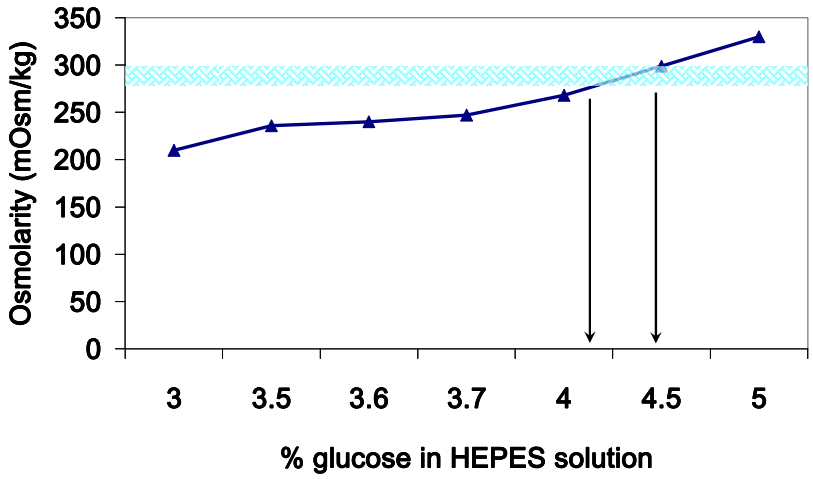

Figure 4.30. Osmolarity of the HEPES buffered glucose (HBG solution) as a function of glucose content (%) in the buffer solution. In light blue is marked the aimed osmolalarity range, the arrows mark the required % glucose concentration in the HEPES solution.

The required range necessary for the above mentioned tests is reached at about 4.3 – 4.5% glucose concentration. That glucose concentration is similar to that used in literature (HBG, 5% glucose) [**Kircheis, 2001; Schwerdt, 2008**].

Additional studies were undertaken in order to determine the effect of the different glucose containing HEPES solutions on nano-emulsion formation as well as the effect on nano-emulsion droplet size and surface charge. With each buffer solution, the nano-emulsions with O/S ratio 70/30 and 95 wt% aqueous solution content were prepared. Nano-emulsions with a translucent appearance were obtained. The results (**Figure 4.31**) show that droplet diameters and surface charge values are constant with increasing glucose concentration in the aqueous solution and are similar to values of the nano-emulsions with the same composition but without glucose (~100 nm and +20 mV). This suggests that glucose incorporated into the HEPES solution has no influence on nano-emulsion droplet size or surface charge.

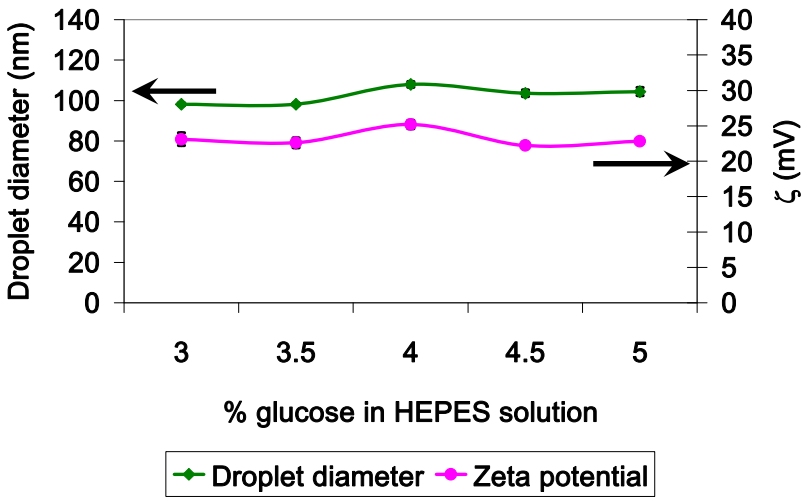

Figure 4.31. Droplet diameter (nm) and zeta potential (ζ) values of the nano-emulsion of the Aqueous solution / [CatA : CEL = 1:1] / [6 wt% EC10 in ethyl acetate] system with an O/S ratio of 70/30 and 95 wt% of aqueous solution content as a function glucose concentration (%) in the HEPES solution, at 25ºC.

Effect of polymer molecular weight

The system was modified by changing the oil component. A polymer of the same type but with a lower molecular weight than EC10, EC4, was used in order to see if nano-emulsions were formed and if it would improve the nano-emulsion properties. The polymer concentration was maintained at 6 wt%. The studies were focussed on nano-emulsions formed with water and HEPES solution (20 mM, pH 7.4) as aqueous solutions.

Figure 4.32a shows the nano-emulsion regions obtained for the Aqueous Solution / [CatA:CEL = 1:1] / [6 wt% EC4 in ethyl acetate] system. Nano-emulsions are formed with water between O/S ratios 40/60 and 90/10 and above 35 wt% water content and with HEPES solution between the O/S ratios 35/65 and 95/05 and above 25 wt% HEPES solution content.

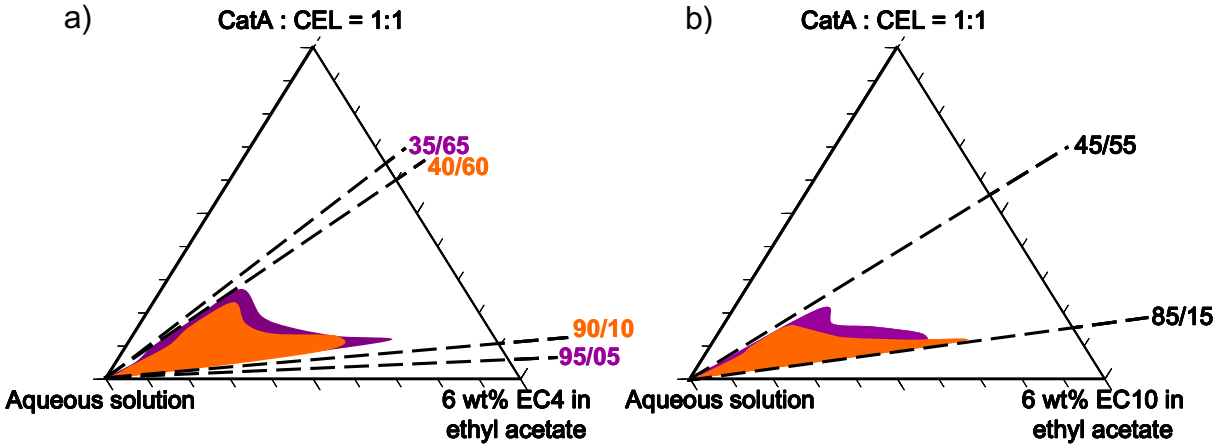

Figure 4.32. Oil-in-water (O/W) nano-emulsion region in the Aqueous solution / [CatA:CEL = 1:1] / 6 wt% polymer solution system with water (pH 5.6) and HEPES solution (20 mM, pH 7.4), for **a)** EC4 and **b)** EC10, at 25°C.

The comparison of the nano-emulsion regions with EC4 (**Figure 4.32a**) to those obtained with EC10 (**Figure 4.32b**) reveals that those formed with 6 wt% EC4 are slightly larger.

Droplet sizes and polydispersity indices (PI) are shown in **Figure 4.33** (and summarized in **Table A 9.8** in the Appendix). The displayed trend is similar to that obtained with 6 wt% EC10 and also to that of the CatA:CWO7 system. Droplet sizes with low O/S ratios are high and decrease with increasing O/S ratio, reaching a minimum/plateau (O/S ratios 70/30 and 80/20) with both aqueous solutions. As observed for 6 wt% EC10, droplet sizes with HEPES solution are slightly smaller than those obtained with water. However, the polydispersity indices are higher.

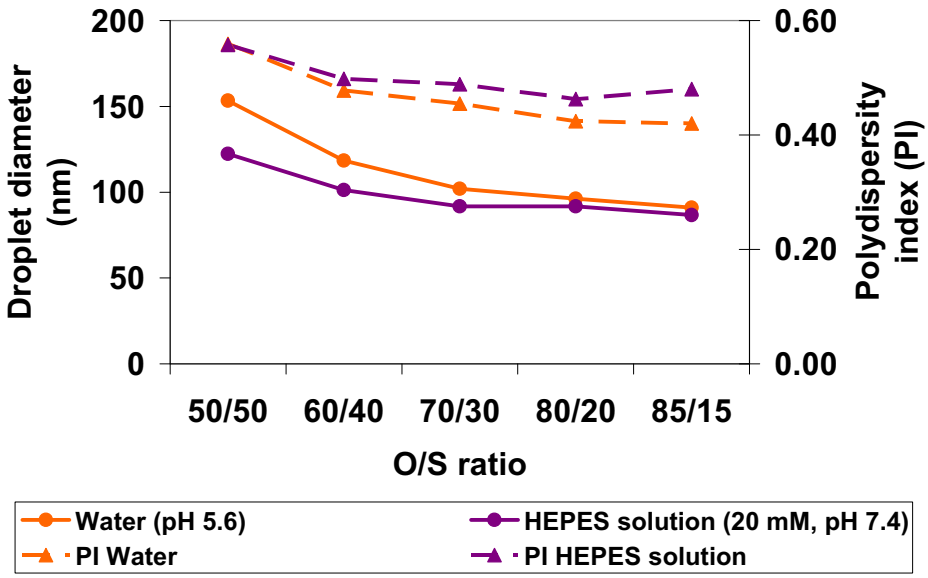

Figure 4.33. Droplet diameters and polydispersity indices (PI) of nano-emulsions of the Aqueous system / [CatA:CEL = 1:1] / [6 wt% EC4 in ethyl acetate] system as a function of the O/S ratio, with 95 wt% aqueous solution content, at 25ºC, as obtained with DLS.

Calculated sedimentation rates (shown in **Table A 9.9** in the Appendix) are between 0.4 and 1.1 nm/s. They are comparable to those obtained with 6 wt% EC10 and indicate a good stability of the nano-emulsions. As with 6 wt% EC10, stability against sedimentation seems to increase with increasing O/S ratio as sedimentation values decrease and are significantly lower than those of the previously studied systems. This suggests a higher stability of nano-emulsions of this system than that of all previously studied.

Zeta potential values are summarized in **Table 4.28** and displayed in **Figure 4.34**. The surface charge values decrease with increasing O/S ratio according to the decrease in amount of cationic surfactant. This trend has been observed previously with 6 wt% EC10 and also for the CatA:Span® 80 system and for the CatA:CWO7 ratio 1:3 system. As with 6 wt% EC10, zeta potential values are higher in water (between +25 and +30 mV) than in HEPES solution (between +15 and +25 mV) which might come from the shielding effect of the HEPES molecules as explained above.

Table 4.28. Electrophoretic mobility (μ) and zeta potential (ζ) values of nano-emulsions of the Aqueous solution / [CatA:CEL = 1:1] / [6 wt% EC4 in ethyl acetate] system with 95 wt% of aqueous solution content, at 25°C.

O/S ratio	Water		HEPES solution	
	μ (μmcm/Vs)	ζ (mV)	μ (μmcm/Vs)	ζ (mV)
50/50	2.3	29.7	1.9	24.0
60/40	2.3	29.6	1.4	17.7
70/30	2.1	26.2	1.4	18.0
80/20	2.0	25.8	1.3	16.1
85/15	1.5	18.6	0.9	11.8

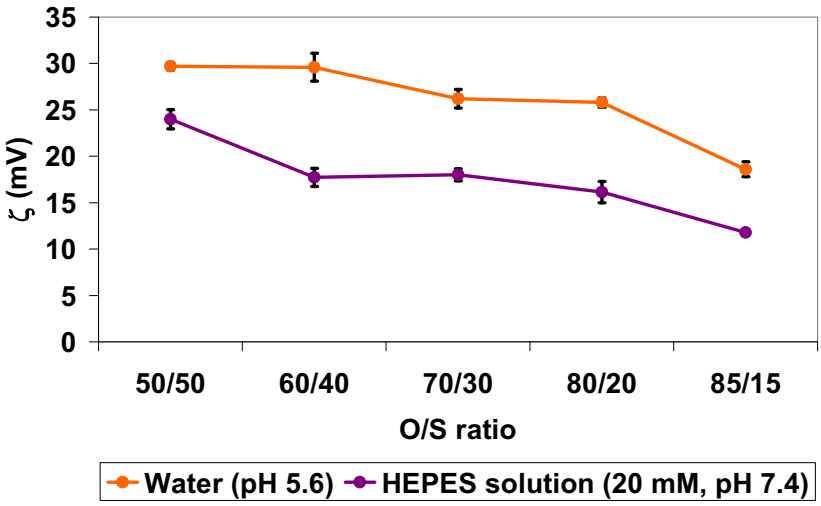

Figure 4.34. Zeta potential (ζ) values of nano-emulsions of the Aqueous solution / [CatA:CEL = 1:1] / [6 wt% EC4 in ethyl acetate] system as a function of O/S ratio, with 95 wt% of aqueous solution content, at 25°C.

The stability of nano-emulsions with an O/S ratio of 70/30 and 95 wt% aqueous solution was assessed by measuring the backscattering intensity and by measuring the droplet diameter as a function of time. Results obtained from the backscattering intensity measurements are provided in **Figure 4.35**. The backscattering intensity keeps steady during the whole sample height. This let assume that samples were homogenous and stable during 24 hours after preparation.

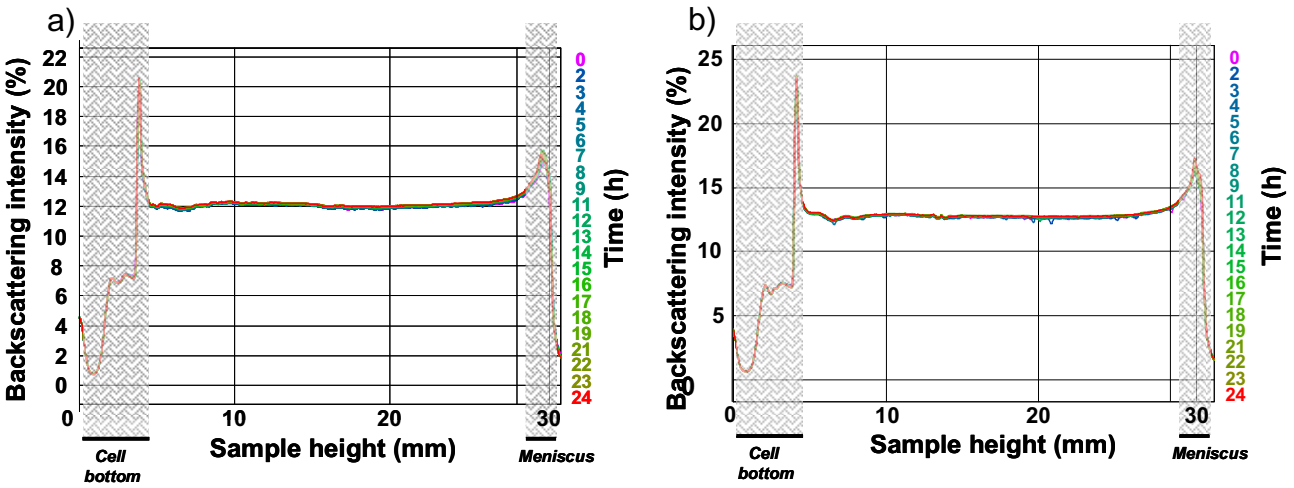

Figure 4.35. Backscattering data of the nano-emulsions of the Aqueous solution / [CatA:CEL = 1:1] / [6 wt% EC4 in ethyl acetate] system with an O/S ratio of 70/30 and 95 wt% **a)** water and **b)** HEPES content, at 25°C.

Stability of the nano-emulsion with an O/S ratio of 70/30 and 95 wt% aqueous solution was furthermore assessed by measuring the droplet diameter as a function of time. As before, the measurements were carried out in the supernatant. No sedimentation was observed in the DLS tubes during that timeframe indicating that nano-emulsions are stable during at least 28 days Figure 4.36).

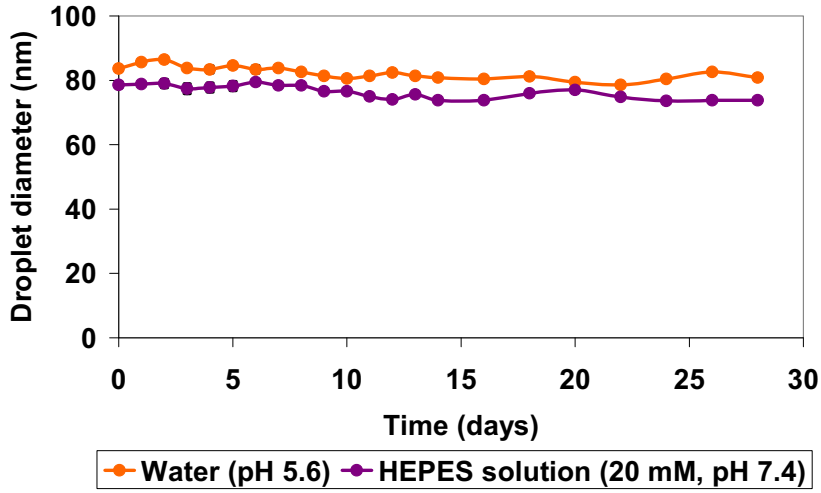

Figure 4.36. Droplet diameter of the nano-emulsion of the Aqueous solution / [CatA:CEL = 1:1] / [6 wt% EC4 in ethyl acetate] system with an O/S ratio of 70/30 and 95 wt% water and HEPES solution, respectively, as a function of time, at 25ºC.

Results obtained with backscattering analysis are in good agreement with those obtained from measuring the droplet size as a function of time and suggest a good stability of the system.

These results suggest that systems with both polymers are suitable for the preparation of nanoparticles.

Summary

Nano-emulsions have been obtained in the Aqueous solution / [CatA:Cremophor® EL = 1:1] / [6 wt% EC10 in ethyl acetate] between O/S ratio 35/65 and 90/10 and above 30 wt% aqueous solution content. The nano-emulsion region formed with Phosphate Buffered Saline (PBS) is slightly larger than those with water or HEPES solution, which have similar shapes and are formed between the same O/S ratios. Nano-emulsion regions, independent of the aqueous solution used, were larger than those obtained with the CatA:Span® 80 or the CatA:CWO7 system. Conductivity measurements, carried out to assess the existence of a phase inversion, were followed for nano-emulsions with O/S ratio 70/30 with all three aqueous solutions. While with water and HEPES solution the conductivity values are similar and phase inversion was detected, no inversion could be determined with PBS as continuous phase due to the ions present in the buffer solution. For instability reasons of nano-emulsions formed with PBS, studies were focused on nano-emulsions with water and HEPES solution as aqueous solutions. Nano-emulsion droplet sizes are small (between 97 and 126 nm) with polydispersity indices between 0.27 and 0.51. Compared to all other studied systems, the smallest droplet size was achieved with this system. The sedimentation rates are low (below 1.0 nm/s). Zeta potential values are between +18 and +36 mV (no dilution) and are higher in water than in HEPES solution. Nano-emulsions with water and HEPES solution show good visual stability with O/S ratios from 60/40 to 70/30. Droplet size measurements (by DLS) over days of these nano-emulsions revealed stability for about 4 weeks.

The effect of a polymer with a lower molecular weight, EC4, on nano-emulsion formation in water and HEPES solution was studied. Nano-emulsion regions formed with 6 wt% EC4 are similar in size and shape to those obtained with EC10. Smaller droplet sizes could be obtained while polydispersity indices remain high (above 0.42) with comparable sedimentation rates. Nano-emulsion stability visually assessed showed sedimentation within less than 1 day.

However, as with 6 wt% EC10, nano-emulsion droplet sizes with O/S ratio 70/30 and 95 wt% of water or HEPES solution was unchanged for at least 28 days.

The following conclusions can be made:

- Nano-emulsion formation using the castor oil derivative surfactant Cremophor® EL was improved compared to that using a sorbitan ester or the hydrogenated castor oil derivative surfactant CWO7. This suggests that not only the structure of the surfactant plays a significant role in nano-emulsion formation but also the HLB number.
- Castor oil derivative surfactants with a high HLB number are likely to favor nano-emulsion formation.
- Nano-emulsions could be formed with different aqueous media, distinctive in pH values and type and quantity of solutes. A high solute concentration (as in PBS) does not favor nano-emulsion formation.
- Glucose has successfully been used to adjust the osmolarity of the HEPES solution to that of blood and does not affect nano-emulsion droplet size and surface charge.
- Droplet diameters of nano-emulsions formed with water and HEPES solution are in the same order and similar stability assessed visually.
- Zeta potential of nano-emulsions with HEPES solution are about 10 mV lower than those with water due to a potential shielding effect of the HEPES zwitterionic molecules on the droplets.
- Also in this system, high O/S ratios (70/30) are favorable for nano-emulsion formation with a good stability.
- Nano-emulsions could successfully be formed with EC4, a polymer of lower molecular weight than the previous used. They are comparable in droplet sizes, surface charge and stability to those with EC10.
- Droplet sizes below 100 nm could be obtained with both polymers.

As nano-emulsions of this system have very suitable features for future applications (small droplet sizes at physiological pH, positive zeta potential of

as-prepared nano-emulsions, stability for more than 24h), the system was studied without the incorporation of the cationic surfactant.

4.1.6. NANO-EMULSIONS IN THE WATER / CREMOPHOR® EL / POLYMER SOLUTION SYSTEM

Comparing all previously studied systems, the CatA:CEL system yielding the smallest nano-emulsion droplet sizes among all, positive surface charge values and a good stability was identified as most favorable for nano-emulsion formation. Trials had shown that nano-emulsions could not be obtained in the Water / CatA / [6 wt% EC10 in ethyl acetate] system. It was considered of interest to study if formation of nano-emulsions was feasible in the system containing only the nonionic surfactant.

Nano-emulsion formation region and Phase Inversion determination

Nano-emulsions were obtained between O/S ratios 55/45 and 85/15 and water contents above 30 wt%, as shown in **Figure 4.37**, and had a transparent or translucent appearance at higher water contents. Also the region formed in the Water / [CatA:CEL = 1:1] / [6 wt% EC10 in ethyl acetate] system is indicated in the figure.

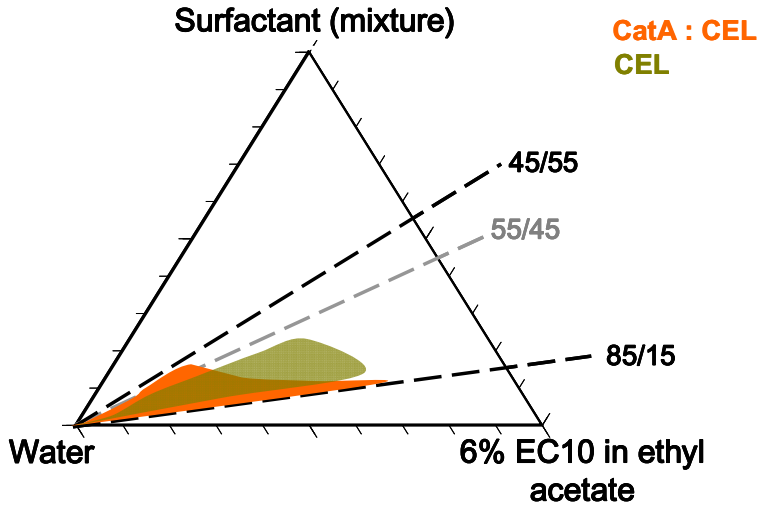

Figure 4.37. Oil-in-water (O/W) nano-emulsion region in the Water / CEL / [6 wt% EC10 in ethyl acetate] system compared to the region of the Water / [CatA:CEL = 1:1] / [6 wt% EC10 in ethyl acetate] system, at 25ºC.

Figure 4.37 shows that the nano-emulsion region formed with only CEL is narrower than that obtained with the CatA:CEL system in water. However, it is broader to lower water contents (about 30 wt% water) at higher O/S ratios (between O/S ratio 60/40 and 80/20) which let conclude that nano-emulsion formation is favored with these O/S ratios.

To evaluate if the nano-emulsions were formed through phase inversion, conductivity measurements were carried out with constant O/S ratio at 25°C (**Section 3.3.1**). Conductivity values in **Figure 4.38** increase with the increase of water content, reaching a maximum (at about 110 μS/cm) and then gradually decrease due to the effect of dilution of the conducting species. This trend has already been observed in previously studied systems. The conductivity values are significantly lower than those obtained with the other studied systems, which is associated with the absence of the cationic surfactant. It is believed that phase inversion takes place when the drastic increase in conductivity occurred, which is at around 30 wt% water, the same phase inversion region assessed for the systems studied in the previous sections.

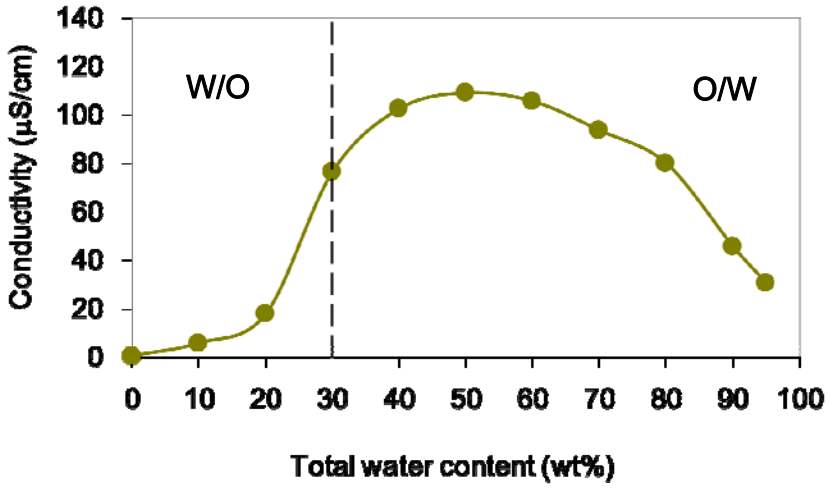

Figure 4.38. Conductivity as a function of total water content in the Water / CEL / [6 wt% EC10 in ethyl acetate] system along the dilution path at the O/S ratio 70/30, at 25ºC. Water-in-oil (W/O) and oil-in water (O/W) regions are indicated.

Nano-emulsion characterization

Nano-emulsions with 95 wt% water were obtained only in a small region of O/S ratios. **Table 4.29** shows droplet diameters and polydispersity indices of the

nano-emulsions obtained as well as those of the system with the surfactant mixture CatA:CEL system.

Table 4.29. Droplet diameters and polydispersity indices (PI) of nano-emulsions of the Water / CEL / [6 wt% EC10 in ethyl acetate] system compared to those of the CatA:CEL ratio 1:1 system, with 95 wt% of water content, obtained by DLS at 25ºC.

O/S ratio	CEL system		CatA:CEL system	
	droplet diameter (nm)	PI	droplet diameter (nm)	PI
70/30	187.6	0.24	98.4	0.32
75/25	149.2	0.26	not studied	not studied
80/20	155.0	0.25	101.4	0.29

The droplet diameters are between 150 and 200 nm and polydispersity indices around 0.25 at room temperature. The droplet diameter is minimal with the O/S ratio 75/25. This behavior could be explained with before-mentioned effects: Ethyl acetate might diffuse out of the droplets into the water phase, which leads to a decrease in droplet size. However, an increase in dispersed phase fraction can lead to an increase of droplet size which is recognized at the O/S ratio 80/20. Droplet sizes are significantly smaller when the cationic surfactant is present in the system, showing comparable polydispersity indices. Hence, these results clearly indicate that although no nano-emulsions were formed in the system containing only Cat A, this component contributes to a striking decrease of the nano-emulsion droplet size when combined with CEL. An explanation to this size decrease may be that mixed surfactant films are stronger and allow higher stability [Tadros, 2005] favoring the formation of smaller droplets and stabilizing them against destabilization mechanisms such as coalescence or Ostwald ripening.

The theoretical sedimentation rate was calculated as for previous systems applying the Law of Stokes using the hydrodynamic diameters, obtained by DLS (Table A 9.10 in the Appendix). Values are between 1.1 and 1.7 nm/s whereby those of the CatA : CEL ratio 1:1 system are significantly lower (about 0.5 nm/s), indicating a higher stability, as expected from their lower droplet size and the more rigid interfacial film obtained in mixed surfactant systems which prevent droplet size increase.

Surface charges of nano-emulsion droplets were measured with the Zetasizer Nano Z and are given in **Table 4.30,** again in comparison to those obtained with the CatA:CEL ratio 1:1 system. As expected, zeta potential values without the cationic component are in the negative range, at around – 28 mV, while when incorporating the cationic surfactant in the system, values are in the positive range (about +30 mV). However, the absolute values without and with CatA are of the same order. This may indicate that electrostatic stabilization may be comparable in both systems. **Figure 4.39** combines droplet diameter and surface charge values of the CEL system in one graph.

Table 4.30. Electrophoretic mobility (μ) and zeta potential (ζ) values of nano-emulsions of the Water / CEL / [6 wt% EC10 in ethyl acetate] system, compared to those obtained with the CatA:CEL ratio 1:1 system, at room temperature.

O/S ratio	CEL system		CatA:CEL system	
	μ (μmcm/Vs)	ζ (mV)	μ (μmcm/Vs)	ζ (mV)
70/30	-2.0	-25.7	2.5	32.2
75/25	-2.0	-25.7	not studied	not studied
80/20	-2.4	-30.9	2.4	30.2

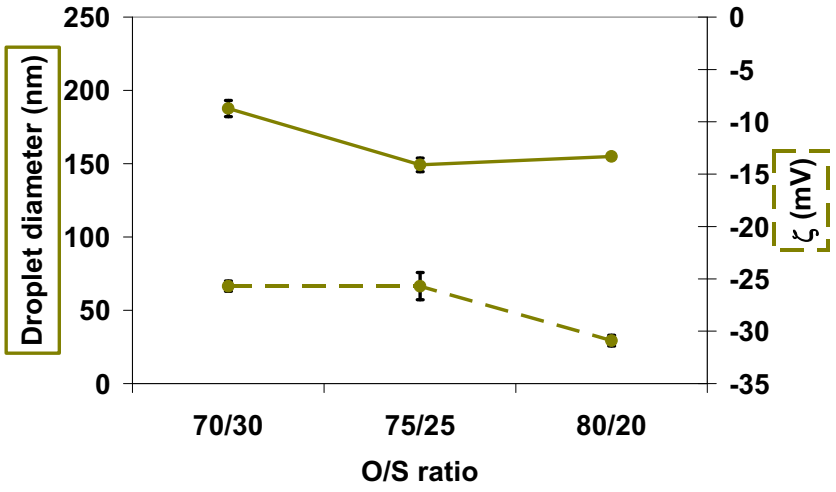

Figure 4.39. Droplet diameters and zeta potential (ζ) values of nano-emulsions of the Water / CEL / [6 wt% EC10 in ethyl acetate] system as a function O/S ratio with 95 wt% of water content, at 25°C.

Nano-emulsion stability was assessed by visual observation. Samples show sedimentation within one hour after nano-emulsion preparation. The nano-

emulsion with the O/S ratio 70/30 and 95 wt% water content of the CatA:CEL ratio 1:1 system showed a stability of one week.

Effect of polymer molecular weight

The effect of a polymer with a lower molecular weight, EC4, on nano-emulsion formation and characteristics was investigated. Nano-emulsions were obtained at the same O/S ratios as with 6 wt% EC10 (between O/S ratios of 55/45 and 85/15 and water contents above 30 wt%, **Figure 4.37**). As with 6 wt% EC10, nano-emulsions had a transparent appearance at higher water contents.

Figure 4.40 shows the graph obtained from conductivity measurements at the constant O/S ratio of 70/30 compared to that obtained with EC10, at 25°C. As with previous systems, this experiment was performed in order to determine if the nano-emulsions were formed through a phase inversion mechanism. As expected, the polymer has no effect on the conductivity. The values of both systems are in the same range and showing the same trend upon water addition which was observed previously with all other studied systems. As explained before, conductivity values increase with increasing addition of water and reach a maximum. Then, they gradually decrease due to the effect of dilution of the conducting species. As with 6 wt% EC10, values are notably lower (maximum at about 150 μS/cm) than those obtained in the other systems (maximum at about 1500 μS/cm) due to the missing cationic species.

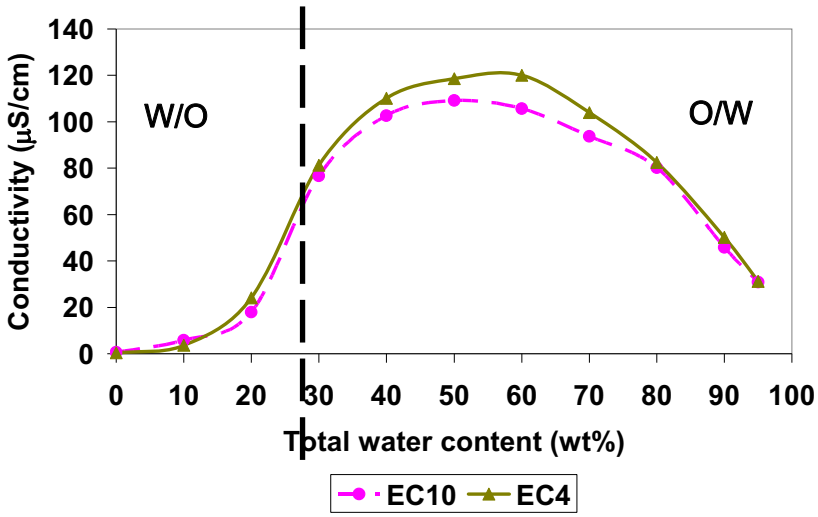

Figure 4.40. Conductivity as a function of total water content in the Water / CEL / [6 wt% polymer in ethyl acetate] system along the dilution path at the O/S ratio 70/30 at 25ºC. The graph in green represents the values obtained with **EC10** and in brown those with **EC4**.

The droplet sizes of nano-emulsions formed with 6 wt% EC4, determined by DLS, are shown together with polydispersity indices in Table 4.31. Due to the high polydispersity indices (about 0.45), the droplet sizes have to be considered cautiously. The droplet size is minimal with the O/S ratio 75/25 which has also been observed with EC10 and can be explained with the same argument used above. Compared to values obtained with 6 wt% EC10, droplet diameters are smaller (around 40 nm) and polydispersity indices are almost twice as big. A possible reason for the smaller droplet size could be that shorter polymer chains form smaller droplets and also have a reduced swelling effect in solution compared to long polymer chains. A potential consequence of the high polydispersity could be a stronger Ostwald ripening effect with EC4 than with EC10 as droplets are maybe formed less dense/compact which might facilitated the ethyl acetate to migrate from smaller to larger droplets. The more compact structure formed with EC10 might act as a barrier and prevent diffusion of the solvent to the continuous phase in the same matter as the addition of hydrophobic solvents (i.e. Squalene) to the dispersed phase in other nano-emulsion systems [Izquierdo, 2002].

Table 4.31. Droplet size, polydispersity index (PI), electrophoretic mobility (μ) and zeta potential (ζ) values of nano-emulsions of the Water / CEL / [6 wt% EC4 in ethyl acetate] system with 95 wt% of water content, at 25ºC.

O/S ratio	Droplet size		Surface charge	
	Droplet diameter (nm)	PI	μ (μmcm/Vs)	ζ (mV)
70/30	134.1	0.44	-2.0	-25.5
75/25	111.5	0.44	-1.8	-22.6
80/20	116.5	0.48	-2.1	-26.7

Table 4.31 also shows the surface charge values of nano-emulsion droplets. These are in the negative range (around -25 mV) and similar to those obtained with EC10. As above, no clear trend is notable as expected. Figure 4.41 illustrates droplet diameters and surface charge values as a function of O/S ratio.

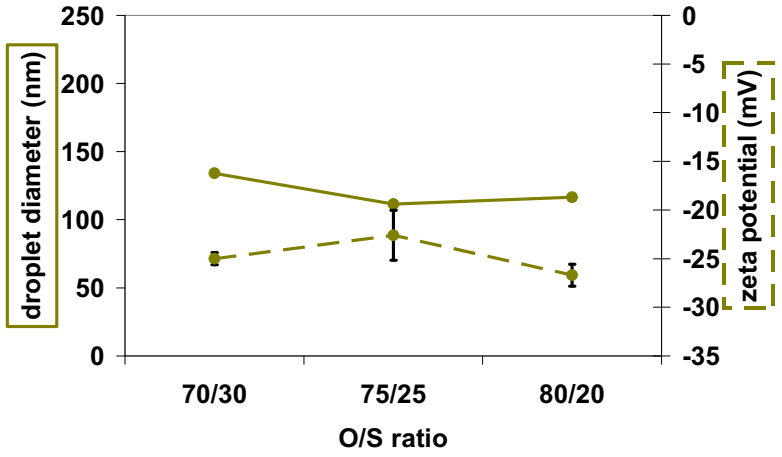

Figure 4.41. Droplet diameters and zeta potential values of nano-emulsions of the Water / CEL / [6 wt% EC4 in ethyl acetate] system as a function O/S ratio with 95 wt% of water content, at 25°C.

Nano-emulsions have been kept in a water bath at 25°C after preparation and were checked visually in order to assess their stability. Sedimentation was observed already one hour after nano-emulsion preparation. The sedimentation rates were calculated and are shown in Table A 9.11 in the Appendix. The rates are lower (around 0.7 nm/s) than those obtained with 6 wt% EC10 and rather in the range of those obtained with the CatA:CEL system, indicating a higher stability.

Summary

Nano-emulsions have been obtained in the Water / CEL / [6 wt% EC10 in ethyl acetate] system. The nano-emulsion region is formed between the O/S ratios 55/45 and 85/15 and above 30 wt% water content. Compared to the regions obtained with the CatA:CEL = 1:1 system, the region is narrower with respect to the O/S ratio but broader at lower water contents. The appearance at higher water contents is transparent. Phase Inversion was confirmed for nano-emulsions with an O/S ratio of 70/30 by conductivity measurements and takes place at about 30 wt% water content, comparable to previously studied systems. Conductivity values were significantly lower (more than 10 times) than those of the CatA:CEL ratio 1:1 system due to the missing cationic component. Nano-emulsions with 6 wt% EC10 showed droplet sizes between 150 and 200 nm and polydispersity indices are about 0.25. Droplets are larger than those obtained with the CatA:CEL ratio 1:1 system in water (droplet diameter around

100 nm). Zeta potential values for nano-emulsions are negative (around -28 mV). However, values of the corresponding nano-emulsion compositions of the CatA:CEL ratio 1:1 system are in the positive range (about +30mV) due to the cationic surfactant present. Stability assessment reveals that nano-emulsions of the CEL system show sedimentation shortly after their preparation (within hours), whereas nano-emulsions of the CatA:CEL ratio 1:1 system showed higher stability.

Nano-emulsions could also be obtained in the Water / CEL / [6 wt% EC4 in ethyl acetate] system. Nano-emulsions are formed in the same region as with EC10 (between O/S ratios 55/45 and 85/15 and above 30 wt% water content). Also in this system, phase Inversion was confirmed for the O/S ratio 70/30 by conductivity measurements and takes place at about 30 wt% water content with conductivity very similar to those of EC10. Nano-emulsions with 6 wt% EC4 show smaller droplet sizes (100 – 150 nm) than those with EC10 (150 - 200 nm) with higher polydispersity indices (0.45). Droplets formed with this polymer of lower molecular weight are larger than those obtained with the CatA:CEL ratio 1:1 system in water (around 100 nm). Zeta potential values for nano-emulsions formed with EC4 are negative (around -25 mV) and do not differ significantly from those of EC10. Nano-emulsions with EC4 show, as those with EC10, sedimentation within hours after preparation.

The following conclusions can be made:

- Nano-emulsion droplets of the system without CatA are larger with negative zeta potential values and lower stability assessed visually compared to the system with CatA.
- Using a polymer with lower molecular weight (EC4), smaller droplets could be obtained than those with EC10 but still larger than those of the CatA:CEL system. Zeta potential and stability (visually assessed) are comparable to those obtained with EC10.

4.1.7. SUMMARY ON NANO-EMULSIONS: FORMATION AND CHARACTERIZATION (SECTION 4.1.)

For nano-emulsion formation, water, HEPES solution and phosphate buffers were chosen as aqueous phase. The oil phase consisted mainly of the polymer ethylcellulose EC10 which was dissolved in ethyl acetate. Minor studies were carried out using a polymer with a lower molecular weight, EC4. The quaternized amido amine Varisoft® RTM 50 (CatA) was chosen as cationic surfactant.Among the nonionic surfactants, it was focused on Span® 80, Cremophor® WO7 and Cremophor® EL.

Nano-emulsions of the Water / [CatA:Span® 80 = 1:1] / [6 wt% EC10 in ethyl acetate] system, formed with 90 wt% water, showed droplet sizes larger than 250 nm with high zeta potential values (about 60 mV in water) with few stability visually assessed. The use of the fatty amine oleylamine did not improve the system properties and therefore this strategy was discontinued.

Nano-emulsion properties using the hydrogenated castor oil derivative surfactant Cremophor® WO7 (CWO7), mixed with CatA, were in general improved compared to that using the nonionic surfactant Span® 80, suggesting that the surfactant structure plays a significant role. Nano-emulsions with 90 and 95 wt% of water content showed comparable droplet sizes and visually assessed stability. Compared to the CatA:Span® 80 system, droplet sizes were significantly smaller (about 150 nm) with surface charge values in about the same range (up to 50 mV). Studied cationic:nonionic surfactant ratios ranged from 1:1 to 1:8 with an optimum ratio 1:3 regarding small droplet size and stability. High O/S ratios (e.g. O/S ratio 70/30) favored the formation of nano-emulsions. The use of a higher polymer concentration (10 wt%) did not improve the formation of kinetically stable nano-emulsions.

Mixing CWO7 with Cremophor® EL (CEL), a castor oil surfactant derivative with a significant higher HLB number, did not contribute to a further improvement of the formation of kinetically stable nano-emulsions. Droplet sizes were similar to those of the CatA:CWO7 system with lower stability assessed visually. Also in

this system, the use of a higher polymer concentration (10 wt%) did not improve the formation of kinetically stable nano-emulsions.

Nano-emulsion properties with the CatA:CEL system were improved compared to systems with Span® 80 or CWO7, suggesting that aside from the surfactant structure, the HLB number plays a significant role in nano-emulsion formulation. Nano-emulsions could be formed with different aqueous media, distinctive in pH values and type and quantity of solutes. A high solute concentration (as in PBS) does not favor nano-emulsion formation. Glucose has successfully been used to adjust the osmolarity of the HEPES solution to that of blood and did not influence nano-emulsion droplet size and surface charge. Droplet diameters of nano-emulsions formed with water and HEPES solution are about 100 nm, significantly smaller than those of the CatA:Span® 80 or CatA:CWO7 systems, with a similar stability assessed visually but varying zeta potential values due to a potential shielding effect of the HEPES zwitterionic molecules on the droplets. Also in this system, high O/S ratios (70/30) are favorable for nano-emulsion formation with a good stability. Nano-emulsions could successfully be formed using EC4, a polymer of lower molecular weight than EC10 with comparable droplet sizes, surface charge and stability.

Studies on the system with CEL (without cationic surfactant) revealed that nano-emulsion droplet sizes are larger, zeta potential values are negative and stability (visually assessed) is low, independently of the polymer molecular weight.

4.2. CATIONIC NANOPARTICLES: FORMATION, CHARACTERIZATION

4.2.1. FORMATION OF NANOPARTICLES FROM SELECTED NANO-EMULSIONS AND CHARACTERIZATION

The studies on nano-emulsion formation described in Sections 4.1.2 to 4.1.5 allowed selected systems to be used as templates for nanoparticle preparation. A screening was carried out using all those nano-emulsions showing small droplet sizes, high zeta potential values, good stability and with a transparent or translucent appearance. For clarity reasons, the properties of the selected nano-emulsions and those of the resulting nanoparticles will be described system by system. Nanoparticles were prepared from nano-emulsions by the solvent evaporation method, following a method described previously (Section 1.2.1).

Water / [CatA:Span® 80] / [6 wt% EC10 in ethyl acetate] system

A nano-emulsion with an O/S ratio of 70/30 and 90 wt% of water content was chosen for nanoparticle preparation as it showed the smallest droplet size of all three studied O/S ratios, with high zeta potential values and a stability assessed visually similar to the other compositions (with O/S ratio 50/50 and 60/40, Section 4.1.2). A comparison of nano-emulsion and nanoparticle dispersion characteristics is presented in Table 4.32.

Table 4.32. Main characteristics (diameter, surface charge and stability) of a nano-emulsion (NE) of the Water / [CatA:Span® 80 = 1:1] / [6 wt% EC10 in ethyl acetate] system with an O/S ratio of 70/30 and 90 wt% of water content and of the nanoparticle dispersion (NP) obtained from the nano-emulsion.

DLS - Diameter (nm)[1]		TEM - Diameter (nm)		ζ (mV) diluted in water[2]		ζ (mV) diluted in PB[2]		Stability observed visually (days)	
NE	NP	NE	NP	NE	NP	NE	NP	NE	NP
262	202	-	228 ± 152	55.1	53.6	20.5	25.0	<1	<1

[1] 1/100 dilution with water saturated with ethyl acetate (nano-emulsion) and water (nanoparticle dispersion); [2] Concentration: 20 mg nano-emulsion or nanoparticle dispersion / g solution.

The nanoparticle mean size obtained by DLS (about 200 nm) roughly matches with the mean particle size obtained by TEM analysis (about 230 nm). A size distribution obtained from TEM image analysis is shown in **Figure 4.42**. It can be seen that it is a monomodal size distribution with the main populations in the size range between 150 and 250 nm. Furthermore, there are larger particles with diameters up to 1 μm.

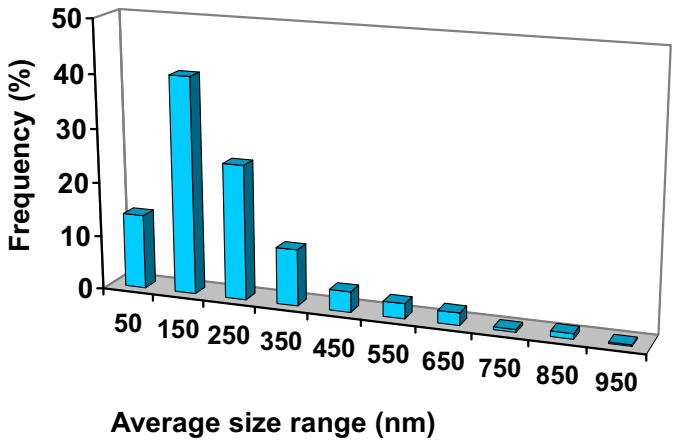

Figure 4.42. Nanoparticle size distribution, assessed from TEM image analysis, of a nanoparticle dispersion obtained from a nano-emulsion of the Water / [CatA:Span® 80 = 1:1] / [6 wt% EC10 in ethyl acetate] system with an O/S ratio of 70/30 and 90 wt% water.

Comparing DLS data, particle size is smaller (about 60 nm) than nano-emulsion droplet size obtained by DLS which is attributed to the evaporation of ethyl acetate from the droplets during the process of nanoparticle preparation. The size decrease after solvent evaporation suggests that the stability of the nano-emulsion system is enough at least during nanoparticle preparation. This is confirmed by stability assessment of the nano-emulsion by Backscattering measurements which revealed no destabilization phenomena during the first 2 hours after nano-emulsions preparation (**Section 4.1.2**).

Micrographs from transmission electron microscopy (TEM) reveal that nanoparticles have a globular shape and are partially aggregated (**Figure 4.43**).

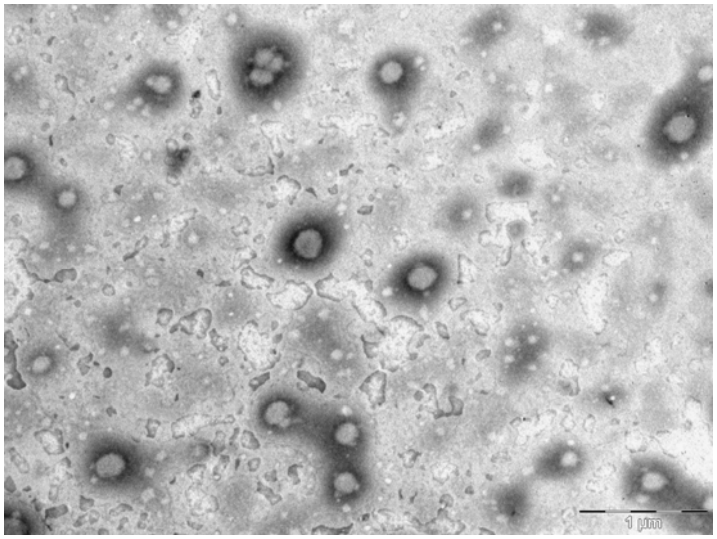

Figure 4.43. TEM micrograph of a negatively stained nanoparticle dispersion obtained from a nano-emulsion of the Water / [CatA:Span® 80 = 1:1] / [6 wt% EC10 in ethyl acetate] system with an O/S ratio of 70/30 and 90 wt% water.

Zeta potential values did not change after solvent evaporation and are around +55 mV. This suggests that the evaporation of the ethyl acetate does not influence the surface charge of the system. As the template nano-emulsions, nanoparticle dispersions showed poor stability (assessed visually). Sedimentation was observed within one day after preparation. Several factors must be taken into account such as the density of the polymer (1.15 g/cm^3) and the high polydispersity of the nanoparticle dispersion (>0.3): The existence of big particles and aggregates of particles (verified from TEM image analysis) suggests that these are very likely to sediment fast. Backscattering measurements of the nanoparticle dispersion during 24 hours, shown in **Figure 4.44**, confirm that sedimentation occurs starting from about 3 hours after nanoparticle preparation. The slight decrease in the backscattering intensity along the central part of the sample height may be due to the sedimentation of the large particles. The peak observed in the upper part of the sample is attributed to the meniscus of the nanoparticle dispersion.

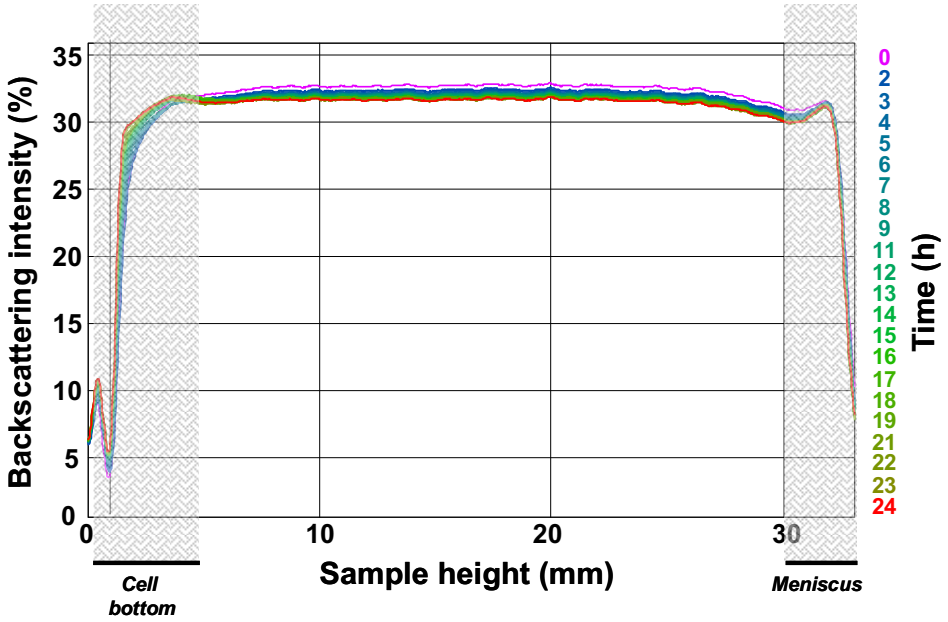

Figure 4.44. Backscattering data during 24 hours of a nanoparticle dispersion obtained from a nano-emulsion of the Water / [CatA:Span® 80 = 1:1] / [6 wt% EC10 in ethyl acetate] system with an O/S ratio of 70/30 and 90 wt% water, at 25ºC. Grey shaded regions indicate the bottom and meniscus of the sample in the glass cell.

Water / [CatA:CWO7] / [6 wt% EC10 in ethyl acetate] system

Table 3.33 and Figures 4.45 and 4.46 show compositions and characteristic properties of the nano-emulsions with 90 wt% of water content, selected for nanoparticle preparation as well as the characteristics of the obtained nanoparticles. Nanoparticle sizes (between 110 and 160 nm) are smaller than those of nano-emulsion droplets (between 120 and 170 nm) as a consequence of ethyl acetate evaporation, as mentioned above (**Figures 4.45a, 4.46a**). Surface charge values of nanoparticle dispersions do not differ significantly from those of the template nano-emulsions (**Figures 4.45b, 4.46b**) which has also been observed for the CatA:Span® 80 system. As observed for corresponding nano-emulsions, the zeta potential for the nanoparticle dispersions decreases with decreasing CatA:CWO7 ratio due to the decreasing amount of cationic surfactant. Stability assessed visually for nanoparticle dispersions is reduced compared to corresponding nano-emulsions (**Figures 4.45c, 4.46c**). As mentioned above, factors like the high polydispersity and the high polymer specific density must be considered carefully.

Table 4.33. Characteristics (diameter with polydispersity index, surface charge and stability assessed visually) of nano-emulsions of the Water / [CatA:CWO7] / [6 wt% EC10 in ethyl acetate] system with 90 wt% water and of nanoparticle dispersions obtained from the nano-emulsions.

Nano-emulsion composition		Nano-emulsion and nanoparticle dispersion characteristics					
CatA : CWO7	O/S ratio	DLS - Diameter (nm)		ζ (mV)[1]		Stability observed visually (days)	
		NE	NP	NE	NP	NE	NP
1:3	65/35	127.3 (0.38)	117.7 (0.36)	39.8	40.6	50	37
	70/30	119.9 (0.41)	109.7 (0.34)	34.4	33.6	66	33
	75/25	167.5 (0.43)	152.8 (0.40)	34.0	36.9	7	1
1:4	70/30	121.8 (0.37)	112.3 (0.36)	32.5	32.6	50	2
1:6	70/30	170.6 (0.32)	159.1 (0.32)	25.5	27.1	12	8

[1] Concentration: 20 mg nano-emulsion or nanoparticle dispersion / g solution (water).

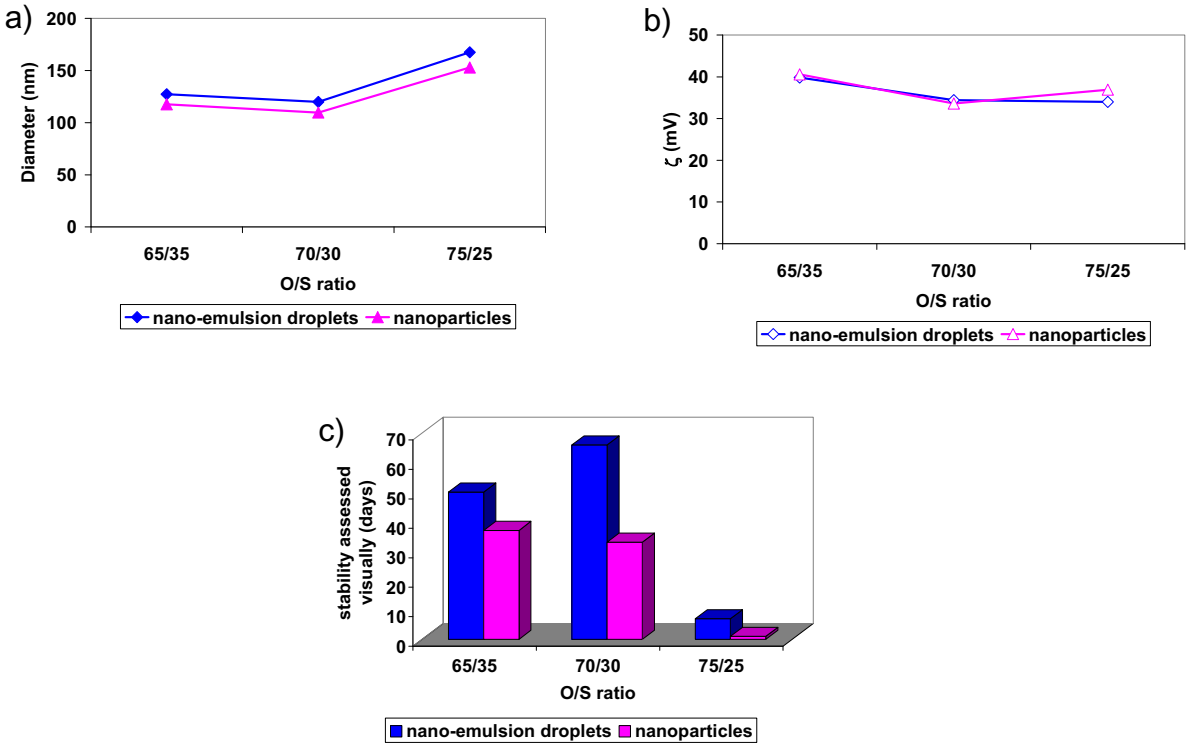

Figure 4.45. Diameter **(a)**, zeta potential (ζ, **b**) and stability assessed visually **(c)** as a function of O/S ratio of nano-emulsions and from those obtained nanoparticle dispersions of the Water / [CatA:CWO7 = 1:3] / [6 wt% EC10 in ethyl acetate] system with 90 wt% water content, at 25°C.

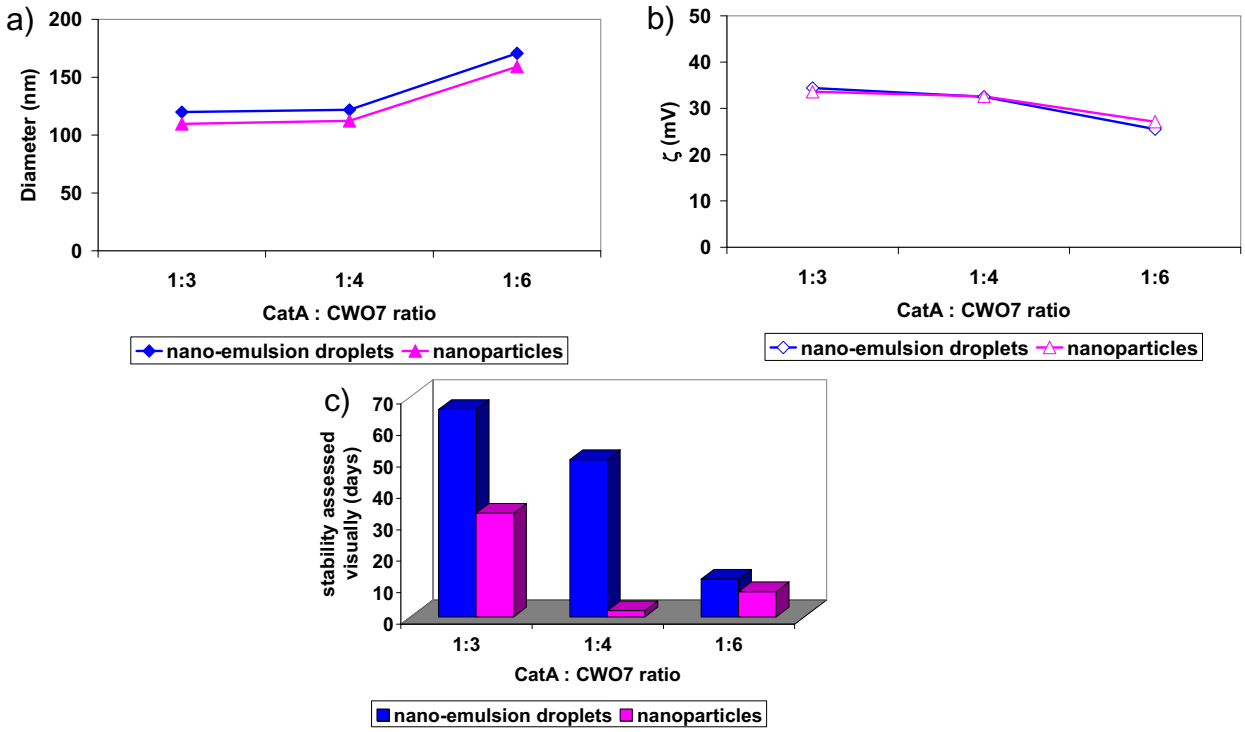

Figure 4.46. Diameter **(a)**, zeta potential (ζ, **b**) and stability assessed visually (**c**) as a function of CatA:CWO7 ratio of nano-emulsions and from those obtained nanoparticle dispersions of the Water / [CatA:CWO7] / [6 wt% EC10 in ethyl acetate] system with 90 wt% water content, at 25°C.

Nano-emulsions with 95 wt% of water content were also chosen for nanoparticle preparation and characterization. **Table 4.34** summarizes and **Figures 4.47** and **4.48** display the properties of the selected nano-emulsions and those of the obtained nanoparticle dispersions.

Table 4.34. Characteristics (diameter with polydispersity index, surface charge and stability assessed visually) of nano-emulsions of the Water / [CatA:CWO7] / [6 wt% EC10 in ethyl acetate] system with 95 wt% water and of nanoparticle dispersions obtained from the nano-emulsions.

Nano-emulsion composition		Nano-emulsion and nanoparticle dispersion characteristics					
CatA : CWO7	O/S ratio	DLS - Diameter (nm)		ζ (mV)[1]		Stability observed visually (days)	
		NE	NP	NE	NP	NE	NP
1:1	60/40	173.1 (0.20)	184.6 (0.20)	49.2	45.0	1	3
	70/30	163.2 (0.36)	186.2 (0.35)	47.2	38.9	2	3
1:3	6040	133.9 (0.41)	108.7 (0.18)	45.7	41.9	5	5
	65/35	130.9 (0.20)	115.5 (0.22)	32.6	37.0	53	37
	70/30	127.6 (0.33)	122.0 (0.30)	30.5	31.7	71	51
	75/25	150.4 (0.32)	133.0 (0.45)	35.1	34.1	1	1
1:4	70/30	133.2 (0.35)	122.8 (0.36)	25.4	25.7	17	17
1:6	70/30	141.6 (0.40)	154.7 (0.37)	16.5	18.8	16	12
1:8	70/30	169.6 (0.30)	184.8 (0.46)	10.3	8.5	15	13

[1] Concentration: 20 mg nano-emulsion or nanoparticle dispersion / g solution (water).

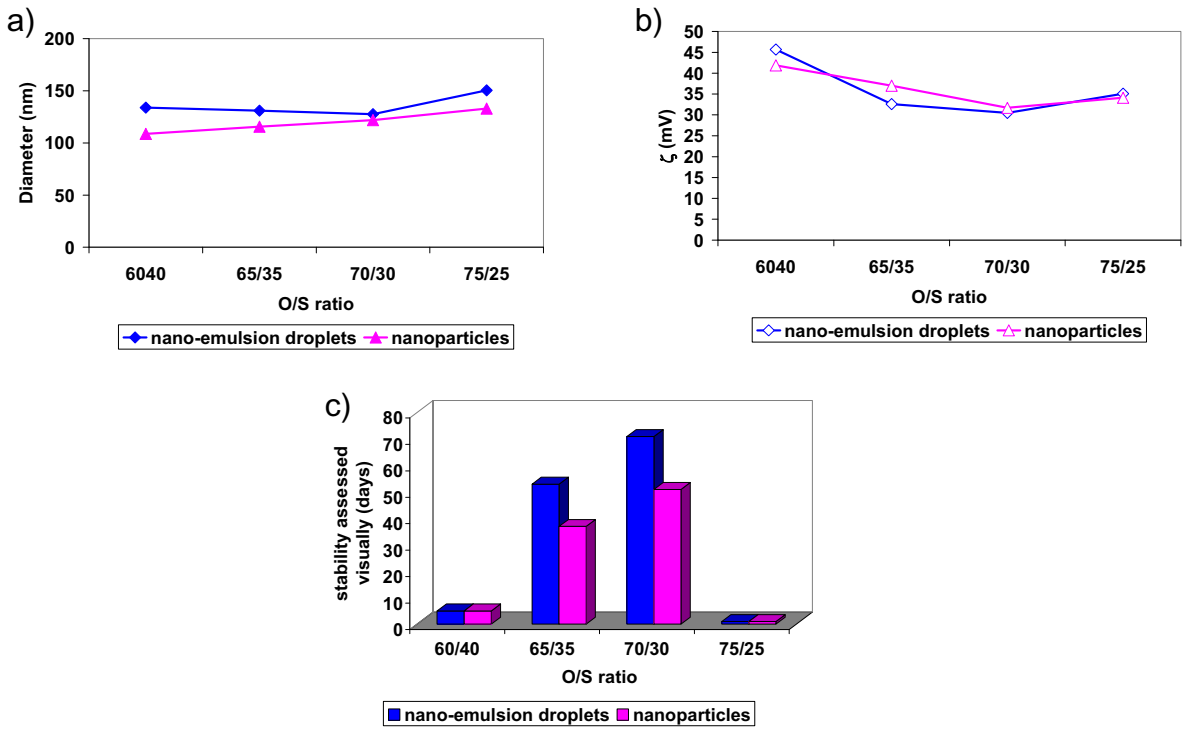

Figure 4.47 Diameter **(a)**, zeta potential (ζ, **b**) and stability assessed visually **(c)** as a function of O/S ratio of nano-emulsions and from those obtained nanoparticle dispersions of the Water / [CatA:CWO7 = 1:3] / [6 wt% EC10 in ethyl acetate] system with 95 wt% water content, at 25°C.

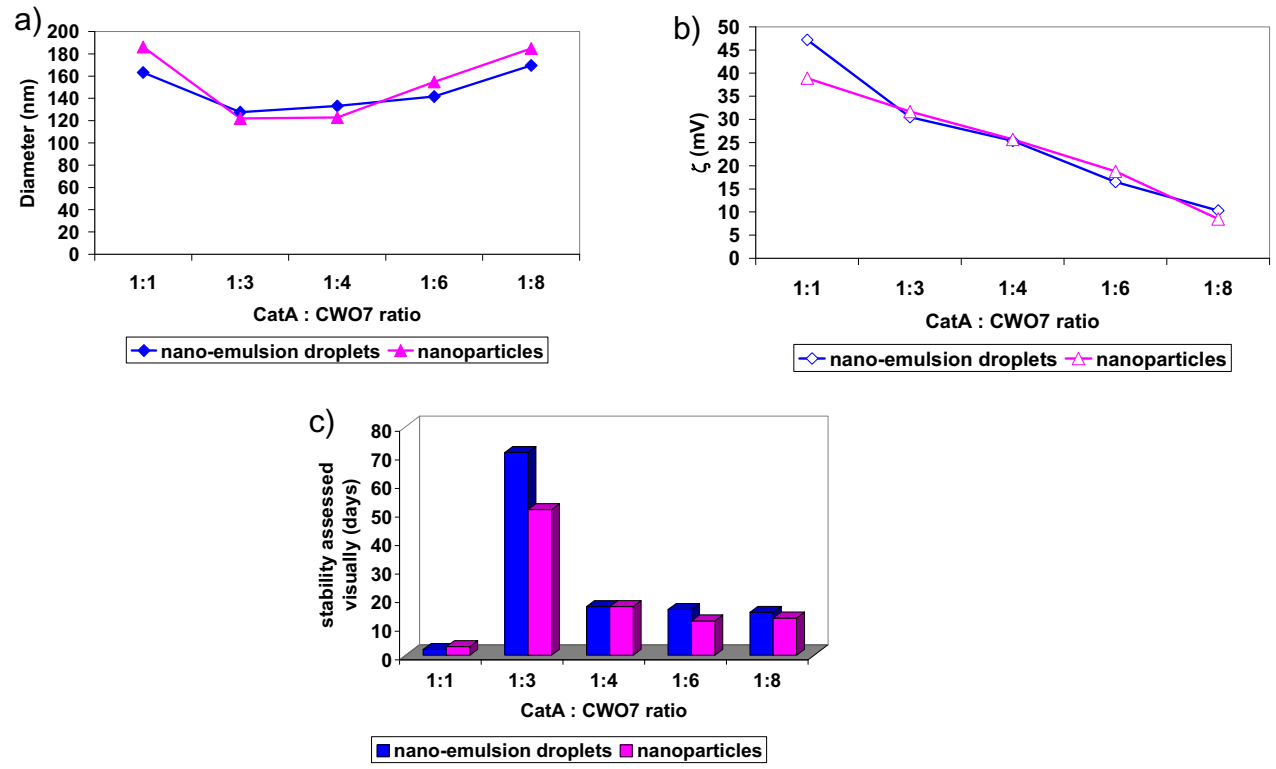

Figure 4.48 Diameter (**a**), zeta potential (ζ, **b**) and stability assessed visually (**c**) as a function of CatA:CWO7 ratio of nano-emulsions and from those obtained nanoparticle dispersions of the Water / [CatA:CWO7] / [6 wt% EC10 in ethyl acetate] system with an O/S ratio of 70/30 and 95 wt% water, at 25°C.

The expected decrease in size of the nanoparticles compared to the droplet size of the corresponding template nano-emulsion could not be observed for all compositions with 95 wt% of water content when changing the CatA:CWO7 ratio (Figure 4.48a). Nanoparticles show larger sizes for the CatA:CWO7 = 1:1, 1:6 and 1:8 systems. This might be due to instability processes during (e.g. Ostwald ripening, coalescence) or after (e.g. aggregation) nanoparticle preparation. Droplet sizes are between 130 and 170 nm for nano-emulsions and between 110 and 180 nm for nanoparticle dispersions.

As observed previously, nanoparticle zeta potential values (Figures 4.47b and 4.48b) are similar to those of the nano-emulsions and, like those, decrease with increasing O/S ratio and decreasing cationic:nonionic surfactant ratio, respectively. Nanoparticle dispersions with 95 wt% water are mostly less stable than the template nano-emulsions (Figures 4.47c and 4.48c), possibly as a consequence of the earlier mentioned instability processes taking place, the high polydispersity and/or higher specific density of the polymer than that of the continuous phase.

Water / [CatA:(CWO7:CEL)] / [6 wt% EC10 in ethyl acetate] system

Nanoparticles have been obtained from nano-emulsions with 95 wt% water. Most of the particle sizes obtained, between 100 and 160 nm, are smaller than those of the template nano-emulsions (Table 4.35, Figures 4.49a and 4.50a). When the opposite was observed, it might be a consequence of destabilization phenomena taking place after nanoparticle preparation or reasons related to the polydispersity and polymer density as mentioned earlier. Nanoparticle surface charge values are comparable to those of the related template nano-emulsions (between 25 and 35 with water and between 10 and 25 with HEPES solution) and follow the same trends (Figures 4.49b and 4.50b). Nanoparticle dispersions as the nano-emulsions show low stability (assessed visually).

Table 4.35. Characteristics (diameter, surface charge and stability assessed visually) of nano-emulsions of the Water / [CatA:(CWO7:CEL)] / [6 wt% EC10 in ethyl acetate] system with an O/S ratio of 70/30 and 95 wt% water and of the nanoparticle dispersions obtained from the nano-emulsions.

Nano-emulsion composition		Nano-emulsion and nanoparticle dispersion characteristics					
CWO7 : CEL	CatA : surfactant ratio	DLS - Diameter (nm)		ζ (mV)		Stability observed visually (days)	
		NE	NP	NE	NP	NE	NP
1:1	1:1	166.4 (0.25)	153.7 (0.27)	24.2	30.2	< 1	< 1
	1:3	149.2 (0.27)	219.3 (0.27)	11.0	11.9		
1:2	1:1	153.2 (0.30)	146.6 (0.31)	30.0	28.7		
	1:3	132.1 (0.32)	127.8 (0.35)	15.4	16.4		
1:1	1:1	148.0 (0.28)	137.7 (0.34)	31.7	33.2		
	1:3	115.8 (0.33)	107.0 (0.34)	18.2	18.3		
2:1	1:1	151.9 (0.32)	147.0 (0.35)	32.9	32.3		
	1:3	116.6 (0.33)	105.0 (0.34)	22.1	24.3		
3:1	1:1	158.2 (0.35)	162.7 (0.30)	32.5	31.3		
	1:3	122.3 (0.36)	98.5 (0.39)	23.3	22.6		

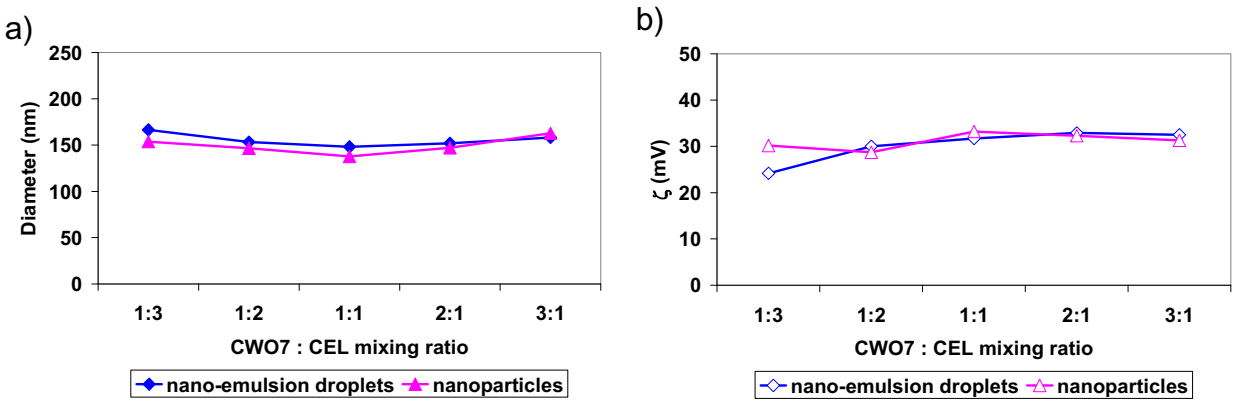

Figure 4.49. Diameter (**a**) and zeta potential (ζ, **b**) as a function of CWO7:CEL mixing ratio of nano-emulsions and from those obtained nanoparticle dispersions of the Water / [CatA:(CWO7:CEL) = 1:1] / [6 wt% EC10 in ethyl acetate] system with an O/S ratio of 70/30 and 95 wt% water, at 25°C.

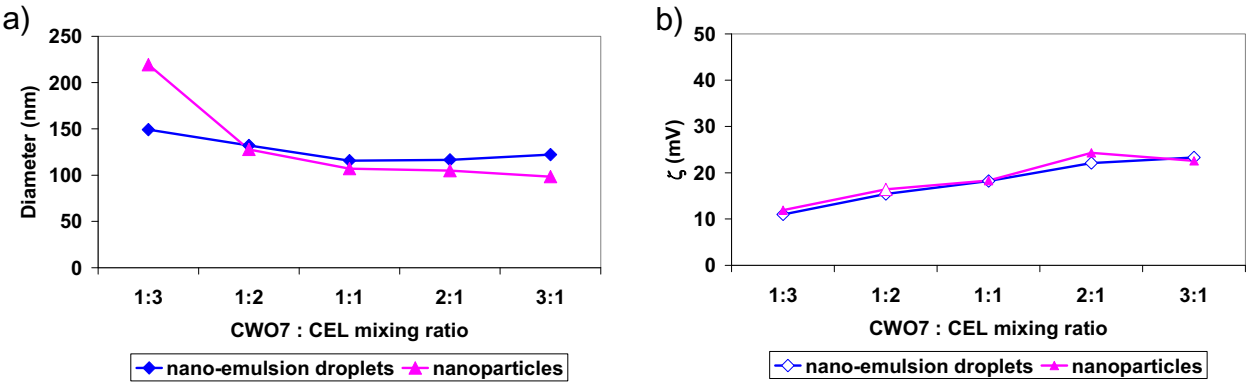

Figure 4.50. Diameter (**a**) and zeta potential (ζ, **b**) as a function of CWO7 : CEL mixing ratio of nano-emulsions and from those obtained nanoparticle dispersions of the Water / [CatA:(CWO7:CEL) = 1:3] / [6 wt% EC10 in ethyl acetate] system with an O/S ratio of 70/30 and 95 wt% water, at 25°C.

Aqueous solution / [CatA:CEL = 1:1] / [6 wt% EC10 in ethyl acetate] system

The nano-emulsions with an O/S ratio of 70/30 and 95 wt% aqueous solution (water or HEPES) showed high stability and smallest droplet sizes and also possessed appropriate zeta potential values (above +20 mV). For these reasons they were selected for nanoparticle preparation. Also nano-emulsions prepared with HEPES buffered glucose solution were selected. **Table 4.36** summarizes the characteristics before (NE) and after solvent evaporation (NP).

Table 4.36. Characteristics (diameter with polydispersity index, surface charge and stability assessed visually) of nano-emulsions of the Aqueous solution / [CatA:CEL = 1:1] / [6 wt% EC10 in ethyl acetate] system with an O/S ratio of 70/30 and 95 wt% aqueous phase and of the nanoparticle dispersions obtained from the nano-emulsions.

Aqueous phase	DLS - Diameter (nm)		TEM - Diameter (nm)		ζ (mV)		Stability observed visually (days)	
	NE	NP	NE	NP	NE	NP	NE	NP
Water	98.4 (0.32)	104.8 (0.35)	N.D.[1]	47 ± 11	32.2	34.3	7	12
HEPES solution	96.9 (0.44)	90.8 (0.46)	N.D.	41 ± 10	19.1	22.0	7	12
HBG (4.3%G[2])	107.4 (0.38)	97.2 (0.37)	N.D.	N.D.	21.7	26.8	N.D.	N.D.
HBG (4.5%G)	104.8 (0.33)	97.7 (0.45)	N.D.	N.D.	22.2	23.3	N.D.	N.D.

[1] N.D.: not determined; [2] G: glucose;

Nano-emulsion droplet sizes are about 100 nm with all aqueous media. Values obtained for nanoparticles are smaller or equal to those of the corresponding nano-emulsions. In water or HEPES solution, the particle size is decreased to the half when evaluated by TEM analysis. As mentioned in **Section 3.2.1** this may be due to the fact that the measurements by DLS provides the size of the solvated particles and for that reason they appear larger than the hard spheres measured from TEM micrographs. Moreover, the polydispersity with nano-emulsions and nanoparticle dispersions is rather high (>0.32). Size distributions in water and HEPES solution are shown in **Figure 4.51**. Both distributions are monomodal with a maximum at about 50 nm (water) and 40 nm (HEPES solution).

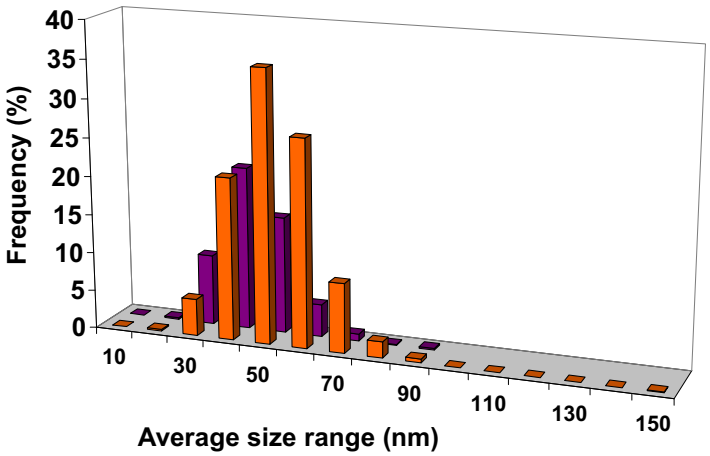

Figure 4.51. Nanoparticle size distribution, assessed from TEM image analysis, of a nanoparticle dispersion obtained from a nano-emulsion of the Aqueous solution / [CatA:CEL = 1:1] / [6 wt% EC10 in ethyl acetate] system with an O/S ratio of 70/30 and 95 wt% water and HEPES solution.

TEM micrographs (Figure 4.52) reveal that nanoparticles have a globular shape in both aqueous solutions.

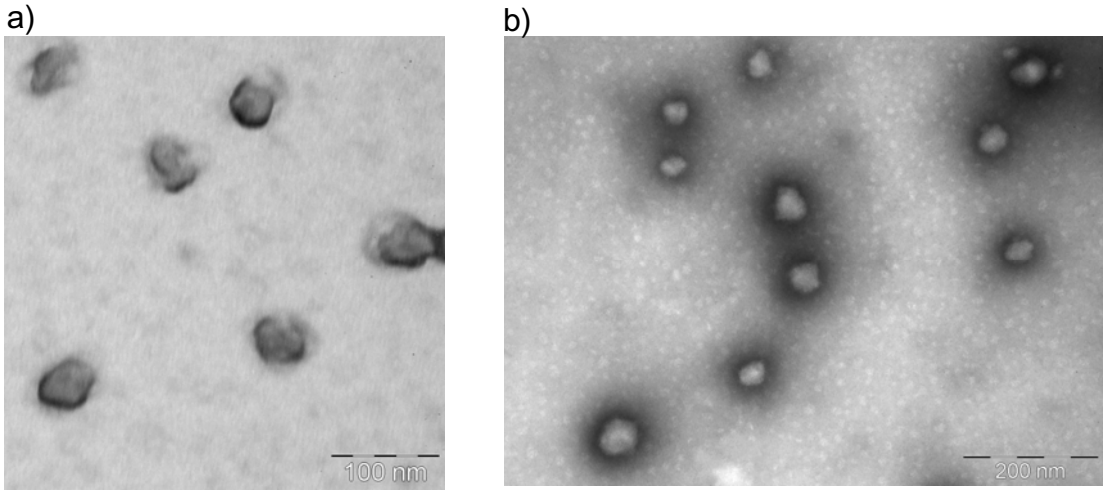

Figure 4.52. TEM micrograph of a negatively stained nanoparticle dispersion obtained from a nano-emulsion of the Aqueous solution / [CatA:CEL = 1:1] / [6 wt% EC10 in ethyl acetate] system with an O/S ratio of 70/30 and 95 wt% **a)** water and **b)** HEPES solution.

Zeta potential values of the nanoparticle dispersions are similar to those of corresponding nano-emulsions and are higher in water than in HEPES solution or HEPES buffered glucose solution. A possible reason could be that the zwitterionic species present in the HEPES solution might have a neutralizing effect, lowering for that reason the zeta potential. Stability assessed visually revealed that nanoparticle dispersions with water or HEPES solution are stable for 12 days which is a higher stability than that observed for the nano-emulsions.

These results are reinforced by particle size measurements as a function of time, carried out by DLS (**Figure 4.53**). Reasons for that might be among others, the smallest particle size and an enhanced stabilization of the nanoparticles as a consequence of a higher surfactant concentration in the interface after solvent evaporation.

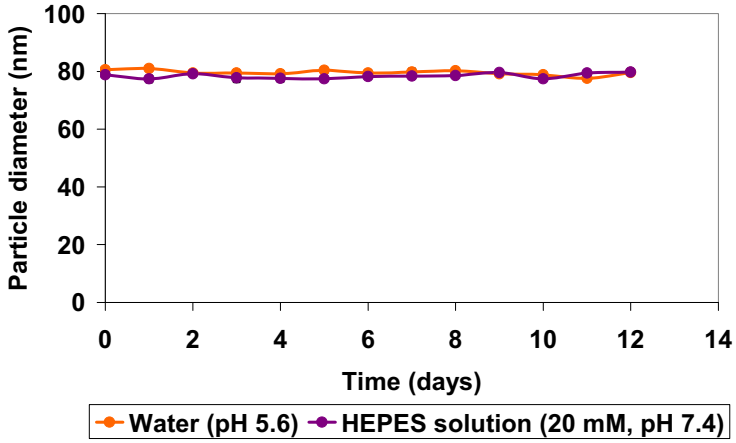

Figure 4.53. Particle diameter of nanoparticle dispersion obtained from nano-emulsion of the Aqueous solution / [CatA:CEL = 1:1] / [6 wt% EC10 in ethyl acetate] system with an O/S ratio of 70/30 and 95 wt% of water and HEPES solution, respectively, as a function of time, at 25ºC.

Effect of polymer molecular weight

Nanoparticles could also be obtained with a lower molecular weight polymer, EC4. For the same reasons as above, the compositions with an O/S ratio of 70/30 and 95 wt% aqueous solution (water or HEPES solution) were chosen for characterization. The main features are summarized in **Table 4.37**.

Table 4.37. Characteristics (diameter with polydispersity index, surface charge and stability assessed visually) of nano-emulsions of the Aqueous solution / [CatA:CEL = 1:1] / [6 wt% EC4 in ethyl acetate] system with an O/S ratio of 70/30 and 95 wt% aqueous phase and of the nanoparticle dispersions obtained from the nano-emulsions.

Aqueous phase	DLS - Diameter (nm)		TEM - Diameter (nm)		ζ (mV)		Stability observed visually (days)	
	NE	NP	NE	NP	NE	NP	NE	NP
Water	102.0 (0.45)	93.8 (0.50)	N.D.(1)	37 ± 14	26.2	26.3	28	28
HEPES solution	91.7 (0.49)	93.6 (0.55)	N.D.	33 ± 11	18.0	21.3	28	28

(1) N.D.: not determined;

As with EC10, nano-emulsion droplet and nanoparticle sizes with EC4 are about 100 nm with both aqueous media and, as before, values obtained for nanoparticles are smaller or equal to those of the corresponding nano-emulsions. Particles measured from TEM micrographs showed in both continuous phases mean diameters of about 35 nm which can be explained with above mentioned reasons. Size distributions in water and HEPES solution are shown in **Figure 4.54**. In both cases, the distribution is monomodal with the main population at about 30 nm (water) and 40 nm (HEPES solution). TEM micrographs (**Figure 4.55**) revealed that in both aqueous media, nanoparticles showed irregular shapes. Aside from rounded shapes, nanoparticles showed also oval shapes. It is worth mentioning that particles are less rounded than those obtained with 6 wt% EC10 with both continuous phases.

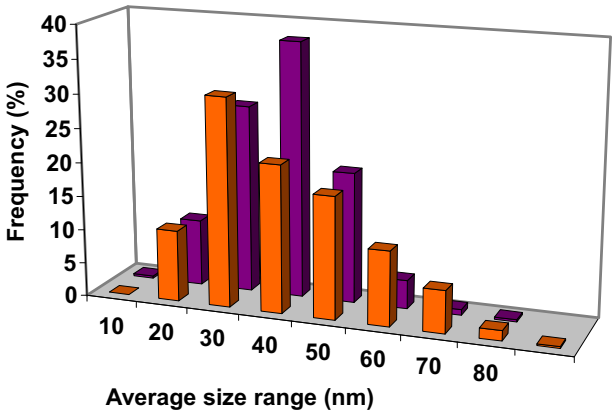

Figure 4.54. Nanoparticle size distribution, assessed from TEM image analysis, of a nanoparticle dispersion obtained from a nano-emulsion of the Aqueous solution / [CatA:CEL = 1:1] / [6 wt% EC4 in ethyl acetate] system with an O/S ratio of 70/30 and 95 wt% water and HEPES solution.

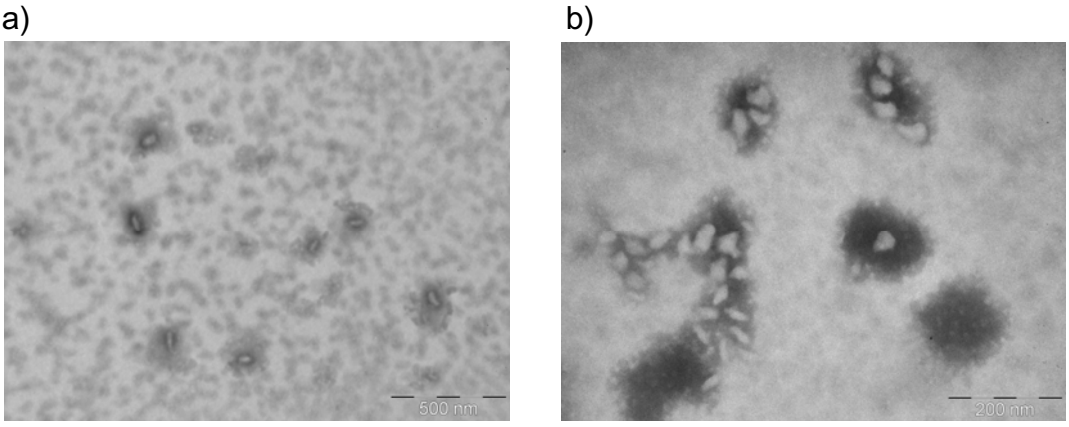

Figure 4.55. TEM micrograph of a negatively stained nanoparticle dispersion obtained from a nano-emulsion of the Aqueous solution / [CatA:CEL = 1:1] / [6 wt% EC4 in ethyl acetate] system with an O/S ratio of 70/30 and 95 wt% **a)** water and **b)** HEPES solution.

Zeta potential values of the nanoparticle dispersions show the same tendencies as described for those with EC10. Stability assessed by DLS revealed for both aqueous media no significant changes during at least 28 days (**Figure 4.56**). These measurements were carried out in the supernatant. No sedimentation was observed in the DLS tubes during the period of study (28 days).

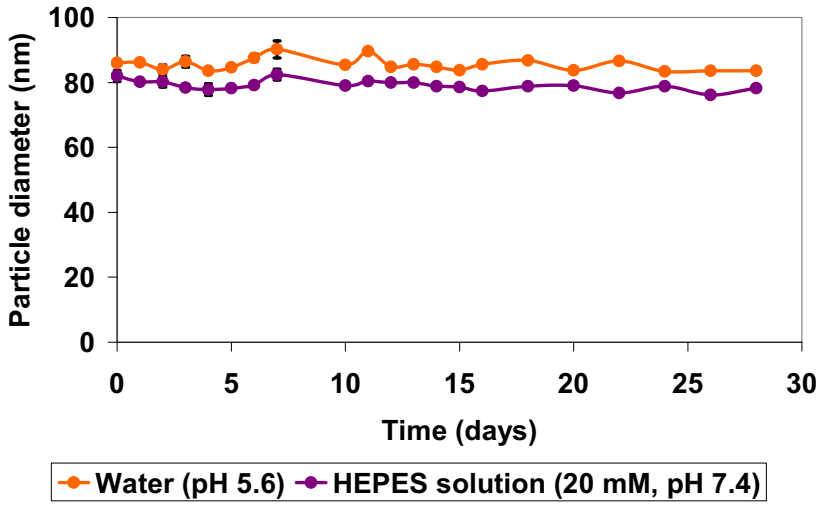

Figure 4.56. Particle diameter of nanoparticle dispersion obtained from nano-emulsion of the Aqueous solution / [CatA:CEL = 1:1] / [6 wt% EC4 in ethyl acetate] system with an O/S ratio of 70/30 and 95 wt% of water and HEPES solution, respectively, as a function of time, at 25ºC.

Based on their small size and good stability, the O/S ratio of 70/30 and aqueous solutions contents of 90 and 95 wt% of different systems with the CatA:nonionic surfactant (mixture) ratio 1:1 or 1:3 were chosen for further studies on excess surfactant removal trials.

As reported in literature [**Hans, 2002; Panyam, 2003; Swami, 2012**], particle size and surface charge play, among others, a key role in the design of therapeutic nanoparticles. Very small (< 10 nm) or very large nanoparticles are rapidly cleared by cells. The nanoparticles obtained with different CatA:nonionic surfactant systems show mostly sizes in the range between 100 and 200. Therefore, they may be acceptable for therapeutic applications.

A high nanoparticle surface charge may cause high immune responses. It was proposed by Davis *et al.* [**Davis, 2009**] that surface charge between – 10 and +10 mV are optimal for preventing phagocytosis. As it is the aim of this work to funcionalize obtained nanoparticles with biomolecules, surface charges higher

than +10 mV are required to ensure electrostatic interactions between the positively charged nanoparticles and negatively charged biomolecules. In this context, surface charges of obtained nanoparticles are mainly appropriate for the intended purpose

SUMMARY on Formation of nanoparticles from selected nano-emulsions and characterization (Section 4.2.1.)

Nanoparticles have been obtained from nano-emulsions of all studied CatA:nonionic surfactant(s) systems. Nanoparticles obtained from nano-emulsions of the CatA:Span® 80 system with 90 wt% water showed high zeta potential values (>50 mV) but large particle sizes (> 200 nm) and few stability visually assessed (<1 day). Nanoparticles obtained with the CatA:CWO7 system with 90 and 95 wt% water content showed particle sizes between 110 and 190 nm with zeta potential values between 10 and 45 mV and visually assessed stabilities up to 51 days. With the CatA:(CWO7:CEL) system, nanoparticle were in about the same range as with CWO7 only (105 – 220 nm) with similar zeta potentials (11 – 30 mV) but with very low stability assessed visually (95 wt% water content). For particles of the CatA:CEL system with 6 wt% EC4 and EC10, respectively, and 95 wt% water, sizes were about 100 nm and surface charges were between 20 and 35 mV with good stabilities (95 wt% water content).

Nanoparticles show sizes mainly between 100 and 200 nm and surface charges in the range 10 – 50 mV whereas the majority of the values are between 20 and 35 mV. These values make them promising candidates for therapeutic applications.

The following conclusions can be made:

- Nanoparticles could successfully be obtained from nano-emulsions with zeta potential values and stability similar to those of corresponding nano-emulsions, and in general lower particle sizes.
- Characteristics (size and surface charge) of nanoparticles formed with polymers of different molecular weight did not change significantly.

- Nanoparticle surface charge values and sizes are mainly appropriate for therapeutical applications

4.2.2. EXCESS SURFACTANT REMOVAL FROM NANOPARTICLE DISPERSIONS

For the removal of surfactant in excess from the nanoparticle dispersion, dialysis was carried out. Dialysis conditions (dialysate composition, nanoparticle dispersion to dialysate volume ratio, duration of dialysis, number of dialysis steps) were investigated in order to achieve an optimum balance between the surfactant removed from the nanoparticle dispersion and the surface charge remaining on the nanoparticles. Too long or too many dialysis steps would wash off too much surfactant while insufficient dialysis would wash off almost no surfactant. Both would be unfavorable conditions for complexation with biomolecules. Nanoparticles with a too high surface charge are known to show a rather high toxicity whereas with a too low surface charge (negative range) they would not undergo complexation. First trials were carried out with water which was later on exchanged for PBS (0.33 M) or HEPES solution (20 mM) in order adapt to physiological conditions (pH 7.4).

Water as dialysate

Dialysis was carried out (0.8 L MilliQ water for 4 g of nanoparticle dispersion) with measuring the conductivity in the dialysate, which was replaced twice, after 30 minutes and 2 hours and then allowed to stand until a plateau was reached. Figure 4.57 shows the conductivity values as a function of the time for the three dialysis tests. It can be observed that during the first two dialysis periods, conductivity in the dialysate strongly increases, indicating a strong washing out-effect. The conductivity increase during the third period is weaker and a plateau is reached after about 20 hours, which was interpreted as an indication that no more ions would be washed out.

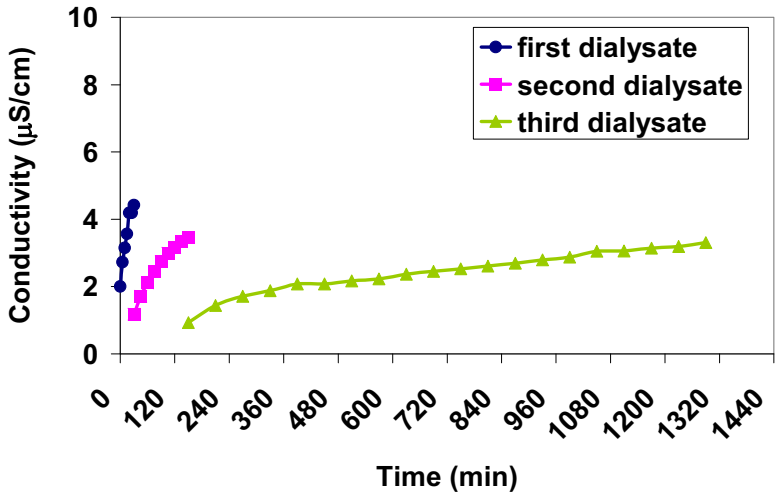

Figure 4.57. Conductivity values as a function of time measured in the dialysate (water) during dialysis of a nanoparticle dispersion obtained from a nano-emulsion of the Water / [CatA:Span® 80 = 1:1] / [6 wt% EC10 in ethyl acetate] system with an O/S ratio of 70/30 and 90 wt% of water content, at 25ºC.

The nanoparticle dispersion with an O/S ratio of 70/30 and 90 wt% of water content was also characterized after dialysis. Micrographs obtained from the nanoparticle dispersion from transmission electron microscopy (TEM) (**Figure 4.58**) reveal that nanoparticle shape after dialysis maintains globular.

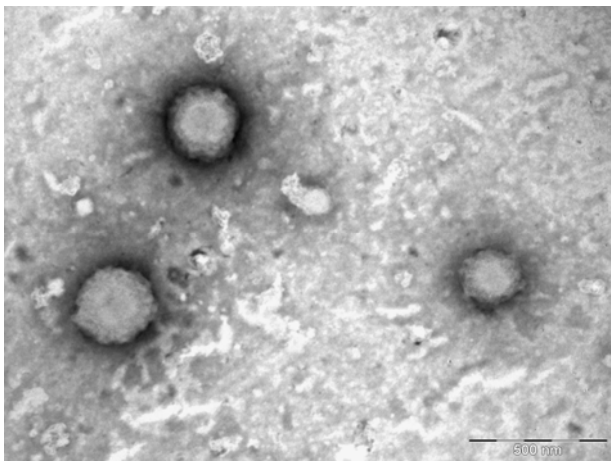

Figure 4.58. TEM micrographs of the negatively stained nanoparticle dispersion of the Water / [CatA:Span® 80 = 1:1] / [6 wt% EC10 in ethyl acetate] system with an O/S ratio of 70/30 and 90 wt% water, after dialysis.

Table 4.38 shows the characteristics of the nanoparticles before and after dialysis. Particle size values before dialysis measured with DLS were around 200 nm and increased significantly after dialysis. This was attributed to aggregation of nanoparticles. The mean diameter measured by TEM is about 30 nm larger than that of the nanoparticle dispersion, with similar polydispersity.

A possible explanation could be that particles grow in size due to swelling of the polymer chains with time. Size distributions of the nanoparticle dispersion before and after dialysis, as described in **Section 3.3.6**, are shown in **Figure 4.59.**

Table 4.38. Particle size (determined by DLS and TEM image analysis) and zeta potential (ζ) values of a nanoparticle dispersion obtained from a nano-emulsion of the Water / [CatA:Span® 80 = 1:1] / [6 wt% EC10 in ethyl acetate] system with an O/S ratio of 70/30 and 90 wt% water content, before and after dialysis.

	Mean diameter by DLS[1] (nm)	Mean diameter by TEM (nm)	ζ (mV) diluted in water[2]	ζ (mV) diluted in PB[2]
Before dialysis	202 (0.34)	228 ± 152	53.6	25.0
After dialysis	824 (0.46)	262 ± 180	24.3	-32.6

[1] 1/100 dilution with water; [2] Concentration: 20 mg nanoparticle dispersion / g solution.

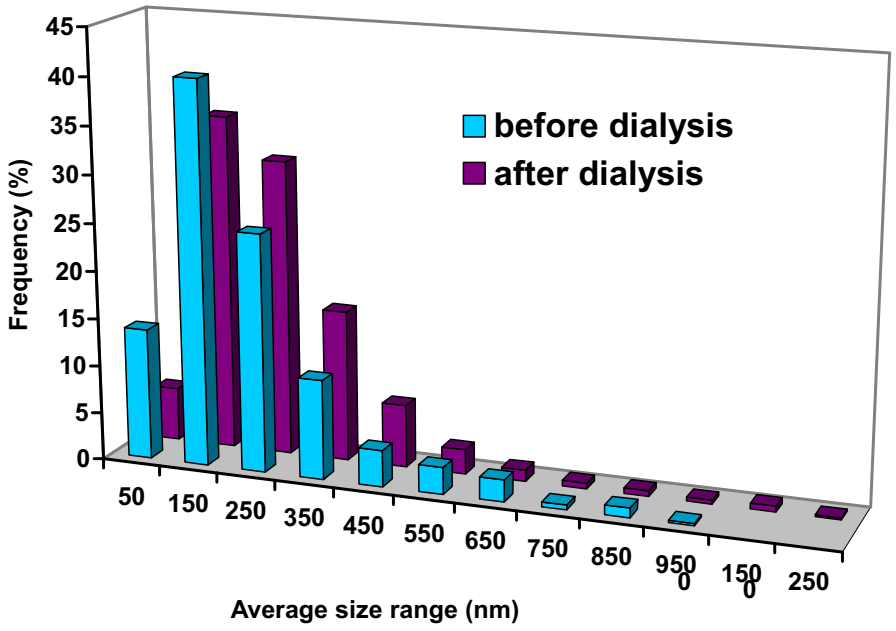

Figure 4.59. Nanoparticle size distribution, assessed from TEM image analysis, of a nanoparticle dispersion obtained from a nano-emulsion of the Water / [CatA:Span® 80 = 1:1] / [6 wt% EC10 in ethyl acetate] system with an O/S ratio of 70/30 and 90 wt% water, before and after dialysis.

The shapes of both distributions are similar and size distribution after dialysis is slightly shifted to larger particle sizes, suggesting that there might be a swelling effect during the dialysis time.

Zeta potential values after dialysis are still in the positive range when diluted with water although they are reduced to about half of the value before dialysis. This allows assuming that there is still cationic surfactant present on the nanoparticle surface. When diluted with PB buffer, values are in the negative range (about -30mV) which might be due to the washing-off effect through dialysis and also due to the shielding effect of the anions present in the PB buffer.

After dialysis, a white solid powder was detected on the bottom of the flexible tube containing the nanoparticle dispersion which was interpreted as sedimentation. The stability of the nanoparticle dispersion after dialysis was assessed by Turbiscan measurements and is shown in **Figure 4.60**.

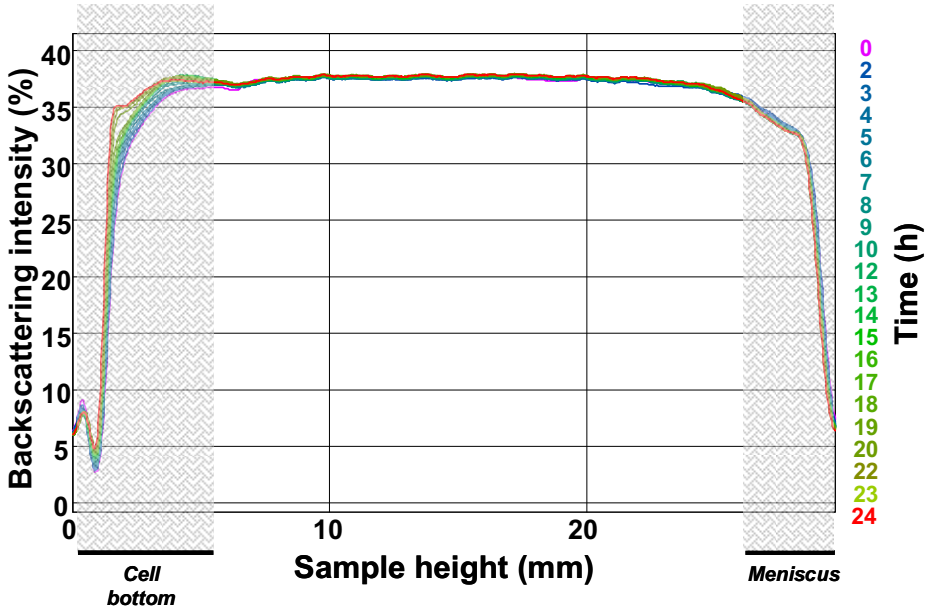

Figure 4.60. Backscattering data during 24 h of a nanoparticle dispersion obtained from a nano-emulsion of the Water / [CatA:Span® 80 = 1:1] / [6 wt% EC10 in ethyl acetate] system with an O/S ratio of 70/30 and 90 wt% water, after dialysis, at 25ºC. Grey shaded regions indicate the bottom and meniscus of the sample in the glass cell.

In **Section 4.1.2**, when the stability of the nano-emulsions of the CatA:Span® 80 system was discussed (**Figure 4.5**), changes in the upper part of the sample were detected which were interpreted as creaming. By contrast, after solvent evaporation (**Figure 4.44**), no changes in the upper part but on the cell bottom

were detected. The increase in backscattering intensity was interpreted as sedimentation. In the spectrum of the nanoparticle dispersion after dialysis (**Figure 4.60**) the same phenomenon can be observed, even slightly more distinctive. This can be seen in good agreement with the visual observation after dialysis.

It was considered of interest to carry out the same dialysis experiment during a shorter timeframe (3 hours) changing the nanoparticle dispersion to dialysate ratio (1 L MilliQ® water for 4 g of nanoparticle dispersion) and replacing the dialysate by fresh one more frequently. **Figure 4.61a** shows the conductivity values obtained. The same trend as in the previous experiment (**Figure 4.57**) can be observed. While during the first dialysis period a strong increase in conductivity in the dialysate is produced, the increase is less distinctive in the following periods, reaching a plateau after 3 hours, indicative that the flux of ions from the nanoparticle dispersion to the dialysate and *vice versa* is reduced.

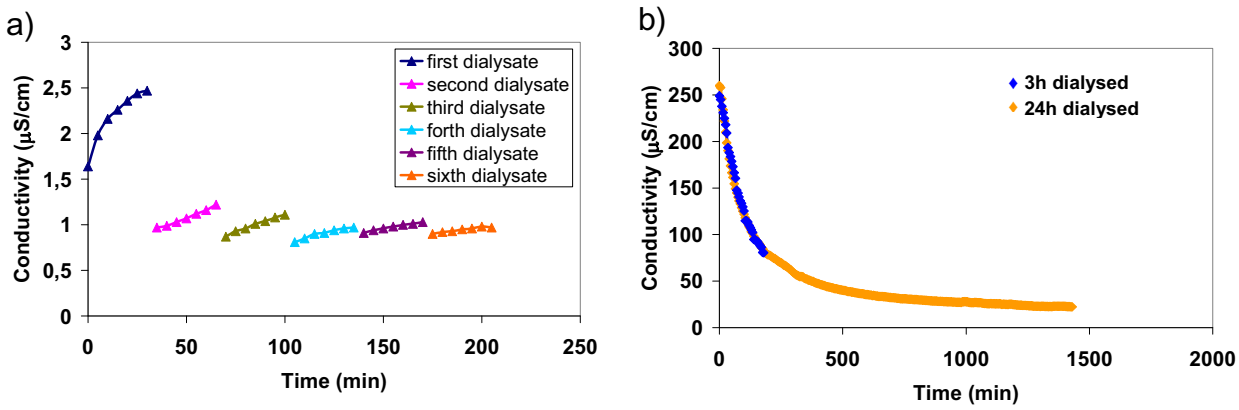

Figure 4.61. Conductivity values as a function of time measured during dialysis of a nanoparticle dispersion obtained from a nano-emulsion of the Water / [CatA:CWO7 = 1:3] / [6 wt% EC10 in ethyl acetate] system with on O/S ratio of 70/30 and 95 wt% water content (**a**) in the dialysate (water) and (**b**) in the nanoparticle dispersion.

The nanoparticle dispersion with an O/S ratio of 70/30 and 95 wt% of water content was characterized after dialysis regarding size and surface charge (**Table 4.39**).

Table 4.39. Particle size (determined by DLS) and zeta potential (ζ) values of a nanoparticle dispersion obtained from a nano-emulsion of the Water / [CatA:CWO7 = 1:3] / [6 wt% EC10 in ethyl acetate] system with an O/S ratio of 70/30 and 95 wt% water, before and after dialysis.

	Mean diameter by DLS (nm)	ζ (mV) diluted in water[1]
Before dialysis	123.1 (0.25)	30.9
After 3h dialysis	111.2 (0.35)	25.2
After 24h dialysis	-	15.0

[1] Concentration: 20 mg nanoparticle dispersion / g solution.

The particle diameter obtained after 3 hours of dialysis is not significantly smaller than that of the nanoparticle dispersion before dialysis. The nanoparticle surface charge measured after 3 hours is decreased for about 5 mV and has decreased to about half of its initial value after 24 hours dialysis, suggesting that surfactant has been washed off. Sedimentation of the nanoparticle dispersion was observed within less than one day after the end of the dialysis.

The conductivity of the nanoparticle dispersion during dialysis was also measured. In these experiments, dialysis (2 L MilliQ® water for 8 g of nanoparticle dispersion) was carried out during 24 hours without changing the dialysate. Conductivity values (**Figure 4.61b**) start at about 250 μS/cm and decrease with time. While conductivity measurements in the dialysate reach a plateau after about 3 hours of dialysis, no plateau is reached in the nanoparticle dispersion within this period of time (blue graph in **Figure 4.61b**). Conductivity values in the nanoparticle dispersion reach a plateau at about 25 μS/cm after 15 hours of dialysis, indicating that equilibrium of ions in the nanoparticle dispersion and in the dialysate is achieved.

Zeta potential of the nanoparticle dispersion was measured during dialysis (2 L MilliQ® water for 8 g of nanoparticle dispersion, up to 12 days of dialysis). **Figure 4.62** shows the surface charge values versus time for two

measurements of different time frames. Zeta potential values in both trials start at about +30 mV and reach neutral values after about 2.5 days. With further dialysis, a plateau in the negative range is reached after about 6 days indicating that all cationic surfactant might have been washed off from the surface of the nanoparticles.

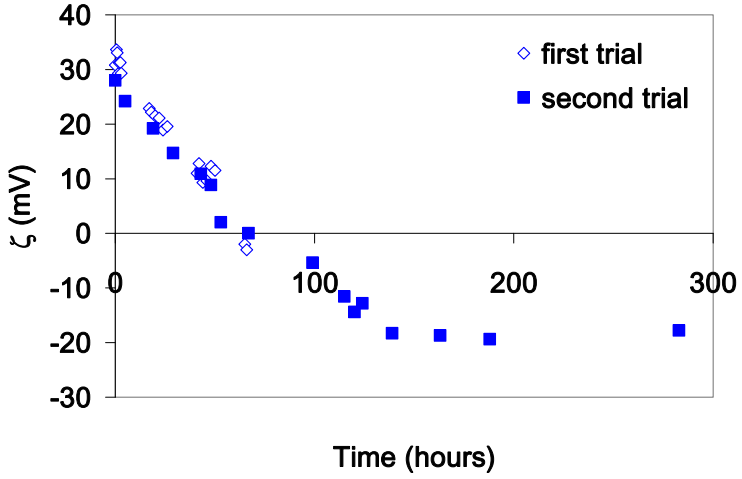

Figure 4.62. Zeta potential (ζ) values as a function of time of a nanoparticle dispersion obtained from a nano-emulsion of the Water / [CatA:CWO7 = 1:3] / [6 wt% EC10 in ethyl acetate] system with an O/S ratio of 70/30 and 95 wt% of water content.

The reason for the differences found in the time needed to attain the plateau by conductivity (15 hours) and zeta potential (6 days) is not clear yet. They might be due to the fact that zeta potential measurements are much more sensitive and may detect with more accuracy changes at the surface of the nanoparticles.

Based on these results, the dialysis conditions were fixed to a time frame of 48 hours using 8 g of nanoparticle dispersion immersed in 2 L of dialysate. By that time, the surface charge was decreased to about the half of the original value (around +30 mV) which was considered to be an appropriate value for complexation studies. Conductivity and zeta potential measurements were carried out in the nanoparticle dispersion during dialysis. Figure 4.63 shows the results.

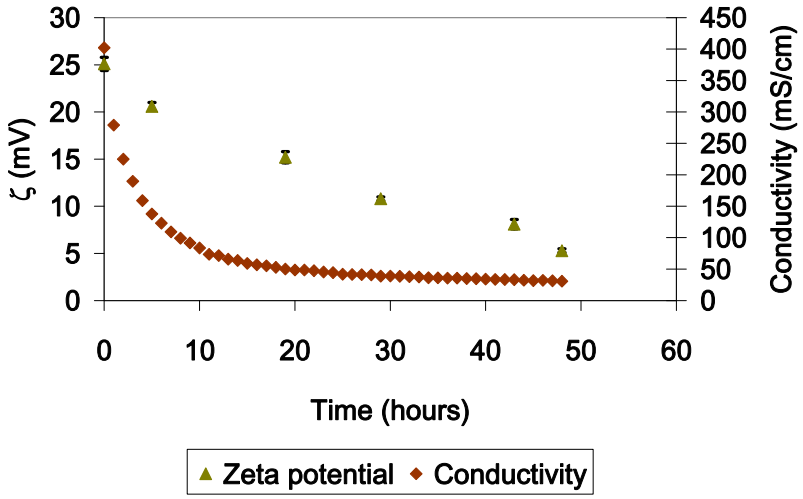

Figure 4.63. Zeta potential (ζ) and conductivity values as a function of time during dialysis of a nanoparticle dispersion obtained from a nano-emulsion with an O/S ratio of 70/30 and 95 wt% water content of the Water / [CatA:CEL = 1:1] / [6 wt% EC10 in ethyl acetate] system with water as dialysate.

At the beginning of the dialysis, conductivity values are about 350 μS/cm and decrease with time, reaching a plateau at around 25 μS/cm after about 35 hours indicating equilibrium of ions, as mentioned above. Nanoparticle surface charge values start around +25 mV, and decrease with time to slightly positive values (about +5 mV).

PBS as dialysate

Removal of excess surfactant from the nanoparticle dispersion during 48 hours was also attempted using PBS (0.33 M) as dialysate (2 L PBS for 8 g of nanoparticle dispersion). Zeta potential and conductivity of the nanoparticle dispersion, measured as a function of time, are shown in Figure 4.64.

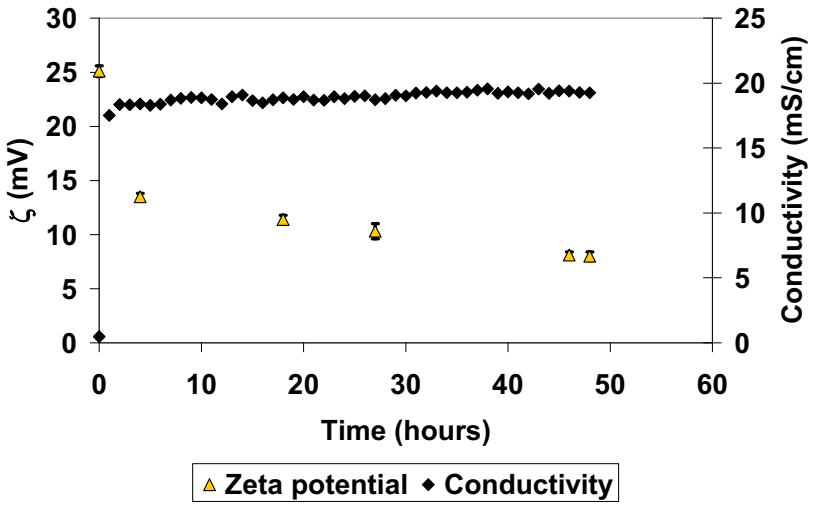

Figure 4.64. Zeta potential (ζ) and conductivity values of the nanoparticle dispersion as a function of time during dialysis of a nanoparticle dispersion obtained from a nano-emulsion with an O/S ratio of 70/30 and 95 wt% water content of the Water / [CatA:CEL = 1:1] / [6 wt% EC10 in ethyl acetate] system with PBS (0.33M) as dialysate.

A pronounced increase in the conductivity of the nanoparticle dispersion from about 0.4 mS/cm to 18 mS/cm can be observed in the first minutes after starting dialysis. The reason for such high conductivity values are the ions present in the buffer solution. Nanoparticle surface charge values start around +25 mV, and decrease with time to about +7 mV, the same trend which has already been observed for dialysis carried out in water as dialysate. It can be interpreted that the nature of the dialysate does not influence the zeta potential of the nanoparticle dispersion.

In this context there was the interest in knowing how much time it would take to attain the pH of the dialysate (pH 7.4) in the nanoparticle dispersion (pH 6.6). Figure 4.65 shows that in the experimental conditions studied, after 15 minutes, the pH of the nanoparticle dispersion is equal to that of the buffer solution.

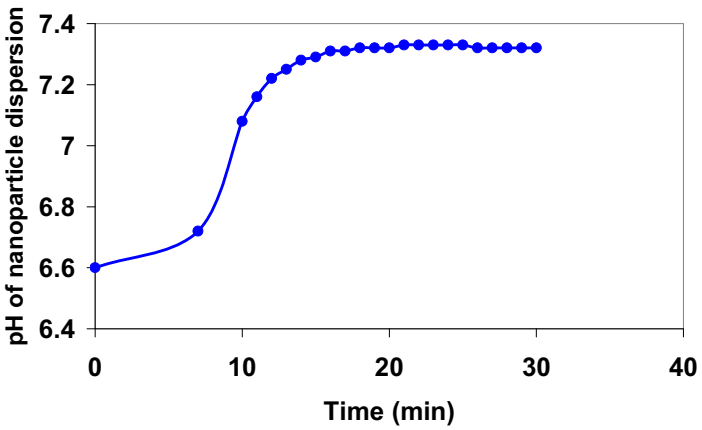

Figure 4.65. pH of a nanoparticle dispersion obtained from a nano-emulsion of the Water / [CatA:CEL = 1:1] / [6 wt% EC10 in ethyl acetate] system with an O/S ratio of 70/30 and 95 wt% water as a function of time with PBS (0.33M) as dialysate.

HEPES solution as dialysate

Another approach to wash off excess of surfactant was carried out using HEPES solution (20 mM, pH 7.4) as dialysate (1 L HEPES solution for 4 g of nanoparticle dispersion) and, moreover, as continuous phase of the nanoparticle dispersion. **Figure 4.66** plots the zeta potential measured in the nanoparticle dispersion and the conductivity measured in the dialysate during the dialysis process (28 hours).

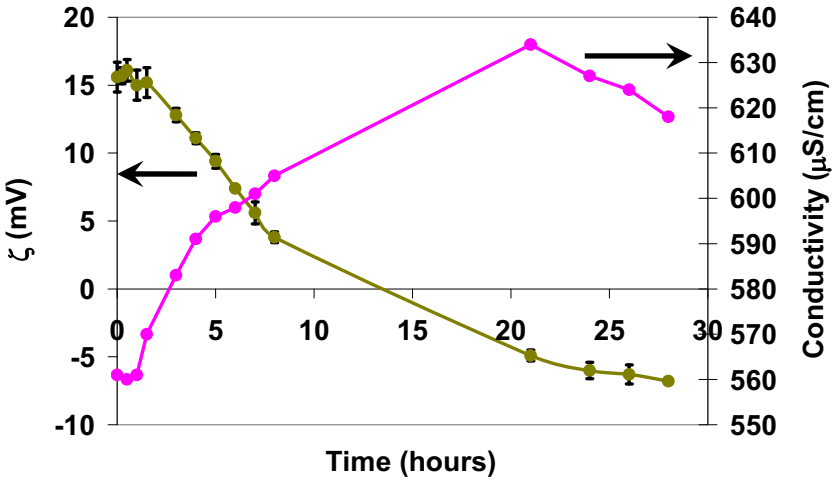

Figure 4.66. Zeta potential (ζ) values of a nanoparticle dispersion obtained from a nano-emulsions of the HEPES solution / [CatA:CEL = 1:1] / [6 wt% EC10 in ethyl acetate] system with an O/S ratio of 70/30 and 95 wt% HEPES solution and conductivity values of the dialysate (HEPES buffer, 20 mM, pH 7.4) as a function of time.

Conductivity values, measured in the dialysate, start at about 560 μS/cm, which are high values compared to water, due to the zwitterionic molecules present in the HEPES solution. Conductivity reaches a maximum value at about 630 μS/cm after 21 hours of dialysis and then decreases slightly. This trend is similar to that observed in **Figures 4.58** and **4.62a**.

Zeta potential values start around +16 mV and are thus slightly lower than values in the dispersion with water as continuous phase. Surface charge values decrease pronouncedly up to 21 hours, reaching neutral values after about 14 hours. With further dialysis, a plateau in the negative scale (about -6 mV) was almost reached. This result allows assuming that most of the cationic surfactant has been washed off of the nanoparticle surface.

In view of the fact that nanoparticles are intended for biomedical applications, a zeta potential of +10 mV is generally considered as a maximum value. In order to obtain this value dialysis was stopped after 5 hours. The nanoparticle dispersion with an O/S ratio of 70/30 and 95 wt% HEPES solution was characterized regarding size and surface charge (**Table 4.40**).

Table 4.40. Particle size (determined by DLS) and zeta potential (ζ) values of a nanoparticle dispersion obtained from a nano-emulsion of the HEPES solution / [CatA:CEL = 1:1] / [6 wt% EC10 in ethyl acetate] system with an O/S ratio of 70/30 and 95 wt% HEPES solution, before and after dialysis.

	Mean diameter by DLS (nm)	ζ (mV)
Before dialysis	80.4 (0.25)	15.8
After 5h dialysis	73.0 (0.49)	11.2

SUMMARY on Excess surfactant removal from nanoparticle dispersions (Section 4.2.2.)

In order to remove surfactant excess, the nanoparticle dispersions were dialysed against water, PBS (0.33 M) or HEPES solution. The dialysis process was followed by conductivity measurements in the dialysate and in the

nanoparticle dispersions but also through measuring the zeta potential of the nanoparticle dispersion as a function of time. Reaching a plateau in conductivity and/or surface charge was interpreted as having reached an equilibrium of ions in and outside of the nanoparticle dispersion. The dialysis process was optimized for the particular systems regarding duration of dialysis and volume of the dialysate and nanoparticle dispersion.

In can be **concluded** that surfactant removal can be achieved successfully by dialysis.

4.2.3. FUNCTIONALIZATION OF CATIONIC NANOPARTICLES

Based on the results of the previous section, the nanoparticle dispersion obtained from the nano-emulsion of the **Aqueous solution / [CatA:CEL = 1:1] / [6 wt% EC10 in ethyl acetate] system** with an O/S ratio of 70/30 and 95 wt% aqueous solution was selected for functionalization studies as it showed small particle size, high enough positive zeta potential values and a good stability.

Complexation with folic acid

Folic acid has been chosen for complexation studies. As mentioned in **Section 3.1.5** the folate receptor is overexpressed on cancerous cells. Due to the high affinity of folic acid/folate for these receptors, this vitamin has been used as targeting ligand for selective delivery of drugs to tumor cells and was used in this work as a model for complex formation with cationic polymeric nanoparticles.

MilliQ® water as continuous phase

In a first attempt, folic acid solution (pH 7.4) and nanoparticle dispersion were prepared with MilliQ® water. As described in **Section 3.3.4**, the nanoparticle dispersion was mixed with folic acid solutions (pH 7.4) at different concentrations in order to obtain complexes with different cationic-to-anionic charge ratios (cationic charge (c^+) from the cationic surfactant present in the

nanoparticle dispersions and anionic charge (a^-) from the anions in the folic acid solution), so-called c^+/a^- ratios, c^+ and a^- expressed as molar ratios. **Figure 4.67** shows the surface charge values of the complexes.

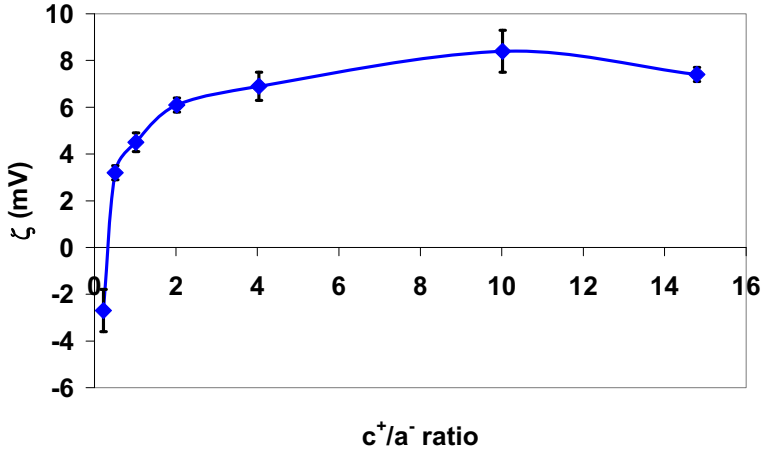

Figure 4.67. Zeta potential (ζ) values as a function of the c^+/a^- ratio between the cationic charges present in a nanoparticle dispersion (c^+) and the negative charges provided by the folic acid (a^-), at 25°C, at pH 7.4. The nanoparticle dispersion was obtained from a nano-emulsion of the Water / [CatA:CEL = 1:1] / [6 wt% EC10 in ethyl acetate] system with an O/S ratio of 70/30 and 95 wt% water.

Initially, the zeta potential of the nanoparticle:folic acid complexes sharply increased with increasing c^+/a^- ratio from slightly negative values (about –4 mV) at low c^+/a^- ratios (≤0.3) to positive values (about +7 mV) for c^+/a^- ratios ≥2 where a plateau is reached. The increase in zeta potential could be explained by ionic interactions between the positively charged nanoparticles and the negatively charged folic acid molecules. At low c^+/a^- ratios the amount of folate anions exceeds the amount of cationic charges on the nanoparticles, resulting in a negative zeta potential. With increasing amount of nanoparticles, the zeta potential increases due to more cationic surface charge present and reaches a plateau in the positive range where it is assumed that the surface of all nanoparticles is saturated with folate anions.

As mentioned previously, the surface charge of nanoparticles plays a major role for biomedical applications. Positively charged nanoparticles have been found to generate a higher immune response compared to neutral or negatively charged nanoparticles. However, a positive surface charge is needed for allowing complex formation with negatively charged bioactive compounds. Davis *et al.* proposed that the optimal surface charge should be between -10

and +10 mV by which nonspecific interactions of nanoparticles will be reduced [Davis, 2009].

Zeta potential values obtained for the nanoparticle:folic acid complexes are significantly lower than those of the nanoparticle dispersion (+34 mV, **Table 4.37** in **Section 4.2.1**) due to the interaction with the negatively charged folate which counteracts the positive charge of the nanoparticles. Therefore, the complexes are within the surface charge range suggested in the literature.

HEPES solution as continuous phase

HEPES solution (20 mM) with a pH of 7.4 (equal to the physiological pH) was used as continuous phase for nanoparticle preparation, and also for the preparation of the folic acid solution and as dialysate. When the nanoparticles are prepared using HEPES solution as the continuous phase, the surface charge of the nanoparticles has a value of about 20 mV, lower than the value when the nanoparticles are prepared using water. As mentioned earlier, this can be attributed to the zwitterionic HEPES molecules which have a shielding effect by placing themselves on the droplet interface and thus lowering the surface charge. For nanoparticle:folic acid complex formation, the same procedure as described previously (using water) was used. The size and surface charge values of the nanoparticle:folic acid complexes are shown in **Figure 4.68**.

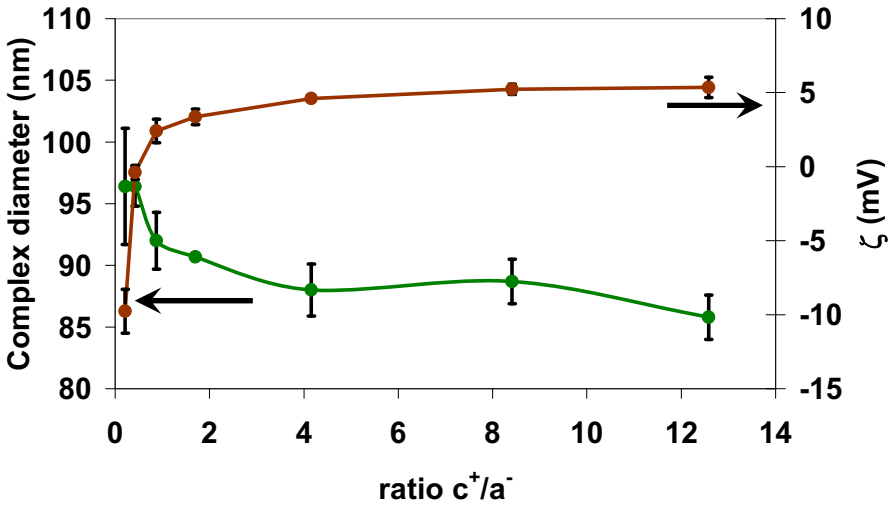

Figure 4.68. Complex size and zeta potential (ζ) values as a function of the c^+/a^- ratio between the cationic charges present in a nanoparticle dispersion (c^+) and the negative charges provided by the folic acid (a^-), at 25°C, at pH 7.4. The nanoparticle dispersion was obtained from a nano-emulsion of the HEPES solution / [CatA:CEL = 1:1] / [6 wt% EC10 in ethyl acetate] system with an O/S ratio of 70/30 and 95 wt% HEPES solution.

There is a pronounced increase in zeta potential of the nanoparticle:folic acid complexes with increasing c^+/a^- ratio from negative values (about -10 mV) at low c^+/a^- ratios (≤0.5) to positive values (about +5 mV) for c^+/a^- ratios ≥5 reaching a plateau. The zeta potential at low c^+/a^- ratios could be explained by a higher amount of anions than cationic surfactant present on the nanoparticle surface, yielding negative surface charge values. With increasing amount of nanoparticles (cationic species), the zeta potential increases reaching a plateau which indicates complete complexation between nanoparticles and folic acid. All obtained zeta potential values are comparable to those obtained when water was used as continuous phase for nanoparticle preparation and are in the range (between -10 and +10 mV) suggested by Davis *et al.* [Davis, 2009]. With increasing c^+/a^- ratio, the nanoparticle:folic acid complex size is decreasing. This decrease is more significant at low c^+/a^- ratios (c^+/a^- ratio < 2) and is diminished at high c^+/a^- ratios (c^+/a^- ratio > 2). This trend may be due to the high ionic interactions at high c^+/a^- ratios, which may lead to the formation of more compact structures and hence to small complex sizes. This has been suggested in the work of Sun *et al.* where similar tendencies in size and surface charge have been obtained for Dextran-adriamycin-polyethylenimine/DNA complexes [Sun, 2011].

Davis *et al.* reported that particle sizes of about 75 ± 25 nm are considered as optimal as delivery systems [Davis, 2009]. Sizes smaller than 10 nm tend to be cleared by either the kidney or through extravasation while larger particles tend to be cleared by the cells or the mononuclear phagocyte system [Swami, 2012]. Also Hans *et al.* [Hans, 2002] reported that the size of nanoparticles must be significant smaller than the micrometer range to avoid the formation of an embolism. The significance of particle size was also reported in the work of Desai *et al.* [Desai, 1997]. It was described that nanoparticles of 100 nm showed a 2.5 fold greater uptake in the Caco-2 cell line compared to those with a size of 1 μm and a 6 fold greater uptake compared to 10 μm big microparticles.

The obtained complex size values (between 100 and 85 nm) are in the range suggested by different authors like Davis *et al.* and Hans *et al.* [Hans, 2002;

Davis, 2009]. Nanoparticle:folic acid complexes are therefore promising candidates for biomedical use.

Based on the results obtained for complex formation with folic acid, it was decided for further experiments to focus on c^+/a^- ratios up to about 4 as a plateau in surface charge has already been reached, meaning that complexation with folic acid molecules is complete.

Effect of glucose

As mentioned in Section 4.1.1, a requirement for some applications in biological environments is the osmolarity adjustment of the system to that of the blood (275 – 300 mOsm/kg). As it was found in previous studies (Section 4.1.5), nano-emulsions prepared with HEPES solutions with 4.3 – 4.5% glucose content fulfilled this requirement. For that reason, the nanoparticle:folic acid complexes were formed under the same conditions. In Figure 4.69 the osmolarity values are plotted against the c^+/a^- ratio of obtained complexes.

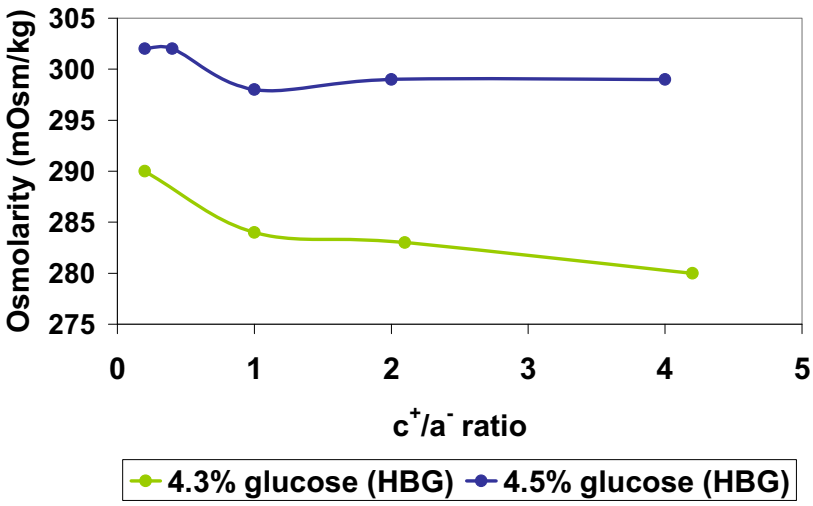

Figure 4.69. Osmolarity values as a function of the c^+/a^- ratio of complexes formed between nanoparticles and folic acid (2 mM), at 25°C. Nanoparticles were obtained from nano-emulsions of the HEPES buffered glucose solution / [CatA:CEL = 1:1] / [6 wt% EC10 in ethyl acetate] system with an O/S ratio of 70/30 and 95 wt% HEPES buffered glucose containing **4.3%** and **4.5%** glucose.

While with 4.5% glucose content in the HEPES solution the values of the nanoparticle:folic acid complexes are near the border of the required range (275–300 mOsm/kg), with 4.3% glucose they are suitable. For that reason, complexes prepared with HEPES solution containing this glucose content were

further characterized in terms of complex size and surface charge. **Figure 4.70** shows the results obtained.

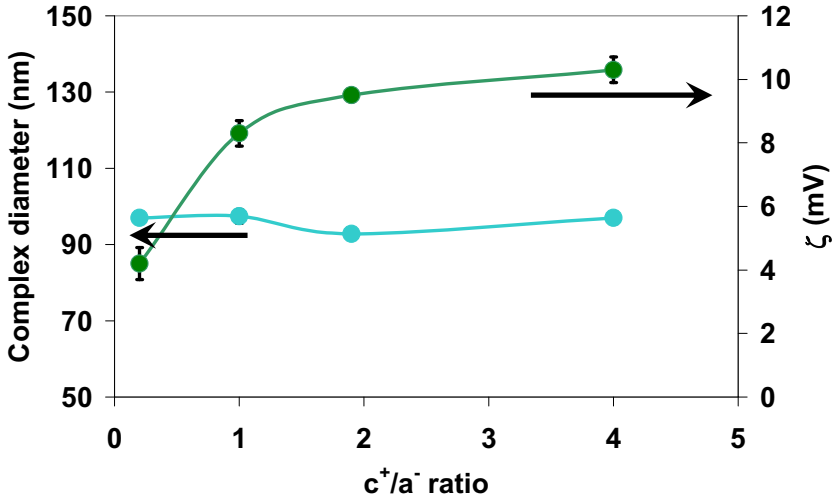

Figure 4.70. Size and zeta potential (ζ) values as a function of the c^+/a^- ratio of complexes formed between nanoparticles and folic acid (2 mM), at 25°C. Nanoparticles were obtained from nano-emulsions of the HEPES buffered glucose solution (HBG, 4.3%glucose, pH 7.4) / [CatA:CEL = 1:1] / [6 wt% EC10 in ethyl acetate] system with an O/S ratio of 70/30 and 95 wt% HBG.

Nanoparticle:folic acid complex size is not significantly changed with increasing c^+/a^- ratio (about 95 nm). The trend in sizes roughly matches that observed without glucose.

In contrast, zeta potential values increase from about +4 mV with the c^+/a^- ratio of about 0.2 to +10 mV at c^+/a^- ratio 4. At higher c^+/a^- ratios, zeta potential values experience only a slight increase, indicating that complex formation between nanoparticles and folic acid is complete. The trend is comparable to those observed previously without glucose addition. Also here, values are in the appropriate range for avoiding a fast nanoparticle clearance from the bloodstream.

Complexation with oligonucleotides

In addition to the complexation studies of polymeric nanoparticles with folic acid, the formation of complexes of antisense phosphorothioate oligonucleotides (ASO) with nanoparticles (using HEPES solution as aqueous phase) was studied. A methodology similar to that described for the formation of folic acid complexes was followed: First, an increasing amount of nanoparticles was

added to a fixed concentration of ASO in order to form complexes with different cationic-to-anionic charge ratios, referred to as N/P ratios, as used in literature for complex formation for DNA [Cheng, 2011; Mohammadi, 2011; Sun, 2011]. The resulting solutions were incubated (37°C, 40 minutes) and size and surface charge were characterized. The results are shown in Figure 4.71.

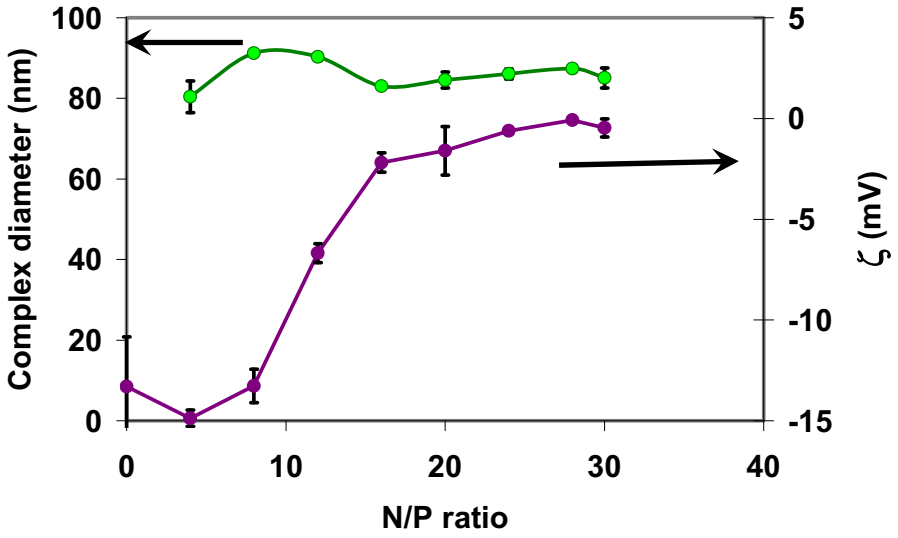

Figure 4.71. Size and zeta potential (ζ) values as a function of the N/P ratio of complexes formed between nanoparticles and the antisense oligonucleotide (ASO) phosphorothioate, at 25°C. Nanoparticles were obtained from nano-emulsions of the HEPES solution / [CatA:CEL = 1:1] / [6 wt% EC10 in ethyl acetate] system with an O/S ratio of 70/30 and 95 wt% HEPES solution.

The nanoparticle:ASO complex size does not change significantly (about 90 nm) with increasing N/P ratio. This has also been reported in literature [Li, 2011]. Compared to the uncomplexed nanoparticle size (determined by DLS), nanoparticle:ASO complex sizes are in the same range of magnitude. They are also in the range suggested by different authors for applications of nanoparticles as therapeutic agents [Hans, 2002; Davis, 2009; Swami, 2012].

Zeta potential values are negative when oligonucleotide is present without nanoparticles or with low nanoparticle concentration (about -15 mV), which is due to the negative backbone of the oligonucleotide. Surface charge values remain in this range up to N/P ratio 8. At N/P ratios ≥ 8, a pronounced increase to almost neutral zeta potential values takes place, an indication of electrostatic interactions between the negatively charged ASO and the positively charged nanoparticles. At N/P ratios ≥ 16, surface charge values are neutral or slightly negative. At these N/P ratios it is assumed that full complexation is achieved.

Putnam *et al.* reports similar behavior for DNA:(polycationic)polymer complexes [**Putnam, 2001**]. Similar results have also been obtained by Ogris *et al.* He showed that the zeta potential of DNA complexes with PEI or TfPEI increased with increasing N/P ratio [**Ogris, 1999**].

The surface charge of the complexes was also measured in the presence of Fetal Bovine Serum (FBS) which is frequently used in transfection studies. As illustrated in **Figure 4.72**, nanoparticle:ASO complexes displayed a negative zeta potential at all N/P charge ratios studied. Zeta potential values are more negative when oligonucleotide and serum without nanoparticles are present (N/P ratio 0, about -25 mV) as additional negative charges are present, coming from serum proteins. Surface charge values increase up to -15 mV for N/P ratio 8 and then only slightly for N/P ratios > 8, staying in the negative range (about -10 mV). These results suggest that negatively charged components in serum might be absorbed onto the surface of the nanoparticle complexes, depending on the charge ratio. Similar results were shown in the work of Li *et al.* dealing with liposome/DNA complexes [**Li, 2011**]. The zeta potential of liposome/DNA complexes (lipoplexes) was studied in the absence and presence of serum. In the absence of serum zeta potential values were positive and increased with increasing N/P ratio. In the presence of serum, however, lipoplexes displayed negative zeta potential values with all studied N/P ratios which was attributed to negatively charged components in serum absorbed onto the surface of the lipoplex particles.

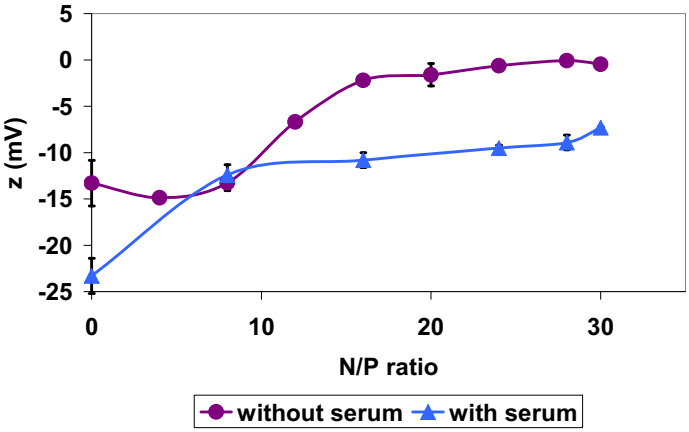

Figure 4.72. Zeta potential (ζ) values as a function of the N/P ratio of complexes formed between nanoparticles and the antisense oligonucleotide (ASO) phosphorothioate in the absence and presence of Fetal Bovine Serum (FBS), at 25°C.Nanoparticles were obtained from nano-emulsions of the HEPES solution / [CatA:CEL = 1:1] / [6 wt% EC10 in ethyl acetate] system with an O/S ratio of 70/30 and 95 wt% HEPES solution.

To assess the complex formation between nanoparticles and ASO, electrophoretic mobility shift assays (EMSA) were performed. This experiment was carried out without FBS and as described in Section 3.3.10. Figure 4.73 shows the results obtained. The numbers between the vertical lines in the figure indicate the N/P ratio.

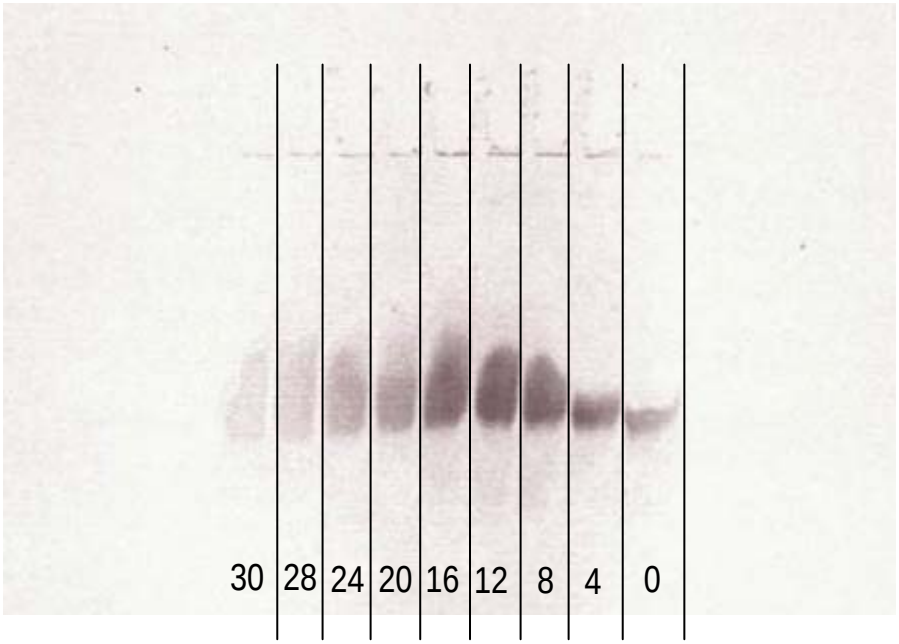

Figure 4.73. EMSA gel shift assay obtained after 8 hours, to analyse the ability of the nanoparticles to form complexes with the antisense oligonucleotide (ASO) phosphorothioate. Nanoparticles were obtained from a nano-emulsions of the HEPES solution / [CatA:CEL = 1:1] / [6 wt% EC10 in ethyl acetate] system with an O/S ratio of 70/30 and 95 wt% HEPES solution. The numbers indicate the N/P ratios.

The negative control is designated 0, i.e. it contains only ASO. With increasing N/P ratio, the band gets broader which was assumed to be due to the formation of complexes with different sizes (polydispersity). For the N/P ratio 20 the band is less intense than for smaller N/P ratios and the higher the N/P ratio is, the more fades the band. The fading of the band is interpreted as a sign of complex formation and retardation. This phenomenon has been described by Lundberg *et al.* [Lundberg, 2007]. In his work, he demonstrated that cell-penetrating peptides could effectively bind siRNA which was followed by gel shift assays. It was for example observed that for the peptide penetratin, complete siRNA retardation took place at a molar ratio of peptide to siRNA of 10:1.

The results obtained are in good agreement with those obtained from surface charge measurements, suggesting that complex formation is achieved at N/P ratios ≥ 16.

Figure 4.74 shows a TEM micrograph obtained from the nanoparticle:ASO complex with an N/P ratio of 30, the highest studied N/P ratio in which complexation took place. Complexes showed a rounded shape and a mean size of 30 nm (by TEM image analysis). This value differs significantly from that obtained by DLS (about 90 nm). As mentioned previously, the sizes measured from TEM micrographs correspond to the hard sphere sizes while DLS provides sizes of the hydrated complexes. Also the high polydispersity (>0.4) has to be taken into account.

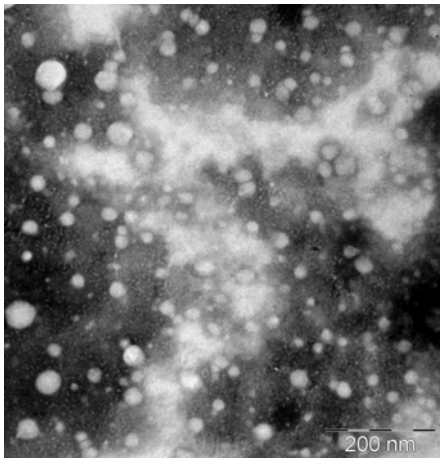

Figure 4.74. TEM micrograph of the negatively stained complex between a nanoparticle dispersion and the antisense oligonucleotide phosphorothioate, in the N/P ratio 30. Nanoparticles were obtained from a nano-emulsion of the HEPES solution / [CatA:CEL = 1:1] / [6wt% EC10 in ethyl acetate] system with an O/S ratio of 70/30 and 95 wt% HEPES solution.

Figure 4.75 compares the size distributions of the nanoparticle dispersion and the complex.

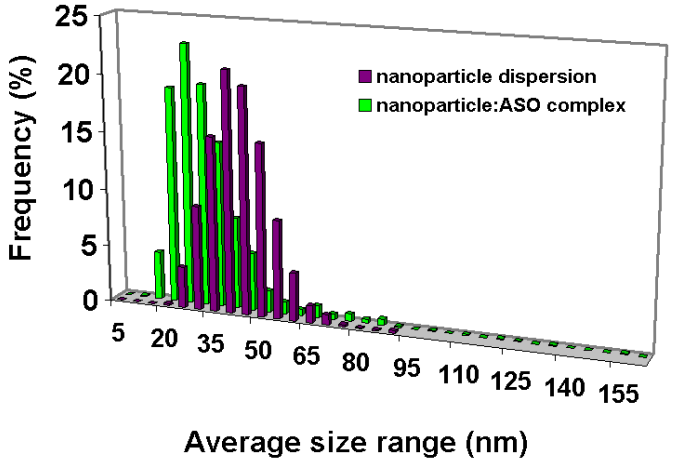

Figure 4.75. Complex size distributions, assessed from TEM image analysis, of a negatively stained nanoparticle dispersion nanoparticle dispersion of the HEPES solution / [CatA:CEL = 1:1] / [6wt% EC10 in ethyl acetate] system with an O/S ratio of 70/30 and 95 wt% HEPES solution and of the complex between nanoparticles and the antisense oligonucleotide phosphorothioate, in the N/P ratio 30.

Both size distributions are monomodal. The main population of the nanoparticle dispersion is at 40 nm and is shifted towards smaller sizes when the complex with ASO is formed. This decrease in mean size has to be taken with caution as the polydispersity with both systems is rather high. However, it should be also considered that electrostatic attractions may favour the compactation of the structure, thus yielding smaller entities, as observed with the nanoparticle:folic acid complexes described above.

SUMMARY on Functionalization of cationic nanoparticles (Section 4.2.3.)

Complexes between folic acid and nanoparticles obtained from a nano-emulsion of the *Aqueous solution / [CatA:CEL = 1:1] / [6 wt% EC10 in ethyl acetate] system* with an O/S ratio of 70/30 and 95 wt% aqueous solution have been obtained with both, water and HEPES solution as aqueous phases. For nanoparticle:folic acid complexes, zeta potential values follow the same trend for both aqueous phases, starting with surface charge values in the negative range for small c^+/a^- ratios and increasing to positive values with increasing nanoparticle concentration.

The incorporation of 4.3% glucose into the aqueous phase is needed to bring osmolarity values of nanoparticle:folic acid complexes in the required range (275 – 300 mOsm/kg) for applications in contact with blood. Complex size did not change significantly and surface charge displayed the same trend described for complexes in water and HEPES solution.

Complexes between the antisense oligonucleotide (ASO) phosphorothioate and nanoparticles obtained from a nano-emulsion of the *HEPES solution / [CatA:CEL = 1:1] / [6 wt% EC10 in ethyl acetate] system* with an O/S ratio of 70/30 and 95 wt% HEPES solution have successfully been obtained. Tendencies regarding complex size and surface charge are similar to those for complexes formed with folic acid. Complex formation was confirmed also by electrophoretic mobility shift assays. The nanoparticle:antisense oligonucleotide complex with the N/P ratio 30 was characterized by TEM image analysis. Complexes possess a higher sphericity than nanoparticles with a mean size of 30 nm, smaller than those obtained for the nanoparticle dispersion (40 nm).

The following **conclusions** can be made:

- Nanoparticle:folic acid complexes with several c^+/a^- ratios were obtained in water and HEPES solution.
- Nanoparticle:folic acid complex sizes were similar to those of the nanoparticles. However, a relevant change in surface charge was noted. The presence of glucose had no significant influence on complex size and complex surface charge.
- Nanoparticle:antisense oligonucleotide complexes with different N/P ratios were successfully obtained.
- Nanoparticle:antisense oligonucleotide complex sizes are smaller than those of the nanoparticles. There is a significant change in zeta potential with increasing N/P ratio, similar to results obtained with folic acid.
- The presence of Fetal Bovine Serum (FBS) had a crucial influence on surface charge values of the nanoparticle:ASO complexes.
- Complexes formed with folic acid and with ASO have appropriate sizes and surface charges for therapeutic applications.

4.2.4. *IN VITRO* STUDIES OF NANOPARTICLE DISPERSIONS

The nanoparticle dispersion obtained from a nano-emulsion of the **HEPES solution / [CatA:CEL = 1:1] / [6 wt% EC10 in ethyl acetate] system** with an O/S ratio of 70/30 and 95 wt% HEPES solution, selected for the complexation studies, was further investigated to determine its toxicity and transfection efficiency.

Cytotoxicity test with 3-(4,5-dimethylthiazol-2-yl)-2,5 diphenyltetrazolium bromide (MTT)

The viability and proliferation of HeLa cells in the presence of nanoparticles was evaluated by performing the MTT cytotoxicity assay on HeLa cells. The studies were carried out as described in **Section 3.3.11**. The absorbance of the colored complex solutions was measured at a wavelength of λ = 570 nm as a function of cationic species concentration present in CatA (40 wt% of active matter).

Keeping in mind that cell viability is directly proportional to the amount of formazan produced (**Section 3.3.11**), dead cells do not show any enzymatic activity and hence will not form formazan crystals. Therefore the absorbance is only due to live cells and gives an idea of the number of viable cells when compared with the control (i.e. cells in the absence of nanoparticles). **Figure 4.76** shows the obtained results.

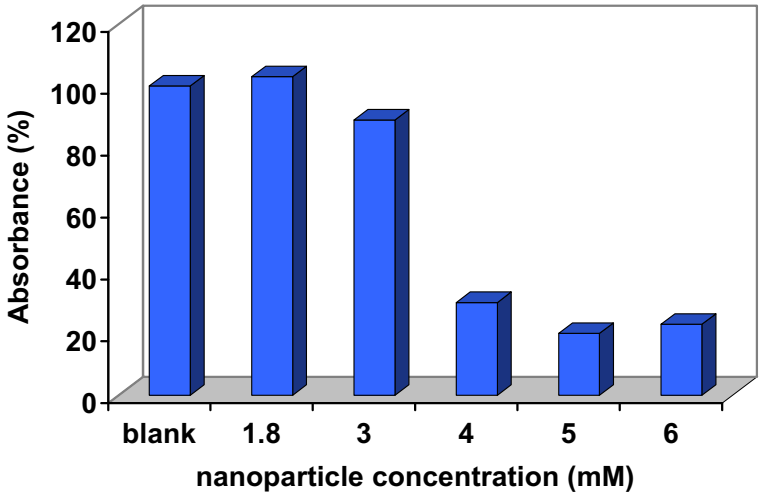

Figure 4.76. Absorbance (at λ = 570 nm) of HeLa cells as a function of nanoparticle concentration after 4 hours of treatment. Nanoparticles were obtained from a nano-emulsion of the HEPES solution / [CatA:CEL = 1:1] / [6 wt% EC10 in ethyl acetate] system with an O/S ratio of 70/30 and 95 wt% HEPES solution. The **blank** bar indicates the sample without nanoparticles.

The graphic shows that absorbance decreases slightly at 3 mM with respect to the blank while at higher concentration it is considerably reduced, indicating that no cytotoxicity occurs up to a concentration of 3 mM, referred to the cationic species. The same trend was reported by Putnam *et al.* [**Putnam, 2001**]. He showed that the cytotoxicity of acid-degradable cationic nanoparticles increased with increasing concentration of cationic polymer.

In vitro hemolysis test

As the nanoparticles are ought to be used as drug carriers, it is important to evaluate their biocompatibility with blood components. The experiments were carried out as described in **Section 3.3.12**. Osmolarities of the samples were adjusted to that required for these tests (between 275 and 300 mOsm/kg) by adding a concentrated glucose solution (30%) to the samples. **Table 4.41**

summarizes the values obtained for the nanoparticle dispersion at different concentrations.

Table 4.41. Osmolarity and percentage of hemolysis (%) of different concentrations of cationic species present in CatA in a nanoparticle dispersion, obtained from a nano-emulsion of the HEPES solution / [CatA:CEL = 1:1] / [6 wt% EC10 in ethyl acetate] system with an O/S ratio of 70/30 and 95 wt% HEPES solution.

Formulation	Cationic species concentration (mM)	Osmolarity (mOsm/kg)	Hemolysis (%)
Nanoparticle dispersion	7.9	279	> 85
	3.0	286	

Nanoparticle dispersions with concentrations of cationic species equal to or above 3 mM (maximum concentration for cytotoxicity tests with HeLa cells, **Section 4.4.1**) were highly hemolytic (>85%).

For complexes formed with folic acid, hemolylsis was greatly reduced (**Table 4.42** and **Figure 4.77**).

Table 4.42. Osmolarity and percentage of hemolysis (%) of complexes with different c^+/a^- ratios formed between a nanoparticle dispersion, obtained from a nano-emulsion of the HEPES solution / [CatA:CEL = 1:1] / [6 wt% EC10 in ethyl acetate] system with an O/S ratio of 70/30 and 95 wt% HEPES solution and varying concentrations of a folic acid solution.

Formulation	c^+/a^- charge ratio	Cationic species concentration (mM)	Osmolarity (mOsm/kg)	Hemolysis (%)
Nanoparticle:folic acid complex	0.1	0.4	280	2
	0.4		278	5
	0.8		280	6
	1.7		279	8

An explanation for this behavior may be not only the complexation but also the very low concentration of cationic species present in the complex (about 20 times lower than that of the nanoparticle dispersion). **Figure 4.77** shows the hemolytic activity as a function of cationic:anionic (c^+/a^-) charge ratio in nanoparticle:folic acid complexes.

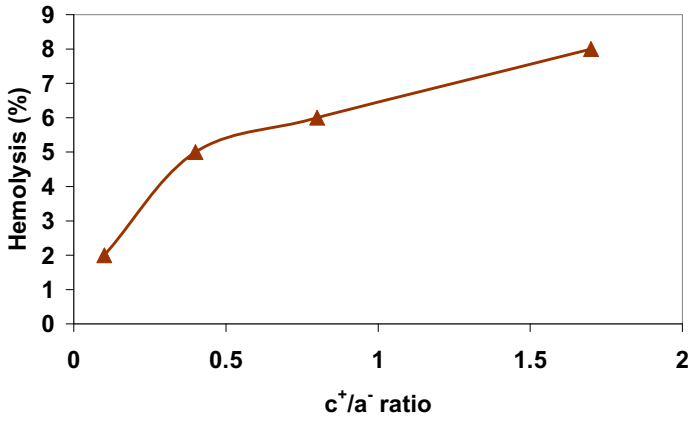

Figure 4.77. Hemolysis (%) as a function of cationic:anionic charge (c^+/a^-) ratio of positively charged nanoparticles and negatively charged folic acid.

Hemolysis is decreasing with decreasing c^+/a^- ratio. As the concentration of cationic species is low, it is assumed that consequently also the zeta potential values are low. Furthermore, as the folic acid content increases with decreasing c^+/a^- ratio, surface charge values are assumed to be lower for low c^+/a^- ratios.
With a minimum hemolysis of 2%, the limits of hemolysis for biomedical purposes (0.8% as per the Council of Europe guidelines and 1% per the US FDA guidelines [**Guide to the preparation, use and quality assurance of blood components, 2000; US License Number. 1986**]) are exceeded. However, the fact that hemolysis is low at low nanoparticle concentration and that folic acid attached to the particles further decreases the hemolytic effect is a promising result in view of achieving lower values of hemolysis.

Transfection efficiency of nanoparticle:oligonucleotide complexes

The ability of the cationic nanoparticles to form complexes with the antisense oligonucleotide (ASO) phosphorothioate through electrostatic interactions was described and proved in **Section 4.3.2**. As mentioned in the introduction, the ASO has been synthesized to inhibit the *Renilla* luciferase gene [**Zhang, 2003; Grijalvo, 2010 and 2012**]. In this chapter, the transfection efficiency of nanoparticles in the absence and presence of Fetal Bovine Serum (FBS) was evaluated. At first, the optimal ratio between the antisense oligonucleotide and the nanoparticles was determined. The experiment was carried out as described in **Section 3.3.13**. Briefly, cells were cotransfected with two luciferase

plasmids (*Renilla* and firefly; target and internal control, respectively). Then the antisense oligonucleotide designed to inhibit the expression of *Renilla* luciferase gene was added with and without nanoparticles. After 24 hours of transfection, the luciferase activities of the samples were measured by using a luminometer. **Figure 4.78** plots the *Renilla* luciferase activity normalized to firefly luciferase as a function of nanoparticle:antisense oligonucleotide (N/P) ratio. In **Section 4.3.2** it was shown by means of zeta potential measurements that formation of nanoparticle:ASO complexes took place at N/P ratios equal to or above 16. As full complexation was assumed in the their described plateau range, which was confirmed by gel shift assays, two N/P ratios of the plateau range (N/P 28 and 30) were selected for transfection assays and a N/P ratio higher than those studied (N/P 35) in order to study the influence of higher nanoparticle concentration. The results show that the luciferase activity of the transfected HeLa cells in the absence and the presence of the antisense oligonucleotide were identical. This confirms that the oligonucleotide alone is not able to reach the nucleus of the HeLa cells to inhibit the expression of the *Renilla* luciferase gene.

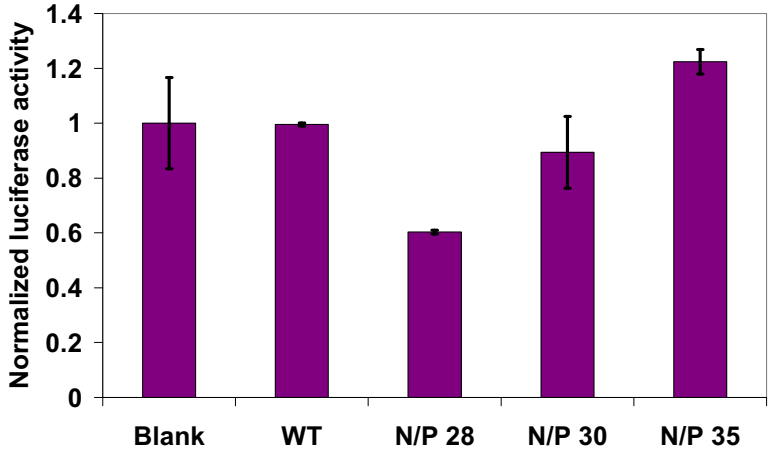

Figure 4.78. Gene-specific silencing activities for phosphorothioate antisense oligonucleotide, targeting the *Renilla* luciferase mRNA expressed in HeLa cells. The N/P (nanoparticle:antisense oligonucleotide) ratios tested for gene knockdown were N/P 28, 30 and 35. The ASO concentration was 60 nM. The bar named **Blank** is the result of luciferase activity of the HeLa cells with the two transfected plasmids. The bar named **WT** is the result without using nanoparticles.

However, it was found that the nanoparticles:ASO complexes were able to transfect the antisense oligonucleotide as the expression of *Renilla* luciferase gene was specifically inhibited. The highest inhibitory properties were found

with nanoparticle:antisense oligonucleotide complexes at the charge ratio of N/P 28 obtaining around 40% inhibition efficiency in serum-free medium. For this reason, the N/P ratio of 28 was chosen to be the optimal for transfecting antisense oligonucleotides with the nanoparticles.

In addition to the transfect cells in cell culture media, it is important to analyse the possibility of using these nanoparticles for intravenous administration. It has been described that in serum nanoparticles:nucleic acids complexes can be displaced by serum proteins, losing the transfecting activity. For this reason, the effect of serum concentration (10% FBS) on the transfection efficiency in HeLa cells was tested. **Figure 4.79** shows the obtained results.

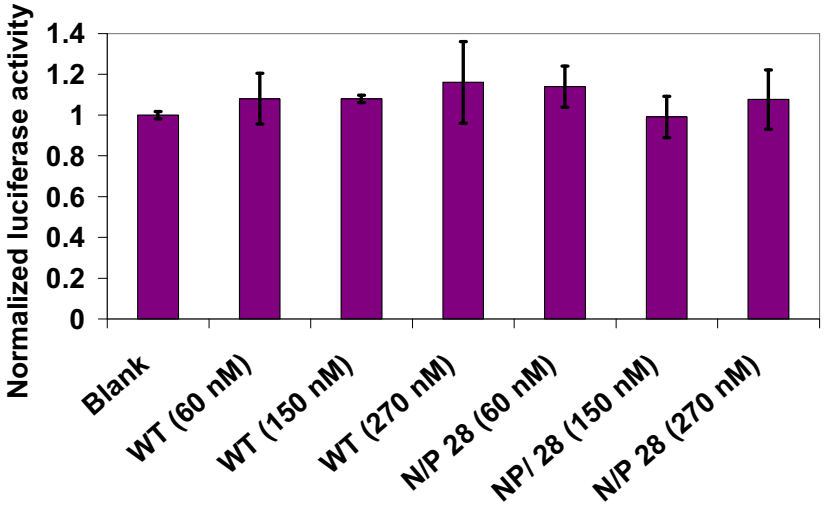

Figure 4.79. Gene-specific silencing activities with 10% serum for unmodified phosphorothioate antisense oligonucleotide (**WT**) at different concentrations (60, 150 and 270 nM) and for the N/P ratio 28 (nanoparticle:antisense oligonucleotide) using mentioned ASO concentrations, targeting the *Renilla* luciferase mRNA expressed in HeLa cells. The bar named **Blank** is the result of luciferase activity of the HeLa cells with the two transfected plasmids.

The N/P charge ratio was set to 28 as it was judged to be the optimal for transfection but, in addition, different ASO concentrations (60, 150 and 270 nM) were tested. As before, the **Blank** and **WT** samples were used as controls. In all cases, the luciferase activity was around 1 which implies that no gene silencing was detected in the presence of serum. This might be due to electrostatic interactions between the positively charged nanoparticles and serum components (e.g. serum proteins), preventing the nanoparticles from entering the cells and thereby reducing the corresponding transfection activity. Hence, further studies are needed for optimizing the transfection efficiency.

SUMMARY on *in vitro* studies on nanoparticle dispersions (Section 4.2.4.)

The cytotoxicity of nanoparticle dispersion of the HEPES solution / [CatA:CEL = 1:1] / [6 wt% EC10 in ethyl acetate] system with an O/S ratio of 70/30 and 95 wt% HEPES solution on HeLa cells was tested. No cytotoxicity occurred up to a concentration of 3 mM of the cationic species present in the nanoparticle dispersion.

In vitro hemolysis tests revealed that nanoparticle dispersions with high concentrations of cationic species showed high hemolytic activity on red blood cells. However, complexes of nanoparticles with folic acid showed significant lower hemolysis.

Transfection efficiency of nanoparticle:antisense oligonucleotide complexes was tested. It was found that the N/P ratio of 28 showed an optimum (40%) in the inhibition of the expression of the *Renilla* luciferase gene in the absence of FBS. However, in the presence of serum proteins, even with changing amount of oligonucleotide, no gene silencing was detected.

The following conclusions can be made:

- Nanoparticles are nontoxic towards HeLa cells up to a concentration of 3 mM of cationic species.
- A low concentration of cationic species is required for obtaining low hemolytic activity. The presence of folic acid attached to the nanoparticles contributes to low hemolysis.
- Transfection efficiency studies preclude the use of these nanoparticles for *in vivo* experiments. However, nanoparticles can be used for gene inhibition in cell cultures.

5. CONCLUSIONS

Polymeric cationic nanoparticles, suitable for biomedical applications, have been obtained by solvent evaporation from cationic nano-emulsions, prepared by a low-energy emulsification method. Nano-emulsions and nanoparticles have been characterized and preliminary *in vitro* studies in biological environment of selected nanoparticles have been carried out. In the following, the main conclusions are summarized.

Formation of O/W cationic nano-emulsions by a low-energy method and their characterization

Nano-emulsions with droplet sizes < 300 nm, positive surface charges and acceptable stability have successfully been obtained in the Aqueous solution / [CatA: nonionic surfactant] / [Polymer in ethyl acetate] system. Nano-emulsion properties have been controlled by the type of the nonionic surfactant, the CatA: nonionic surfactant ratio, the composition of the aqueous solution, the polymer concentration and the polymer molecular weight.

Comparing the different **nonionic surfactants** studied, it can be concluded that nano-emulsion properties using a castor oil surfactant derivative, i.e. Cremophor® WO7 or Cremophor® EL, are more suitable for the intended application than those using sorbitan ester which suggests that the surfactant structure plays a significant role.

The **CatA : nonionic surfactant mixing ratio** of 1:1 was found to be optimum to form nano-emulsions with small droplet size and appropriate surface charge and stability.

The properties of nano-emulsions prepared with **MilliQ water or HEPES solution** did not differ significantly while nano-emulsions prepared with a **phosphate buffer** were highly unstable. The incorporation of glucose in order to adapt the

solution to the osmolarity required for *in vitro* studies had no influence on droplet size or surface charge.

Increasing the **polymer concentration** from 6 wt% to 10wt% did not improve nano-emulsion properties. Decreasing the **polymer molecular weight** (from EC10 to EC4) did not significantly change nano-emulsion properties.

Formation and characterization of cationic nanoparticles

Cationic nanoparticles with small particle sizes (<250 nm), positive surface charges and acceptable stability have been obtained from nano-emulsion templating by the solvent evaporation method.

Nanoparticle surface charge and stability were similar to those of the template nano-emulsions while particle size was smaller.

The nature of the **nano-emulsion aqueous component** did not influence significantly size and stability of the nanoparticles. Surface charge values, however, were lower in HEPES solution than in water.

Decreasing the polymer **molecular weight** (from EC10 to EC4) did not significantly change nanoparticle size and surface charge, independently on the aqueous solution used.

Complex formation between nanoparticles and **folic acid** at different charge ratios was achieved. Complex formation was not influenced by the nature of the nanoparticle aqueous component. The size of the complexes formed with different cationic/anionic (c^+/a^-) charge ratios was not significantly changed compared to that of uncomplexed nanoparticles. However, surface charge values were significantly decreased.

Complexation between nanoparticles and an **antisense oligonucleotide** (ASO) at different nanoparticle:antisense oligonucleotide (N/P) ratios have been achieved. The complexes showed the same trends regarding surface charge and size as

those observed for nanoparticle:folic acid complexes and are hence suitable for therapeutic applications.

In the presence of Fetal Bovine Serum (FBS), surface charge values of the nanoparticle:ASO complexes stayed in the negative range suggesting that serum components were absorbed onto the nanoparticle surface.

In vitro studies of nanoparticle dispersions revealed that nanoparticles are non-toxic to HeLa cells up to a concentration of 3 mM.

A low concentration of cationic species is required for obtaining low hemolytic activity. The presence of folic acid attached to the nanoparticles may contribute to low hemolysis values.

In the absence of Fetal Bovine Serum, *Renilla* luciferase gene inhibition showed an optimum for the N/P ratio 28 (40%) which makes them promising candidates for gene inhibition in cell cultures. However, in the presence of serum proteins, no gene silencing was detected, precluding the use of these nanoparticles for *in vivo* experiments.

6. REFERENCES

Allay, M.C., Scudiero, D.A., Monks, A., Hursey Czerwinski, M.L.M.J., Fine, D.L., Abbott, B.J., Mayo, J.G., Shoemaker, R.H., Boyd, M.R., Feasibility of drug screening with panels of human tumor cell lines using a microculture tetrazolium assay, *Cancer Research*, 1988, 48 (3), 589-601.

Alves, M.P., Scarrone, A.L., Santos, M., Pohlmann, A.R., Guterres, S.S., Human skin penetration and distribution of nimesulfide from hydrophilic gels containing nanocarriers, *International Journal of Pharmaceutics*, 2007, 341 (1-2), 215-220.

Ammar, H.O., Salama, H.A., Ghorab, M., Mahmoud, A.A., Nanoemulsion as a potential ophthalmic delivery system for dorzolamide hydrochloride, *AAPS PharmSciTech*, 2009, 10 (3), 808-819.

Anton, N., Benoit, J-P., Saulnier, P., Design and production of nanoparticles formulated from nano-emulsion templates–a review, *Journal of Controlled Release*, 2008, 128, 185-199.

Anton, N., Vandamme, T.F., The universality of low-energy nano-emulsification, *International Journal of Pharmaceutics*, 2009, 377, (1-2), 142-147.

Aparicio, R.M., García-Celma, M.J., Vinardell, M.P., Mitjans, M., In vitro studies of the hemolytic activity of microemulsions in human erythrocytes, *Journal of Pharmaceutical and Biomedical Analysis*, 2005, 39 (5), 1063-1067.

Arias, J.L., López-Viota, M., Delgado, A.V., Ruiz, M.A., Iron/ethylcellulose (core/shell) nanoplatform loaded with 5-fluorouracil for cancer targeting, *Colloids and Surfaces B: Biointerfaces*, 2010, 77 (1), 111-116.

Arias, J.L., Ruiz, Ma.A., López-Viota, M., Delgado, A.V., Poly(alkylcyanoacrylate) colloidal particles as vehicles for antitumour drug delivery: A comparative study, *Colloids and Surfaces B: Biointerfaces*, 2008, 62 (1), 64-70.

Asua, J.M., Miniemulsion polymerization, Miniemulsion polymerization, *Progress in Polymer Science (Oxford)*, **2002**, 27 (7), 1283-1346.

BASF a Technical data sheet of Cremophor® WO7.

BASF b Technical data sheet of Cremophor® EL.

Benita, S., Levy, M.Y., Submicron emulsions as colloidal drug carriers for intravenous administration: Comprehensive physicochemical characterization, *Journal of Pharmaceutical Sciences*, **1993**, 82, 1069-1079.

Bernas, T., Dobrucki, J., Mitochondrial and nonmitochondrial reduction of MTT: Interaction of MTT with TMRE, JC-1, and NAO mitochondrial fluorescent probes, *Cytometry*, **2002**, 47 (4), 236-242.

Berridge, M.V., Herst, P.M., Tan, A.S., Tetrazolium dyes as tools in cell biology: New insights into their cellular reduction, *Biotechnology Annual Review*, **2005,** 11 (SUPPL.), 127-152.

Bivas-Benita, M., Oudshoorn, M., Romeijn, S., Van Meijgaarden, K., Koerten, H., Van der Meulen, H., Lambert, G., Ottenhoff T., Benita S., Junginger H., Borchard G., Cationic submicron emulsions for pulmonary DNA immunization, *Journal of Controlled Release*, **2004**, 100 (1), 145-155.

Borwankar, R.P., Lobo, L.A., Wasan, D.T., Emulsion stability – kinetics of flocculation and coalescence, *Colloids and Surfaces*, **1992**, 69 (2-3), 135-146.

Bouchemal, K., Briançon, S., Perrier, E., Fessi, H.,Nano-emulsion formation using spontaneous emulsification : solvent, oil and surfactant optimisation, *International Journal of Pharmaceutics*, **2004**, 280, 241-251.

Calderó, G., García-Celma, M.J., Solans, C., Formation of polymeric nano-emulsions by a low-energy method and their use for nanoparticle preparation, *Journal of Colloid and Interface Science*, **2011**, 353, 406-411.

Calderó, G., Montes, R., Llinàs M., García-Celma, M.J., Solans, C., Studies on the formation of polymeric nano-emulsions obtained via low-energy emulsification and their use as templates of drug delivery nanoparticle dispersions, **submitted**.

Calvo, P., Vila-Jato J.L., Alonso M.J., Comparative in vitro evaluation of several colloidal systems, nanoparticles, nanocapsules, and nanoemulsions as ocular drug carriers, *Journal of Pharmaceutical Sciences*, **1996**, 85 (5), 530-536.

Chen, C., Cheng, Y.C., Yu, C.H., Chan, A.W., Cheung, M.K., Yu, P.H.F., In vitro cytotoxicity, hemolysis assay, and biodegradation behavior of biodegradable poly(3-hydroxybutyrate)-poly(ethylene glycol)-poly(3-hydroxybutyrate) nanoparticles as potential drug carriers, *Journal of Biomedical Materials Research – Part A*, **2008**, 87 (2), 290-298.

Chen, D., Anti-reflection (AR) coatings made by sol-gel process: A review, *Solar Energy Materials & Solar Cells*, **2001**, 68, 313-336.

Cheng, M., Li, Q., Wan, T., Hong, X., Chen, H., He, B., Cheng, Z., Xu, H.-X., Ye, T., Zha, B., Wu, J., Zhou, R., Synthesis and efficient hepatocyte targeting of galactosylated chitosan as a gene carrier in vitro and in vivo, *Journal of Biomedical Materials Research – Part B Applied Biomaterials*, **2011**, 99 B (1), 70-80.

Cheng, Q., Feng, J., Chen, J., Zhu, X., Li, Fl, Brain transport of neurotoxin-I with PLA nanoparticles through intranasal administration in rats: A microdialysis study, *Biopharmaceutics and Drug Disposition*, **2008**, 29 (8), 431-439.

Clausse, M., Heil, J., Diffuse phase inversion, percolation and bicontinuous structures in microemulsions*, Lettere al Nuovo Cimento*, **1983**, 36 (12), 369-376.

Cortesi, R., Esposito, E., Luca, G., Nastruzzi, C., Production of lipospheres as carriers for bioactive compounds, *Biomaterials*, **2002**, 23 (11), 2283-2294.

Couvreur, P., Dubernet, C., Puisieux, F., Controlled drug delivery with nanoparticles: Current possibilities and future trends, *European Journal of Pharmaceutics and Biopharmaceutics*, **1995**, 41 (1), 2-13.

Couvreur, P., Vauthier, C., Nanotechnology: Intelligent design to treat complex disease, *Pharmaceutical Research*, **2006**, 23 (7), 1417-1450.

Damgé, C., Maincent, P., Ubrich, N., Oral delivery of insulin associated to polymeric nanoparticles in diabetic rats, *Journal of Controlled Release*, **2007**, 117 (2), 163-170.

Danhier, F., Lecouturier, N., Vroman, B., Jérôme, C., Marchand-Brynaert, J., Feron, O., Préat, V., Paclitaxel-loaded PEGylated PLGA-based nanoparticles : In vitro and in vivo evaluation, *Journal of Controlled Release*, **2009**, 133 (1), 11-17.

Davis, M.E., The first targeted delivery of siRNA in humans via a self-assembling, cyclodextrin polymer-based nanoparticle: From concept to clinic, *Molecular Pharmaceutics*, **2009**, 6 (3), 659-668.

Deminière, B., Colin, A., Calderon, F.L., Bibette, J., Vieillissement par coalescence et duree de vie d'une emulsion concentree, *Comptes Rendus de l'Académie des Sciences - Series IIC - Chemistry,* **1998**, 1, 163-165.

Desai, M.P., Labhasetwar, V., Walter, E., Levy, R.J., Amidon G.L., The mechanism of uptake of biodegradable microparticles in Caco-2 cells is size dependent, *Pharmaceutical Research*, **1997**, 14 (11) 1568-1573.

Desgouilles, S., Vauthier, C., Bazile, D., Vacus, J., Grossiord, J.-L., Veillard, M., Couvreur, P., The design of nanoparticles obtained by solvent evaporation : a comprehensive study, *Langmuir*, **2003**, 19, 9504-9510.

Dixit, T., Van Den Bossche, J., Sherman, D.M., Thompson, D.H., Andres, R.P., Synthesis and grafting of thioctic acid-PEG-folate conjugates onto AU nanoparticles for selective targeting of folate receptor-positive tumor cells, *Bioconjugate Chemistry*, **2006**, 17 (3), 603-609.

Dobrovolskaia, M., Clogson, J.D., Neun, B.W., Hall, J.B., Patri, A.K., McNeil, S.E:, Method for Analysis of nanoparticle hemolytic properties in vitro, *Nano Letters*, **2008**, 8 (8), 2180-2187.

Dow Cellulosics, Ethocel Ethylcellulose Polymers Technical Handbook.

Dubas, S.T:, Kumlangdudsana, P., Potiyaraj, P., Layer-by-layer deposition of antimicrobial silver nanoparticles on textile fibers, *Colloids and Surfaces A: Physicochemical and Engineering Aspects*, **2006**, 289 (1-3), 105-109.

El-Aasser, M.C., Sudol, E.D., Miniemulsions: overview of research and applications, *Journal of Coatings Technology Research*, **2004**, 1 (1), 21-31.

Ferguson, W.J., Braunschweiger, K.I., Braunschweiger, W.R:, Smith, J.R., McCormick, J.J., Wasmann, C.C., Jarvis, N.P., Bell, D.H., Good, N.E., Hydrogen ion buffers for biological research, *Analytical Biochemistry*, **1980**, 104 (2), 300-310.

Fernández-Urrusuno, R., Calvo, P., Remuñan-López, C., Vila-Jato, J.L., Alonso, M.J., Enhancement of nasal absorption of insulin using chitosan nanoparticles, *Pharmaceutical Research*, **1999**, 16 (10), 1576-1581.

Fisichella, M., Dabboue, H., Bhattacharyya, S., Saboungi, M.-L., Salvetat, J.-P., Hevor, T., Guerin, M., Mesoporous silica nanoparticles enhance MTT formazan exocytosis in HeLa cells and astrocytes, *Toxicology in Vitro*, **2009**, 23 (4), 697-703.

Fitzgerald, K.T., Holladay, C.A., McCarthy, C., Power, K.A., Pandit, A., Gallagher, W.M., Standardization of models and methods used to assess nanoparticles in cardiovascular applications, *Small*, **2011**, 7 (6), 705-717.

Forgiarini, A., Esquena, J., González, C., Solans, C., Formation of Nano-emulsions by Low-Energy Emulsification Methods at Constant Temperature, *Langmuir*, **2001**, 17, 2076-2083.

Fotakis, G., Timbrell, J.A., In vitro cytotoxicita assays: Comparison of LDH, neutral red, MTT and protein assay in hepatoma cell lines following exposure to cadmium chloride, *Toxicology Letters*, **2006**, 160, 171-177.

Gabizon, A., Shmeeda, H., Horowitz, A.T., Zalipsky, S., Tumor cell targeting of liposome-entrapped drugs with phospholipid-anchored folic acid-PEG conjugates, *Advanced Drug Delivery Reviews*, **2004**, 56 (8), 1177-1192.

Gelderblom H., Verweij, H., Nooter, K., Sparreboom, A., Cremophor EL: The drawbacks and advantages of vehicle selection for drug formulation, *European Journal of Cancer*, **2001**, 37 (13), 1590-1598.

Generalova, A.N., Sizova, S.V., Oleinikov, V.A., Zubov, V.P., Artemyev M.V., Spernath, L., Kamyshny, A., Magdassi, S., Highl y fluorescent ethyl cellulose nanoparticles containing embedded semiconductor nanocrystals, *Colloids and Surfaces A: Physicochemical and Engineering Aspects*, **2009**, 342 (1-3), 59-64.

Gleave, M.E., Monia, B.P., Antisense therapy for cancer, *Nature Reviews Cancer*, **2005**, 5 (6), 468-479.

Good, N.E:, Winget, G.D., Winter, W., Connolly, T.N., Izawa, S., Singh, R.M.M., Hydrogen ion buffers for biological research, *Biochemistry*, **1966**, 5 (2), 467-477.

Grijalvo, S., Terrazas, M., Aviñó, A., Eritja, R., Stepwise synthesis of oligonucleotide-peptide conjugates containing guanidinium and lipophilic groups in their 3'-termini, *Bioorganic and Medicinal Chemistry Letters*, **2010**, 20 (7), 2144-2147.

Grijalvo, S., Eritja, R., Synthesis and In vitro inhibition properties of oligonucleotide conjugates carrying amphiphatic proline-rich peptide derivatives of the sweet arrow peptide (SAP), *Molecular Diversity*, **2012**, 16 (2), 307-317.

Guide to the preparation, use and quality assurance of blood components. 6th ed. Strasbourg Cedex Germany: Council of Europe Publishing; 2000.

Gutierrez, J.M., González, C., Maestro, A., Solè I., Pey, C.M., Nolla, J., Nano-emulsions: New applications and optimization of their preparation, *Current Opinion in Colloid & Interface Science*, **2008**, 13 (4), 245-251.

Hadjipanays, C.G., Bonder, M.J., Balakrishnan, S., Wang, X., Mao, H., Hadjipanays, G.C., Metallic iron nanoparticles for MRI contrast enhancement and local hyperthermia, *Small*, **2008**, 4 (11), 1924-1929.

Hagigit, T., Nasser, T., Behar-Cohen, F., Lambert, G., Benita, S., The influence of cationic lipid type on in-vitro release kinetic profiles of antisense oligonucleotide from cationic nanoemulsions, *European Journal of Pharmaceutics and Biopharmaceutics*, **2008**, 70, 248-259.

Hans, M.L., Lowman, A.M., Biodegradable nanoparticles for drug delivery and targeting, *Current Opinion in Solid State and Materials Science*, **2002**, 6, 319-327.

Harris, J., Roos, C., Djalali, R., Rheingans, O., Maskos, M., Schmidt, M., Application of the negative staining technique to both aqueous and organic solvent solutions of polymer particles, *Micron*, **1999**, 30 (4), 259-298.

Hart, B.A., Lee, C.H., Shukla, G.S., Shukla, A., Ossier, M., Eneman, J.D., Chiu, J.F., Characterization of cadmium-induced apoptosis in rat lung epithelial cells: Evidence for the participation of oxidant stress, *Toxicology*, **1999**, 133 (1), 43-58.

Hart, M., Jarelöv, A., Kühn, I., McKenzie, D., Möllby, R., Evaluation of redox indicators and the use of digital scanners and spectrophotometer for quantification of microbial growth in microplates, *Journal of Microbiological Methods*, **2002**, 50, 63-73.

Heunemann, P., Prévost, S., Grillo, I., Michelina Marino, C., Meyer, J., Gradzielski, M., Formation and structure of slightly anionically charged nano-emulsions obtained by the phase inversion concentration (PIC) method, *Soft Matter*, **2011**, 7, 5697-5710.

Hilgenbrink, A.R., Low, P.S., Folate receptor-mediated drug targeting: From therapeutics to diagnostics, *Journal of Pharmaceutical Sciences*, **2005**, 94 (10), 2135-2146.

Hiller, J., Mendelsohn, J.D., Rubner, M.F., Reversibly erasable nanoporous anti-reflection coatings from polyelectrolyte multilayers, *Nature Materials*, **2002**, 1 (1), 59-63.

Huang, Q., Yu, H., Ru, Q., Bioavailability and delivery of nutraceuticals using nanotechnology, *Journal of Food Science*, **2010**, 75 (1), R50-R57.

Ishiyama, M., Tominaga, H., Shiga, M., Sasamoto, K., Ohkura, Y., Ueno, K., A combined assay of cell viability and in vitro cytotoxicity with a highly water-soluble tetrazolium salt, neutral red and crystal violet, *Biological and Pharmaceutical Bulletin*, **1996**, 19 (11), 1518-1520.

Izquierdo, P., Esquena, J., Tadros, T.F., Dederen, J.C., Feng, J., Garcia-Celma, M.J., Azemar, N., Solans, C., Phase Behavior and nano-emulsion formation by the phase inversion temperature method, *Langmuir*, **2004**, 20 (16), 6594-6598.

Izquierdo, P., Esquena, J., Tadros, Th.F., Dederen, C., Garcia, M.J., Azemar, N., Solans, C., Formation and stability of nano-emulsions prepared using the phase inversion temperature method, *Langmuir*, **2002**, 18 (1), 26-30.

Jafari, S.M., He, Y., Bhandari, B., Optimization of nanoemulsion production by microfluidization, *Journal of Food Engineering*, 2007, 82, 478-488.

Janes, K.A., Fresneau, M.P., Marazuela, A., Fabra, A., Alonso, M.J., Chitosan nanoparticles as delivery systems for doxorubicin, *Journal of Controlled Release*, 2001, 73 (2-3), 255-267.

Kabalnov, A.S., Shchukin, E.D., Ostwald ripening theory: applications to fluorocarbon emulsion stability, *Advances in Colloid and Interface Science*, 1992, 38 (C), 69-97.

Kaur, A., Jain, S., Tiwary, A.K., Mannan-coated gelatin nanoparticles for sustained and targeted delivery of didanosine: In vitro and in vivo evaluation, *Acta Pharmaceutica*, 2008, 58 (1), 61-74.

Kelmann, R.G., Kuminek, G., Teixeira, H.F., Koester, L.S., Carbamazepine parenteral nanoemulsions prepared by spontaneous emulsification process, *International Journal of Pharmaceutics*, 2007, 342 (1-2), 231-239.

Kim, D., El-Shall, H., Dennis, D., Morey, T., Interaction of PLGA nanoparticles with human blood constituents, *Colloids and Surfaces B: Biointerfaces*, 2005, 40, 83-91.

Kircheis, R., Blessing, T., Brunner, S., Wightman, L, Wagner, E., Tumor targeting with surface-shielded ligand-polycation DNA complexes, *Journal of Controlled Release*, 2001, 72, 165-170.

Kohler, N., Sun, C., Wang, J., Zhang, M., Methotrexate-modified superparamagnetic nanoparticles and their intracellular uptake into human cancer cells, *Langmuir*, 2005, 21 (19), 8858-8864.

Krogman, K.C., Druffel, T., Sunkara, M.K., Anti-reflective optical coatings incorporating nanoparticles, Nanotechnology, 2005, 16 (7), S338-S343.

Kumari, A., Yadav, S.K., Yadav S.C., Biodegradable polymeric nanoparticles based drug delivery systems, *Colloids and Surfaces B: Biointerfaces*, 2010, 75, 1-18.

Kuntsche, J., Horst, J., Bunjes, H., Cryogenic transimission electron microscopy (cryo-TEM) for studying the morphology of colloidal drug delivery systems, *International Journal of Pharmaceutics*, **2011**, 417, 120-137.

Labhasetwar, V., Song, C., Humphrey, W., Shebuski, R., Levy, R.J., Arterial uptake of biodegradable nanoparticles: Effect of surface modifications, *Journal of Pharmaceutical Sciences*, **1998**, 87 (10), 1229-1234.

Landfester, K., The generation of nanoparticles in miniemulsions, *Advanced Materials*, **2001**, 13 (10), 765-768.

Lee, H.J., Yeo, S.Y., Jeong, S.H., Antibacterial effect of nanosized silver colloidal solutions on textile fabrics, *Journal of Material Science*, **2003**, 38 (10), 2199-2204.

Li, L., Song, H., Luo, K., He, B., Nie, Y., Yang, Y., Wu, Y., Gu, Z., Gene transfer efficacies of serum-resistant amino acids-based cationic lipids: Dependence on headgroup, lipoplex stability and cellular uptake, *International Journal of Pharmaceutics*, **2011**, 408 (1-2), 183-190.

Lifshitz, I., Slyozov, V., The kinetics of precipitation from supersaturated solid solutions, *Journal of Physics and Chemistry of Solids*, **1961**, 19, 35-50.

Liu, Q., Yu, S.-Y., Cationic nanoemulsions as non-viral vectors for plasmid DNA delivery, *Colloids and Surfaces B: Biointerfaces*, **2010**, 79 (2), 509-515.

Lu, Z., Yeh, T.-K., Tsai, M., Au, J.L.-S., Wientjes, M.G., Paclitaxel-loaded gelatin nanoparticles for intravesical bladder cancer therapy, *Clinical Cancer Research*, **2004**, 10 (22), 7677-7684.

Lucock, M., Folic acid: Nutritional biochemistry, molecular biology, and role in disease process, *Molecular Genetics and Metabolism*, **2000**, 71 (1-2), 121-138.

Lundberg P., El-Andaloussi, S., Sütlü, T., Johansson, H., Langel, Ü., Delivery of short interfering RNA using endosomolytic cell-penetrating peptides, *FASEB Journal*, **2007**, 21 (11), 2664-2671.

Mainardes, R.M., Gremião, M.P.D., Brunetti, I.L., Luiz Fonseca, M.D., Khalil, N.M., Pharmaceutical nanotechnology zidovudine-loaded PLA and PLA-PEG blend nanoparticles: Influence of polymer type on phagocytic uptake by

polymorphonuclear cells, *Journal of Pharmaceutical Sciences*, **2009**, 98 (1), 257-267.

Matijević, E., Preparation and properties of uniform size colloids*, Chemistry of Materials*, **1993**, 5 (4), 412-426.

Maurer, N., Wong, K.F., Stark, H., Louie, L., McIntosh, D., Wong, T., Scherrer, P., Semple, S.C., Cullis, P.R., Spontaneous entrapment of polynucleotides upon electrostatic interaction with ethano-destabilized cationic liposomes, *Biophysical Journal*, **2001**, 80 (5), 2310-2326.

McClements, D.J., Decker, E.A., Weiss, J., Emulsion-based delivery systems for lipophilic bioactive components, *Journal of Food Science*, **2007**, 72 (8), R109-R124.

McClements, D.J., Edible nanoemulsions: fabrication, properties, and functional performance, *Soft Matter*, **2011**, 7, 2297-2316.

McClements, D.J., Nanoemulsions versus microemulsions: terminology, differences and similarities, *Soft Matter*, **2012**, 8, 1719-1729.

Merkel, O.M., Zheng, M., Mintzer, M.A., Pavan, G.M., Librizzi, D., Maly, M., Höffken, H., Danani, A., Simanek, E.E., Kissel, T., Molecular modeling and in vivo imaging can identify successful flexible triazine dendrimer-based siRNA delivery sistems, *Journal of Controlled Release*, **2011**, 153 (1), 23-33.

Meziani, A., Zradba, A., Touraud, D., Clausse, M., Kunz, W., Can aldehydes participate in the nanostructuration of liquids containing charged micelles?, *Journal of Molecular Liquids*, **1997**, 73-74, 107-118.

Mishra, S., Tyagi, V.K., Esterquats: the novel class of cationic fabric softeners, *Journal of oleo science*, **2007**, 56 (6), 269-276.

Mohammadi, Z., Abolhaassani, M., Dorkoosh, F.A., Hosseinkhani, S., Gilani, K., Amini, T., Najafabadi, A.R., Tehrani, M.R., Preparation and evaluation of chitosan-DNA-FAB-B nanoparticles as a novel non-viral vector for gene delivery to the lung epithelial cells*, International Journal of Pharmaceutics*, **2011**, 409 (1-2), 307-313.

Moinard-Chécot, D., Chevalier, Y., Briançon S., Beney, L, Fessi, H., Mechanism of nanocapsules formation by the emulsion-diffustion process, *Journal of Colloid and Interface Science*, **2008**, 50 (1-3), 31-40.

Morales, D., Gutiérrez, J.M., García-Celma, M.J., Solanc, C., A study of the relation between bicontinuous microemulsions and oil/water nano-emulsion formation, *Langmuir*, **2003**, 19, 7196-7200.

Morales, D., Solans C., Gutiérrez, J.M., Garcia-Celma M.J., Olsson U., Oil/Water Droplet Formation by Temperature Change in the Water /$C_{16}E_6$/Mineral Oil System, *Langmuir*, **2006**, 22, 3014-3020.

Morral-Ruíz, G., Melgar-Lesmes, P., García, M.L., Solans, C., García-Celma, M.J., Design of biocompatible surface-modified polyurethane and polyurea nanoparticles, *Polymer*, **2012**, 53, 6072-6080.

Mosmann, T., Rapid colorimetric assay for cellular growth and survival: Application to proliferation and cytotoxicity assays, *Journal of Immunological Methods*, **1983**, 65, 55-63.

Na, H.B:, Song, I.C., Hyeon, T., Inorganic nanoparticles for MRI contrast agents, *Advanced Materials*, **2009**, 21 (21), 2133-2148.

Némati, F., Dubernet, C., De Verdiere, A.C., Poupon, M.F., Treupel-Acar, L., Puisieux, F. Couvreur, P., Some parameters influencing cytotoxicity of free doxorubicin and doxorubicin-loaded nanoparticles in sensitive and multidrug resistant leucemic murine cells : Incubation time, number of nanoparticles per cell, *International Journal of Pharmaceutics*, **1994**, 102 (1-3), 55-62.

Nicolaos, G., Crauste-Manciet, S., Farinotti, R., Brossard, D., Improvement of cefpodoxime proxetil oral absorption in rats by an oil-in-water submicron emulsion, *International Journal of Pharmaceutics*, **2003**, 263 (1-2), 165-171.

Ogris, M., Brunner, S., Schüller, S., Kircheis, R., Wagner, E., PEGylated DNA/transferrin-PEI complexes: Reduced interaction with blood components, extended circulation in blood and potential for systemic gene delivery, *Gene Therapy*, **1999**, 6 (4), 595-605.

Ogris, M., Wagner, E., Steinlein, P., A versatile assay to study cellular uptake of gene transfer complexes by flow cytometry, *Biochimica et Biophysica Acta – General Subjects*, **2000**, 1474 (2), 237-243.

Osol, A., Remington's Pharmaceutical Sciences, 16th edition, Mack Publishing company, Easton, Pennsylvania, **1980**.

Ott, G., Singh, M., Kazzaz, J., Briones, M., Soenawan, E., Ugozzoli, M., O'Hagan, D.T., A cationic sub-micron emulsion (MF59/DOTAP) is an effective delivery system for DNA vaccines, *Journal of Controlled Release*, **2002**, 79, 1-5.

Pan, G., Shawer, M., Øie, S., Lu, D.R., In vitro gene transfection in human glioma cells using a novel and less cytotoxic artificial lipoprotein delivery system, *Pharmaceutical Research*, **2003**, 20 (5), 738-744.

Pan, J., Feng, S.-S., Targeting and imaging cancer cells by Folate-decorated, quantum dots (QDs)-loaded nanoparticles of biodegradable polymers, *Biomaterials*, **2009**, 30 (6), 1176-1183.

Panyam, J., Labhasetwar, V., Biodegradable nanoparticles for drug and gene delivery to cells and tissue, *Advanced Drug Delivery Reviews*, **2012**, 64 (SUPPL.), 61-71.

Perugini, P., Simeoni, S., Scalia, S., Genta, I., Modena, T., Conti, B., Pavanetto, Fl, Effect of nanoparticle encapsulation on the photostability of the sunscreen agent, 2-ethylehxyl-p-methoxycinnamate, *International Journal of Pharmaceutic*s, **2002**, 246 (1-2), 37-45.

Pey, C.M., Maestro, A., Solè, I., González, C., Solans, C., Gutiérrez J.M., Optimization of nano-emulsions prepared by low-energy emulsification methods at constant temperature using a factorial design study, *Colloids and Surfaces A: Physicochemical and Engineering Aspects*, **2006**, 288, 144-150.

Pinto Reis, C., Neufeld, R.J., Ribeiro, A.J., Veiga, F., Nanoencapsulation I: Methods for preparation of drug-loaded polymeric nanoparticles, *Nanomedicine: Nanotechnology, Biology, and Medicine*, **2006**, 2, 8-21.

Putnam, D., Gentry, C.A., Pack, D.W., Langer R., Polymer-based gene delivery with low cytotoxicity by a unique balance of side-chain termini, *Proceedings of*

the National Academy of Sciences of the United States of America, **2001**, 98 (3), 1200-1205.

Rao, J.P., Geckeler, K.E., Polymer nanoparticles: preparation techniques and size-control parameters, *Progress in Polymer Science*, **2011**, 36, 887-913.

Rekhi, G.S., Jambhekar, S.S., Ethylcellulose – A polymer review, *Drug Development and Industrial Pharmacy*, **1995**, 21 (1), 61-77.

Roger, K., Cabane, B., Olsson, U., Emulsificaiton through surfactant hydration: The PIC Process Revisited, *Langmuir*, **2011**, 27, 604-611.

Rother, R.P., Bell, L., Hillmen, P., Gladwin, M.T., The clinical sequelae of intravascular hemolysis and extracellular plasma hemoglobin: A novel mechanism of human disease, *Journal of the American Medical Association*, **2005**, 293 (13), 1653-1662.

Rowe, R.C., Sheskey, P.J., Quinn, M.E., Handbook of Pharmaceutical Excipients, 6th edition, Pharmaceutical Press. London, **2009**.

Sadurní, N., Solans, C., Azemar, N., García-Celma, M.J., Studies on the formation of O/W nano-emulsions, by low-energy emulsification methods, suitable for pharmaceutical applicatins, *European Journal of Pharmaceutical Sciences*, **2005**, 26 (5), 438-445.

Sah, H., Microencapsulation techniques using ethyl acetate as a dispersed solvent: Effects of its extraction rate on the characteristics of PLGA microspheres*, Journal of Controlled Release*, **1997**, 47 (3), 233-245.

Sahraneshin, A., Takami, S., Hojo, D., Arita, T., Minami, K., Adschiri, T., Mechanistic study on the synthesis of one-dimensional yttrium aluminium garnet nanostructures under supercritical hydrothermal conditions in the presence of organic amines, *CrystEngComm*, **2012**, 14 (18), 6085-6092.

Santos-Magalhães, N.S., Pontes, A., Pereira, V.M.W., Caetano, M.N.P., Colloidal carriers for benzathine penicillin G: Nanoemulsions and nanocapsules, *International Journal of Pharmaceutics*, **2000**, 208, 71-80.

Schwerdt, A., Zintchenko, A., Concia, M., Roesen, N., Fisher, K., Lindner, L.H., Issel, R., Wagner, E., Ogris, M., Hyperthermia-induced targeting of

thermosensitive gene carriers to tumors, *Human Gene Therapy*, **2008**, 19 (11), 1283-1292.

Sheng, Y., Yuan, Y., Liu, C., Tao, X., Shan, X., Xu, F., In vitro macrophage uptake and in vivo biodistribution of PLA-PEG nanoparticles loaded with hemoglobin as blood substitutes: Effect of PEG content, *Journal of Materials Science: Materials in Medicine*, **2009**, 20 (9), 1881-1891.

Shinoda, K., Saito, H., The effect of temperature on the phase equilibria and the types of dispersions of the ternary system composed of water, cyclohexane, and nonionic surfactant, *Journal of Colloid and Interface Science,* **1968**, 26, 70-74.

Shultz, M.D., Calvin, S., Fatouros, P.P., Morrison, S.A., Carpenter, E.E., Enhanced ferrite nanoparticles as MRI contrast agents, *Journal of Magnetism and Magnetic Materials*, **2007**, 311, 464-468.

Silva, H.D., Cerqueira, M.A., Vicente, A.A., Nanoemulsions for Food Applications: Development and Characterization, *Food and Bioprocess Technology*, **2012**, 5 (3), 854-867.

Slater, T.F., Sawyer, B., Sträuli, U.,Studies on succinate-tetrazolium reductase systems. III. Points of coupling of four different tetrazolium salts III. Points of coupling of four different tetrazolium salts, *BBA – Biochimica et Biophysica Acta*, **1963**, 77 (C), 383-393.

Solans, C., Izquierdo, P., Nolla, J., Azemar, N., Garcia-Celma, M.J., Nano-emulsions, *Current Opinion in Colloid & Interface Science*, **2005**, 10, 102-110.

Solans, C., Solè, I., Nano-emulsions: Formation by low-energy methods, *Current Opinion in Colloid & Interface Science*, **2012**, 17, 247-254.

Solè, I., Maestro A., González, C., Solans, C., Gutiérrez, J.M., Optimization of nano-emulsion preparation by low-energy methods in an ionic surfactant system, *Langmuir*, **2006**, 22, 8326-8332.

Solè, I., Pey, C.M., Maestro, A., González, C., Porras, M., Solans, C., Gutiérrez, J.M., Nano-emulsions prepared by the phase inversion composition method:

Preparation variables and scale up, *Journal of Colloid and Interface Science*, **2010**, 344 (2), 417-423.

Song, C.X., Labhasetwar, V., Murphy, H., Qu, X., Humphrey, W.R., Shebuski, R.J., Levy, R.J., Formulation and characterization of biodegradable nanoparticles for intravascular local drug delivery, *Journal of Controlled Release*, **1997**, 43 (2-3), 197-212.

Sonneville-Aubrut, O., Babayan, D., Bordeaux, D., Lindner, P., Rata, G., Cabane, B., Phase transition pathways for the production of 100 nm oil-in-water emulsions, *Physical Chemistry Chemical Physics*, **2009**, 11, 101-110.

Sonneville-Aubrut, O., Simmonet, J.T., Alloret F.L., Nanoemulsions: a new vehicle for skin care products, *Advances in Colloid and Interface Science*, **2004**, 108-109, 145-149.

Soppimath, K.S., Aminabhavi, T.M., Kulkarni, A.R., Rudzinski, W.E., Biodegradable polymeric nanoparticles as drug delivery devices, *Journal of Controlled Release*, **2001**, 70, 1-20.

Spernath, L., Magdassi, S., Preparation of ethyl cellulose nanoparticles from nano-emulsion obtained by inversion at constant temperature, *Micro and Nano Letters*, **2007**, 2 (4), 90-95.

Stoimenov, P.K., Klinger, R.L., Marchin, G.L., Klabunde, K.J., Metal oxide nanoparticles as bactericidal agents, *Langmuir*, **2002**, 18 (17), 6679-6686.

Stoll, V.S., Blanchard, J.S., Chapter 6 Buffers. Principles and Practice1, *Methods in Enzymology*, **2009**, 463 (C), 43-56.

Sudimack J., Lee, R.J., Targeted drug delivery via the folate receptor, *Advanced Drug Delivery Reviews*, **2000**, 41 (2), 147-162.

Sun, K., Wang, J., Zhang, J., Hua, M., Liu, C., Chen, T., Dextran-g-PEI nanoparticles as a carrier for co-delivery of adriamycin and plasmid into osteosarcoma cells, *International Journal of Biological Macromolecules*, **2011**, 49 (2), 173-180.

Swami, A., Shi, J., Gadde, S., Vortuba, A.R., Kolishetti, N., Farokhzad, O.C., Nanoparticles for targeted and temporally controlled drug delivery in S. Svenson

and Prud'homme R.K. (eds.), Multifunctional Nanoparticles for Drug Delivery Applications: Imaging, Targeting and Delivery, Springer, 2012, 9-29.

Sweetman, S.C., Martindale The complete drug reference, 34th edition, Pharmaceutical Press, London, 2005.

Szakács Z., Noszál, B., Determination of dissociation constants of folic acid, methotrexate, and other photolabile pteridines by pressure-assisted capillary electrophoresis, *Electrophoresis*, 2006, 27, 3399-3409.

Tadros, T.F., Applied Surfactants: Principles and Applications, WILEY-VCH Verlag GmbH & Co. KGaA, Weinheim, 2005.

Tadros, T.F., Emulsion Science and Technology, WILEY-VCH Verlag GmbH & Co. KGaA, Weinheim, 2009.

Tadros, T.F., Izquierdo, P., Esquena, J., Solans C., Formation and stability of nano-emulsions*, Advances in Colloidal and Interface Science*, 2004, 108-109, 303-318.

Tamilvanan, S., Oil-in-water lipid emulsions: Implications for parenteral and ocular delivering systems, *Progress in Lipid Research*, 2004, 43 (6), 489-533.

Taylor, P., Ostwald ripening in emulsions, *Advances in Colloid and Interface Science*, 1998, 75, 107-163.

Teixeira, H., Dubernet, C., Puisieux, F., Benita, S., Couvreur, P., Submicron cationic emulsions as a new delivery system for oligonucleotides, *Pharmaceutical Research*, 1999, 16 (1), 30-36.

The United States Pharmacopeia, 21st revision, The National Formulary, 16th edition, United States Pharmacopeial Convention Inc., Rockville, MD, 1985.

Tiwari, S.B., Amiji, M.M., Improved oral delivery of paclitaxel following administration in nanoemulsion formulations, *Journal of Nanoscience and Nanotechnology*, 2006, 6 (9-10), 3215-3221.

Torchilin, V.P., Multifunctional nanocarriers, *Advanced Drug Delivery Reviews*, 2006, 58, 1532-1555.

Troncoso E., Aquilera, J.M., McClements, D.J., Fabrication, characterization and lipase digestibility of food-grade nanoemulsions, *Food Hydrocolloids*, **2012**, 27 (2), 355-363.

Twentyman, P.R., Luscombe, M., A study of some variables in a tetrazolium dye (MTT) based assay for cell growth and chemosensitivity, *British Journal of Cancer*, **1987**, 56 (3), 279-285.

Ubrich, N., Bouillot, P., Pellerin, C., Hoffman, H., Maincent, P., Preparation and characterization of propanolol hydrochloride nanoparticles: A comparative study, *Journal of Controlled release*, **2004**, 97 (2), 291-300.

Ugelstad, J., El-Aasser, M.S., Vanderhoff, J.W., Emulsion polymerization: Initiation of polymerization in monomer droplets. *Journal of Polymer Science: Polymer Letters*, **1973**, 11, 503-513.

US License Number. 1986. Applicant-Department of the Navy, Naval Hospital. Bethesda, MD, FDA summary basis of approval of red blood cells frozen and red blood cells deglycerolized (reference no. 86-0335) pp. 635–10.

Usón, N., Garcia, M.J., Solans, C., Formation of water-in-oil (W/O) nano-emulsions in a water/mixed non-ionic surfactant/oil system prpared by a low-energy emulsification method, *Colloids and Surfaces A: Physicochemical and Engineering Aspects*, **2004**, 250, (1-3 SPEC.ISS.), 415-421.

Vanderhoff, J.W., El Aasser, M.S., Ugelstad, J., Polymer emulsification process. US Patent 4,177,177 (**1979**).

Varga, C.M., Wickham, T.J., Lauffenburger, D.A., Receptor-mediated targeting of gene delivery vectors: Insights from molecular mechanisms for improved vehicle design, *Biotechnology and Bioengineering*, **2000**, 70 (6), 593-605.

Vauthier, C., Bouchemal, K., Methods for the preparation and manufacture of polymeric nanoparticles, *Pharmaceutical Research*, **2009**, 26 (5), 1025-1058.

Wagner, C., Theorie der Alterung von Niederschlägen durch Umlösen (Ostwald-Reifung), *Zeitschrift für Elektrochemie, Berichte der Bunsengesellschaft für physikalische Chemie*, **1961**, 65, 581-591.

Walstra, P., Emulsion stability. In: Becher, P. (Ed.), Encyclopedia of Emulsion Technology, Vol. 4., Marcel Dekker, New York, pp. 1–62, **1996**.

Wang, H., Cheng, H., Wang, F., Wei, D., Wang, X., An improved 3-(4,5-dimethylthiazol-2-yl)-2,5 diphenyl tetrazolium bromide (MTT) reduction assay for evaluating the viability of Escherichia coli cells, *Journal of Microbiological Methods*, **2010**, 82, 330-333.

Wang, L., Mutch, K.J., Eastoe, J., Heenan, R.K., Dong, J., Nanoemulsions prepared by a two-step low-energy process, *Langmuir*, **2008**, 24, 6092-6099.

Wang, L., Tabor, R., Eastoe, J., Li, X., Heenan, R.K., Dong, J., Formation and stability of nano-emulsions with mixed ionci-nonionic surfactants, *Physical Chemistry Chemical Physics*, **2009**, 11, 9772-9778.

Weitman, S.D., Lark, R.H., Coney, L.R., Fort, D.W., Frasca, V., Zurawski, Jr.,V.R., Kamen, B.A., Distribution of the folate receptor GP38 in normal and malignant cell lines and tissues, *Cancer Research*, **1992**, 52 (12), 3396-3401.

Willert, M., Rothe, R., Landfester, K., Antonetti, M., Synthesis of inorganic and metallic nanoparticles by miniemulsification of molten salts and metals, *Chemistry of Materials*, **2001**, 13 (12), 4681-4685.

Wu, H., Ramachandran, C., Bielinska, A.U., Kingzett, K., Sun, R., Weiner, N.D., Roessler, B.J., Topical transfection using plasmid DNA in a water-in-oil nanoemulsion, *International Journal of Pharmaceutics*, **2001**, 221, 23-34.

Wu, Y., Yang, W., Wang, C., Hu, J., Fu, S., Chitosan nanoparticles as a novel delivery system for ammonium gylcyrrhizinate, *International Journal of Pharmaceutics*, **2005**, 295 (1-2), 235-245.

Xu, X., Asher, S.A., Synthesis and utilization of monodisperse hollow polymeric particles in photonic crystals, *Journal of the American Chemical Society*, **2004**, 126 (25), 7940-7945.

Xu, Y., Szoka Jr., F.C., Mechanism of DNA release from cationic liposome/DNA complexes used in cell transfection, *Biochemistry*, **1996**, 35 (18), 5616-5623.

Yang, S.C., Benita, S., Enhanced absorption and drug targeting by positively charged submicron emulsions, *Drug Development Research*, 2000, 50 (3-4), 476-486.

Zhang, H.-Y., Mao, J., Zhou, D., Xu, Y., Thonberg, H., Liang, Z., Wahlestedt, C., mRNA accessible site tagging (MAST): a novel high throughput method for selecting effective antisense oligonucleotides, *Nucleic acids research*, 2003, 31 (14), e72.

Zheng, D., Li, X., Xu, H., Lu, X., Hu, Y., Fan, W., Study on docetaxel-loaded nanoparticles with high antitumor efficacy against malignant melanoma, *Acta Biochimica et Biophysica Sinica*, 2009, 41 (7), 578-587.

Zimmer, A., Antisense oligonucleotide delivery with polyhexylcyanoacrylate nanoparticles as carriers, *Methods: A Companion to Methods in Enzymology*, 1999, 18 (3), 286-295.

7. GLOSSARY

7.1. ABBREVIATIONS

a^-	anionic charge (coming from folic acid)
ASO	Antisense oligonucleotide
c^+	cationic charge (coming from the nanoparticle dispersion)
CatA	Cationic Amphiphile (Varisoft® RTM 50)
CEL	Cremophor® EL
cryoTEM	cryogenic Transmission Electron Microscopy
CWO7	Cremophor® WO7
DLS	Dynamic Light Scattering
DNA	Deoxyribonucleic acid
e.g.	Example given
EC10	Ethocel Std 10 Premium
EC4	Ethocel Std 4 Premium
EMSA	Electrophoretic Mobility Shift Assay
etc.	And other things (from Latin *et cetera*)
FBS	Fetal Bovine Serum
h	Hour
HBG	Hepes-buffered glucose
HLB	Hydrophilic-Lipophilic Balance
i.e.	That is (from Latin *id est*)
min	Minute(s)
MTT	3-(4,5-dimethylthiazol-2-yl)-2,5 diphenyltetrazolium bromide
MW	Molecular Weight
n.s.	Not studied
N/P ratio	cationic-to-anionic charge ratio
NE	Nano-emulsion

NP	Nanoparticle dispersion
O	Oil
O/S ratio	Oil to surfactant weight ratio
O/W	Oil-in-water
OA	Oleylamine
PB	Phosphate Buffer
PBS	Phosphate Buffered Saline
PI	Polydispersity index
PIC	Phase Inversion Composition
PIT	Phase Inversion Temperature
ppm	Parts per million
PS	Phosphorothioate oligonucleotide
PTA	Phosphotungstic acid
RI	Refractive index
rpm	Revolutions per minute
S	Surfactant
TEM	Transmission Electron Microscopy
W/O	Water-in-oil
wt%	Weight percent

7.2. ROMAN LETTERS

A	Interfacial area
C_∞	Solubility of the dispersed phase in the continuous phase
D	Diffusion coefficient
f	Friction coefficient of the solute
$f(\kappa r)$	Henry's function
g	Gravitational acceleration
G_T	Total free energy (Gibbs)
k_B	Boltzmann constant
M	Mass of polymer in the medium
r	Droplet radius

R	Gas constant
r_0	Droplet radius at t=0
R_H	Hydrodynamic radius of the solute
S	Configuration entropy
T	Temperature
t	time
V_m	Molar volume of the dispersed phase

7.3. GREEK LETTERS

ρ	Density
γ	Interfacial tension
ω	Rate (coalescence or Ostwald ripening)
ε	Dielectric constant in medium
ε_0	Dielectric contant in vacuum
η	Viscosity
κ	Inverse of the Debye length
λ	Wavelength
μ	Electrophoretic mobility
ν_{Stokes}	Creaming/sedimentation velosity
ζ	Zeta potential

7.4. SYMBOLS

$<$	Less than
$\leq$	Less than and equal to
$>$	Greater than
$\geq$	Greater than and equal to
Ø	Diameter

8. SUMMARY IN SPANISH

1. Introducción

1.1. NANO-EMULSIONES

Definición y características

Las nano-emulsiones son emulsiones (dispersiones de al menos dos líquidos inmiscibles, en forma de gotas estabilizadas por moléculas tensioactivas) que se caracterizan por poseer un tamaño de gota en el rango nanómetrico. Generalmente, uno de los líquidos es polar (por ejemplo agua), mientras que el otro es no polar (denominado aceite). Según la naturaleza de las fases, las nano-emulsiones se pueden clasificar en aceite-en-agua (O/W) cuando la fase dispersa es oleosa y agua-en-aceite (W/O) cuando la fase dispersa es acuosa [Solans, 2005; Tadros, 2006; McClement, 2011 y 2012]. En la literatura, se utilizan términos tales como emulsiones submicrométricas [Benita, 1993; Yang, 2000], miniemulsiones [Ugelstad, 1973; Asua, 2002; El-Aasser, 2004], etc. para denominar a las nano-emulsiones. Los tamaños de gota de las nano-emulsiones son típicamente entre 20 y 500 nm y por ello presentan una apariencia transparente o translúcida y estabilidad cinética frente a la separación gravitacional (sedimentación o cremado). Las nano-emulsiones, por ser sistemas termodinámicamente inestables (sistemas fuera del equilibrio) no se forman espontáneamente. Por tanto, es necesaria la aportación de energía para su formación.

La formación de nano-emulsiones implica la generación de nuevas interfases agua-aceite que requieren la presencia de un tercer componente estabilizador. Debido a su carácter anfifílico (con una parte hidrófila y otra parte lipófila en la misma molécula), los tensioactivos se adsorben en la interfase. De este modo, disminuyen la tensión interfacial y por tanto la energía libre total del sistema, lo

cual favorece la formación de gotas pequeñas. Las moléculas de tensioactivo forman una monocapa en la interfase de las gotas que funciona como una barrera estérica, mecánica y / o eléctrica que evita el contacto directo entre las gotas y por lo tanto fenómenos de destabilización como floculación o coalescencia [Tadros, 2004].

Estabilidad

Dado que las nano-emulsiones son sistemas termodinámicamente inestables, tienden a la separación de fases con el tiempo. Los mecanismos de desestabilización se representan esquemáticamente en la Figura 6.1.

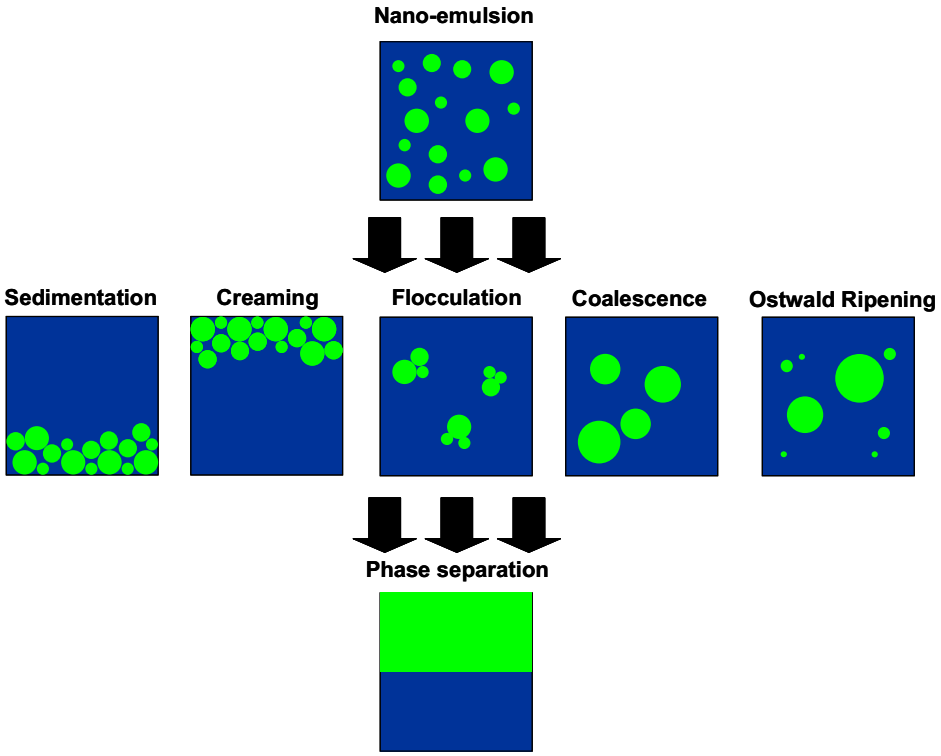

Figura 8.1. Representación esquemática de los procesos de desestabilización de las nano-emulsiones.

La *sedimentación/cremado* es un proceso reversible que tiene lugar debido a las densidades relativas de la fase dispersa y la fase continua. Como se mencionó anteriormente, la elevada estabilidad cinética de las nano-emulsiones frente a estos procesos es debido al pequeño tamaño de gota pues el movimiento Browniano es suficiente para evitar la sedimentación (o cremado) debido a la fuerza d la gravedad. Sin embargo, cuando las gotas son

polidispersas se puede producir sedimentación o cremado de las gotas grandes, mientras que las pequeñas permanecen dispersas.

La *floculación* es la formación de agregados de gotas de la fase dispersa, un proceso que es en principio reversible. Las fuerzas de atracción de van der Waals son las responsables de este fenómeno. La floculación conduce a la formación de unidades grandes de gotas que pueden experimentar coalescencia d [Borwankar, 1992; Tadros, 2009].

La *coalescencia* es la fusión de dos o más gotas por rotura del film interfacial y puede producirse cuando las gotas entran en contacto debido al movimiento browniano o cuando están ya en contacto debido a la floculación o sedimentación. Se trata de un proceso irreversible.

La *maduración de Ostwald* describe el crecimiento irreversible de gotas más grandes a expensas de los más pequeños. Este efecto es el resultado de polidispersidad y por lo tanto de los diferentes potenciales químicos en las gotas de distinto tamaño debido a los diferentes radios de curvatura. También es el resultado de la solubilidad de la fase dispersa en la continua. Por ello ese produce difusión de las moléculas de la fase dispersa y un aumento del radio medio de las gotas.

Métodos de preparación

Las nano-emulsiones se preparan generalmente por métodos de alta energía, en los que la energía puede provenir de dispositivos como homogeneizadores de alta presión, generadores de ultrasonidos, etc. [Tadros, 2004; Solans, 2005; Jafari, 2007; Anton, 2008]. Sin embargo, se pueden también preparar por métodos de baja energía que aprovechan el potencial químico de los componentes y se requiere sólo simple agitación. Estos métodos permiten la formación de gotitas más pequeñas que con los métodos de alta energía [Walstra, 1983; Forgiarini, 2001; Bouchemal, 2004; Usón, 2004; Solé, 2006; Kelmann, 2007; Anton, 2009]. Entre los diferentes métodos de emulsificación de baja energía, destacan los métodos de inversión de fase en los que se produce inversión de la curvatura espontánea de las moléculas de tensioactivos durante el proceso de la emulsificación, ya sea por cambio de

temperatura a composición constante (método PIT) o mediante el cambio de composición a temperatura constante (método PIC).

El método **PIT** se basa en los cambios en la curvatura espontánea de tensioactivo que se inducen por cambios de temperatura [**Izquierdo, 2002; Solans, 2005; Morales, 2006; Anton, 2008 and 2009**]. Este método sólo se puede aplicar a tensioactivos sensibles a la temperatura, como los tensioactivos noionicos etoxilados. A bajas temperaturas (T<PIT), las moléculas de tensioactivo se hallan hidratadas y por tanto son solubles en agua (dando lugar a nano-emulsiones de tipo O/W). Al aumentar la temperatura, los grupos hidrófilos de las moléculas tensioactivas se van deshidratando por lo que disminuyen las propiedades hidrófilicas. A la temperatura PIT, el tensioactivo es igualmente soluble en la fase acuosa y en la fase oleosa produciéndose estructuras de tipo bicontinuo. Al aumentar aún más la temperatura (T>PIT), el tensioactivo es fundamentalmente lipófilo y se forman nano-emulsiones W/O.

En el método de **PIC,** se añade uno de los componentes (agua o aceite) progresivamente a una mezcla de los otros dos componentes (aceite-tensioactivo o agua-tensioactivo, respectivamente). La **Figura 6.2** muestra una representación esquemática de los distintos tipos de agregados tensioactivos implicados en el proceso de emulsificación.

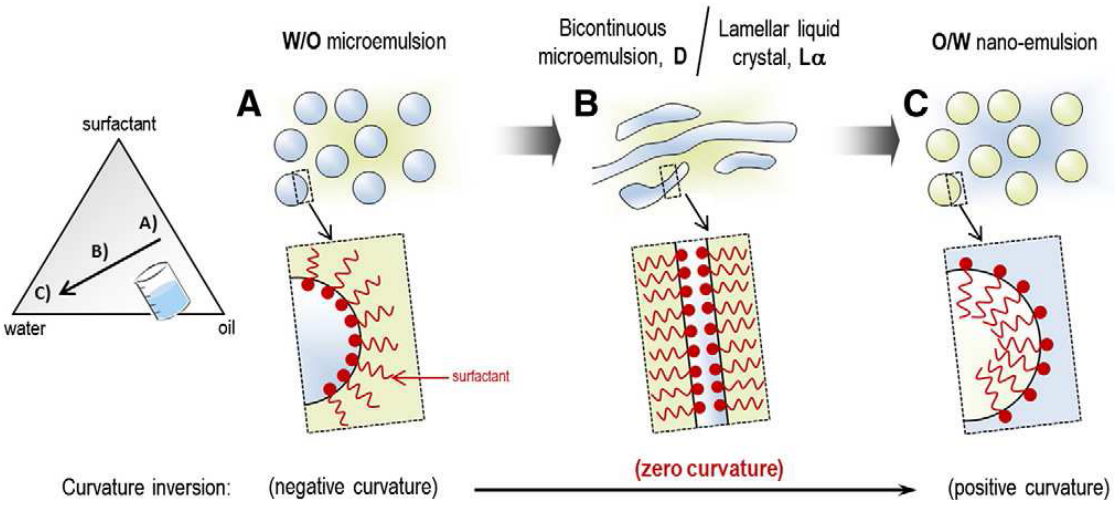

Figura 8.2. Representación esquemática de la formación de nano-emulsión por el método de composición de inversión de fase (PIC).

Cuando se añade agua a la fase oleosa que contiene el agente tensioactivo, inicialmente, se parte de microemulsiones de tipo agua-en-aceite (W/O).

Adicionando más agua, la curvatura espontánea del tensioactivo cambia de negativo a cero y, por consiguiente, se forman estructuras bicontinuas. Por adición de más agua se forman nano-emulsiones aceite-en-agua (O/W) [Forgiarini, 2001; Pey, 2006; Wang, 2008 and 2009; Solè, 2006 and 2010; Calderó, 2011; Solans, 2012].

Aplicaciones

Debido a sus propiedades características, las nano-emulsiones son interesantes para aplicaciones en muchos campos como alimentos, productos de cuidado personal y las industrias médicas y farmacéuticas. En este último ámbito, las nano-emulsiones se utilizan como vehículos, por ejemplo, para vacunas, medicamentos codificados de ADN o antibióticos a través de diversas rutas de administración. Otra aplicación importante de las nano - emulsiones es su uso como plantillas para la preparación de nanopartículas, que es el objetivo de esta investigación.

1.2. NANOPARTÍCULAS

Definición y características

Las nanopartículas son materiales sólidos con tamaños, por lo general, por debajo de 500 nm. Pueden clasificarse en nanoesferas y nanocápsulas. Las nanoesferas consisten en matrices homogéneas, en general esférica. Las nanocápsulas son partículas con una cáscara sólida que rodea un núcleo líquido o semisólido Soppimath, 2001; Pinto Reis, 2006; Anton, 2008; Kumari, 2010; Rao, 2011]. Dependiendo de cada aplicación particular, las propiedades de las nanopartículas se pueden optimizar por la elección de los materiales y método de preparación. Los materiales utilizados para la preparación de nanopartículas son materiales inorgánicos como óxidos de metales [Matijević, 1993; Willert, 2001; Stoimenov, 2002] u orgánicos como polímeros [Fernández-Urrusuno, 1999; Xu, 2004].

Métodos de preparación

Las nanopartículas se pueden preparar a partir de una variedad de materiales inorgánicos y orgánicos. Entre los materiales orgánicos, los polímeros (naturales, sintéticos, semisintéticos) se han utilizado con frecuencia para la preparación de nanopartículas poliméricas. Hay dos métodos generales: la preparación por polimerización de monómeros [**Landfester, 2001; Asua, 2002; Rao, 2011**] o por aplicación de polímeros preformados [**Soppimath, 2001; Pinto Reis, 2006; Calderó, 2011; Rao, 2011**]. El segundo enfoque tiene varias ventajas sobre la polimerización de monómeros. Se evitan procesos de purificación, necesarios para eliminar los productos de reacción secundarios no deseados o exceso de reactivos (monómeros, tensioactivos, etc.) y la aplicación de componentes reactivos adicionales (por ejemplo, iniciadores) [**Pinto Reis, 2006; Calderó, 2011**]. Hay varios métodos para obtener nanopartículas poliméricas mediante el uso de un polímero preformado tal como por ejemplo el método de desplazamiento del disolvente, el método de evaporación del disolvente o mediante la aplicación de la tecnología de fluidos supercríticos (SCF) [**Soppimath, 2001; Vauthier, 2009; Rao, 2011**]. El método de evaporación del disolvente fue el primer método desarrollado para preparar nanopartículas poliméricas a partir de un polímero preformado [**Vanderhoff, 1979**]. La **Figura 6.3** muestra una representación esquemática de este método.

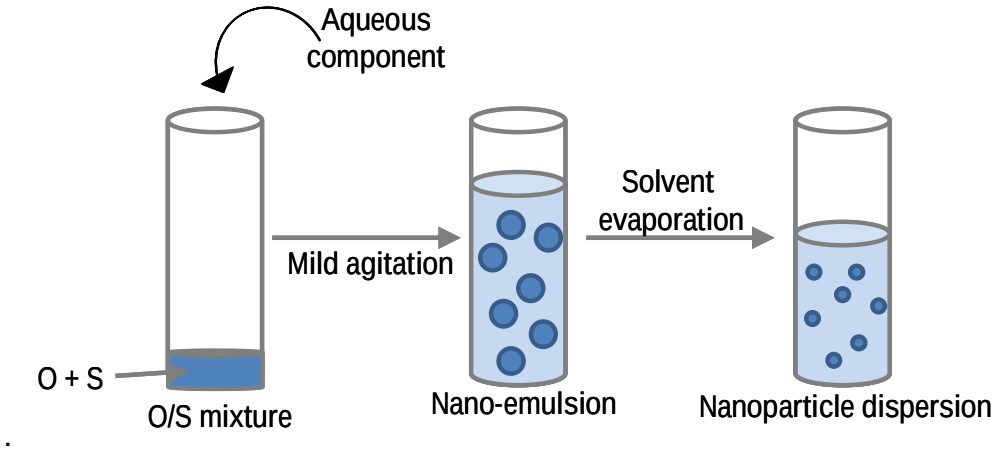

Figura 8.3. Representación esquemática del processo de preparación de nanopartículas con la fase de aceite abreviado con O y el tensioactivo (mezcla) con S.

En una primera etapa, la nano-emulsión O/W se formula con un disolvente volátil, como fase oleosa que contiene el polímero. En una segunda etapa y mediante la evaporación del disolvente, se forma la dispersión de nanopartículas La evaporación del disolvente se consigue, por ejemplo, por agitación continua a temperatura ambiente o por presión reducida [Pinto Reis, 2006; Rao, 2011]. En el trabajo de Calderó *et al.*, para obtener nanopartículas de etilcelulosa, el disolvente, acetato de etilo, se evaporó durante unas doce horas con agitación continua a temperatura ambiente [Calderó, 2011]. El acetato de etilo fue también el disolvente orgánico en el trabajo de Desgouilles *et al.* donde las nanopartículas de etilcelulosa y poli (ácido láctico) se formaban por evaporación del disolvente bajo vacío y a temperatura elevada (30 °C) durante 30 minutos [Desgouilles, 2003].

Aplicaciones

Las nanopartículas encuentran aplicación en diversos campos como en la industria textil, la óptica, dispositivos magnéticos así como en las industrias farmacéutica y médica donde son ampliamente utilizados como vehículos para compuestos bioactivos.

El uso de nanopartículas para mejorar la eficacia in vivo de fármacos ha sido bien establecido en los últimos años en la investigación farmacéutica y clínica. Modificando la superficie de las nanopartículas se puede controlar sus propiedades biológicas y simultáneamente se las puede dotar de varias funciones terapéuticas y/o diagnósticas. La vectorización de las nanopartículas con la ayuda de ligandos específicos de la superficie celular permite la entrada selectiva de fármacos a las células. En este contexto se han desarrollado una variedad de métodos para anclar vectores tales como anticuerpos, péptidos, ácido fólico y otros a la superficie de las nanopartículas.

La incorporación de medicamentos / ácido nucleico a nanopartículas se realiza a través de diferentes metodologías que implican unión covalente, adsorción, encapsulación o interacciones electrostáticas. En relación a los interacciones electrostáticas, la carga superficial positiva de una nanopartícula puede provenir de la incorporación de un polímero o tensioactivo catiónico. Li *et al.* [Li, 2011] ha estudiado la eficiencia de la transfección de genes de liposomas

catiónicas que contienen lípidos basados en amino-ácidos. La transfección generalmente se refiere a la introducción de ácido nucleico en las células.
Muchos compuestos biológicamente activos deben ser transportados al interior de las células para ejercer su acción terapéutica en el núcleo u otros orgánulos específicos. No obstante, la naturaleza lipófila de las membranas biológicas restringe la entrada intracelular directa. Además, las moléculas grandes, tales como ADN, son degradadas por enzimas. Desde este punto de vista, el desarrollo de nanopartículas para transportar ADN o oligonucleótidos en el citoplasma de las células diana sería altamente deseable. El uso de lípidos catiónicos y polímeros catiónicos como vectores de transfección para la administración intracelular de ADN se sugirió en las últimas décadas.

2. Objectivos

El objetivo general de esta investigación fue el diseño de nanopartículas poliméricas catiónicas, a partir de nano-emulsiones obtenidas por métodos de baja energía, para aplicaciones biomédicas. Este objetivo incluye los siguientes objetivos parciales:

- Preparación de nano-emulsiones catiónicas de tipo aceite en agua (O/W) con métodos de baja energía y su caracterización.
- Preparación y caracterización de nanopartículas poliméricas catiónicas utilizando los nano-emulsiones catiónicas O/W como plantilla.
- Funcionalización de las nanopartículas poliméricas
- Estudios in vitro de las nanopartículas funcionalizadas.

3. Resultados y discusión

3.1. NANO-EMULSIONES: FORMACIÓN Y CARACTERIZACIÓN

3.1.1. Selección de componentes y de ensayos preliminares de formación de nano-emulsiones

El primer objetivo específico de la tesis fue el de la formación de nano-emulsiones de tipo aceite en agua (O/W) en sistemas Agua / Tensioactivo / Aceite por métodos de baja energía para aplicaciones farmacéuticas. Uno de los puntos centrales era obtener nano-emulsiones catiónicas por lo que se incorporaron tensioactivos con carga positiva Otro objetivo era utilizar estas nano-emulsiones catiónicas como plantilla para la preparación de nanopartículas poliméricas. Por esta razón, se disolvió un polímero preformado en un disolvente volátil, que constituye la fase oleosa de la nano-emulsión. Los componentes utilizados y por lo tanto las nano-emulsiones y nanopartículas tienen que cumplir los requisitos para la ruta farmacéutica de administración deseada y tiene que ser biocompatible y no tóxico o, al menos, eficaz en un rango de concentración no tóxico. Las nano-emulsiones se formularon a temperatura ambiente. A temperaturas elevadas, el disolvente volátil se evapora fácilmente y los componentes farmacéuticos podrían ser degradados.

Selección de componentes

Para la formación de nano-emulsiones, se utilizó, además de agua, solución de HEPES y soluciones de fosfatos reguladoras de pH como *fase acuosa*. La *fase oleosa* consistió principalmente en el polímero etilcelulosa que se disolvió en acetato de etilo, un solvente orgánico y volátil, que es apropiado para la preparación de nanopartículas según el método de evaporación del disolvente. Como uno de los objetivos era obtener nanopartículas con una carga superficial positiva, se decidió usar un tensioactivo noniónico en combinación con un *tensioactivo catiónico* pues ensayos previos pusieron de manifiesto que no se formaban nano-emulsiones utilizando sólo tensioactivo catiónico.

Ensayos preliminares de formación de nano-emulsiones O/W en sistemas Agua / cationico:nonionico / EC10 en acetato de etilo

Se llevaron a cabo ensayos de formación de nano-emulsiones usando diferentes tensioactivos catiónicos (elegido entre los anfífilos biocompatibles y

biodegradables cuaternizados disponibles comercialmente) en combinación con varios tensioactivos noniónicos con diferentes números de HLB. En base a este screening, el tensioactivo derivado de amido amina cuaternizada, *Varisoft ® RTM 50 (CatA*), fue seleccionado para estudios sistemáticos, ya que produjo nano-emulsiones en combinación con diversos agentes tensioactivos noniónicos, a diferencia de otros tensioactivos catiónicos ensayados. Entre los tensioactivos noniónicos, se seleccionaron *Span® 80, Cremophor® WO7 y Cremophor® EL.* Se estudiaron, principalmente, los relaciones tensioactivos catiónico:noniónico de *1:1 y 1:3* con las concentraciones de polímero de *6 y 10 wt%*.

3.1.2. Nano-emulsiones en el sistema Agua / CatA:Span® 80 / solución de polímero

Se formaron nano-emulsiones O/W en el sistema Agua / [CatA:Span® 80 = 1:1] / [6 wt% EC10 en acetato de etilo] con relaciones de aceite/tensioactivo (O/S) entre 25/75 y 85/15 con un contenido de agua superior a 75 wt%. Se confirmó que las nano-emulsiones se formaban por inversión de fases mediante determinaciones de conductividad. Se obtuvieron nano-emulsiones con tamaños de gota de 300 nm y una polidispersidad inferior a 0.15. Los valores de potencial zeta en muestras diluidos (concentración: 20 mg/g en agua y PB) fueron de aproximadamente 60 mV (en agua) y 30 mV (en PB). Se observó que la incorporación de oleilamina producía un aumento del potencial zeta de las nano-emulsiones (67 mV en agua y 35 mV en PB) debido a la carga positiva adicional procedente de la amina. Con oleilamina, el diámetro de gota en las nano-emulsiones era ligeramente más pequeño (250 nm) que en nano-emulsiones sin la amina, pero, las nano-emulsiones eran menos estables. Como el uso de oleilamina no mejoraba las propiedades de las nano-emulsiones, no se llevaron a cabo más estudios con esta amina.

3.1.3. Nano-emulsiones del sistema Agua / CatA:Cremophor® WO7 / solución de polímero

Se formaron nano-emulsiones en el sistema Agua / [CatA:CWO7] / [6 wt% EC10 en acetato de etilo] para relaciones de aceite/tensioactivo (O/S) entre

55/45 y 75/25 con un contenido de agua superior a 88 wt% con las relaciones CatA:CWO7 = 1:1 y 1:3. La inversión de fases desde un sistema agua-en-aceite (W/O) a un sistema aceite-en-agua (O/W) fue confirmada por mediciones de conductividad. La región de formación de nano-emulsiones era ligeramente más estrecha que para el sistema CatA:Span® 80 y aparecía para contenidos de agua más altos. Las nano-emulsiones del sistema CatA:CWO7 = 1:3 eran más transparentes que los de los sistemas CatA:CWO7 = 1:1 y CatA:Span® 80. La inversión de fases desde un sistema agua-en-aceite (W/O) a un sistema aceite-en-agua (O/W) fue confirmada por mediciones de conductividad y se encontraron en el mismo rango de contenido de agua que en el sistema CatA:Span® 80 (aproximadamente a 30 wt%). Los valores de conductividad eran comparativamente más altos que los obtenidos con el sistema CatA:Span® 80. Las nano-emulsiones con las dos relaciones tensioactivo catiónico:noniónico mostraron tamaños de gota inferiores a 260 nm y una polidispersidad entre 0.20 y 0.46. En comparación con el sistema CatA:Span® 80, los tamaños de gota son significativamente más pequeños y con una polidispersidad mayor. Los valores de potencial zeta, tal como se esperaba eran positivos, y se hallaban entre +30 y +50 mV (dilución de 20 mg/g en agua). Los valores de la carga superficial son más altos con la relación CatA:CWO7 1:1 que con la relación 1:3 debido a la presencia de mas tensioactivo catiónico. La evaluación de la estabilidad visual mostraba que las nano-emulsiones de CatA:CWO7 = 1:3 son más estables que las de 1:1 o de CatA:Span® 80. La disminución de relación CatA:CWO7 no mejoraba el tamaño de gota, la carga superficial o la estabilidad (evaluado visualmente) de nano-emulsiones en comparación con el sistema CatA:CWO7 1:3.

Se estudió asimismo el efecto de la concentración de polímero en las propiedades de las nano-emulsiones. Con 10 wt% de polímero sólo se obtenían nano-emulsiones con la mescla CatA:CWO7 = 1:3 y la relación O/S de 70/30. Los valores de tamaño de gota eran más grandes y la carga superficial era más baja que los de nano-emulsiones correspondientes formadas con 6 wt% de polímero y además eran visualmente menos estable. Es importante mencionar que el uso del tensioactivo CWO7 mejoraba ligeramente la formación de nano-emulsiones con respecto al sistema

CatA:Span® 80. Esto sugiere que la estructura del agente tensioactivo juega una función importante.

3.1.4. Nano-emulsiones en el sistema Agua / CatA:(Cremophor® WO7:Cremophor® EL) / solución de polímero

Se estudió este sistema para comprobar si la mezcla de tensioactivo CWO7 (con número HLB bajo) con otro tensioactivo noniónico con una estructura similar, Cremophor® EL (CEL), y con un número HLB alto (12-14) podría contribuir a una mejora adicional de la formación y propiedades de nano-emulsiones. Los estudios se centraron en la caracterización de nano-emulsiones con la relación O/S de 70/30 y con 95 wt% agua. El tensioactivo catiónico se mezclaba con diferentes relaciones de los dos tensioactivos noniónicos con las relaciones CatA:(CWO7:CEL) de 1:1 y de 1:3.

Se obtuvieron nano-emulsiones en el sistema Agua / [CatA:(CWO7:CEL)] / [6 wt% EC10 en acetato de etilo] con la relación de aceite/tensioactivo (O/S) 70/30 y con un contenido de agua de 95 wt% con las relaciones CatA:(CWO7:CEL de 1:1 y 1:3. Los tamaños de gota eran entre 115 y 160 nm y la polidispersidad entre 0.25 y 0.37. Estos valores son similares a los obtenidos con el sistema CatA:CWO7. Las cargas superficiales, entre +11 y +33 mV, eran más elevados al aumentar el contenido de CWO7. Los valores de potencial zeta eran bastante menores con la relación CatA:(CWO7:CEL) 1:3 que con la relación CatA:(CWO7:CEL) 1:1 debido al menor contenido de tensioactivo catiónico. La estabilidad (evaluada visualmente) de todas las nano-emulsiones era inferior a un día.

En relación al efecto de la concentración de polímero, se formaban nano-emulsiones con 10 wt% polímero con tamaños de gota más grande que con 6 wt% y con cargas superficiales en el mismo rango que las de 6 wt% y menos estables. Asi se confirmó que el uso de una concentración de polímero más alta (10 wt%) no mejora la formación de nano-emulsiones cinéticamente estables.

La mezcla de los dos tensioactivos derivados de aceite de ricino con significativamente diferentes números de HLB no contribuyó a una mejora adicional de la formación de nano-emulsiones cinéticamente estable.

3.1.5. Nano-emulsiones en el sistema Solución acuosa / CatA:Cremophor® EL / solución de polímero

Se consideró de interés estudiar si se favorecía la formación de nano-emulsiones mezclando el tensioactivo CatA sólo con el tensioactivo de HLB alto, CEL. Se eligió la relación CatA:CEL 1:1 para tener una carga superficial adecuada para aplicaciones futuras (por ejemplo, la formación de complejos con biomoléculas). Se utilizaron diferentes tipos de soluciones acuosas, tales como solución salina tamponada con fosfato o solución de HEPES que tienen valores de pH fisiológicos. El contenido de la solución acuosa se fijó en 95 wt%. Tal como se evidenció en los estudios con los sistemas CatA:CWO7 y CatA:(CWO7:CEL), la formación de nano-emulsiones no se mejoró con una elevada concentración de polímero (10%). Por eso, el contenido de la solución de polímero se mantuvo al 6 wt%.

Se obtuvieron nano-emulsiones en los sistemas Solución acuosa / [CatA:CEL] / [6 wt% EC10 en acetato de etilo] con relaciones de aceite/tensioactivo (O/S) entre 35/65 y 90/10 con un contenido de solución acuosa 30 wt%. La región de formación de nano-emulsiones con tampón fosfato salino (PBS) es un poco mayor que con agua o con la solución de HEPES, que tienen formas similares y las nano-emulsiones se forman entre las mismas relaciones O/S (**Figura 6.4**).

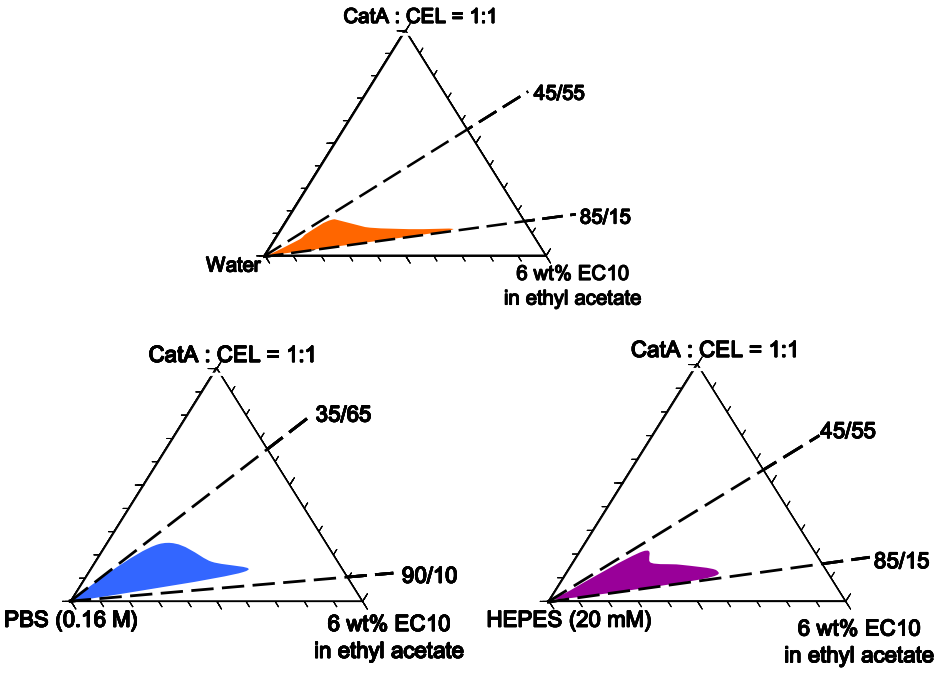

Figura 8.4. Región de formación de nano-emulsiones aceite-en-agua (O/ W) en el sistema solución acuosa / [CatA:CEL = 1:1] / [6 wt% de EC10 en acetato de etilo], a 25 °.

Las zonas de nano-emulsión, independientemente de la solución acuosa utilizada, eran mayores que las obtenidas con los sistemas CatA:Span® 80 o CatA:CWO7. Por razones de inestabilidad de las nano-emulsiones formadas con PBS, los estudios se centraron en las nano-emulsiones formados con agua y solución de HEPES como soluciones acuosas. Los tamaños de gota eran entre 97 y 126 nm con polidispersidades entre 0.27 y 0.51. En comparación con todos los otros sistemas estudiados, con este sistema se obtuvieron nano-emulsiones con tamaño de gota más pequeño. Los valores de potencial zeta, entre +18 y +36 mV (sin dilución) eran más elevados con agua que con HEPES. Las nano-emulsiones con agua y HEPES mostraban una buena estabilidad visual para relaciones O/S entre 60/40 y 70/30. Las determinaciones del tamaño de gota por DLS en función del tiempo revelaron estabilidad durante aproximadamente 4 semanas. Por otra parte, se estudió el efecto de un polímero con un peso molecular más bajo, EC4. Las regiones de nano-emulsiones eran similares en tamaño y forma a las de EC10. El tamaño de las gotas era más pequeño con polidispersidades altas (0.42). La estabilidad visual era peor que con EC10. La estabilidad de nano-emulsiones por medidas del tamaño de gota por DLS en función del tiempo para la relación O/S de 70/30 y 95 wt% de agua o HEPES reveló que el tamaño de gotas no variaba durante al menos 28 días.

Como las nano-emulsiones de este sistema presentaban características muy adecuadas para aplicaciones futuras (pequeños tamaños de gota a pH fisiológico, potencial zeta positivo, estabilidad superior a 24 horas), se estudió el sistema con el tensioactivo no iónico CEL sin la incorporación del tensioactivo catiónico.

3.1.6. Nano-emulsiones en sistema Agua / Cremophor® EL / solución de polímero

La región de formación nano-emulsiones en el sistema Agua / CEL / [6 wt% EC10 en acetato de etilo] comprende las relaciones aceite/tensioactivo (O/S) entre 55/45 y 85/15 con un contenido de agua superior a 30 wt%. En comparación con las regiones obtenido con el sistema CatA:CEL 1:1, la región es más estrecha con respecto a la relación O/S pero más amplia a contenidos

de agua más bajos. La inversión de fases se confirmó por mediciones de conductividad. Los valores de conductividad eran significativamente más bajos (más de 10 veces) que las del sistema CatA:CEL 1:1 debido a la falta de la componente catiónico. Los tamaños de gota eran entre 150 y 200 nm con una polidispersidad de 0.25. Los tamaños de gota eran más grande que los obtenidos con CatA:CEL 1:1 y los valores de potencial zeta negativos (alrededor de -28 mV). Es de destacar que las nano-emulsiones de este sistema sedimentan poco después de su preparación mientras que los del sistema CatA:CEL 1:1 mostraban una mayor estabilidad. Estudios con el polímero con un peso molecular más bajo, EC4, mostraron que la región de formación de nano-emulsiones era similar a la del sistema con EC10, que los tamaños de gota eran más pequeños, con elevada polidispersidad y que los valores del potencial zeta eran similares. Por otra parte, las nano-emulsiones eran poco estables.

3.2. NANOPARTÍCULAS CATIONICAS: FORMACIÓN Y CARACTERIZACIÓN

3.2.1. Formación y characterización de nanopartículas a partir de las nano-emulsions seleccionadas

Los estudios sobre la formación de nano-emulsiones permitieron seleccionar las nano-emulsiones que se utilizarían como plantilla para la preparación de nanopartículas. Se seleccionaron las nano-emulsiones que mostraban pequeños tamaños de gota, valores de potencial zeta elevado, buena estabilidad y con un aspecto transparente o translúcido. Las nanopartículas se prepararon a partir de las nano-emulsiones por el método de evaporación del disolvente.

Las nanopartículas obtenidas de nano-emulsiones del sistema Agua / CatA:Span® 80 / solución de polímero mostraron tamaños grandes (>200 nm) con potenciales zeta altos (>50 mV) y con poca estabilidad (< 1día). Las nanopartículas obtenidas de nano-emulsiones del sistema Agua / CatA:CWO7 / solución de polímero mostraban tamaños de partícula entre 110 y 190 nm, con

valores de potencial zeta entre 10 y 45 mV y estabilidades (evaluados visualmente) hasta 51 días.

Con el sistema **Agua / CatA:(CWO7:CEL) / solución de polímero** se obtenían nanopartículas en aproximadamente el mismo rango de tamaños que con el sistema CatA:CWO7 (105 – 220 nm) con valores de potencial zeta similares (11-30 mV) pero con una estabilidad muy baja (evaluado visualmente).

Para nanopartículas del sistema **Solución acuosa / CatA:CEL / solución de polímero** (EC4 y EC10) los tamaños eran de alrededor 100 nm (**Figura 6.5**) con cargas superficiales entre 20 y 35 mV y presentaban estabilidades aceptables.

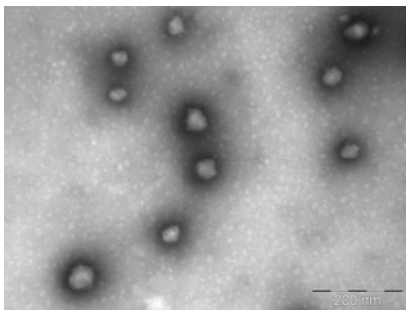

Figura 8.5. Micrografía TEM de una dispersión de nanopartículas obtenida a partir de una nano-emulsión del sistema Solución de HEPES / [CatA: CEL = 1:1] / [6 wt% de EC10 en acetato de etilo] con una relación O / S de 70/30 y 95 wt% de solución HEPES.

3.2.2. Eliminación del exceso de tensioactivo de dispersiones de nanopartículas

Para eliminar el exceso de tensioactivo, las dispersiones de nanopartículas se **dializaron** frente a agua, PBS (0.33 M) o solución de HEPES. El proceso de diálisis fue seguido por mediciones de la conductividad en el líquido de diálisis y en las dispersiones de nanopartículas y también fue seguido por mediciones del potencial zeta de la dispersión de nanopartículas en función del tiempo. El plateau en conductividad y/o en carga superficial fue interpretado como un equilibrio de iones dentro y fuera de la dispersión de nanopartículas.

El proceso de diálisis se optimizó para cada sistema con respecto a la duración de la diálisis y el volumen de la solución de diálisis y nanopartículas dispersión.

3.2.3. Funcionalización de nanopartículas catiónicas

Se seleccionó la dispersión de nanopartículas obtenida de la nano-emulsión del sistema **Solución acuosa / [CatA:CEL = 1:1] / [6 wt% EC10 en acetato de etilo]**

con la relación O/S de 70/30 y con 95 wt% de solución acuosa para los estudios de funcionalización pues el tamaño de nanopartícula era pequeño, los valores de potencial zeta suficientemente altas positivos y presentaba buena estabilidad.

Se eligió ácido fólico para estudios de formación de complejos nanopartícula:ligando. Debido a la alta afinidad de ácido fólico/folato para los receptores de folato, que se sobreexpresan en células cancerosas, esta vitamina se utilizo como ligando dirigido para la entrega selectiva de fármacos a células tumorales y se ha utilizado en este trabajo como un modelo para la formación de complejos con nanopartículas poliméricas catiónicas.

Se formaron complejos entre **ácido fólico** y nanopartículas obtenidas de una nano-emulsión del sistema Solución acuosa / [CatA:CEL = 1:1] / [6 wt% EC10 en acetato de etilo] con la relación O/S de 70/30 y con 95 wt% de agua o solución HEPES como fases acuosas. Los complejos se formaron con diferentes relaciones de carga catiónica-a-aniónica c^+/a^- (la carga catiónica (c^+) del tensioactivo catiónico presente en la dispersión de nanopartículas y la carga aniónica (a^-) de los aniones en la solución de ácido fólico), expresado en equivalentes. Los valores de potencial zeta siguen la misma tendencia en todas las fases acuosas. La **Figura 6.6** muestra los valores en agua.

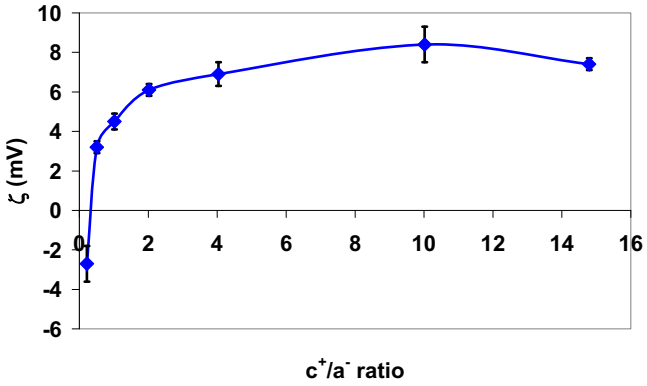

Figura 8.6. Potencial zeta en función de la relación carga catiónica/aniónica (c^+/a^-) de una dispersión de nanopartículas obtenida a partir de una nano-emulsión del sistema Agua / [CatA:CEL = 1:1] / [6 wt% EC10 en acetato de etilo] con la relación O/S de 70/30. La carga aniónica corresponde a ácido fólico.

Los valores son negativos para relaciones c^+/a^- pequeñas y aumentan a valores positivos con el aumento de concentración de nanopartículas. Los valores de

potencial zeta no exceden +10 mV, el límite superior para aplicaciones biomédicas [**Davis, 2009**]. Los tamaños de los complejos son similares en ambas fases acuosas (90 nm). Para ajustar los valores de osmolaridad de nanopartículas en el rango requerido para aplicaciones en contacto con la sangre (275 – 300 mOsm/kg), se necesita la incorporación de 4.3% de glucosa en la fase acuosa. La glucosa no afecta el tamaño de complejos y el potencial zeta sigue la misma tendencia descrita para los complejos formados con agua y solución de HEPES.

Aparte de los estudios de formación de complejos con el ácido fólico, se ha estudiado la formación de complejos de **oligonucleótidos de fosforotioato antisentido (ASO)** con nanopartículas obtenidas de una nano-emulsión de solución HEPES / [CatA:CEL = 1:1] / [6 wt% EC10 en acetato de etilo] con la relación O/S de 70/30 y con 95 wt% de solución HEPES. Las diferentes relaciones entre la carga positiva del tensioactivo catiónico presente en la dispersión de nanopartículas (N) y la carga negativa que viene de los grupos fosfato del oligonucleótido (P) se indicaban como relaciones N/P. Las tendencias en tamaño de complejo y carga superficial de complejos son similares a aquellos con ácido fólico. Mientras que, en ausencia de suero bovino fetal (FBS), los valores de potencial zeta aumentan con el aumento de la relación N/P para valores neutros, en presencia de FBS, los valores eran negativos (**Figura 6.7**).

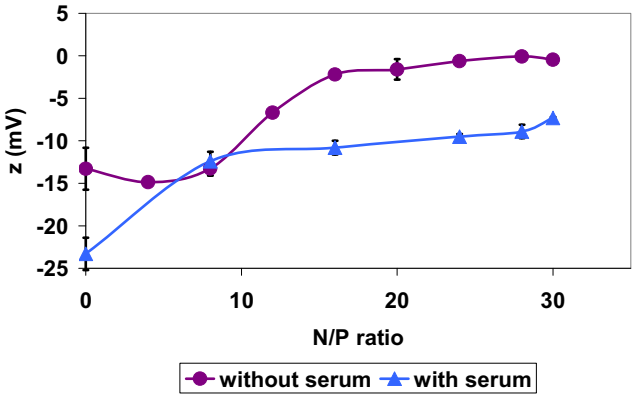

Figura 8.7. Valores del potencial zeta (ζ) en función de la relación N/P de los complejos formados entre las nanopartículas y el oligonucleótido antisentido (ASO) fosforotioato en ausencia y en presencia de suero bovino fetal (FBS), a 25 °C. Las nanopartículas se obtuvieron a partir de nano-emulsiones del sistema solución de HEPES / [CatA:CEL = 1:1] / [6 wt% de EC10 en acetato de etilo] con una relación O/S de 70/30 y 95 wt% de solución de HEPES.

Esto indica que los componentes cargados negativamente en el suero son, dependiendo de la relación de carga, adsorbidos sobre la superficie de los complejos de nanopartículas/ASO. La formación del complejo también fue confirmada por ensayos EMSA. El complejo nanopartícula:oligonucleótido antisentido con N/P 30 se caracterizó por análisis de imagen TEM. Los complejos poseen una esfericidad más alta que las nanopartículas, con un tamaño medio de 30 nm, más pequeños que los obtenidos para la dispersión de nanopartículas (40 nm). Se puede concluir que los complejos formados con ácido fólico y con ASO tienen tamaños y cargas superficiales adecuadas para aplicaciones terapéuticas [Davis, 2009].

3.2.4. Estudios *in vitro* de dispersiones de nanopartículas

Se seleccionó la dispersión de nanopartículas obtenida de la nano-emulsión del sistema Solución HEPES / [CatA:CEL = 1:1] / [6 wt% EC10 en acetato de etilo] con la relación O/S de 70/30 y con 95 wt% de solución HEPES para una investigación adicional de su toxicidad y la eficiencia de transfección.

La viabilidad y la proliferación de las células HeLa en presencia de nanopartículas se evaluó mediante la realización del ensayo de citotoxicidad MTT (Figura 6.8). No se produjo citotoxicidad hasta una concentración de 3 mM de la especie catiónica presente en la dispersión de nanopartículas.

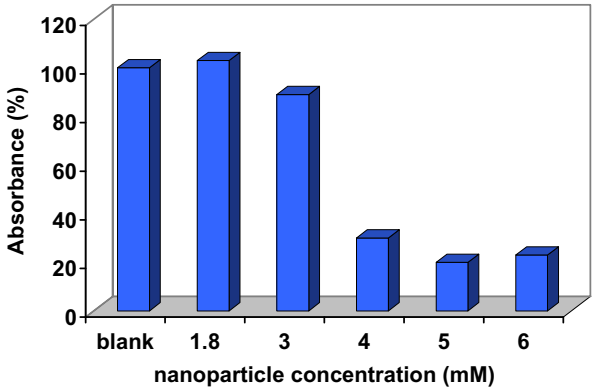

Figura 8.8. Absorbancia (λ = 570 nm) de células HeLa en función de la concentración de nanopartículas después de 4 horas de tratamiento. Las nanopartículas se obtuvieron a partir de una nano-emulsión del sistema solución de HEPES / [CatA:CEL = 1:1] / [6 wt% de EC10 en acetato de etilo] con una relación O/S de 70/30 y 95 wt% de solución de HEPES. La barra **blank** indica la muestra sin nanopartículas.

Las **pruebas de hemólisis** *in vitro* revelaron que las dispersiones de nanopartículas con altas concentraciones de especies catiónicas mostraron una alta actividad hemolítica en las células rojas de la sangre. Sin embargo, los complejos de nanopartículas con ácido fólico mostraron valores de hemólisis significativamente menores.

Los ensayos de **eficiencia de transfección** de los complejos de nanopartículas:oligonucleótidos antisentido pusieron de manifiesto que la relación N/P 28 mostraba un óptimo en la inhibición (40%) de la expresión del gen de la luciferasa de *Renilla* en ausencia de FBS. Sin embargo, en presencia de proteínas de suero, incluso con el cambio de concentración de oligonucleótido, no se detectó el silenciamiento del gen.

4. Conclusiones generales

Los resultados de la tesis demuestran la posibilidad de obtener nanopartículas catiónicas a partir de nano-emulsiones del tipo aceite-en-agua (O/W) por la incorporación de un tensioactivo catiónico en un sistema Solución acuosa / tensioactivo(s) / Aceite. Los nano-emulsiones se han podido preparar por un método de emulsificación de baja energía y el tamaño y estabilidad se puede controlar con una variedad de parámetros tales como naturaleza del tensioactivo noniónico, la relación tensioactivo catiónico:nonionico, tipo de solución acuosa, concentración de polímero y el peso molecular del polímero.

Se han obtenido nanopartículas catiónicas poliméricas utilizando estos nano-emulsiones como plantilla, utilizando un polímero preformado que era incorporado en la fase oleosa. Se confirmó la posibilidad de formar complejos entre nanopartículas seleccionadas y compuestos bioactivos, tales como ácido fólico y oligonucleótido de fosforotioato antisentido (ASO). Las características (tamaño y la carga superficial) de las nanopartículas y de los complejos formados con ácido fólico o ASO estaba en un rango que permitiría su aplicación como agentes terapéuticos.

Los estudios *in vitro* de nanopartículas y de los complejos de nanopartículas:oligonucleótido revelaron que

- las nanopartículas no son tóxicos para las células HeLa hasta una concentración de 3 mM
- la concentración de especie catiónica de las nanopartículas debe ser baja para obtener valores bajas de hemólisis y la presencia de ácido fólico unido a las nanopartículas contribuye a una hemólisis baja.
- los complejos de nanopartícula:oligonucleótidos mostraban una inhibición de genes en ausencia de suero bovino fetal (FBS), por lo que son candidatos prometedores para la inhibición de genes *in vitro*. En la presencia de proteínas de suero, no se detectó “gene silencing” que impide el uso de estas nanopartículas para experimentos *in vivo*.

9. APPENDIX

9.1. NANO-EMULSIONS IN THE WATER / CATA:CREMOPHOR® WO7 / POLYMER SOLUTION SYSTEM

Table A 9.1. Droplet diameters and polydispersity indices (PI) of nano-emulsions of the Water / [CatA:CWO7] / [6 wt% EC10 in ethyl acetate] systems with the O/S ratio 70/30 and 90 and 95 wt% of water content at 25ºC, as obtained with DLS. Shadowed cells correspond to samples diluted (1/100) with water saturated with ethyl acetate.

CatA : CWO7 surfactant ratio	90 wt% water		95 wt% water	
	droplet diameter (nm)	PI	droplet diameter (nm)	PI
1:1	218.6	0.29	173.1	0.20
1:3	119.9	0.41	127.6	0.33
1:4	121.8	0.37	133.2	0.35
1:6	170.6	0.32	141.6	0.40
1:8	222.0	0.48	169.6	0.30

Table A 9.2. Visually assessed stability of nano-emulsions of the Water / [CatA:CWO7] / [6 wt% EC10 in ethyl acetate] system with the O/S ratio 70/30 and 90 and 95 wt% water content, at 25ºC.

CatA : CWO7 surfactant ratio	Stability (days)	
	90 wt% water	95 wt% water
1:1	1	2
1:3	66	70.5
1:4	50	17
1:6	12	16
1:8	17	15

9.2. NANO-EMULSIONS IN THE WATER / CATA:(CREMOPHOR® WO7:CREMOPHOR® EL) / POLYMER SOLUTION SYSTEM

Table A 9.3. Droplet diameters and polydispersity indices (PI) of nano-emulsions of the Water / [CatA:(CWO7:CEL)] / [6 wt% EC10 in ethyl acetate] system with the O/S ratio 70/30 and 95 wt% of water content at 25ºC, as obtained with DLS.

CWO7:CEL mixing ratio	CatA:(CWO7:CEL) = 1:1		CatA:(CWO7:CEL) = 1:3	
	droplet diameter (nm)	PI	droplet diameter (nm)	PI
1:3	166.4	0.25	149.2	0.27
1:2	153.2	0.30	132.1	0.32
1:1	148.0	0.28	115.8	0.33
2:1	151.9	0.32	116.6	0.33
3:1	158.2	0.35	122.3	0.36

Table A 9.4. Theoretical stability assessment of nano-emulsions of the Water / [CatA:(CWO7:CEL)] / [6 wt% EC10 in ethyl acetate] system with the O/S ratio 70/30 and 95 wt% water content, calculated from Stokes' law.

CWO7:CEL mixing ratio	CatA:(CWO7:CEL) = 1:1	CatA:(CWO7:CEL) = 1:3
	Rate of sedimentation (nm/s)	
1:3	1.3	1.1
1:2	1.1	0.8
1:1	1.1	0.6
2:1	1.1	0.7
3:1	1.2	0.7

Table A 9.5. Theoretical stability assessment of nano-emulsions of the Water / [CatA:(CWO7:CEL)] / [10 wt% EC10 in ethyl acetate] system with the O/S ratio 70/30 and 95 wt% water content, calculated from Stokes' law.

CWO7:CEL mixing ratio	CatA:(CWO7:CEL) = 1:1	CatA:(CWO7:CEL) = 1:3
	Rate of sedimentation (nm/s)	
1:3	x	x
1:2	x	x
1:1	1.3	1.3
2:1	x	1.1
3:1	1.2	0.9

9.3. NANO-EMULSIONS IN THE AQUEOUS SOLUTION / CATA:CREMOPHOR® EL / POLYMER SOLUTION SYSTEM

Table A 9.6. Droplet diameters and polydispersitiy indices (PI) of nano-emulsions of the Aqueous solution / [CatA:CEL = 1:1] / [6 wt% EC10 in ethyl acetate] system in water (pH 5.6) and HEPES solution (20 mM, pH 7.4), as obtained with DLS, at 25°C.

O/S ratio	Water		HEPES	
	droplet diameter (nm)	PI	droplet diameter (nm)	PI
55/45	x(1)	x(1)	116.7	0.51
60/40	125.6	0.27	103.9	0.47
65/35	107.2	0.31	101.0	0.42
70/30	98.4	0.32	96.9	0.44
80/20	101.4	0.29	97.0	0.36
85/15	104.6	0.32	x(1)	x(1)

(1) As nano-emulsions were very unstable, values are not included.

Table A 9.7. Theoretical stability assessment of nano-emulsions of the Aqueous solution / [CatA:CEL = 1:1] / [6 wt% EC10 in ethyl acetate] system with the O/S ratio 70/30, calculated from Stokes' law.

O/S ratio	Rate of sedimentation (nm/s)	
	Water	HEPES
55/45	x[(1)]	0.7
60/40	0.8	0.5
65/35	0.6	0.5
70/30	0.5	0.5
80/20	0.5	0.5
85/15	0.5	x[(1)]

[(1)] As nano-emulsions were very unstable, values are not included.

Table A 9.8. Droplet diameters and polydispersity indices (PI) of nano-emulsions of the Aqueous solution / [CatA:CEL = 1:1] / [6 wt% EC4 in ethyl acetate] system with 95 wt% of aqueous solution content at 25ºC, as obtained with DLS.

O/S ratio	water		HEPES	
	droplet diameter (nm)	PI	droplet diameter (nm)	PI
50/50	153.4	0.56	122.3	0.56
60/40	118.4	0.48	101.2	0.50
70/30	102.0	0.45	91.7	0.49
80/20	96.2	0.42	91.6	0.46
85/15	91.0	0.42	86.6	0.48

Table A 9.9. Theoretical stability assessment of nano-emulsions of the Aqueous solution / [CatA:CEL = 1:1] / [6 wt% EC4 in ethyl acetate] system with 95 wt% aqueous solution content, calculated from Stokes' law.

O/S ratio	Water	HEPES
	Rate of sedimentation (nm/s)	
50/50	1.1	0.7
60/40	0.7	0.5
70/30	0.5	0.4
80/20	0.4	0.4
85/15	0.4	0.4

9.4. NANO-EMULSIONS IN THE AQUEOUS SOLUTION / CREMOPHOR® EL / POLYMER SOLUTION SYSTEM

Table A 9.10. Theoretical stability assessment of nano-emulsions of the Water / CEL / [6 wt% EC4 in ethyl acetate] system, compared to that of the CatA:CEL system, with 95 wt% of water content, calculated from Stokes' law.

O/S ratio	CEL system	CatA:CEL system
	Rate of sedimentation (nm/s)	
70/30	1.7	0.5
75/25	1.1	-(1)
80/20	1.2	0.4

(1) no nano-emulsion formed.

Table A 9.11. Theoretical stability assessment of nano-emulsions of the Water / CEL / [6 wt% EC4 in ethyl acetate] system with 95 wt% of water content, calculated from Stokes' law, compared to that of the CatA:CEL system.

O/S ratio	CEL system	CatA:CEL system
	rate of sedimentation (nm/s)	
70/30	0.9	0.5
75/25	0.6	-
80/20	0.7	0.4